1977

Development Of Sulfide-hosting Structures And Mineralization, Pine Point, Northwest Territories

James Richard Kyle
Western University, rkyle@jsg.utexas.edu

DEVELOPMENT OF SULFIDE-HOSTING STRUCTURES AND MINERALIZATION, PINE POINT, NORTHWEST TERRITORIES

by

James Richard Kyle

Submitted in partial fulfillment
of the requirements for the degree of
Doctor of Philosophy

Faculty of Graduate Studies
The University of Western Ontario
London, Ontario
March, 1977

ABSTRACT

The Pine Point district contains about 40 Pb-Zn ore bodies within a Middle Devonian carbonate barrier complex which developed along a tectonic hinge zone separating contemporaneous evaporite and shale basins. The ore bodies occur in two trends along the North and Main Hinge Zones and are stratabound in dolostones of several depositional facies over a 200-meter section of the barrier. The sulfide bodies range in size from 100,000 tons to more than 15 million tons and contain up to 20 percent combined Pb-Zn as sphalerite and galena. Marcasite and pyrite are ubiquitous accessories, and Fe content of ore bodies ranges from less than 1 percent to above 10 percent. The overall Pb:Zn:Fe ratio for the district is about 2:5:3. Ore bodies are "prismatic" with large vertical relative to horizontal dimensions, and "tabular" with large horizontal relative to vertical dimensions. Prismatic ore bodies are Pb-rich with Pb/(Pb + Zn) ratios averaging about 0.4; tabular ore bodies are Zn-rich with ratios averaging less than 0.3. Individual ore bodies are zoned with a Pb-rich, high grade core passing outward into a Zn-rich, high grade zone which grades into an Fe-rich, low grade envelope. The sulfide concentrations have abrupt contacts with barren host rocks. A district-wide study of major metal distribution shows that the ore bodies in both the Main and North Trends are more Pb-rich and less Fe-rich from southeast to northwest.

Detailed stratigraphic investigations reveal major paleo-solution structures related to post-middle Givetian subaerial exposure of the barrier complex. Numerous irregularly elliptical dolines as much as 400 meters long and 35 meters deep developed through dissolution of limestones by meteoric water. These dolines subsequently were filled with erosional detritus. Caves and tabular zones of increased permeability were formed in the upper part of the phreatic zone. The coarse-crystalline Facies K dolostone was created by mixing of fresh water and sea water during subaerial exposure, as indicated by stratigraphic relations, paleogeography, hydrologic principles, dolostone Na-content, and comparison with recent carbonates. These paleo-solution features were aquifers and loci for sulfide deposition in the coarse-crystalline Facies K dolostone. Dolines host prismatic ore bodies, whereas caves and tabular permeable zones contain tabular ore bodies. Origin of the breccias which host sulfides in the fine-crystalline dolostone of the lower barrier is less apparent, but these are believed to be solution features as well.

Ore textures are complex and exhibit paragenetically early marcasite and pyrite with rare pyrrhotite followed by colloform and banded sphalerite with skeletal galena. Large, well-formed sphalerite and galena crystals are late. Dolomite is both earlier and later than sulfides; calcite, celestite, gypsum, fluorite, sulfur, and bitumen are later and generally not associated with the sulfides. Sphalerite ranges from tan to dark brown, generally depending on variations in Fe content from 0.15 to 10.3 weight percent; Pb, Mn, Cu, and Cd are present in minor amounts. Galena, pyrite, and marcasite are extremely

low in trace elements, with Cu erratically present.

Fluid inclusion evidence indicates that the Pine Point sulfides were deposited by highly saline, 50° to 100° C brines, probably upon encountering reduced sulfur. These brines appear to have originated within the sedimentary sequence, but the immediate metal source cannot be defined by present data. The most likely source of sulfur is the Middle Devonian evaporites. Lead isotope analyses of different galena types confirm their non-radiogenic nature and indicate a mean $^{206}Pb/^{204}Pb$ ratio of about 18.1. These data suggest a mid-Carboniferous (310 million years) age of mineralization, considerably younger than the middle Givetian (375 million years) dolostone host. Colloform sphalerite and skeletal galena indicate rapid early sulfide deposition, while coarse crystals suggest slower late sulfide growth. Evidence for both sulfide-carbonate equilibrium and disequilibrium conditions is apparent, perhaps relating to periodic fluctuations in the supply of reduced sulfur. Sulfide concentrations are localized in paleodolines and breccia zones because these transgressive structures were bypasses between different aquifers and loci for mixing of fluids of different character, one of which contained metals and the other reduced sulfur.

ACKNOWLEDGEMENTS

The author is grateful to R. W. Hutchinson for his helpful advice throughout the course of the project and to C. G. Winder for his constructive criticism of the original drafts. I am particularly indebted to D. F. Sangster for his interest and valuable discussions while serving as an external thesis advisor. The excellent advice and assistance provided by Edwin Roedder concerning fluid inclusion measurements and the use of the heating and freezing stage facilities of the United States Geological Survey are greatly appreciated. Discussions with William Back concerning hydrology and with Paul B. Barton, Jr., concerning sulfide geochemistry and sphalerite stratigraphy were also very enlightening. C. F. Kahle generously provided a tour and discussion of paleokarst features in Silurian reefal carbonates near Toledo, Ohio. I am grateful to R. L. Barnett for microprobe analyses, J. Forth for preparation of thin and polished sections, and J. R. L. Ellis, G. Barker, and particularly M. W. Delich for their assistance with various aspects of the computer work. The author would like to thank T. W. Muraro for suggesting and initiating this project and for handling much of the logistics within Cominco Limited. I am grateful to J. A. Collins for his interest, helpful comments, and encouragement during the course of the study. W. R. Sproule, W. E. Wiley, and Z. Nikic provided recommendations concerning the release of previously unpublished information. I would like to thank these geologists and D. H. Adams, J. P. Balmer, K. M. Newman, P. J. Santos, H. Skall, and

J. M. West for many unselfish discussions which enabled the author to become more familiar with the geologic details of the Pine Point district. This cooperation has hopefully allowed the present study to build on existing geologic knowledge. However, the interpretations presented in this thesis do not necessarily agree with the views of these geologists and are the sole responsibility of the author. I am grateful to Pine Point Mines Limited and Cominco Limited for providing summer employment in the study area and for permission to work on and to release the material contained herein. Cominco Limited furnished financial support and facilities for computer work. The Geological Survey of Canada provided funds for the lead isotope analyses. I am especially indebted to my wife, Linda, not only for her technical assistance, but also for her understanding, patience, and constant encouragement during the lean times of graduate school.

TABLE OF CONTENTS

LIST OF TABLES

LIST OF PLATES

LIST OF FIGURES

LIST OF APPENDICES

CHAPTER ONE

INTRODUCTION

Statement of the Problem

The Pine Point mining district consists of about 40 lead-zinc ore bodies in a Middle Devonian carbonate barrier complex exposed on the south shore of the Great Slave Lake, Northwest Territories. The geological setting of the district has been used to define a widely accepted model for the genesis of carbonate-hosted lead-zinc deposits of the so-called Mississippi Valley-type (Beales and Jackson, 1966; Jackson and Beales, 1967). Although the district has been the subject of a number of studies and information on many aspects is available, previous research may be considered to fall into two general fields:

1. General studies primarily concerned with the regional geologic setting.
2. Detailed studies of various mineralogical aspects such as isotopes, sulfide textures, trace elements, and fluid inclusions.

Little information is available on such fundamental aspects as geometry of the mineralized zones, relationships between sulfide concentrations and hosting structures, and variations in metal percentages and ratios, mineralogy, textures, and isotopic composition within individual ore bodies and throughout the district. Earlier analytical work was performed on samples from a limited area and reflects only a small

proportion of the geological variables in the entire district. This study bridges the gap between the previous megascopic and microscopic research and provides additional analytical data to enable a more comprehensive understanding of the geology of the district. The main objectives are to:

1. Investigate the diagenetic processes affecting the barrier complex, particularly with regard to development of ore-hosting structures.
2. Study the distribution of lead, zinc, and iron within four geologically dissimilar ore bodies and within the district.
3. Determine and interpret the distribution of lead isotopes in galena.
4. Document and interpret the significance of mineralogical and textural variations, sulfide-carbonate relationships, sulfide trace element distributions, and isotopic and fluid inclusion data for various ore and gangue mineral generations.

Many of the stratigraphic complexities of the barrier complex have been unraveled (Skall, 1975), and the results of 10 years of intense production and over a million feet of diamond core drilling are available. Therefore, the foundation has been established for documenting fundamental relationships between host rocks and sulfide concentrations with the ultimate goal of solving some aspects of ore genesis at Pine Point.

Location and Access

The Pine Point mining district is located on the south shore of Great Slave Lake in the District of Mackenzie, Northwest Territories, about 800 kilometers north of Edmonton, Alberta, and 180 kilometers south of Yellowknife, N. W. T. (Fig. 1). The study area of about 1,700 square kilometers is defined by the Buffalo River on the west, the Great Slave Lake shore on the north, the Little Buffalo River on the east, and a northeasterly trending line approximately 25 kilometers south of the Lake shore (Fig. 2). Known sulfide bodies occur in a zone about 10 kilometers wide trending N 65° E through the center of this area (Fig. 2). The Pine Point townsite with a population of about 1,200 is located at latitude 60° 49' N., longitude 114° 28' W.

The area is accessible by commercial airline to Hay River, 75 kilometers to the west. An airstrip for light planes is located five kilometers northeast of the Pine Point townsite. Access can be gained also by an all-weather road from the Mackenzie Highway in Hay River. A spur from the Great Slave Railroad at Hay River provides freight and concentrate shipping facilities.

Topography and Vegetation

The area is a muskeg terrain with many shallow ponds and a cover of black spruce and pine with some deciduous trees and shrubs. Elevations range from 136 meters above sea level at the Great Slave Lake to as much as 250 meters above sea level on the higher beach ridges from the ancestral lake which once extended many kilometers

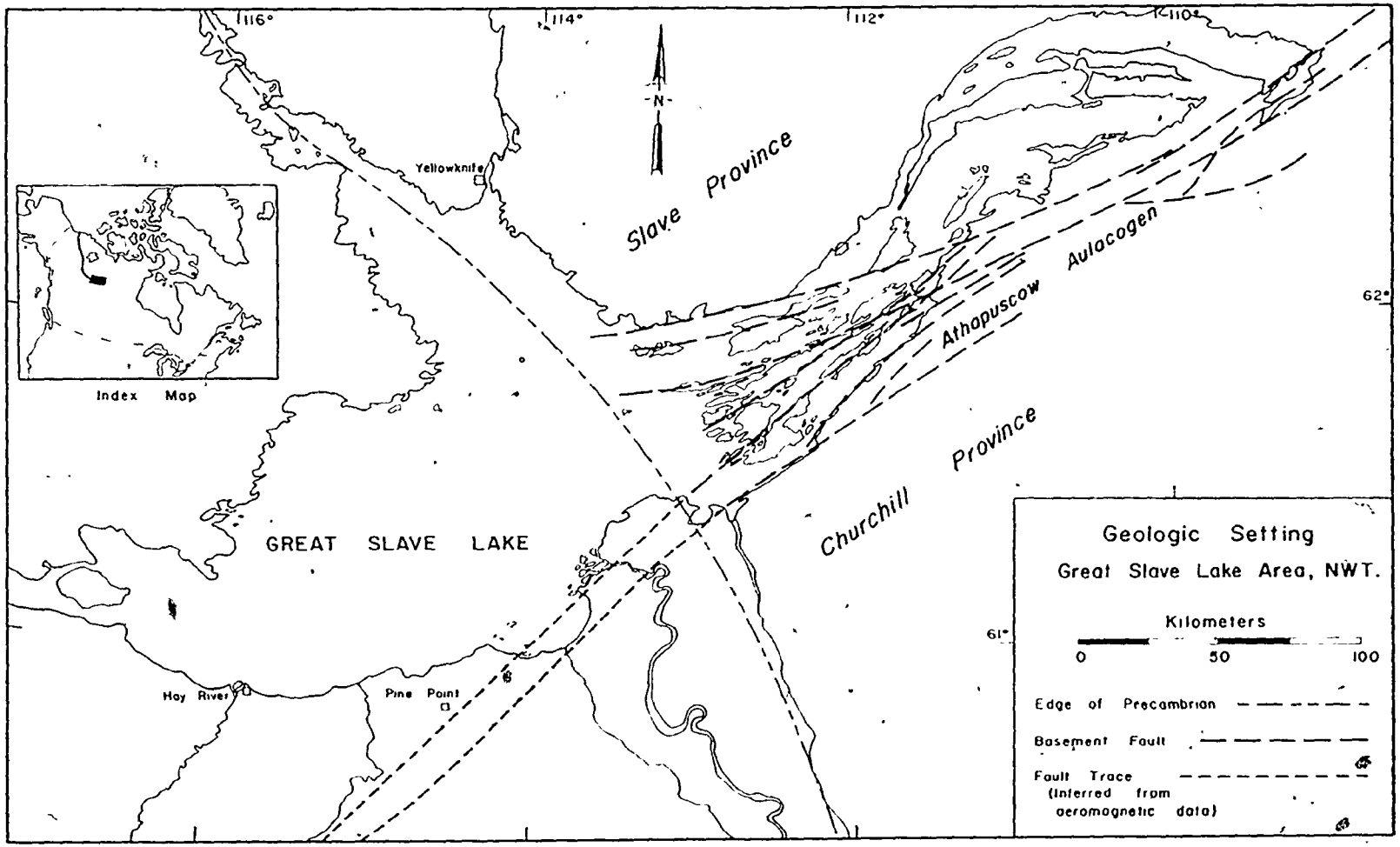

Fig. 1. Location and Geologic Setting of the Great Slave Lake Area, Northwest Territories. Modified after Norris (1965) and Hoffman et al. (1974)

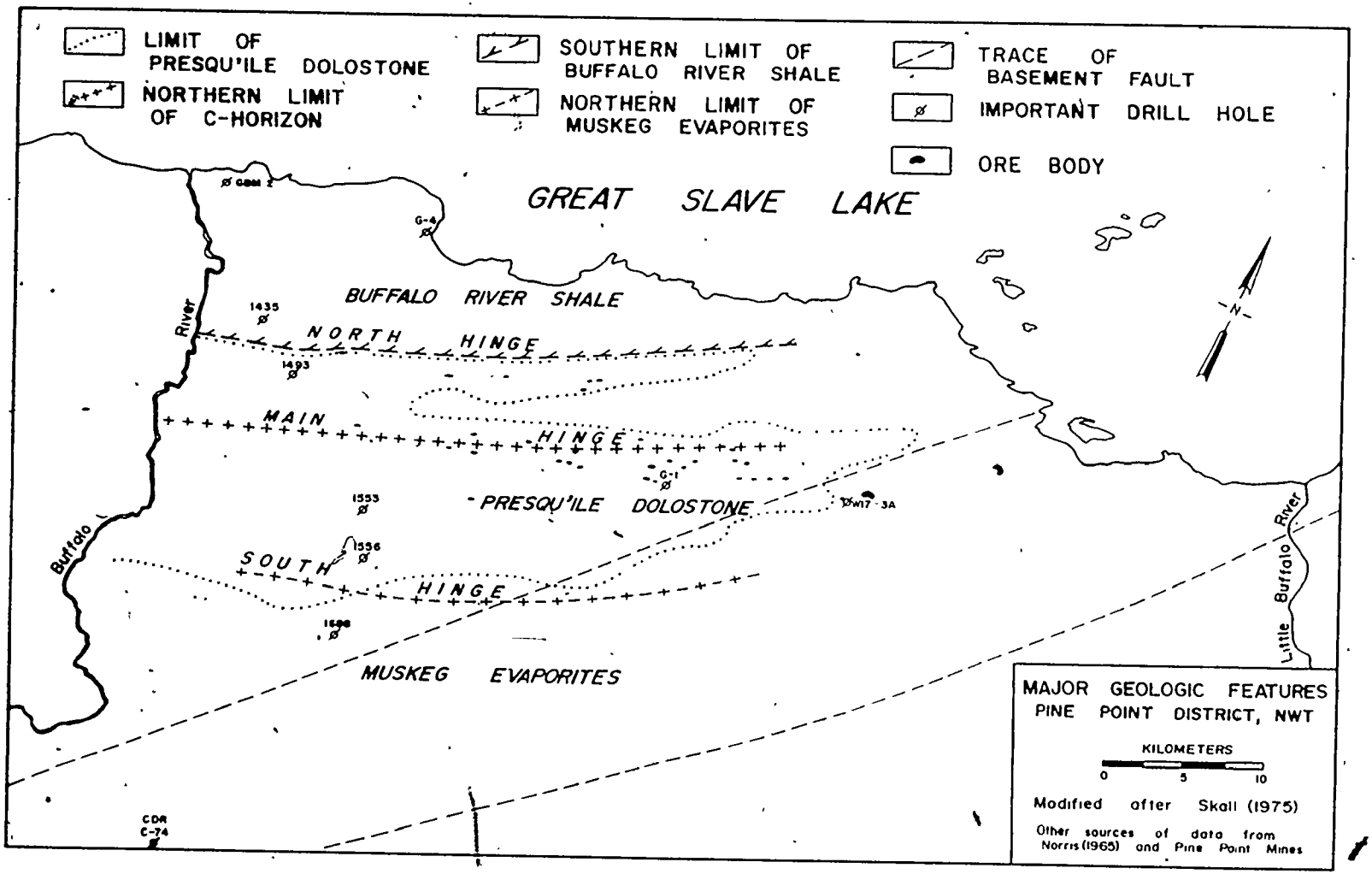

Fig. 2. Major Geological Features of the Pine Point Mining District

south of the present shore. Outcrops are virtually nonexistent with only a few exposures near the lake shore and river banks.

History

The lead-zinc occurrences on the south shore of the Great Slave Lake were examined by prospectors enroute to the gold fields of Alaska and the Yukon in 1898 (Bell, 1899). Campbell (1966) and Jackson (1971) provide summaries of early exploration work in the area, and only a few important events will be mentioned here. Bell (1929) classified the deposits as Mississippi Valley-type and identified the host rock as the Presqu'ile Dolostone of Middle Devonian age. Reserves of only 500,000 tons of ore grade material had been outlined during exploration to the late 1930's. The exploration program of The Consolidated Mining and Smelting Company of Canada Limited from 1940 to 1955 was based on the concept that the Pine Point sulfide deposits were related to the MacDonald Fault which could be traced southwestward from the Precambrian Shield in the East Arm of the Great Slave Lake and projected beneath Paleozoic cover to the Pine Point area. If numerous concealed ore bodies lay along a linear trend in the Devonian dolostones overlying the projection of the fault zone, the aggregate reserves from many isolated near surface deposits might make a major mining operation feasible in spite of the remote location. This concept resulted in the discovery of ore bodies with no surface expression, and mining operations became economically viable in 1961 with the decision of the Canadian Government to build a railroad to the Great Slave Lake. Increased exploration drilling, aided by induced polarization

techniques, resulted in the establishment of substantial reserves, and the first ore shipment was made in late 1964. The coarse-crystalline Presqu'ile Dolostone was considered to be the favorable host rock during this stage of exploration, but Pyramid Mines Limited discovered two large ore bodies (X15 and W17) in the fine-crystalline dolostones of the Pine Point Formation which underlie the Presqu'ile. Further exploration revealed the presence of a large mineralized zone (N204) at the contact of the Pine Point Formation and the Keg River Formation near its subcrop in the eastern part of the property and another mineralized trend in the Presqu'ile parallel to and north of the Main Trend. Recent preliminary drilling results of Western Mines Ltd. indicate the presence of substantial sulfide concentrations along the Main Trend west of the Buffalo River (The Northern Miner, October 14, 1976). A total of about 40 ore bodies has been outlined in the district, some of which have been mined completely. Pine Point Mines Limited is the sole producer in the district, and Cominco Limited is the operator, holding a 69.1 percent interest. Total production of the district to the end of 1975 is 33.7 million tons of ore grading 7.3 percent zinc and 3.7 percent lead (Table 1). Mine production is currently 11,000 tons per day. Present official ore reserves are 39.2 million tons of 5.4 percent zinc and 2.0 percent lead (Pine Point Mines Ltd. Annual Report, 1975).

Field and Laboratory Work Performed

The author spent a total of six months in the study area in the summers of 1974 and 1975. Cores from closely spaced diamond drill holes

TABLE 1

Pine Point District Production and Reserves 1964 - 1975

Compiled from Pine Point Mines Limited Annual Reports 1964 - 1975

	RESERVES			PRODUCTION				
	Tons Ore $\times 10^6$	Pb%	Zn%	Tons Ore	Pb%	Zn%	Tons Pb $\times 10^3$	Tons Zn $\times 10^3$
1964				14,070	18.6	25.8	2.6	3.6
1965	21.5	4.0	7.2	75,356	4.27	7.63	3.2	5.6
				364,168	22.5	29.1	81.9	106.0
1966	37.8	2.9	6.8	1,457,990	4.9	10.5	71.4	153.1
				282,309	18.8	26.3	53.1	74.2
1967	40.5	2.6	6.8	1,521,000	4.7	9.7	71.5	100.4
				333,000	18.0	27.9	59.9	92.9
1968	39.3	2.6	6.8	2,138,000	3.5	6.6	74.8	141.1
				353,000	19.0	25.0	67.1	88.3
1969	41.8	2.4	6.3	3,605,000	3.2	7.4	115.4	266.8
1970	43.5	2.5	6.0	3,860,000	3.0	7.1	115.8	274.1
				92,600	14.5	21.5	13.4	19.9
1971	41.9	2.4	6.0	3,892,000	2.6	6.5	101.2	253.0
1972	40.9	2.4	6.0	3,810,000	2.7	6.2	102.9	236.2
1973	38.3	2.3	5.7	3,896,000	2.9	6.0	113.0	233.8
1974	39.5	2.2	5.7	4,135,000	2.5	5.3	103.4	219.2
1975	39.2	2.0	5.4	3,905,000	2.4	4.9	93.7	191.3
Total Milled				32,295,346	3.0	6.4	966.3	2,074.8
Total Direct Shipping				1,439,147	19.3	26.7	278.0	384.9
TOTAL				33,734,493	3.7	7.3	1,244.3	2,459.7

in a number of ore bodies were examined, and relationships determined from drilling were compared with those observable in mining exposures in an attempt to determine controls of sulfide concentration. K57, A70, and W17 ore bodies were selected for detailed studies (Fig. 3). Cores from close-spaced drilling were logged totaling 30,000 feet for K57, 6,500 feet for A70, and 14,000 feet for W17, and samples of ore and host rock were collected. In addition 1,000 feet of N204 core were logged, and selected cores from other ore bodies were examined to study variations within the district. Because these cores were from ore outline drilling, all significantly mineralized intervals had been split, and half of the core had been removed for assaying purposes. Occasionally, mineralized intervals had been taken in their entirety for metallurgical testing. In these cases the original descriptions were used in conjunction with the remaining core, and increased emphasis was placed on adjacent drill holes. Several thousand feet of core from widely spaced exploration drilling were examined to familiarize the author with regional stratigraphic variations, and samples were collected for study of diagenetic modifications of barrier lithologic units. Geologic relationships were documented by field notes and photographs in all accessible mining operations (X15, W17, O28, P29, N31, P31, N32, O32, P32, N38A, M40, N42, O42, J44, K57, R61, and K62), and samples were collected for study.

Approximately 175 mine specimens and 400 core samples were slabbed, polished, and examined with a binocular microscope. Some rock slabs were stained with Alizarin red-S as an aid in differentiating between generations of carbonate cements. Approximately 150 polished

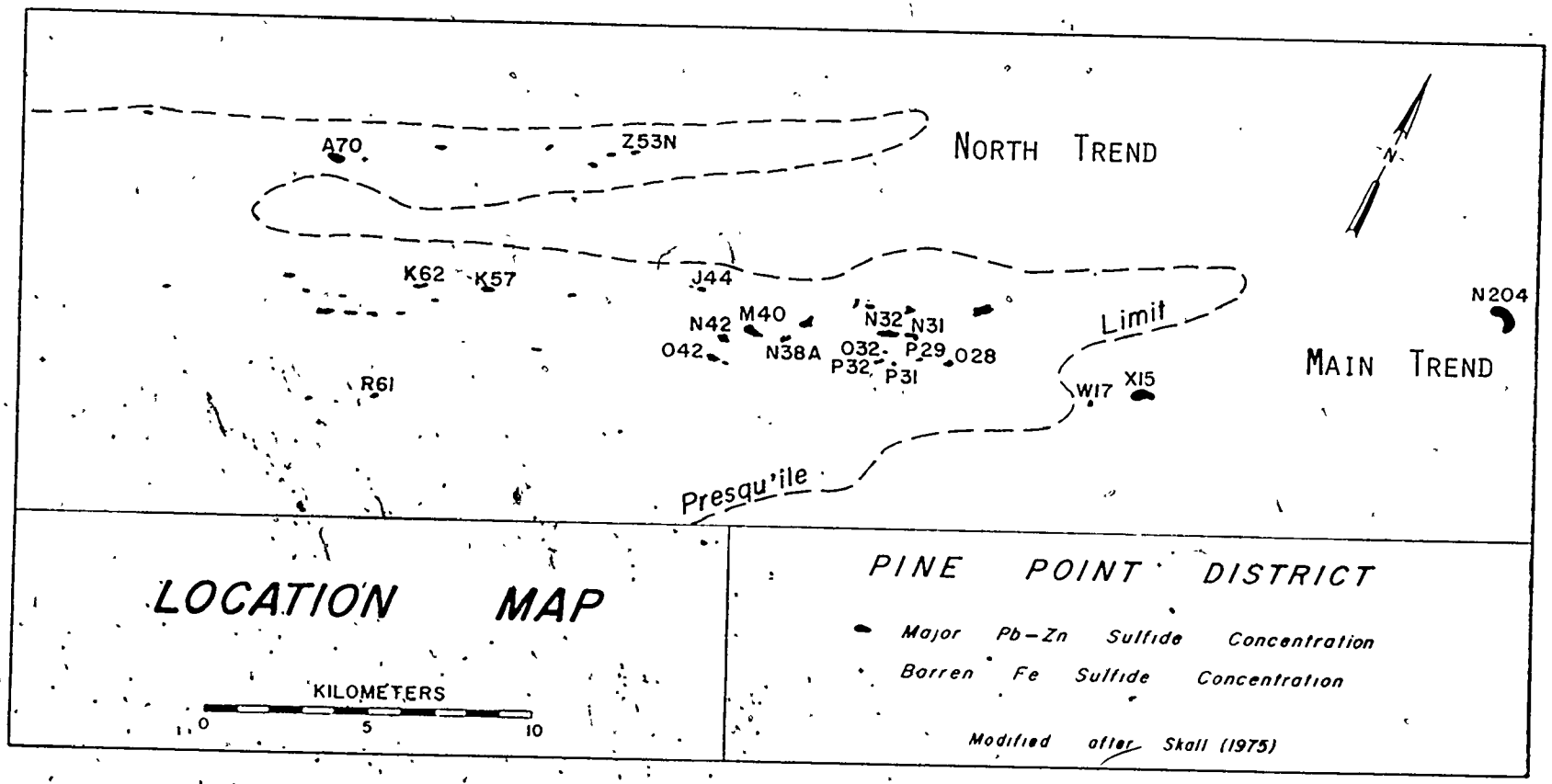

Fig. 3. Major Sulfide Concentrations

sections, polished thin sections, and thin sections were examined with a petrographic microscope and described as to their mineralogy and textural relationships. Visually and optically unidentifiable minerals and fine-crystalline mineral aggregates were identified by x-ray diffraction. Cathodoluminescence techniques using a Nuclide Model ELM-2A LUMINOSCOPE were attempted to differentiate carbonate and sphalerite generations; initial results were only modestly encouraging, and the technique was not pursued to its fullest potential. Polished doublets were made from sphalerite-bearing samples at the University of Western Ontario and at the United States Geological Survey National Headquarters, Reston, Virginia, and homogenization and freezing temperatures of fluid inclusions in 15 of these specimens were measured using the facilities of the U. S. Geological Survey. Thirteen hand-separated galena concentrates for lead isotope analyses were selected from mine samples and drill cores to represent as many variables as possible in terms of district-wide geographic, stratigraphic, and paragenetic distribution of ore leads. Approximately 100 hand-separated galena, sphalerite, and pyrite/marcasite concentrates were prepared for a later district-wide study of sulfide sulfur isotope distribution by D. F. Sangster and the author. Selected sphalerite, galena, pyrite, and marcasite samples were analyzed for trace element compositions using microprobe facilities of the University of Western Ontario. The study of metal zoning in K57, A70, and W17 used diamond drill core assay data provided by Pine Point Mines Limited and the modified MEPS program and facilities of Cominco Limited Data Processing Section in Trail, B. C.

CHAPTER TWO

GEOLOGIC SETTING

Stratigraphy

Pre-Givetian Strata

Three diamond drill holes (G-1, G-4, and W17-3A) extend to the Precambrian basement in the study area (Fig. 2). Pre-Givetian stratigraphy in these holes and for the southern Great Slave Lake region as defined by Norris (1965) from subsurface and outcrop data is summarized in Table 2. The easternmost mineralized zone (N204) in the Pine Point district is about 75 kilometers southwest of the first exposure of Precambrian rocks in the Churchill Province (Fig. 1). The nature of the Precambrian underlying the immediate Pine Point area is little known; G-1 and G-4 penetrate short sections of micaceous quartzite and biotite granodiorite, respectively.

The Middle Ordovician or older Old Fort Island Formation unconformably overlies the Precambrian (Plate 1:1). The Mirage Point Formation transitionally overlies the Old Fort Island Formation or unconformably overlies the Precambrian basement where the basal sandstone unit is absent (Plate 1:2,3). The early Middle Devonian (Eifelian) Chinchaga Formation (Plate 1:4) unconformably overlies the Mirage Point Formation (Norris, 1965).

TABLE 2

Pre-Givetian Stratigraphy, Pine Point Area, N.W.T.

After Norris, 1965

AGE	FORMATION	THICKNESS (meters) W17-3A	G-1	G-4	Regional Variation	DESCRIPTION
Middle Devonian (Eifelian)	Chinchaga	111	92	97	90 - 129?	Light gray to brown anhydrite and gypsum, with minor amounts of limestone, dolostone, limestone and dolostone breccia, salt, and green shale.
UNCONFORMITY						
Upper to Middle Ordovician or older	Mirage Point	70	57	88	17 - 178	Red beds of dolostone; dolomitic silty mudstone breccia, gypsiferous and sandy dolostone, shale, siltstone, anhydrite, gypsum, and salt.
Middle Ordovician or older	Old Fort Island	26+*	0	4.5	0 - 40	White and red, friable, fine to medium grained, quartz sandstone with minor greenish gray siltstone and green shale.
UNCONFORMITY						
Precambrian	Basement					

* Drill hole W17-3A was abandoned in "sand" after penetrating 26 m. of Old Fort Island Formation strata; this interval probably represents most of the true thickness of the basal clastic unit.

Givetian Strata

Generalized Givetian stratigraphic features of the Pine Point area are shown in plan in figure 2 and in section in figure 4; stratigraphic positions of selected ore bodies are illustrated schematically in figure 5. The nomenclature and definitions of Skall (1975) will be closely followed for Givetian facies relationships of the Pine Point barrier complex; figure 6 is a correlation chart for comparison of the stratigraphic terminology of earlier workers in the area. Skall (1975) has shown that previous subdivisions of Givetian stratigraphy are inadequate to represent the highly variable strata of the Pine Point barrier complex. Formational nomenclature has been replaced by facies designated A through P (Table 3); these facies and subfacies are clearly defined by composition, fabric, and paleoecology, although the contacts are generally gradational and interdigitated (Skall, 1975).

The early Givetian Keg River Formation (Facies A) conformably overlies the Eifelian Chinchaga Formation (Plate 1:5). One to three widely distributed thin shale beds, termed E-Shale markers (Campbell, 1950), occur about 35 to 50 meters above the base (Plate 1:6). Middle Givetian strata consist regionally of a narrow carbonate barrier, the Pine Point barrier complex, which separates a carbonate and shale sequence deposited in the deep water environment of the Mackenzie Basin from extensive back-reef evaporite deposits of the Elk Point Basin (Fig. 7). The Pine Point Group has been defined to include the middle Givetian strata (Facies B through K) which form integral parts of the barrier complex (Skall, 1975). It includes the Sulphur Point Formation,

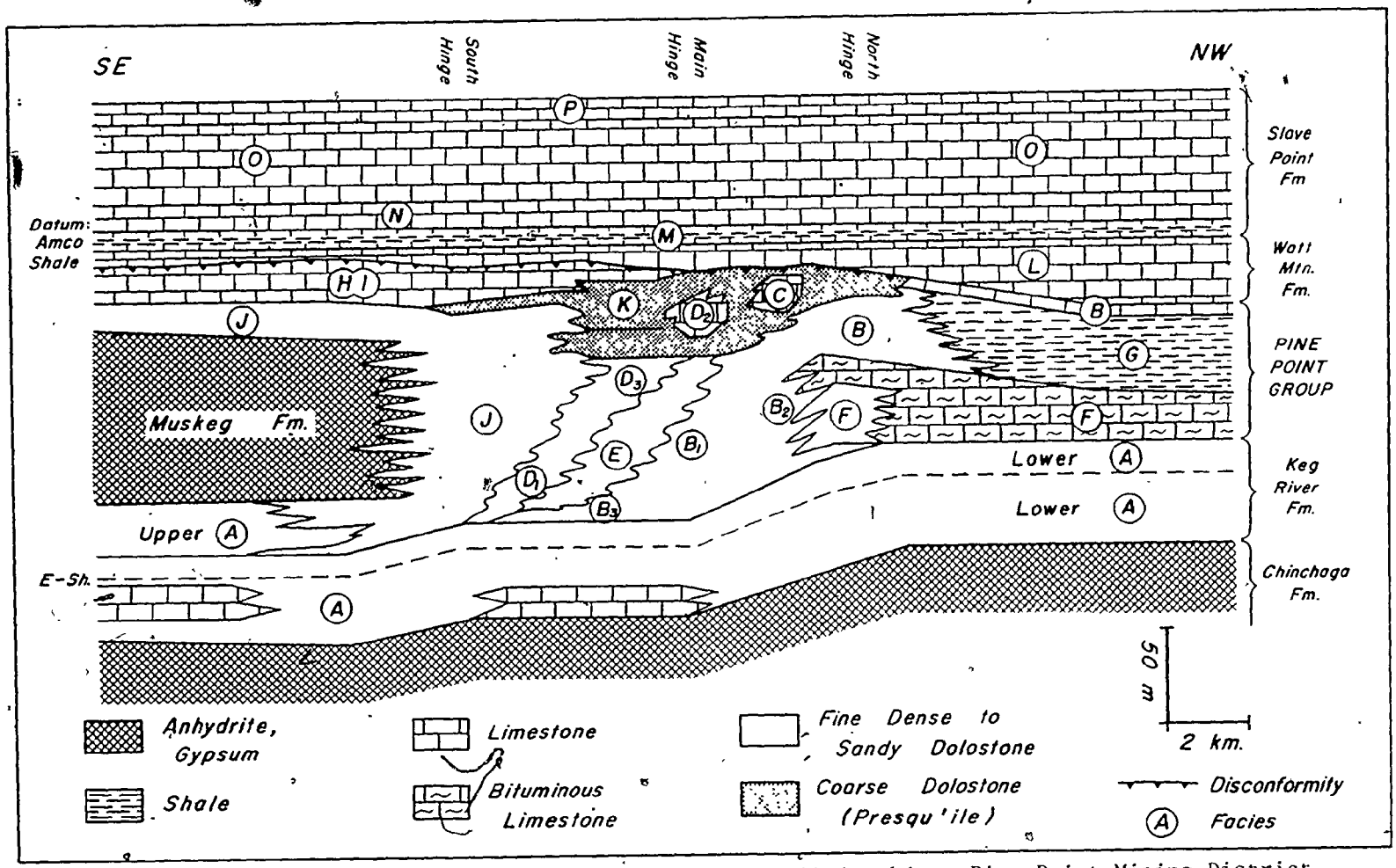

Fig. 4. Generalized Middle Devonian Stratigraphic Relationships, Pine Point Mining District
Modified after Skall (1975) and Adams (1975)

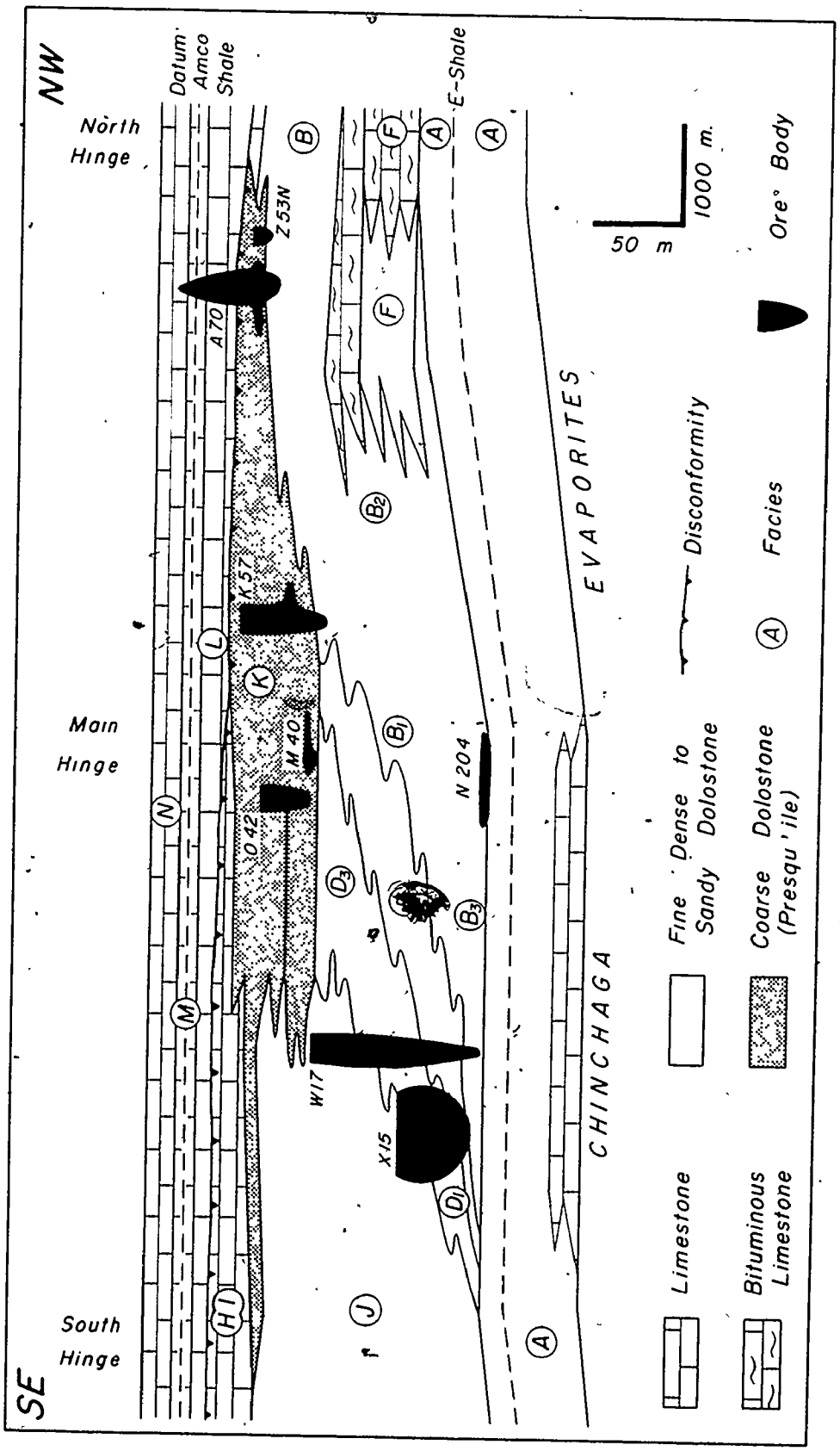

Fig. 5. Cross Section of Pine Point Barrier Complex showing Stratigraphic Positions of Selected Ore Bodies

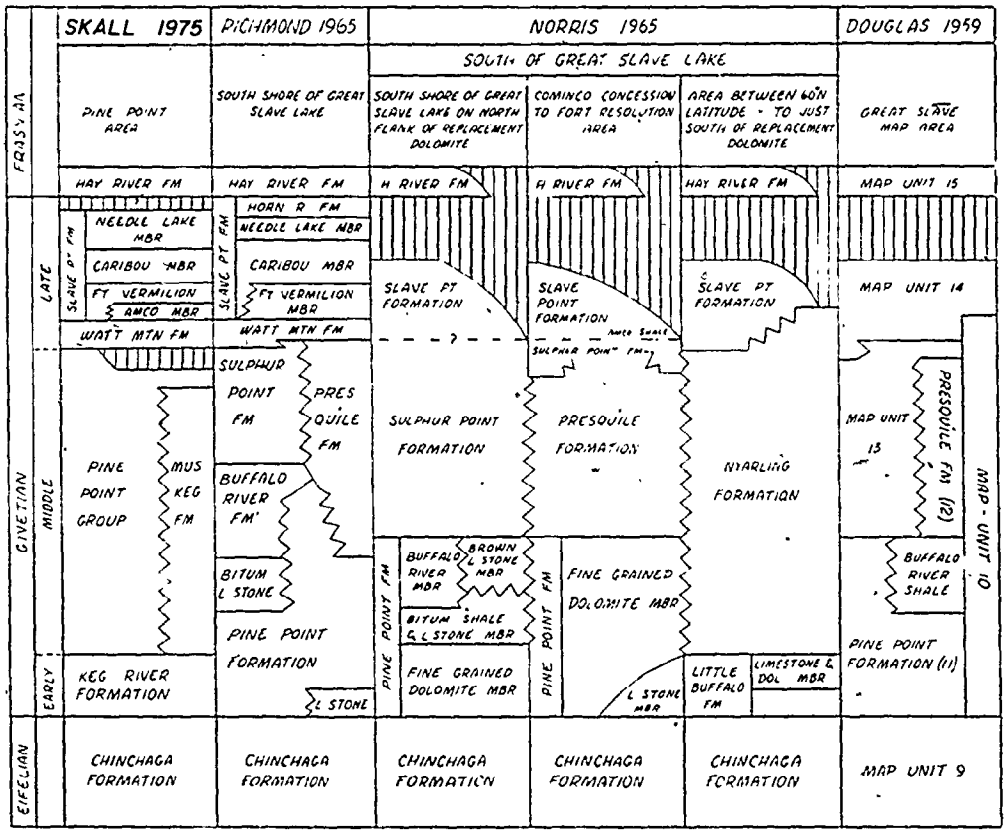

Fig. 6. Middle Devonian Stratigraphic Correlations,

Southern Great Slave Lake Area

Modified after Skall (1975)

Table 3

Givetian Stratigraphy, Pine Point, Northwest Territories

After Skall (1975) and Adams (1975)

AGE	FORMATION	FACIES	MAXIMUM THICKNESS (METERS)	DESCRIPTION	FAUNA*	DEPOSITIONAL ENVIRONMENT
LATE GIVETIAN	SLAVE POINT	P	12	Limestone, dark brown, dense micrite, slightly argillaceous, intraclasts common	Massive corals and stromatoporoids (+++), Amphipora (+), thin-shelled brachiopods (+), Stachyodes (+), crinoids (++)	Deep Marine Platform
		O	50	Limestone, light to dark brown, micrite or sand, large intraclasts common, slightly argillaceous to common shaley laminae, burrowed	Massive stromatoporoids (+), Amphipora (+ to +++), thin-shelled brachiopods (++)	Shallow Marine Platform
		N	18	Limestone, often dolomitic, light gray, dense micrite; blotchy bedding, stromatolite, and fenestrate structures common	Amphipora (+), calcispheres (+), Charophyta (+), brachiopods (-), ostracods (-)	Tidal Flat
		M	10	1. Shale, gray to blue-gray, usually calcareous and mottled with disseminated sulfides 2. Limestone or dolostone, light to medium brown, sand or micrite, argillaceous	Crinoids (-), thick-shelled brachiopods (-) Brachiopods (+ to +++), massive stromatoporoids (++), crinoids (+)	Marine Marine Shoal
	WATT MOUNTAIN	L	45	Limestone, may be dolostone or dolomitic; very light gray, light gray, buff, light green gray; micrite with minor sandy beds; laminite, stromatolite, blotchy bedding and fenestrate structures common; minor gypsum; waxy green shale interbeds	Charophyta (+ to ++), calcispheres (+), gastropods (+), ostracods (+), Amphipora (+)	Predominately Tidal Flat, Lacustrine
DISCFM.						

* Faunal Abundance --- Abundant (+++), Common (++), Minor (+), Rare (-)

Table 3 (Continued)

MIDDLE DEVONIAN	PINE POINT GROUP	K	65	Dolostone, buff to light gray, coarse-crystalline, often with large vugs; uniform granular, mottled, zebra, and breccia-moldic textures common; white dolomite may be abundant	Rarely recognizable, variable depending on original lithology	Secondary effect imposed on B,C,D,E,H,I, and J facies
		Muskeg	120	Anhydrite and gypsum, white to light brown, dense; massive, laminated, and nodular bedding; may be interbedded with J facies dolostone		Restricted Evaporitic
		J	145	1. Dolostone, light gray to blue-gray, dense to sucrosic; laminite, blotchy bedding, stromatolite, and fenestrate structures common	Charophyta (+)	Tidal Flat
				2. Dolostone, light to medium brown, sucrosic with intergranular porosity; slightly argillaceous to laminated		Subtidal to Tidal Flat
				3. Dolostone, light brown to buff, sucrosic to sandy with good intergranular porosity; some faint argillaceous wisps	Amphipora (+), corals (+), stromatoporoids (+), brachiopods (+)	Backreef Subtidal
				4. Dolostone, buff to medium brown, sucrosic with some argillaceous wisps, may be vuggy	Amphipora (++ to +++)	Lagoonal
				5. Dolostone, very light gray, dense micrite	Corals (+), dendroid stromatoporoids (+)	Lagoonal
		I	30	Limestone, very light gray, pelleted micrite and sand; fenestrate, laminite, and stromatolite structures common	Amphipora (++ to +++), gastropods (+), corals (+), stromatoporoids (+), Stachyodes (+), brachiopods (+), calcispheres (+)	Backreef Platform Lagoonal and Tidal Flat
		H		Limestone, very light gray, micrite with bioclastic debris	Gastropods (+ to +++), stromatoporoids (++), Stachyodes (++), corals (++), brachiopods (++) Amphipora (+)	Backreef Platform Tidal Flat and Lagoonal
		G	60	Shale, dark gray to blue-gray, fissile, calcareous, disseminated iron sulfides	Thin-shelled brachiopods (-)	Marine Pelagic
		F	35	Limestone, occasionally dolomitic, dark brown to black, dense micrite, very bituminous and argillaceous	Crinoids (+), Tentaculites and Styliolina (+ to +++), thin-shelled brachiopods (+ to +++)	Basinal Deep Marine

Table 3 (Continued)

MIDDLE GIVETIAN	PINE POINT GROUP	E	45	Dolostone, buff to light brown, sucrosic to sandy with good intergranular porosity, often friable; lacks argillaceous material	Stromatoporoids (-), corals (-), thick-shelled brachiopods (-), Amphipora (-)	Forereef
		D	30	1. Dolostone, light brown to buff, sucrosic to sandy matrix with abundant fossils; may have large vugs and good intergranular porosity	Tabular stromatoporoids (++ to +++), massive stromatoporoids (- to ++), Stachyodes (++), dendroid corals (++ to +++), Alveolites (+)	Organic Barrier Reef in Part
				2. Limestone, very light gray, skeletal sand and clasts cemented by sparry calcite	Massive stromatoporoids (++ to +++), Stachyodes (++ to +++), massive corals (++), thick-shelled brachiopods (++), gastropods (++) cephalopods (-)	
				3. Dolostone, buff to blue-gray, dense, fragmental (often vague due to diagenetic modifications)	Massive and dendroid stromatoporoids (+++), tabular stromatoporoids (+ to ++), dendroid corals (+ to ++)	
		C	20	Limestone, buff to very light gray, micrite and bioclastic sand; lacks argillaceous material	Crinoids (+ to +++), thick-shelled brachiopods (++ to +++), corals (+), dendroid and massive stromatoporoids (+)	Shallow Forereef
		B	60	1. Dolostone, rarely limestone, light to medium gray-brown, sandy to sucrosic, slightly argillaceous	Crinoids (+ to ++), dendroid corals (+ to ++)	Offreef Marine
				2. Dolostone, rarely limestone, medium to dark gray-brown to black, dense to sucrosic, very argillaceous, common chert nodules and secondary silicification	Thin-shelled brachiopods (+ to +++), crinoids (++ to +++), dendroid corals (+ to ++)	
				3. Dolostone, light to medium brown, sandy to dense matrix with zones of good intergranular porosity; many large vugs after leached fossils	Massive stromatoporoids (+ to +++), crinoids (+), brachiopods (+)	Offreef to Shallow Platform
EARLY GIVETIAN	KEG RIVER	A	70	Dolostone and limestone, medium to dark brown, dense to sucrosic, varying amounts of argillaceous and carbonaceous wisps, minor chert nodules; E-shale marker beds (1 to 3) occur 35 to 50 meters above base	Crinoids (+ to +++), brachiopods (+ to ++), gastropods (+), tabular stromatoporoids (+), cephalopods (-)	Marine to Shallow Platform

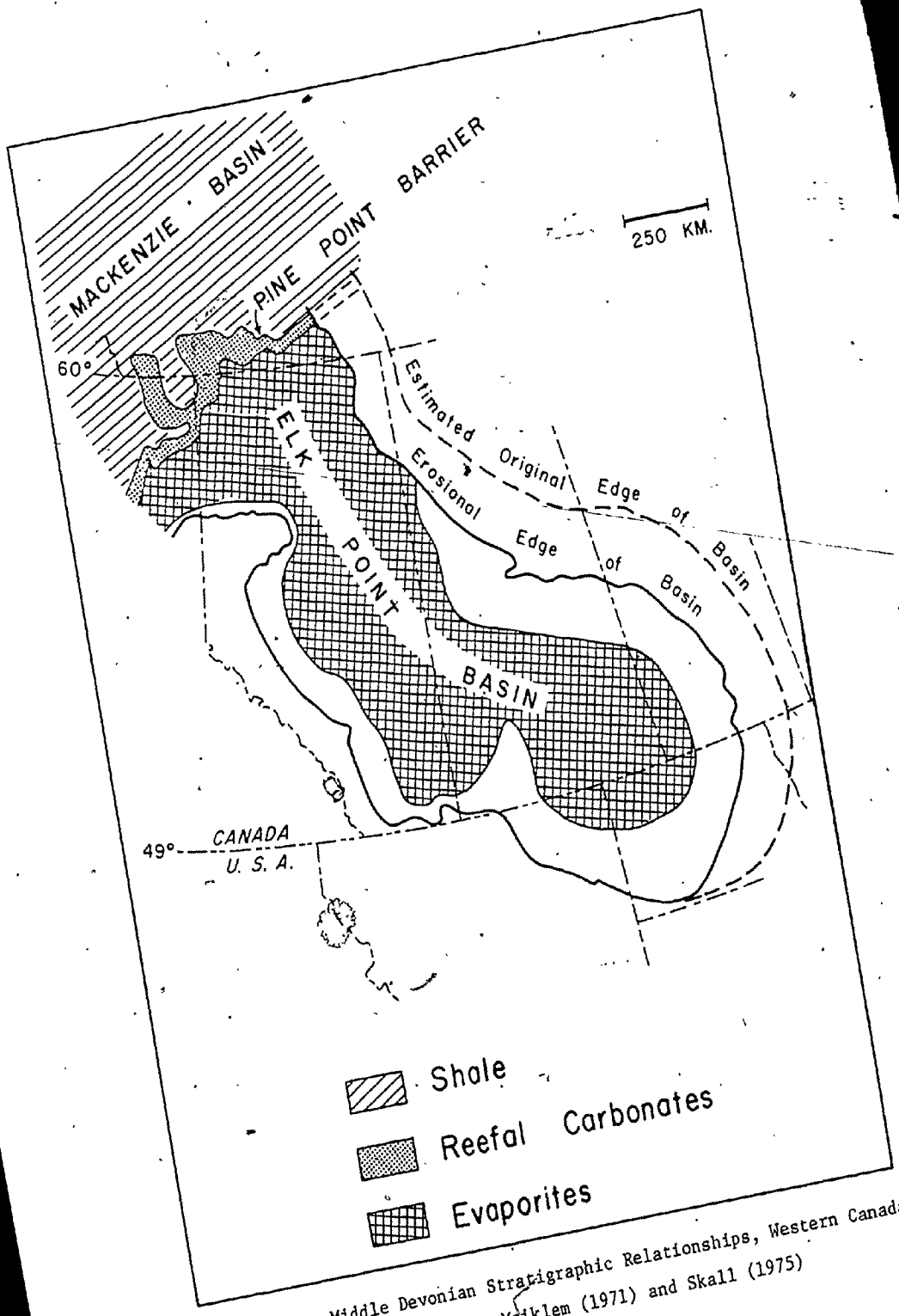

Fig. 7. Middle Devonian Stratigraphic Relationships, Western Canada
Modified after Meiklem (1971) and Skall (1975)

the Presqu'ile Formation, and most of the Pine Point Formation of Norris (1965). The lower part of the barrier (Fig. 4) consists largely of the fine-crystalline dolostones of Facies B (Off-reef), D (Organic Barrier), E (Fore-reef), and J (Back-reef) and of the bituminous limestones of Facies F (Marine); the evaporite strata of the Muskeg Formation are, in part, lateral equivalents of these units. The upper part of the barrier (Fig. 4) consists of limestones of Facies B, C (Fore-reef), D, and H and I (Back-reef), the coarse-crystalline dolostone of Facies K developed from these units, and the Buffalo River Shale of Facies G (Marine). A partial disconformity separates the upper barrier from the late Givetian Watt Mountain Formation (Facies L). The Slave Point Formation (Facies M through P) conformably overlies Facies L and is overlain by the Upper Devonian (Frasnian) Hay River Shale. Facies M contains a shale member, termed the Amco Shale, which can be used as a stratigraphic marker in conjunction with the E-Shales to document development of the Pine Point barrier complex. The Givetian lithologies of the Pine Point area are illustrated in Plates 1 through 6, and the reader is referred to the excellent work of Skall (1975) for details of stratigraphic relationships among the facies.

Structural Evolution in the Pine Point Area

Pre-Givetian Tectonics

The fault zone trending N 45° E can be traced for over 500 kilometers in Precambrian rocks of the Churchill Province of the

Canadian Shield before it is covered by Paleozoic rocks northeast of Pine Point (Fig. 1); a similar structural trend is present along its projection in the subsurface of northeast British Columbia (Sikabonyi and Rogers, 1959). This trend marks a major zone of prolonged tectonic disturbance which first became active in early Proterozoic time. Detailed sedimentologic and structural investigations by Hoffman (1969) have revealed that the Proterozoic succession in the East Arm of Great Slave Lake was deposited in a long-lived, deeply subsiding linear trough, and Hoffman et al. (1974) have interpreted the zone to be an aulacogen. It is not known how far this feature extends to the west of the exposed Precambrian rocks under Phanerozoic cover and the Great Slave Lake. Hoffman et al. (1974) suggest that aulacogens are especially susceptible to reactivation and may control sedimentation even after long periods of dormancy.

Development of the Pine Point Barrier Complex

The detailed stratigraphic analysis of Skall (1975) has permitted documentation of the development of the carbonate sediments of the Pine Point barrier (Fig. 8). Following deposition of the platform carbonates of the Keg River Formation (Facies A), gentle tectonic arching of the area between early and middle Givetian was responsible for establishment of shoal conditions and initiation of barrier development. During this first stage (Fig. 8A), the depositional environments of the Organic Barrier Facies (D), the Clean Arenite Facies (E), the South Flank Facies (J), and probably the Tentaculites Facies (F) came into existence (Skall, 1975). The

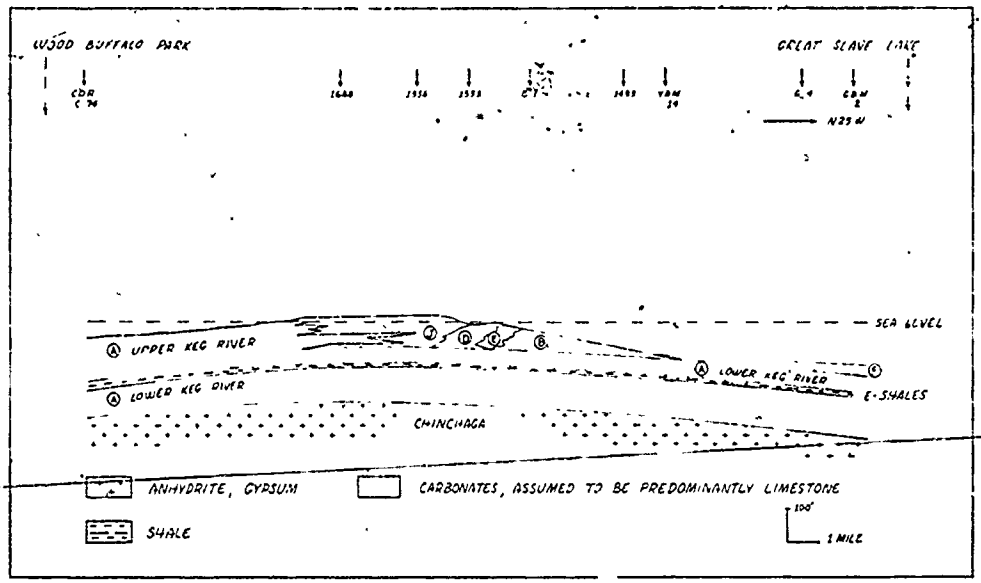

FIG. 8A Initiation of the barrier at early to middle Givetian.

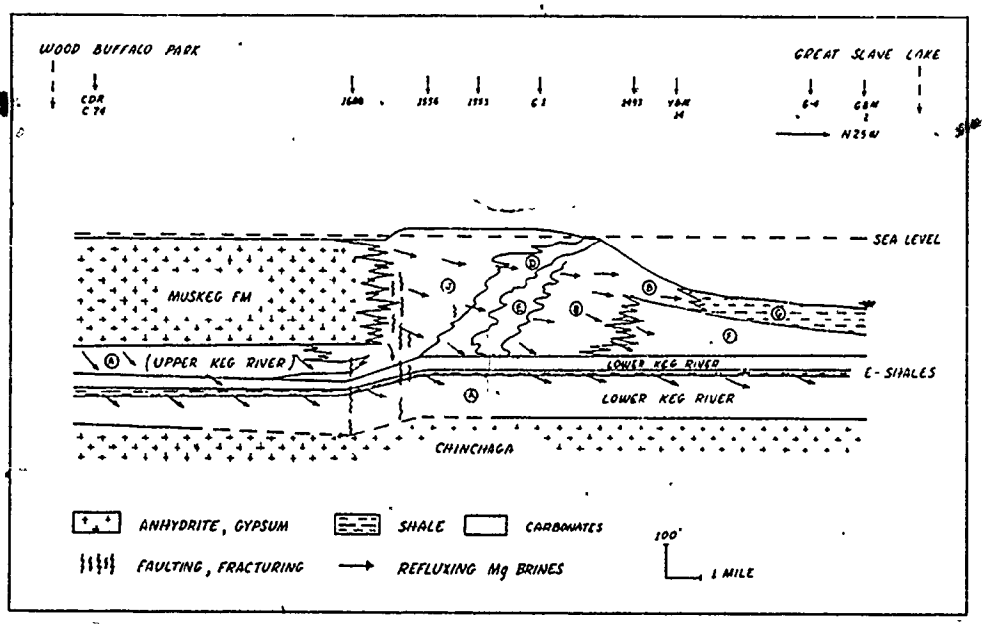

FIG. 8B Higher rate of subsidence in the south causes South Hinge and precipitation of Muskeg evaporites during middle Givetian.

Fig. 8. Development of the Pine Point Barrier Complex
From Skall (1975)

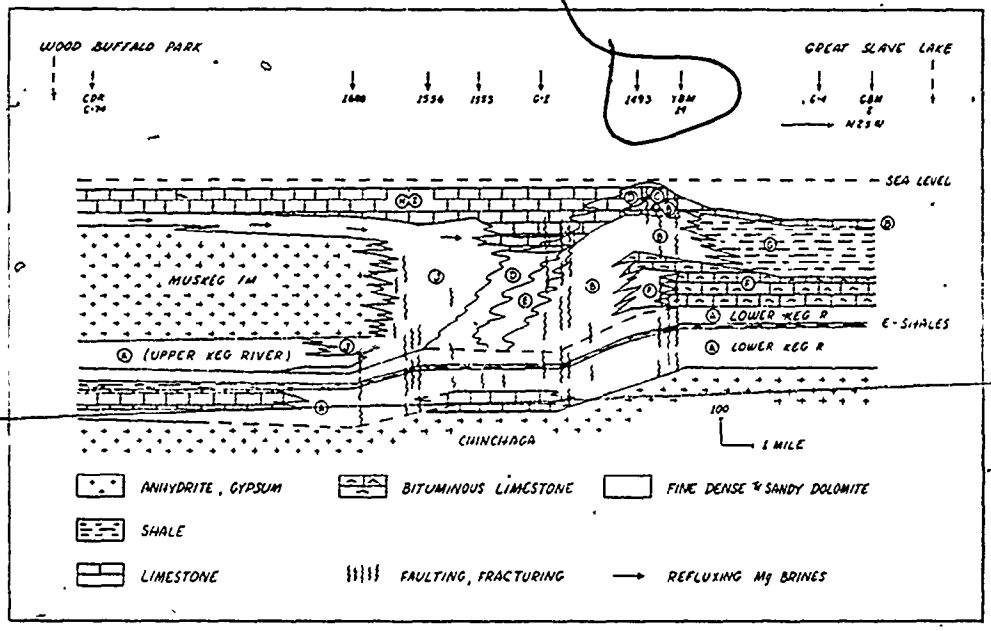

FIG. 8C Main and North Hinge maintain a higher rate of subsidence in the south but terminate the precipitation of evaporites in favor of subtidal back-reef deposits during the late middle Givetian.

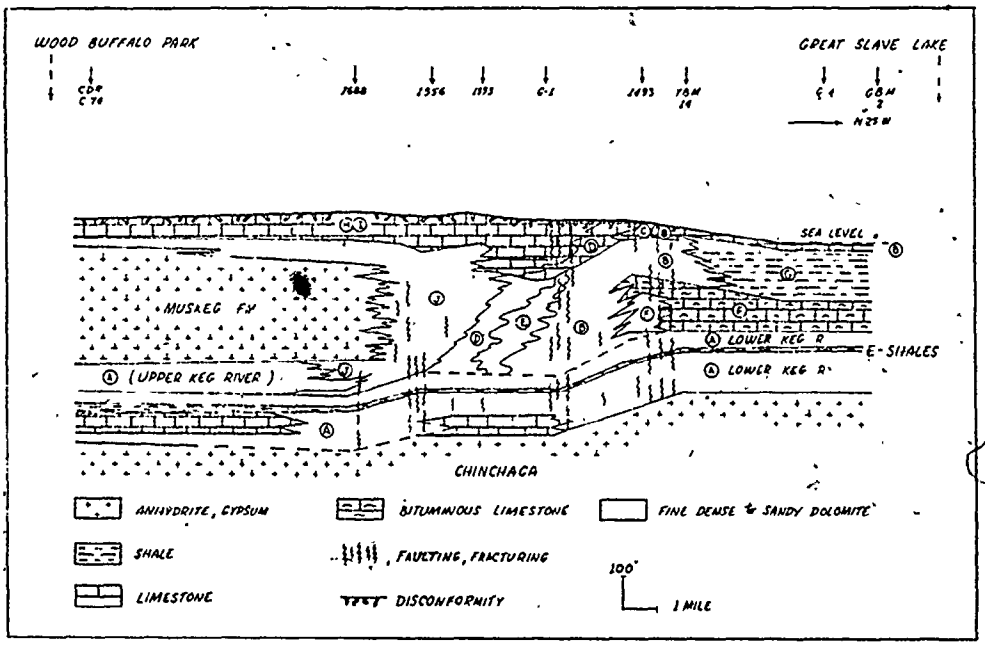

FIG. 8D Marine regression and karst development between middle and late Givetian.

Fig. 8 (Continued)

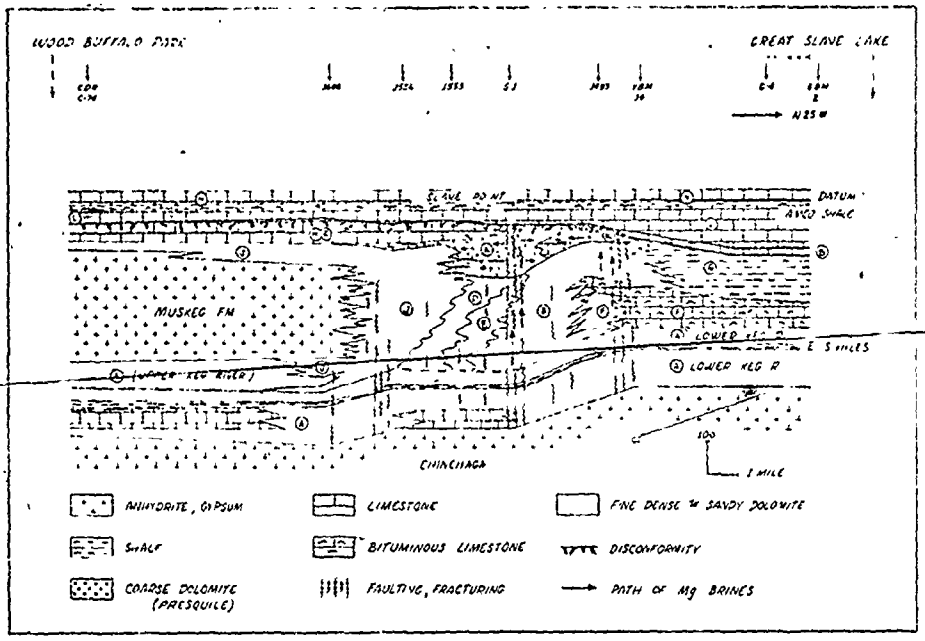

FIG 8E Alteration of vulnerable limestone to coarse Presqu'ile dolomite during post-(?) Givetian.

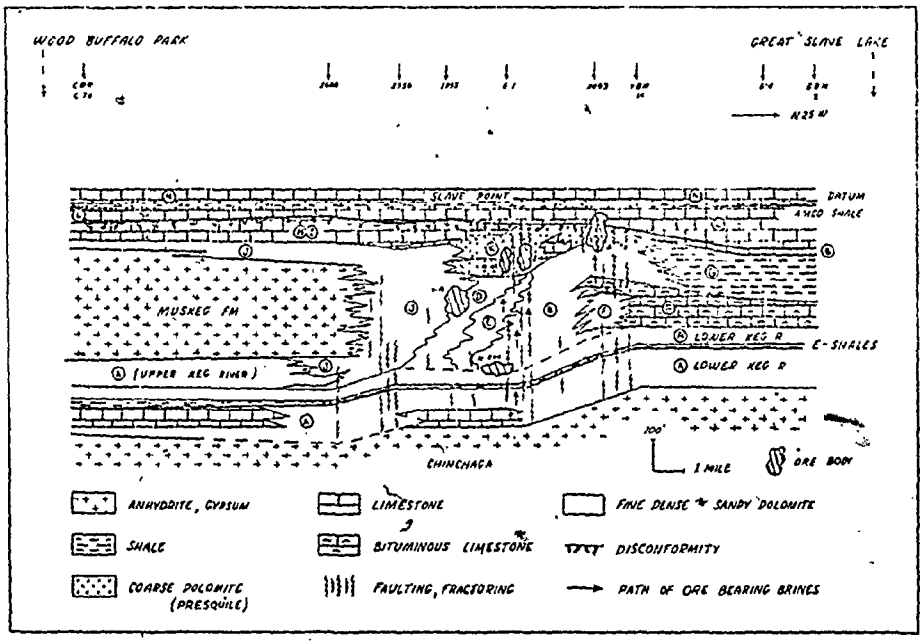

FIG. 8F Post-Middle Devonian emplacement of sulfides.

Fig. 8 (Continued)

barrier apparently emerged hundreds of kilometers from the nearest coast and exerted only minor influence on regional sedimentation during initial development. Marine conditions were maintained on both sides of the barrier (Skall, 1975). With additional tectonic adjustments and concomitant stabilization of the organic framework of the barrier, more restricted sedimentary environments were created.

The sudden increase in thickness of sediments between the Amco and E-Shales in the southern part of the Pine Point area (Fig. 2 and 4) is interpreted to be the result of tectonic adjustments along what is referred to as the South Hinge (Skall, 1975). This subtle tectonic movement caused a higher rate of subsidence to the south and resulted in the establishment and maintenance of restricted conditions which promoted precipitation of calcium sulfates in vast evaporate pans in the back-reef area. The barrier became firmly established during this time and was effectively separated from the evaporite area by the extensive tidal flat zone of the South Flank Facies (Fig. 8B). Precipitation of evaporites continued as long as the higher rate of subsidence was maintained in the south and resulted in the deposition of 120 meters of interbedded evaporite and dolostone strata of the Muskeg Formation. Displacement along the South Hinge amounted to only 20 meters over a prolonged period of time but was responsible for the rapid facies change between the South Flank Facies and the Muskeg Formation.

While evaporites were being deposited south of the South Hinge, the barrier continued to grow on the more stable north slope. The Organic Barrier Facies (D) grew seaward in time over its own fore-reef deposits because of the very slow rate of subsidence (Fig. 8B). Skall

(1975) recognized that during its total development, the barrier migrated horizontally about ten kilometers and climbed vertically about 165 meters. Therefore the barrier units represent diachronous development and form an angle between 1° and 2° with the time units of the Amco and E-Shales. Intricate facies relationships are the result of sporadic barrier growth, presumably due to minor sea-level fluctuations. The Clean Arenite Facies (E) continued to accumulate from the diminution of skeletal material in the fore-reef area. Further downslope the skeletal debris became gradually mixed with argillaceous material and formed the Off-Reef Facies (B). Facies B graded basinward into the Tentaculites Facies (F); with time Facies F was overlain and eventually replaced by the Buffalo River Facies (G). During this early stage of barrier development, the limestones were converted to fine dense to sandy dolostones (Skall, 1975). Maiklem (1971) and Bebout and Maiklem (1973) present evidence for subaerial exposure during early development of the Middle Devonian barrier carbonates in the Elk Point Basin. Although differences in stratigraphic nomenclature and area of study between these and the work of Skall (1975) make exact correlations difficult, it appears that this time period is approximately that marked by termination of early development of the barrier and cessation of evaporite deposition in the Pine Point area. Skall (1975) does not recognize evidence for subaerial exposure at this time, but sedimentation at this point was dominated by the supratidal deposits of the South Flank Facies (Fig. 8B). Ephemeral exposure of the barrier complex would require only minor sea level fluctuation; evidence for such exposure

may be somewhat masked by later diagenetic effects.

Growth of the barrier was interrupted by a second phase of tectonic adjustments that created the Main and North Hinges and resulted in a marked change in sedimentary facies (Fig. 2 and 8C). Again, the exact time of tectonic adjustment is not known; it occurred after deposition of the E-Shales but prior to deposition of the Watt Mountain Formation. Skall (1975) suggests that the second tectonic phase began at a late stage of barrier development and probably lasted throughout the late middle Givetian. Pre-Amco displacement along the Main and North Hinges was responsible for thinning of the barrier by 45 meters between the E-Shales and Amco markers. A higher rate of subsidence was maintained in the south and now affected the previous tidal flat area as well (Fig. 8C). Evaporite precipitation was terminated, and tidal flat conditions were only occasionally affected in the back-reef. Instead, the extensive lagoonal deposits of the Gastropod and Amphipora Facies (H and I) dominated the back-reef area. The Organic Barrier Facies was represented by subfacies D-2. The Clean Arenite Facies (E) was replaced by the Shallow Fore-Reef Facies (C), and sedimentation of the Off-Reef Facies (B) and the Buffalo River Facies (G) continued (Skall, 1975). The upper part of the barrier was not affected by the processes that converted the lower barrier lithologies into fine dense to sandy dolostones, and the facies of the upper part of the barrier remained limestones (Fig. 8C).

Growth of the Pine Point barrier was terminated by marine regression that resulted in a partial disconformity and the development of a karst surface. Subaerial exposure and diagenesis affected the

topographically higher parts of the barrier (Facies C, D. H, and I), but shallow-water sedimentation continued in the lower-lying off-reef area (Facies B) (Fig. 8D). Skall (1975) reconstructed the post-erosional topography of the barrier using the overlying Amco Shale as the datum. The higher areas of the barrier are within 12 meters of this marker, but the Off-Reef Facies is only within 42 meters. Therefore, most of the barrier was at least 30 meters above sea level and was probably more, for it cannot be determined how much of the barrier was eroded during this time (Fig. 8D). The erosional period has been timed by ostracod data to mark the boundary between the middle and late Givetian (Skall, 1975).

Following the erosional period, the late Givetian Watt Mountain Formation (Facies L) was deposited during initial marine transgression (Fig. 8E). The irregular surface on the eroded barrier and the sporadic nature of marine encroachment resulted in the several ephemeral shallow water depositional environments that are represented by the varied lithologies of Facies L. Wiley (1970) recognized five phases of marine transgression separated by periods of minor regression. Marine transgression enveloped the eroded barrier from the north; basinward the Watt Mountain Formation is thicker and conformably overlies the Off-Reef Facies B (Wiley, 1970). Facies M was the result of short-lived, deepening marine conditions; this unit was followed by the tidal flat sedimentation of Facies N. Facies O and P and the Hay River Shale reflect slow but steady increase in subsidence which was prevalent over the entire Pine Point area (Skall, 1975).

Therefore, the subtle tectonic adjustments along a N 65° E

trend were responsible for pronounced facies development of the Pine Point barrier complex during middle Givetian time. Displacements along the South, Main, and North Hinge zones were compensated for by faulting in consolidated strata, slumping of unconsolidated sediments, and shifts in depositional environments. The South Hinge coincides with the northern-most occurrence of evaporites of the Muskeg Formation, and the Main Hinge marks the northern-most extension of the C-horizon. The North Hinge is slightly south and parallel to the southern limit of the Buffalo River Facies (Fig. 2 and 4). Middle Devonian faulting and fracturing is concentrated along the hinge zones but is not restricted to them (Skall, 1975). Numerous gentle folds trending parallel to the hinge zones are also present. Although successful exploration of the Pine Point district was based on the concept of relationship of mineralization to basement faults projected from the East Arm of Great Slave Lake, Norris (1965) pointed out that the N 65° E structures do not parallel the trace of the basement faults on aeromagnetic data (Fig. 2) and suggested that the two trends are tectonically unrelated. Although both sets of structures are tensional features, the exact relationship between basement faults and the Middle Devonian tectonic adjustments must be regarded as uncertain.

Post-Devonian Tectonics

Little is known about post-Devonian tectonics in the southern Great Slave Lake area largely because of the absence of late Paleozoic and younger strata in most of the region. Skall (1969) has recognized faults with post-Amco displacement in the Pine Point area. Late

Paleozoic and Cretaceous strata are preserved in some areas west of Great Slave Lake (De Wit et al., 1973) and probably once extended much further to the east of the present outcrop areas. De Wit et al. (1973) feel that the most important uplifts in the region took place during late Paleozoic and early Mesozoic and during Late Cretaceous and Tertiary (?). These tectonic movements may have caused further displacement along older fault zones and are responsible for the present southwesterly dip of the Pine Point barrier complex.

CHAPTER THREE

CARBONATE DIAGENESIS AND DEVELOPMENT OF SULFIDE-HOSTING STRUCTURES

Introduction

Diagenesis is used here in the sense of Murray and Pray (1965) to include ". . . those natural changes which occur in sediments or sedimentary rocks between the time of initial deposition and the time--if ever--when the changes created by elevated temperature, or pressure, or by other conditions can be considered to have crossed the threshold into the realm of metamorphism." The boundary between diagenesis and low-grade metamorphism is not well defined as seen at Pine Point where late-stage dolomitization has been considered by some to be a metamorphic effect (Campbell, 1966). Others have considered all processes that have affected the Pine Point barrier, including sulfide mineralization, to be within the realm of diagenesis (Jackson and Beales, 1967; Dunsmore, 1973). The diagenetic approach will be followed in this study, although the economic importance of the lead and zinc sulfides merits separate discussion.

A carbonate rock is the end product of a complex history of sedimentation, diagenetic processes, and sequence of diagenetic modification (Matthews, 1974). An exhaustive examination of diagenesis is not possible within the purposes and physical limits of this study, but some useful information can be synthesized from existing information

on Pine Point geology by comparison with analogous situations in other areas and by utilization of recent geochemical studies of diagenesis. Dolomitization and karstification are major aspects of carbonate diagenesis at Pine Point which were of great importance in the preparation of the fluid-transporting and sulfide-hosting structures.

Dolomitization

General

Although recent geochemical studies and documentation of occurrences of modern dolostones have contributed greatly toward solving the "dolomite problem," the origin of thick sequences of ancient dolostones has not been resolved. Also, it is common for several types of interbedded dolostone units to occur in a stratigraphic section; these dolostones have been referred to as primary, syngenetic, supratidal, early diagenetic, late diagenetic, epigenetic, replacement, recrystalline, secondary, and many other equally indefinite and, therefore, unsatisfactory terms. It has been generally accepted that, although present-day sea water is supersaturated with respect to dolomite, dolomite apparently does not precipitate directly because of kinetic effects (Füchtbauer, 1974). This chemical restriction together with stratigraphic relationships and studies of modern carbonate sedimentation indicates that bedded dolostones originate by introduction of Mg^{2+} into pre-existing calcium carbonate sediments or rocks. The most obvious requirement for dolomitization is a mechanism capable of supplying sufficient magnesium to account for the volume of

the various generations of dolostone that are apparent from field relationships. The basic cause for disagreement concerns the origin, nature, and timing of the solutions responsible for creating these various types of dolostone. An understanding of the geologic history of the Middle Devonian strata in the Pine Point area, particularly that of the coarse-crystalline Presqu'ile Dolostone, may contribute greatly to the general knowledge of dolomitization of ancient carbonate rocks.

Dolomitization of the Pine Point Barrier Complex

A comparison of the descriptive terminology of Fritz and Jackson (1972) and Skall (1975) for the various dolostone types in the Pine Point area is presented as Table 4. The classification of Fritz and Jackson (1972) appears to be the more acceptable because it is based on detailed petrographic, isotopic, and geochemical investigations of samples for which stratigraphic relationships had been previously determined. Their work largely concerned the Presqu'ile Dolostone (Facies K) and the scattered dolostone units in the Watt Mountain and Slave Point Formations. Detailed geochemical data are not available for the extensive dolostones of the Pine Point Group, and it may be incorrect to assume that the data for the upper dolostones apply also to the lower units. Although the depositional environments of the upper dolostones were similar to those of the Facies J units, extensive contemporaneous evaporite strata are not associated with the upper dolostones, and many of the upper tidal flat units remain as limestones in contrast with the completely dolomitized Facies J. Also, organic

TABLE 4

Types of Dolostones, Middle Devonian, Pine Point area, Northwest Territories

Reference	Units Considered (Revised Terminology)	Method of Division	Divisions			
			$<20\mu$	$20-50\mu$	$50-150\mu$	$\gg 200\mu$
Fritz and Jackson (1972)	Mostly K,L,M,N	Stratigraphic/ Petrographic	Group I	Group II	Group III	Group IV
		Isotopic/ Geochemical	high $CaCO_3$, high Na,Sr, "clay"	low Na, Sr	low Na, Sr, "clay"	
Skall (1975)	A through N	Stratigraphic relationships and field petrology	Fine-crystalline (dense to sandy)			Coarse-crystalline
This Study	B through K	Stratigraphic and petrographic relationships	Fine-crystalline Type I		Type II	Coarse-crystalline Type III

barrier and associated lithologies are not present locally in the Watt Mountain and Slave Point Formations which would be comparable to the dolomitized Facies D, E, and B of the Pine Point Group. Therefore, the scattered dolostones of the Watt Mountain and Slave Point Formations may not completely represent the conditions responsible for the dolostones of the lower Pine Point Group. The differences between the upper and lower fine-crystalline dolostones may be in degree rather than process, but for the purposes of this study, descriptive parameters will be used for dolostone division (Table 4). The following discussion will be concerned mainly with the dolostones of the Pine Point Group (Facies B through K) which may be divided into three types (Types I, II, and III) on the basis of stratigraphic relationships and gross petrographic features.

Fine-Crystalline Dolostones

The "fine dense to sandy" dolostones of Skall (1975) may be divided into Types I and II. Type I includes all fine-crystalline dolostones for which field and petrographic relationships suggest that deposition took place in a supratidal to intertidal environment. These dolostones consist of very uniform, very fine-crystalline (generally less than 20 microns), dense rocks with laminite, stromatolite, intraclast, blotchy bedding, and fenestrate structures and without megafossils. Subfacies J-1 and J-2 are probably of this type, and the Group I (Fritz and Jackson, 1972) dolostones of the Watt Mountain and Slave Point Formations probably formed under similar conditions.

Type II includes all fine-crystalline dolostones for which stratigraphic, petrologic, and faunal evidence indicates that these units were deposited as calcium carbonate sediments in a subtidal normal marine to slightly restricted environment. These lithologies generally consist of fine-crystalline (20 to 150 microns), dense to sandy dolostone with varying amounts of coarser skeletal material. The dolostones of facies B-1, B-2, B-3, D-1, D-3, E, J-3, J-4, and J-5 of the Pine Point Group are of this type.

With the exception of a minor amount of Facies B limestone, the Type I and II dolostones in the Pine Point Group have no preserved calcium carbonate precursors (Fig. 4). Thus, it appears that dolomitization was a relatively early process which equally affected lithologies of many differing depositional environments within the barrier complex. Not only are the tidal flat units (Type I) dolomitized, but the subtidal barrier lithologies (Type II) are completely dolomitized as well. This phase of early dolomitization requires a mechanism to supply sufficient Mg^{2+} for conversion of the lower Pine Point Group sediments to dolostone.

Skall (1975) proposed that all of the fine dense to sandy dolostones of the lower Pine Point Group were the result of the migration of dense, high Mg/Ca brines from the vast evaporite pans represented by the Muskeg Formation through the lower barrier (Fig. 8B), the so-called reflux mechanism for dolomitization popularized by Adams and Rhodes (1960). However, Hsu and Siegenthaler (1969) have calculated that the slight difference in density between a hypersaline brine and normal sea water does not furnish the amount of hydrostatic

head necessary to permit effective flow through fine-grained sediments and, therefore, cannot supply sufficient Mg^{2+} for extensive dolomitization. They demonstrated the potential for dynamic flow of sea water by evaporative pumping through carbonate sediments in a coastal plain region where evaporation results in major loss of pore fluids. The supratidal flat acts as a sink for the hydrodynamic system, and the flow direction and source of magnesium by evaporative pumping is exactly opposite that of evaporative refluxing. The experiments of Hsu and Siegenthaler (1969) indicate that evaporative pumping is virtually independent of sediment permeability, in contrast to movement due to density or height differences which is controlled by permeability. In defense of the refluxing mechanism as applied to Pine Point, the objections are largely that reflux cannot account for "extensive" dolomitization, and that it requires precipitation of vast quantities of gypsum (Hsu and Siegenthaler, 1969). Certainly the Elk Point Basin contains enormous amounts of evaporites, and the volume of dolostone in the lower Pine Point Group is not extensive. In the Pine Point area, the barrier is roughly 150 meters in thickness and 16 kilometers in width (Fig. 4).

Maiklem (1971) suggested that diagenesis of the lower Pine Point barrier carbonates was the result of water-level lowering of at least 30 meters by evaporative drawdown within the Elk Point Basin. He documents occurrences of breccia, pisolites, and internal silt which are characteristic of modern vadose diagenetic environments. As mentioned earlier, it is difficult to relate Maiklem's large-scale study to the detailed stratigraphic setting at Pine Point (Skall, 1975),

but it appears that the period of subaerial exposure corresponds to the cessation of tectonic adjustments along the South Hinge (Fig. 8B). No evidence for vadose diagenesis at this time has been recognized in the Pine Point area. In this model, magnesium would be supplied by evaporative pumping of sea water through the barrier where it would mix with meteoric water causing dolomitization of barrier strata.

It is suggested that the very fine-crystalline supratidal and intertidal dolostones (Type I) of Facies J may be the result of dolomitization closely related to its depositional surface. Capillary movements might have been important in concentrating Mg^{2+} as suggested by Fritz and Jackson (1972) because of high sodium contents of Group I dolostones, but periodic flooding of the sabkha by meteoric water might have been the precipitation mechanism (Folk and Land, 1975). Origin of the remaining fine-crystalline dolostones (Type II) is even less well understood. The passage of sea water through the barrier would supply sufficient Mg^{2+} for dolomitization and is hydrologically feasible; mixing with CO_2-rich meteoric water may have occurred. It is not clear whether dolomitization is a single-stage event, as Maiklem (1971) envisages, or perhaps a more-or-less continuous process of evaporative pumping of sea water related to tidal flat and evaporite sedimentation as Hsu and Siegenthaler (1969) propose. The proximity of major contemporaneous evaporite strata, the limited amount of Type II dolostone, and the presence of introduced gypsum within the barrier makes it difficult to eliminate the reflux mechanism. Additional stratigraphic, geochemical, and isotopic data are needed before the nature of the processes responsible for dolomitization of the lower Pine Point barrier complex can be deciphered.

Coarse-Crystalline Dolostone -- Facies K

Skall (1975) defined Facies K (Presqu'ile) as the coarse-crystalline dolostone which occurs between the lower barrier units and the Watt Mountain Formation (Fig. 4). The distribution of the coarse-crystalline dolostone is further restricted to the area between the Hinge Zones and below the post-middle Givetian disconformable surface (Fig. 2 and 4). This lithology consists of dolomite crystals greater than 200 microns in size (Type III), and the unit is a diagenetic facies superimposed on back-reef, reef, and fore-reef strata (Skall, 1975). In contrast to the ubiquitous fine-crystalline dolostones of the lower barrier, the original limestone lithologies are preserved as isolated remnants within the coarse-crystalline dolostone (Plate 5:1-5) and as extensive back-reef strata of Facies H and I (Fig. 4). Contacts between coarse-crystalline dolostone and limestone commonly transect bedding, are irregular, and relatively sharp. Relic depositional textures are preserved locally in the coarse-crystalline dolostone, particularly in the lower units (Plates 4 and 5). White dolomite is a ubiquitous accessory, and its pervasive introduction has obliterated much of the original nature of the upper part of Facies K in some areas (Plate 4). The contact of the coarse-crystalline dolostone with the underlying fine-crystalline dolostones of the lower barrier is commonly abrupt but locally is gradational over a few meters. These relationships indicate that the coarse-crystalline dolostone is distinctly different from the fine-crystalline dolostone and originated by a different mechanism.

Most earlier workers have considered the coarse-crystalline dolostone to be the result of dolomitization of coarse-grained reefal limestones or of recrystallization of fine-crystalline dolostones (Norris, 1965; Campbell, 1967). These explanations appear inadequate. The coarse-crystalline nature of Facies K does not reflect an original coarse-grained sediment because it is not restricted to the reefal facies and because the coarse-grained reefal lithologies of the lower barrier have not been converted to coarse-crystalline dolostone (Skall, 1975). Adjacent to the N42 ore body, beds of Facies I micritic limestone can be traced laterally into coarse crystalline Facies K dolostone (Plate 5:2-4). The extensive recrystallization of fine-crystalline dolostone into Facies K is unlikely because of the thin beds of fine-crystalline Facies J dolostone (C-Horizons) preserved within the coarse-crystalline dolostone. The coarse-crystalline dolostone is not an alteration effect directly related to sulfide mineralization because it is much more extensive than sulfide mineralization, is not associated with the ore bodies (X15, W17, and N204) in the lower barrier, and is not present above the disconformity in those ore bodies that extend into the Watt Mountain Formation.

The problem is to supply enough Mg^{2+} to convert limestone into coarse-crystalline dolostone. Facies K is less extensive than the fine-crystalline dolostones of the lower barrier; in the Pine Point area, it is not more than 13 kilometers in width and attains a maximum thickness of 65 meters along the Main Hinge (Fig. 4).

Both the reflux and evaporative pumping mechanisms can be eliminated as possible methods of generating the coarse-crystalline

dolostone because the evaporitic conditions responsible for the deposition of the Muskeg evaporites and tidal flat lithologies of Facies J had ceased to exist in the Pine Point area by the time of upper barrier sedimentation. Instead, predominantly lagoonal sedimentation resulted in Facies H and I (Fig. 8C), and the existence of bedded evaporites in the upper Pine Point Group cannot be demonstrated. Skall (1975) acknowledged that the distribution of the coarse-crystalline dolostone below the Watt Mountain disconformity suggests an origin related to the erosional surface. He chose to relate its development to post-Givetian circulation of warm, magnesium-rich fluids along the Hinge Zones (Fig. 8E). Skall suggested that the erosional period represented by the disconformity served to increase the permeability of the barrier and that the Watt Mountain shale beds overlying the disconformity restricted the upward migration of dolomitizing fluids. This interpretation is influenced greatly by fluid-inclusion data (Roedder, 1968a) which indicate that the distinctive white dolomite associated with sulfide ore minerals was formed at temperatures of about 90° to 100° C from brines which contained 15 to 20 weight percent total salts, that is, brines similar to those which deposited the sulfides. Not only is the development of the coarse-crystalline dolostone genetically unrelated to sulfide mineralization, but also as Skall (1975) suggests, white dolomite is the product of late alteration primarily of the coarse-crystalline dolostone by fluids of the sulfide-depositing system. In fact, a great deal of the white dolomite may post-date the period of major sulfide deposition. Consequently, there is no evidence to indicate

that relatively hot, strongly saline fluids were responsible for the development of the coarse-crystalline dolostone. Further, the influence of non-saline water in the formation of the coarse-crystalline dolostones is suggested by their sodium contents of generally less than 100 ppm; in contrast, the fine-crystalline dolostones contain as much as 600 ppm Na (Fritz and Jackson, 1972).

The strongest evidence concerning the origin of the coarse-crystalline Facies K dolostone is its distribution below the Watt Mountain disconformity and immediately "landward" of the most "seaward" extent of the partial erosional surface (Fig. 4). The disconformity is not exposed in the Pine Point area, but the abundant drill hole information indicates that the paleo-erosional surface is one of relatively low relief with a characteristic karst topography. Using the Amco shale as datum, regional topography on the karstified barrier can be shown to be gently sloping seaward, generally at less than one meter per kilometer. Carbonate rubble and discontinuous green shale layers commonly mark the surface and probably represent regolith resedimented by the sporadically advancing sea which deposited the late Givetian Watt Mountain Formation (Skall, 1975). A possible modern analogue of the karstified Pine Point barrier with roughly similar geologic, topographic, and hydrologic features is the northern Yucatan Peninsula (Back and Hanshaw, 1970).

The influence of meteoric ground water on dolomitization has received considerable attention in recent literature following the initial hypothesis by Hanshaw et al. (1971). This model is based on the dynamic mixing of ground water and normal marine water which will

produce a mixture with chemical characteristics that may be a more effective diagenetic agent than either of the parent solutions (Runnells, 1969; Badiozamani, 1973; Matthews, 1974; Plummer, 1975). Because most dolomitization involves the intimate dissolution of calcium carbonate followed by precipitation of dolomite, it may be an effective dolomitizing mechanism, particularly for those "late" dolostones which have been created from non-supratidal calcium carbonate strata. Reduction of pore water salinity by CO_2-rich meteoric water would promote the formation of dolostone during the dissolution of aragonite and magnesian calcite if there were sufficient mixing with marine water to provide the required magnesium (Hanshaw et al., 1971). Badiozamani (1973) proposed the term "Dorag dolomitization" for this mechanism and demonstrated the geochemical potential for dolomitization to occur until a mixture containing 30 percent sea water was achieved. Folk and Land (1975) suggested that Mg/Ca ratio and salinity are the major controls over crystallization of dolomite and that dolomite can be formed from solutions with Mg/Ca ratios near the theoretical value of 1:1. Land (1973a, b) promotes present-day mixing of CO_2-rich meteoric water with marine water to account for addition of 14 weight percent dolomite to Pleistocene reefal carbonates of northern Jamaica in a geologically short period of time. He further suggests that the degree of dolomitization is related to the local meteoric hydrologic conditions. Rapid flushing with meteoric water results in sparry calcite cementation without dolomitization, whereas slow mixing over a long period of time creates very coarse-crystalline, pure dolomitic rocks (Land, 1973a).

The diagenetic environments resulting from prolonged subaerial exposure of the Pine Point barrier complex during post-middle Givetian time are shown schematically in figure 9. Of importance to the development of the coarse-crystalline Facies K dolostone is the zone of brackish water resulting from the mixing of fresh meteoric water and normal marine water. The flow lines and configuration of the mixing zone are generalized after Kahout (1960) and show the salt-water intrusion wedge common below most coastal aquifers. The actual size, configuration, and flow patterns were undoubtedly affected by a large number of variables including seasonal changes in meteoric water supply, short and long term climatic changes, tectonic and eustatic sea level adjustments, topography of the erosional surface, and initial and evolved porosity and permeability. The low relief and lack of major surface drainage on the erosional surface and the apparent lack of stratigraphic restrictions to vadose water flow in the upper barrier suggest that the water table was not much above sea level. A representative figure of one meter above mean sea level approximately 10 kilometers from the point of termination of the partial disconformable surface (that is, the middle Givetian "shore") is reasonable in comparison with the analogous modern hydrologic system of the northern Yucatan Peninsula (Back and Hanshaw, 1970). Assuming that the permeability of the upper Pine Point barrier complex was relatively homogeneous during the erosional period, the Ghyben-Herzberg principle can be applied (Back and Hanshaw, 1970). This principle states that for every unit of fresh water above the mean sea level, the thickness of the fresh water lens floating on salt water of ocean water density

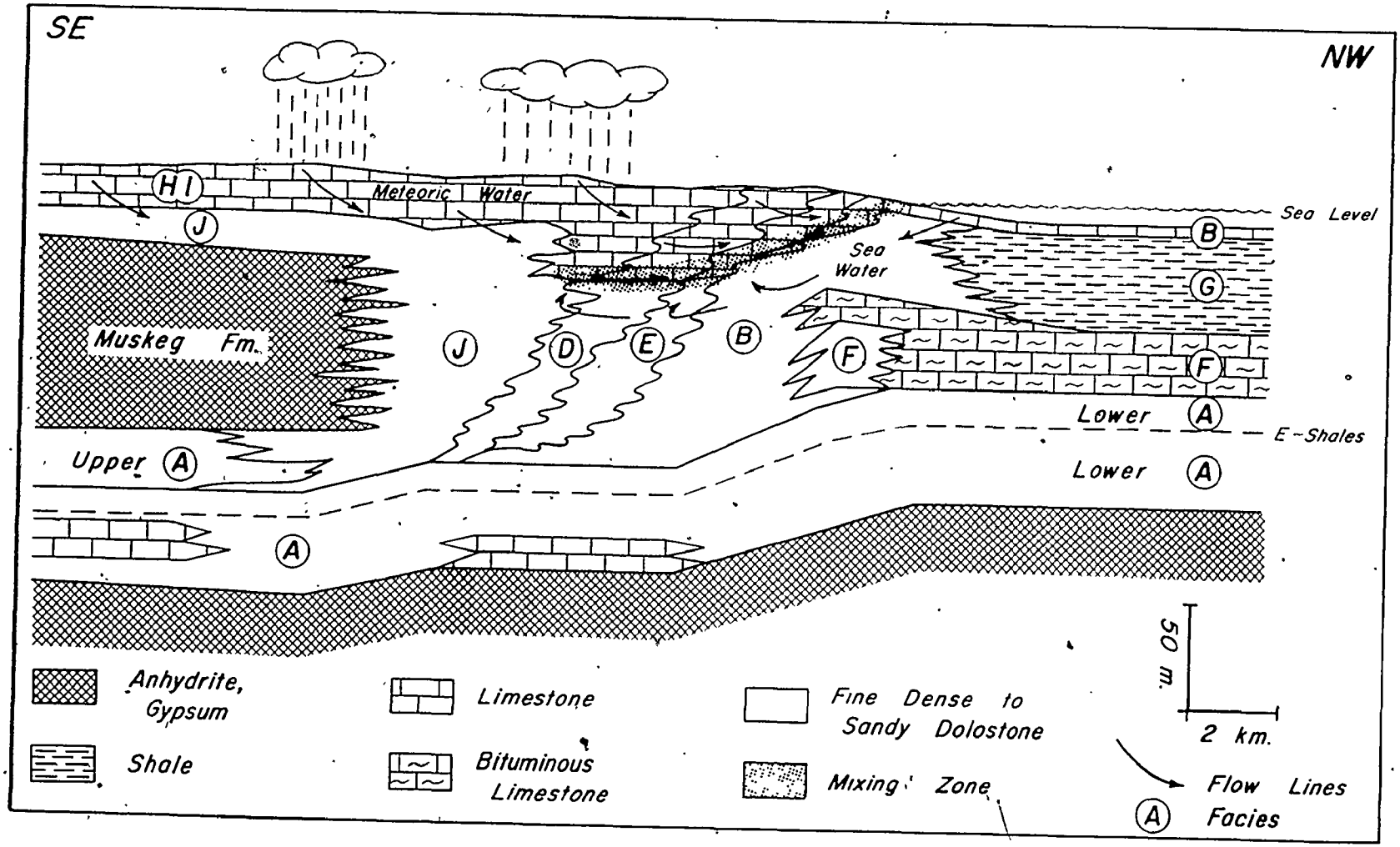

Fig. 9. Generalized Diagenetic Environments, Post-Middle Givetian Erosional Period

is about 40 units. With a hydraulic head of one meter, the fresh water lens would have extended within the upper barrier to a depth of about 40 meters below mean level of the post-middle Givetian sea. A zone of meteoric water and sea water mixing would have existed below this depth and would account for the position of the maximum thickness of coarse-crystalline Facies K dolostone about 10 kilometers "landward" from "shore" and sloping gently upward to mean sea level (Fig. 4 and 9).

The zone of dynamic mixing is capable of concentrating the magnesium required for dolomitization of the upper Pine Point barrier. Most proponents of the mixing model for dolomitization support sea water or hypersaline water as the dominant source of Mg^{2+} (Hanshaw et al., 1971; Badiozamani, 1973; Folk and Land, 1975; Land et al., 1975). An additional source which should be considered is the Mg^{2+} content of the original carbonate sediment. Most modern shallow-water carbonate sediments are composed of aragonite and high-magnesium calcite; in contrast ancient carbonate rocks are composed of low-magnesium calcite and dolomite. A compilation by Milliman (1974) shows that the Mg-calcites in some recent shallow-water limestones contain 15 to 30 mole percent $MgCO_3$; low-Mg calcites in ancient limestones contain less than 4 mole percent $MgCO_3$. Studies of modern carbonate diagenesis in Barbados (Matthews, 1974) and elsewhere (Friedman, 1975) indicate that the mineralogic stabilization of carbonate sediments, that is, conversion from aragonite and high-Mg calcite to low-Mg calcite, occurs in the fresh-water phreatic zone. Because magnesium release undoubtedly was taking place in the meteoric zone overlying the lens of mixed water, this mechanism has the

potential to supply much of the Mg^{2+} required to convert part of the upper barrier to coarse-crystalline dolostone, especially considering the volumetrically much larger amount of high-Mg sediment which must have been affected by fresh-water diagenesis (Fig. 9).

In summary, it is suggested that the development of the coarse-crystalline Facies K dolostone was related to the dynamic mixing of meteoric water with sea water as an integral part of barrier diagenesis during the post-middle Givetian erosional period (Fig. 9). Magnesium required for dolomitization was supplied by sea water and by magnesium expulsion during mineralogic stabilization of upper barrier carbonates in the fresh-water phreatic zone. The mixing zone was probably rather thin at any particular time, but short and long-term fluctuations in sea level, including the sporadic advance of the Watt Mountain sea, resulted in migration of the mixing zone and concomitant dolomitization of the entire area now represented by Facies K (Fig. 4). Slow mixing of CO_2-rich meteoric water with sea water over a long period of time resulted in coarse-crystalline dolostone as each cycle of mixing dissolved calcite and deposited dolomite by enlargement of pre-existing crystals.

It should be emphasized that this model is a greatly simplified version of the actual case; for example, Matthews (1974) provides an excellent summary of the complexities of multiple superimposed diagenetic environments in modern carbonates. In the case of Pine Point, it is difficult to evaluate the possible effects of lesser periods of subaerial exposure earlier than the post-middle Givetian erosional interval on the development of the coarse-crystalline

dolostone; one such period is reflected by a slightly undulating surface with minor truncation of underlying beds and a thin green shale mantle just below the tidal flat C-Horizon in the N38A open pit (first recognized by W. E. Wiley). These ephemeral periods of exposure may have served to increase the overall permeability of the barrier sediments, thus facilitating fluid movement and dolomitization during the post-middle Givetian interval of prolonged subaerial exposure.

Karstification and Development of Sulfide-Hosting Porosity

General

Although Beales and Jackson (1968) and Jackson and Folinsbee (1969) suggested that subaerial exposure and karstification of the Pine Point barrier could have been important in the preparation of the host rock for sulfide concentration, it was not until the work of Skall (1970, 1975) and Wiley (1970) that the existence of the post-middle Givetian, pre-late Givetian partial disconformable surface was documented. To date little information is available concerning the consequences of this period of prolonged emergence, particularly with regard to creation of sulfide-hosting structures. The probable influence of meteoric water in the formation of the vuggy, coarse-crystalline dolostone of Facies K has already been discussed, but dolomitization of upper barrier limestone is only one of several features resulting from subaerial exposure.

Karstification

Surface Configuration

The disconformity is present in the southern and central part of the Pine Point area (Fig. 2 and 6) where the basal late Givetian Watt Mountain Formation, Facies L, overlies the coarse-crystalline dolostone of the Presqu'ile Facies K or the undolomitized upper barrier limestones of Facies C, D-2, H and I. North of the coarse-crystalline dolostone development, a considerably thicker Facies L directly overlies Facies B without apparent disconformity (Skall, 1975). The disconformable contact commonly consists of a zone of green clay and carbonate rock fragments overlying the upper Pine Point Group strata which may contain minor green clay in vugs, fractures, and bedding planes for some distance below the rubble contact. Thickness of the rubble zone is highly variable, apparently depending on the local topography on the disconformable surface, but generally is less than five meters. In the A70 area, a waxy green shale bed as much as four meters thick usually overlies and grades into the rubble zone.

Solution Features

Detailed stratigraphic studies within and around several mineralized zones have revealed the presence of major solution features. These features appear to control the distribution of sulfides and to account for the geometry of the "prismatic" ore bodies with restricted horizontal dimensions relative to vertical extent and of the "tabular" ore bodies with restricted vertical extent relative to the horizontal

dimensions (Skall, 1972). Within many prismatic ore bodies in the upper Pine Point barrier are strata which are not present in standard Facies K sections, even immediately adjacent to the mineralized zones (Plate 7:1). Generally this material is light gray, fine- to coarse-crystalline dolostone which is often friable with good intercrystalline porosity (Plate 7); calcite may occlude much of this porosity. In the following discussion this material will be referred to as detritus. The detritus may be laminated (Plate 7:1, 2, 4) and may contain fragments of green clay and fine-crystalline tidal flat dolostone, particularly in the upper portion (Plate 7:3, 5, 6). Generally these fragments are only a few centimeters in the longest dimension but are occasionally as much as a meter (Plate 7:5).

Although this material is often observable in broken ore in the open pits, the current mining methods at Pine Point seldom permit the study of undisturbed detritus. The most acceptable means of determining the nature, geometry, and significance of the detritus is through a study of drill core from closely spaced holes. Despite poor recovery and limited sample size of cores, disruption of the detritus zones by the introduction of sulfide minerals, and truncation of the upper part of most of these zones by the present-day erosion, a reliable composite description can be developed from a study of drill cores from a number of these detritus zones, combined with observations in the open pits.

Z53N is the most northeasterly mineralized zone within the coarse-crystalline dolostone of Facies K (Presqu'ile) along the North Hinge (Fig. 3). Since this area is near the erosional pinchout of the

Presqu'ile, the coarse-crystalline dolostone is generally less than 15 meters in thickness, and the upper part of the mineralized zone undoubtedly has been eroded. Within the sulfide-bearing zone of Z53N is an irregularly elliptical area (Fig. 10) which contains light gray, fine- to coarse-crystalline, friable dolostone with fragments of green clay and fine-crystalline dolostone. In its current preservation, this detritus zone is about 350 meters in length and 100 meters in width and is surrounded by the standard coarse-crystalline Facies K. It contains a maximum preserved thickness of about 15 meters of detritus, and three areas of increased thickness are indicated by structural contours on the base of the detritus zone (Fig. 10). The detritus occupies a depression overlying Facies B and has steep contacts with Facies K around the margins of the zone (Fig. 11).

A70 is a zone of extensive sulfide concentration within Facies K along the North Hinge about nine kilometers southwest of Z53N (Fig. 3). The middle Givetian stratigraphic sequence has not been truncated by recent erosion in this area. The coarse-crystalline Presqu'ile dolostone reaches a maximum of about 25 meters in thickness but is entirely absent locally; the lower part of Facies K often retains the textural features of Facies B. A northward prograding depositional sequence of fore-reef, reef, and back-reef limestone facies is common away from the zone of maximum coarse-crystalline dolostone development (Figs. 12 and 13); these limestones are interbedded with and laterally equivalent to Facies K. A major elliptical zone of detritus about 400 meters in length and 175 meters in width is surrounded by standard coarse-crystalline Facies K dolostone (Fig. 14). Maximum detritus

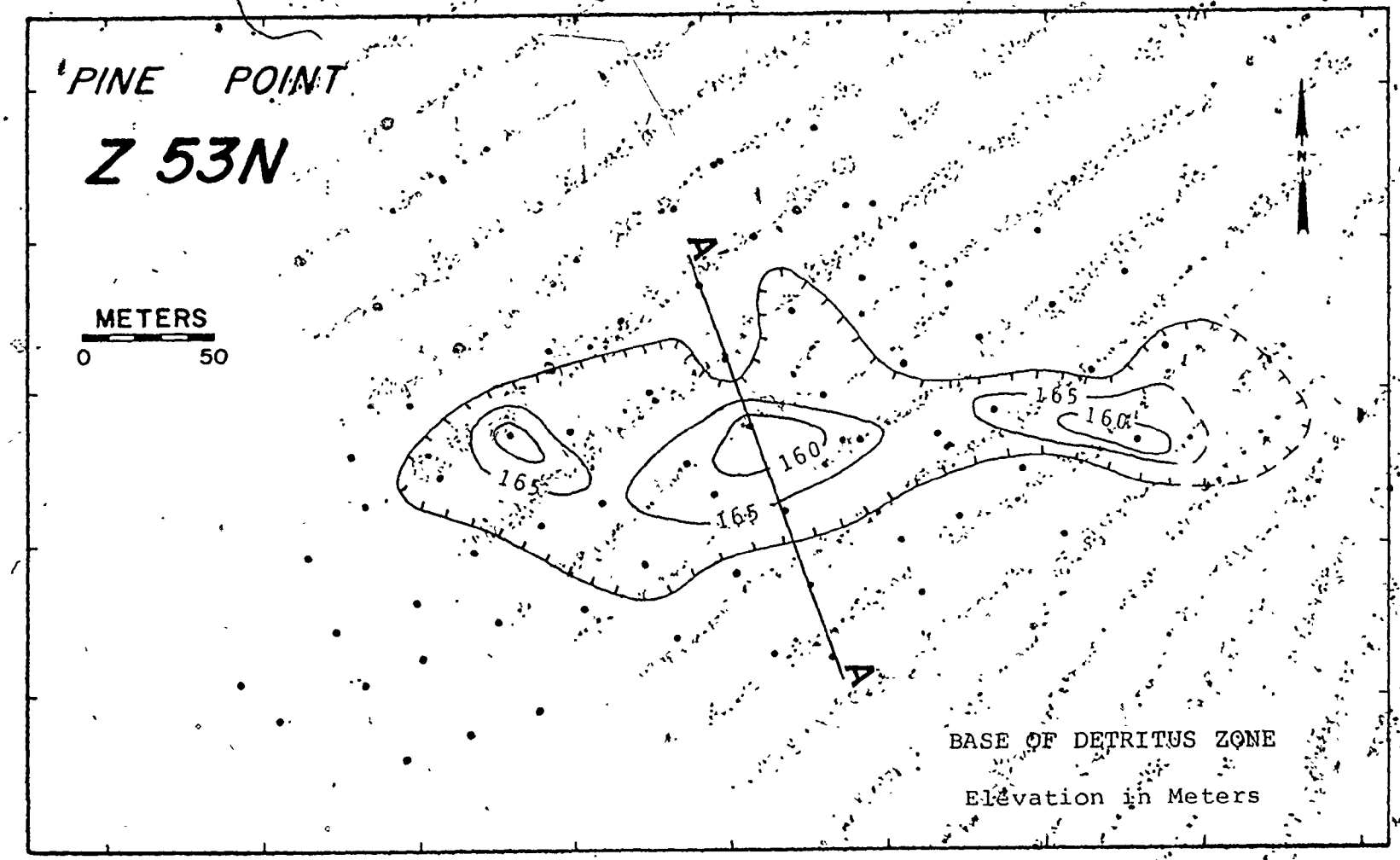

Fig. 10. Structural Contour Map on Base of Detritus Zone, Z53N Area.
Extent of detritus is delineated by hachures; dots indicate location of diamond drill holes.

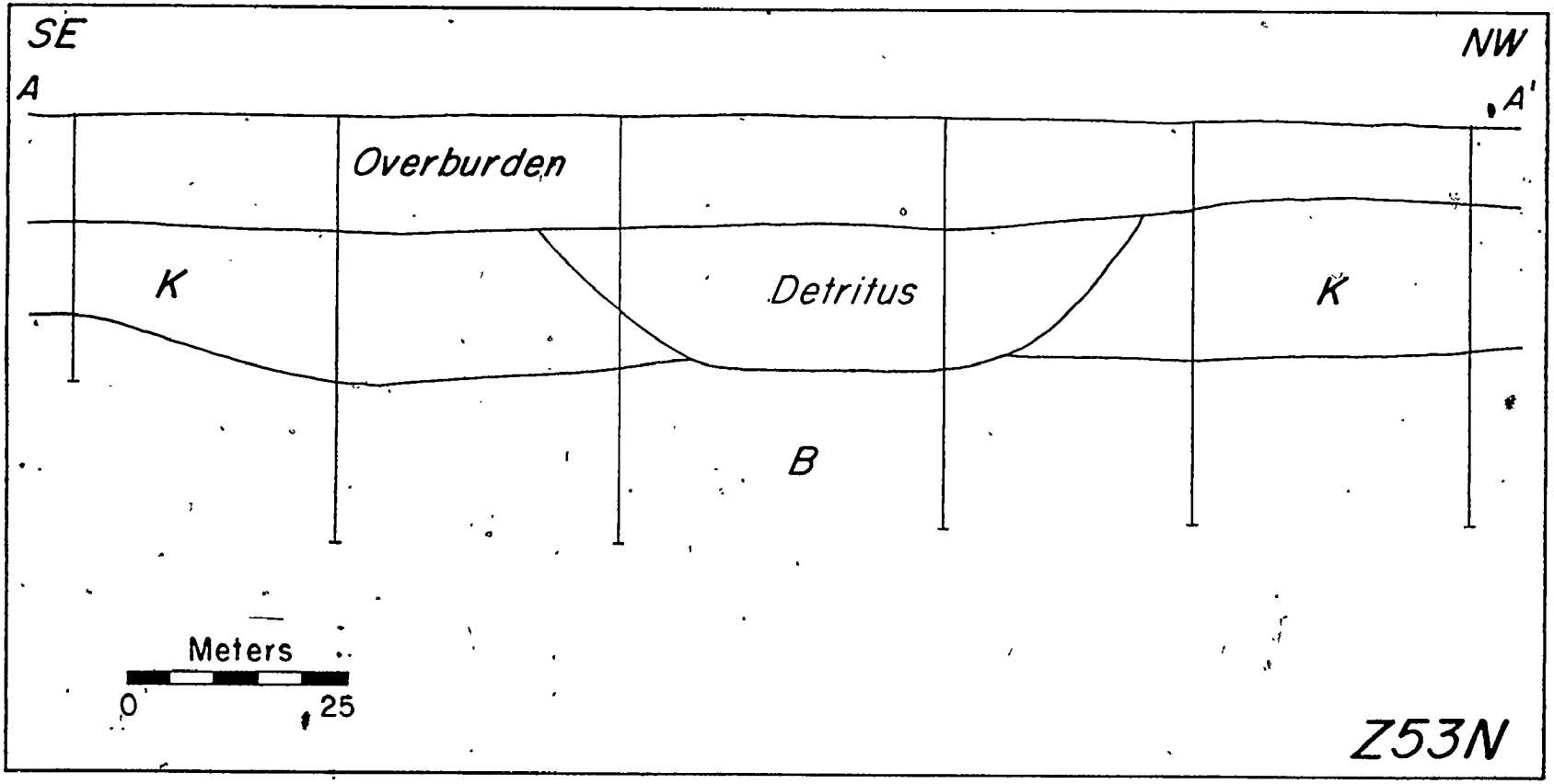

Fig. 11. Geologic Cross Section, Z53N Area.

Vertical lines represent diamond drill holes.

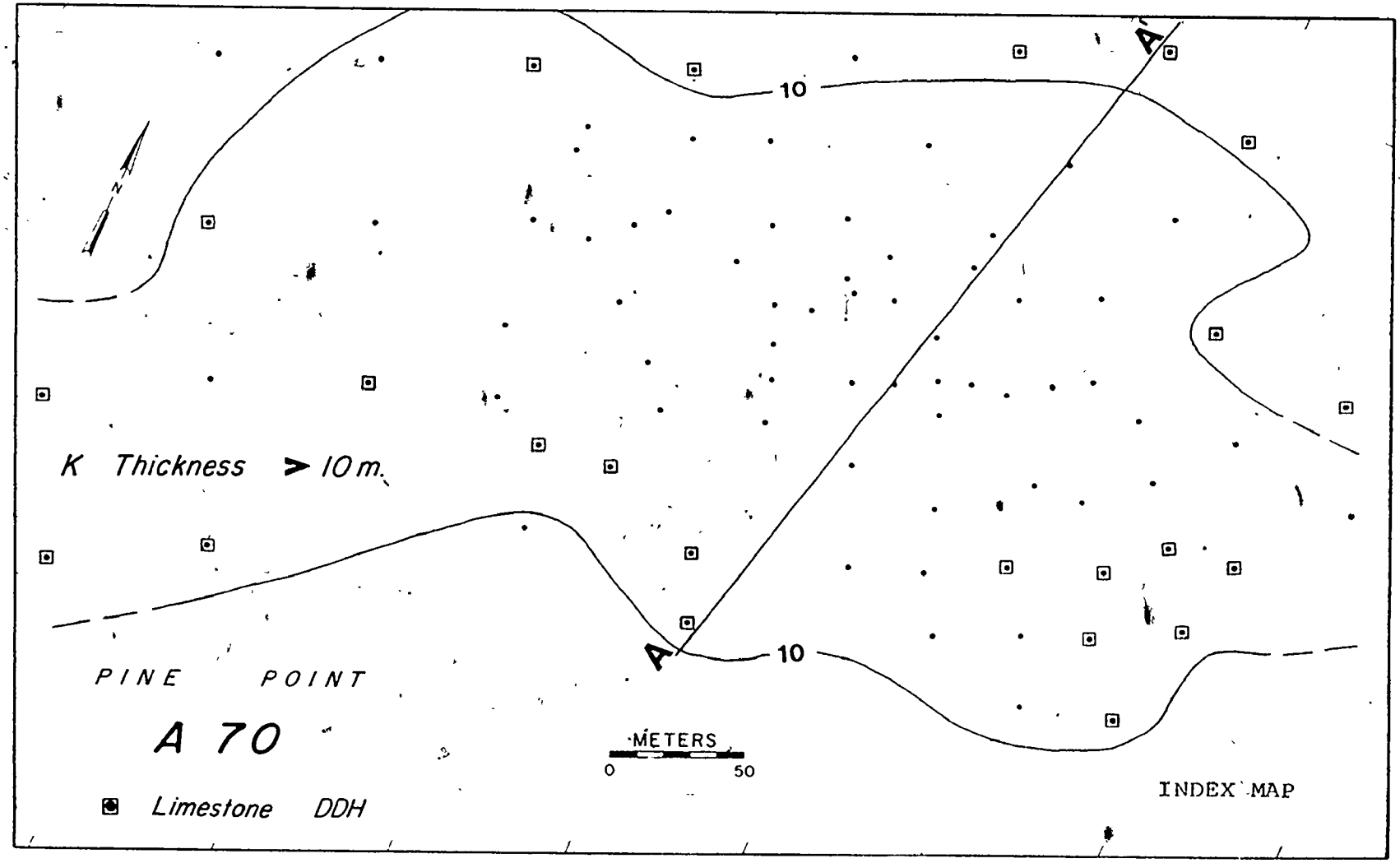

Fig. 12. General Geologic Features of the A70 Area.

Limestone drill holes indicate areas of Upper Pine Point Group limestone preserved within Facies K.

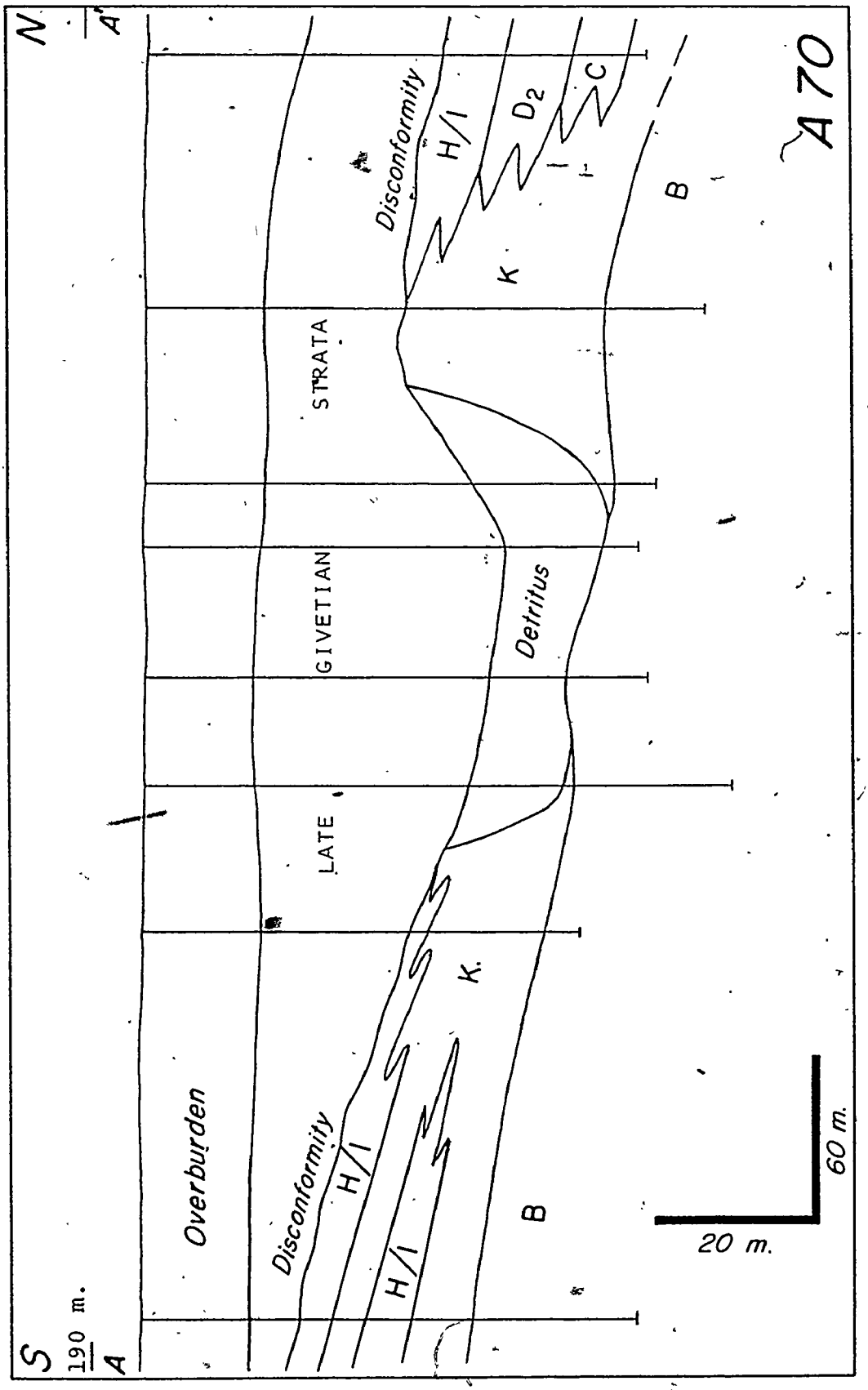

Fig. 13. Geologic Cross Section, A70 Area

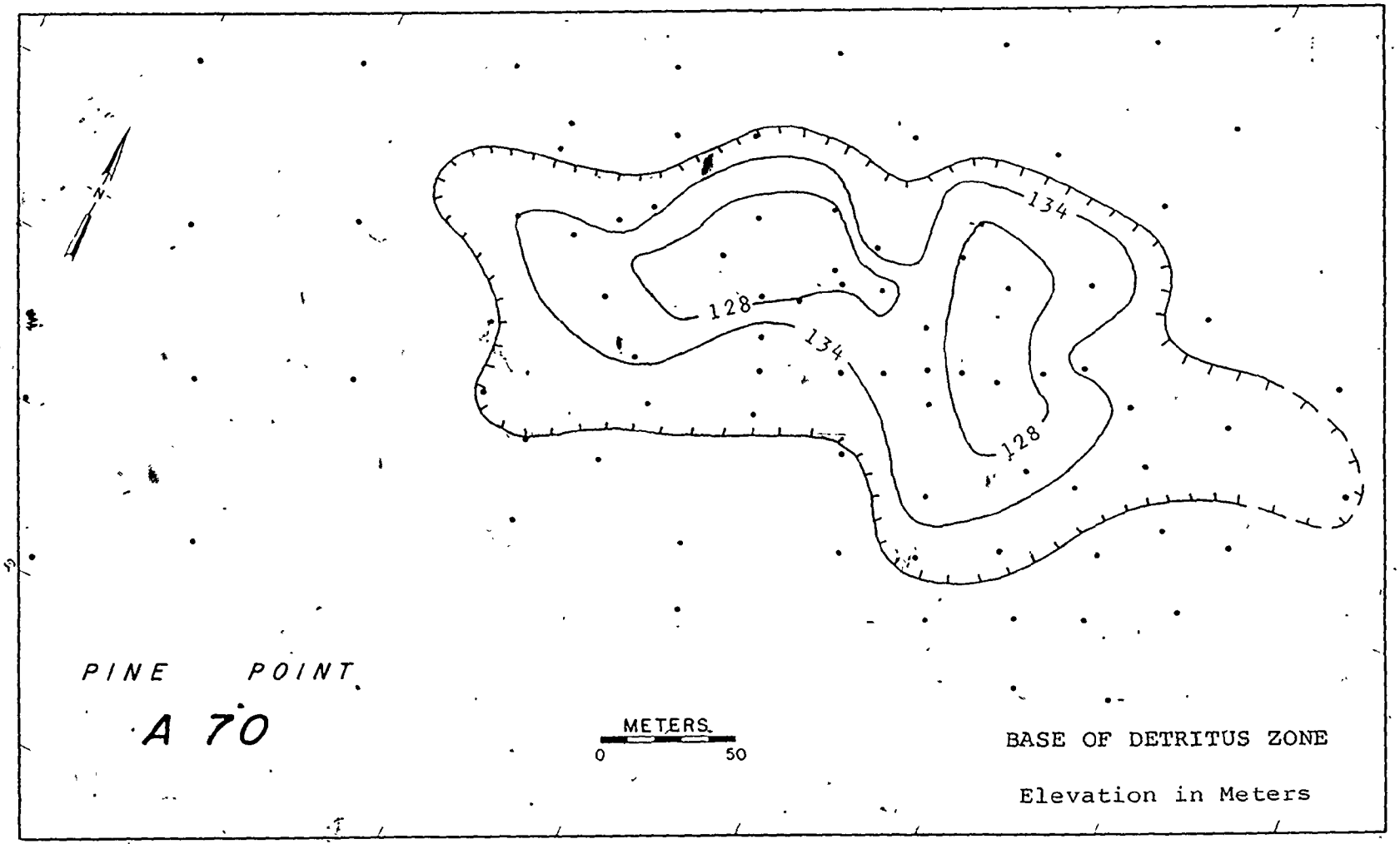

Fig. 14. Structural Contour Map on Base of Detritus Zone, A70 Area
Extent of detritus is delineated by hachures.

thickness is about 20 meters, and two depocenters are indicated by structural contours on the base of the detritus zone (Fig. 14) and by thickness contours of the detritus interval (Fig. 15). The waxy green shale bed which overlies the disconformity rubble contact also is present on top of the detritus zone. In cross-section the detritus zone is broad and shallow and is overlain by late Givetian units (Fig. 13). As in the case of Z53N, the detritus zone overlies Facies B where thickest and Facies K around its margins.

The K57 area was chosen for the most detailed study because it has been drilled on a 12-meter (40-foot) grid (Fig. 16) and because it includes sulfide concentrations of both the prismatic and tabular types (Skall, 1972). The lower part of the K57 ore body and the upper part of the nearby and similar K62 ore body were accessible for detailed study during mining operations, thus providing excellent comparisons with features determined from drill core data. K57 lies within the coarse-crystalline Presqu'ile dolostone along the Main Hinge Zone in the western part of the district (Fig. 3). In this area, Facies K has a maximum preserved thickness of about 45 meters and may be divided into upper and lower units. The lower unit consists of buff to light gray, coarse-crystalline dolostone which contains megafossil (Plate 4:8a, b) and uniform granular (Plate 4:8c, d) lithologic types. These rocks are interpreted to represent reefal and proximal fore-reef depositional environments, respectively. Reefal limestone, Facies D-2, was exposed within the coarse-crystalline dolostone in the south side of the K57 pit during construction of the ramp (K. Newman, pers. commun.). An irregular, interfingering facies

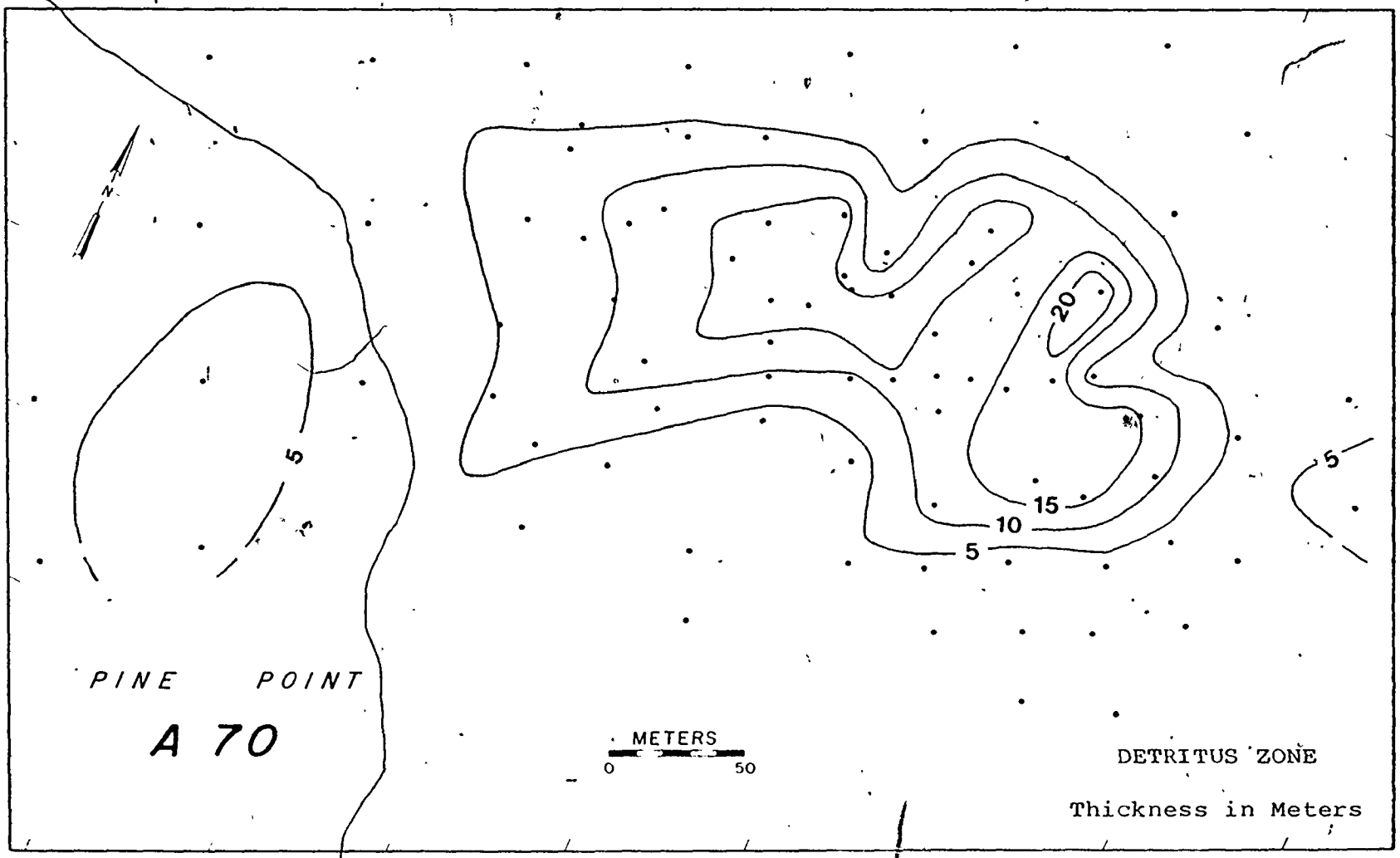

Fig. 15. Isopach Map of Detritus Zone, A70 Area.

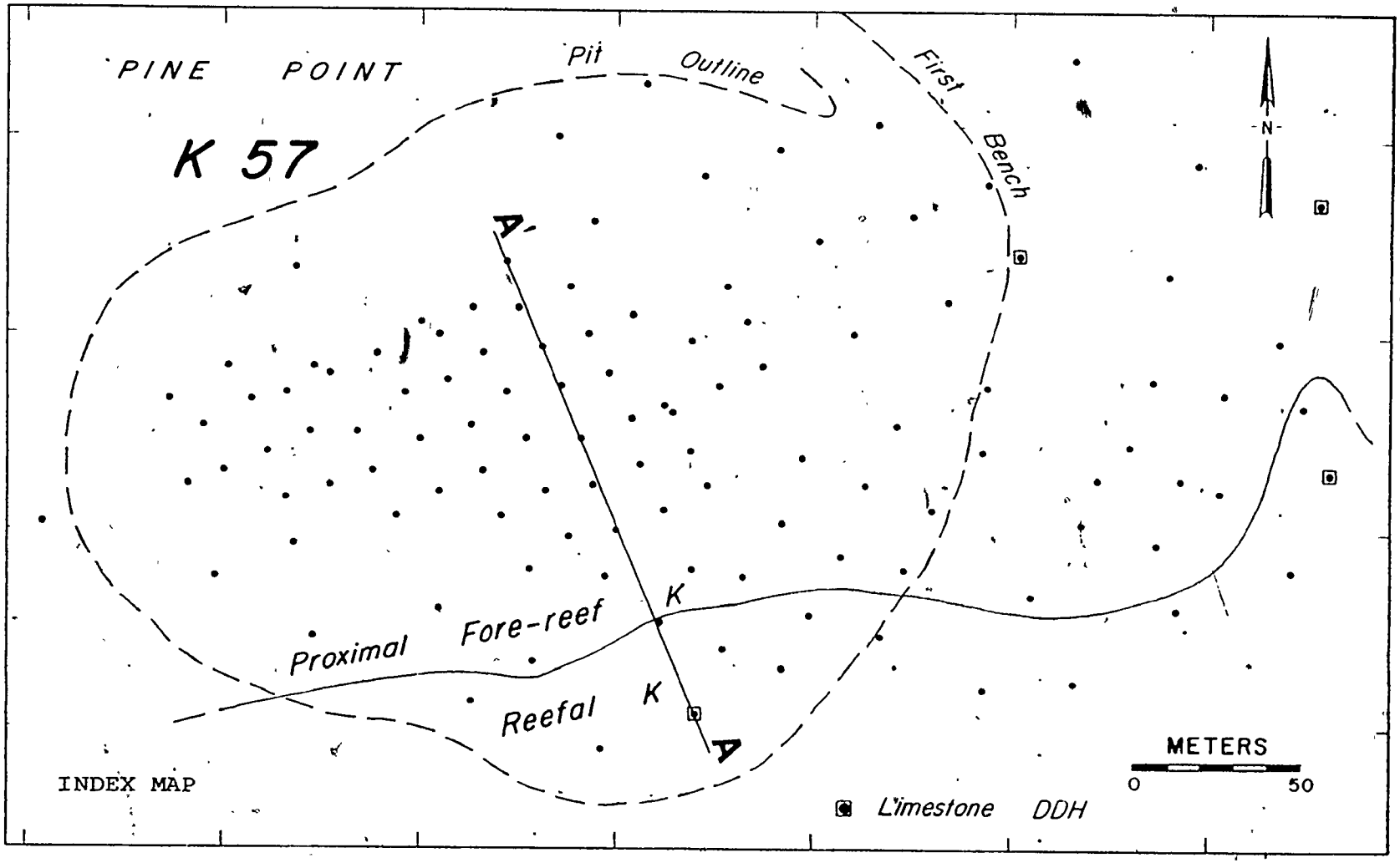

Fig. 16. General Geologic Features of K57 Area.

Limestone drill holes indicate areas of Upper Pine Point Group limestone preserved within Facies K.

boundary between the two lithologic types of the lower Facies K is present just to the south of the mineralized zone (Figs. 16 and 17). Direct evidence concerning the original nature of the upper Facies K unit has been largely obliterated by the pervasive introduction of white dolomite (Plate 4:4-7). Isolated limestone remnants lateral to this unit (Figs. 16 and 17) suggest that this material was originally the lagoonal Facies H/I. This relationship would be anticipated due to the general northwestward progradation of depositional environments in the area (Skall, 1975).

Within the zone of coarse-crystalline dolostone is an irregularly elliptical area containing light gray, fine- to coarse-crystalline, friable dolostone detritus (Fig. 18). The detritus zone is about 190 meters long and 100 meters wide and has a maximum detritus thickness of about 35 meters in two areas (Fig. 19). Although the top of most of the detritus zone is truncated at its subcrop, Facies L units are present in four drill holes, thus suggesting that the present detritus thickness represents most of the original material. Again, the thickest detritus overlies Facies B (Fig. 17). Near the detritus zone, the contact between Facies B and Facies K is indistinct because the upper part of Facies B is medium- to coarse-crystalline with poorly preserved faunal components. Detailed study of the detritus zone in K57 reveals the presence of three stratigraphic units (Fig. 17). The stratigraphically lowest unit consists of relatively clean, fine- to coarse-crystalline dolostone which contains blocks of coarse-crystalline Facies K dolostone, particularly near the base. Minor amounts of detritus may be present in fractures and along bedding

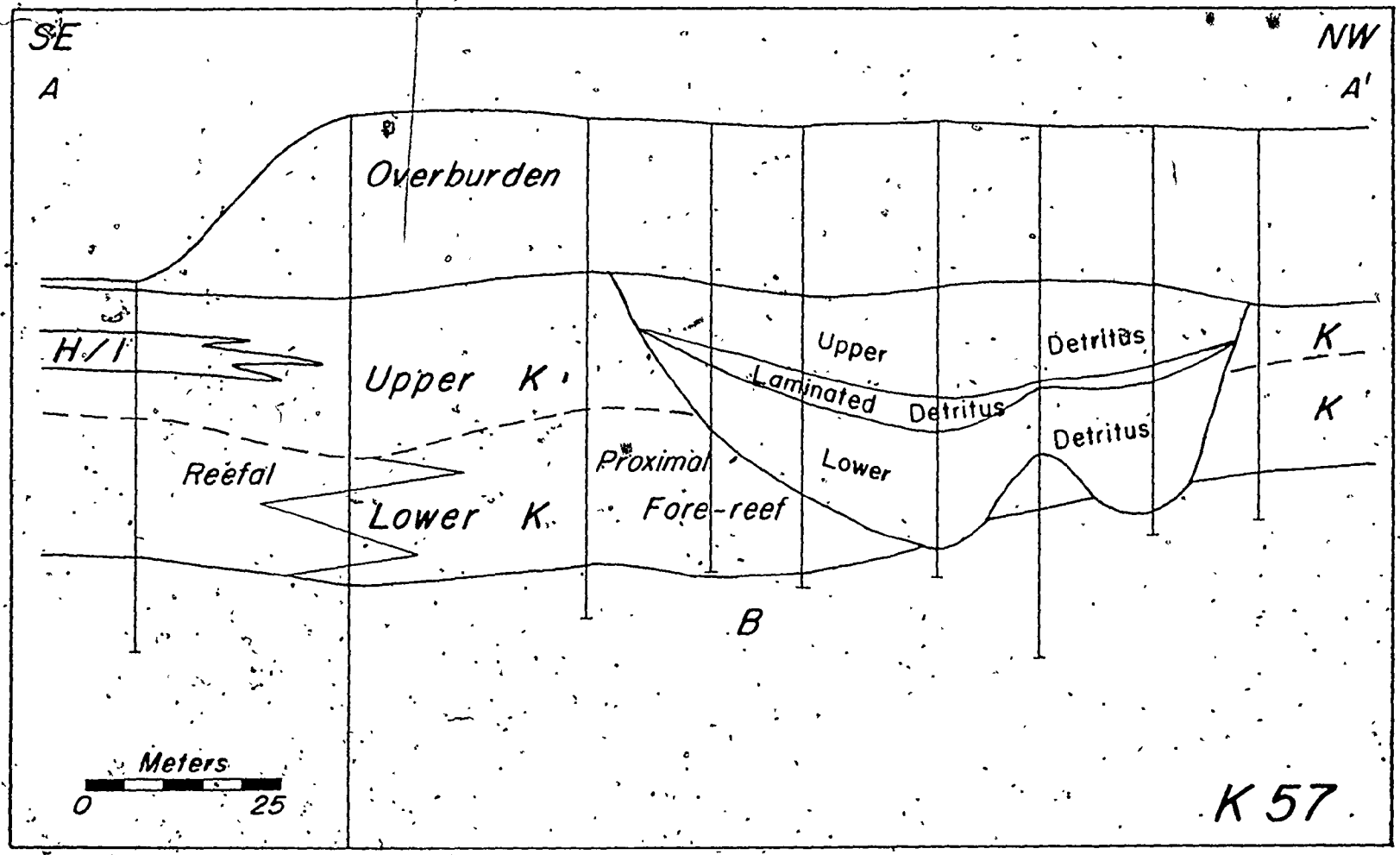

Fig. 17. Geologic Cross Section, K57 Area.

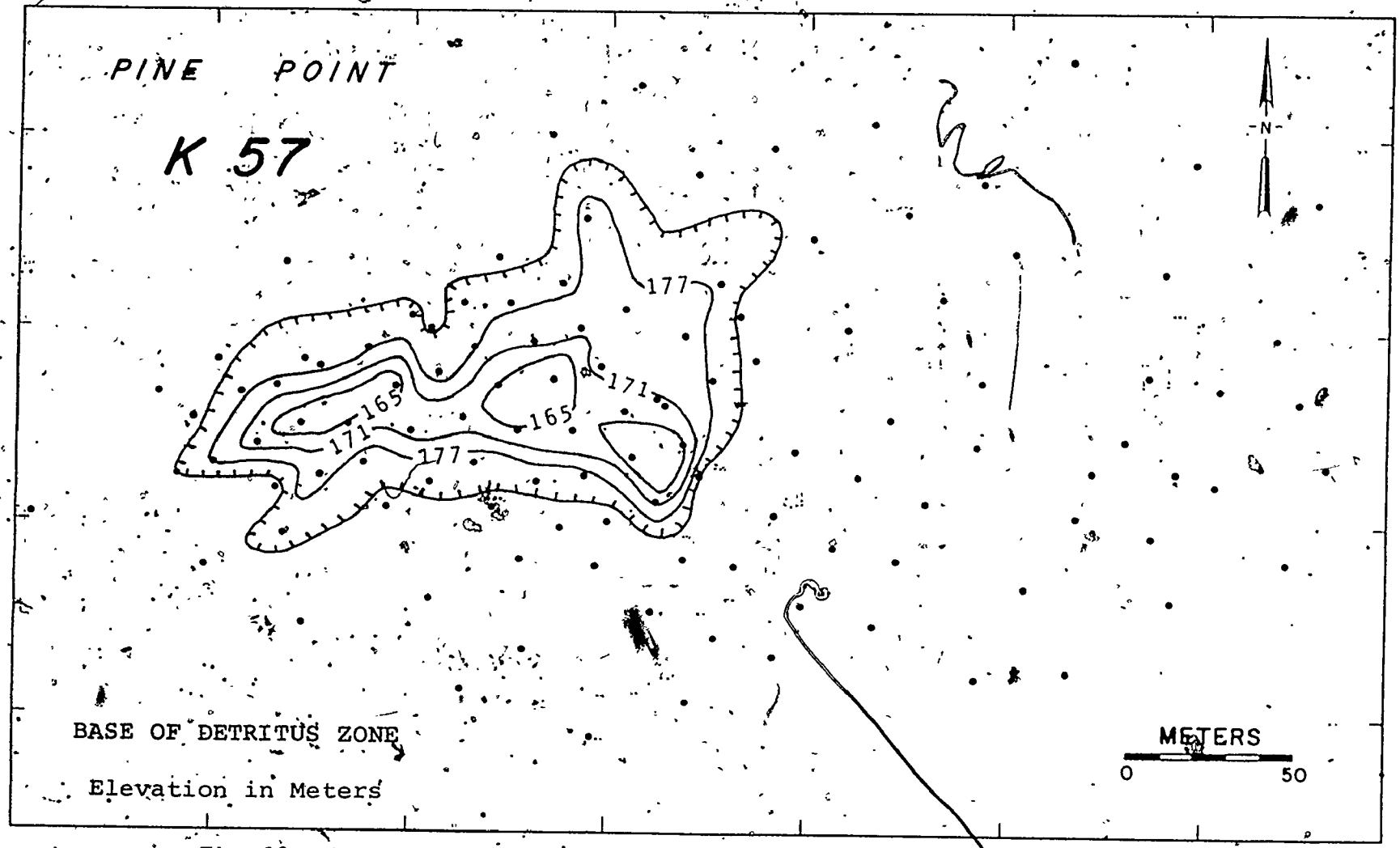

Fig. 18. Structural Contour Map on Base of Detritus Zone, K57 Area
Extent of detritus is delineated by hachures.

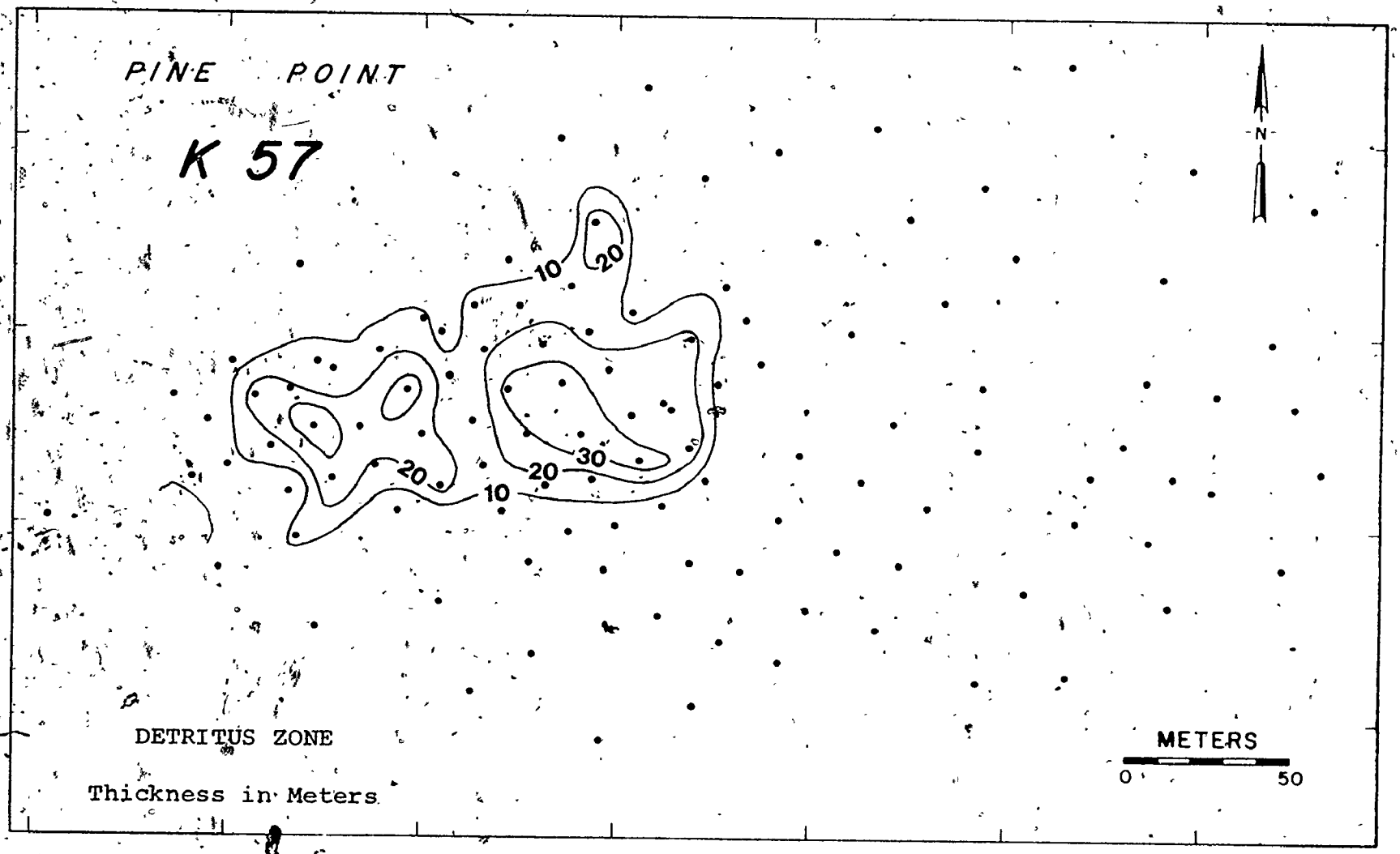

Fig. 19. Isopach Map of Detritus Zone, K57 Area.

planes for some distance in the units underlying the detritus zone. Thickness of the lower unit is highly variable and attains a maximum of 18 meters. A thinner unit of laminated detritus, consisting of alternating bands of light and medium gray dolostone with rare green clay blebs (Plate 7:2-4), overlies the lower detritus unit (Fig. 17). Thickness of this unit is also variable, largely due to disruption by sulfide introduction, and is a maximum of five meters. The upper unit consists of nonlaminated detritus with common small fragments of green clay and fine-crystalline dolostone, particularly in the upper part (Plate 7:5-10), and is a maximum of 15 meters in thickness. These lithologic types have been observed in other detritus zones, but additional work is needed to establish the consistency of the sequence.

Dolostone detritus is a common associate of the prismatic ore bodies within the coarse-crystalline dolostone of the upper barrier and has been observed in drill core or broken ore in the N38A, N42, 042, J44, Z53N, Y54N, K57, K62, R61, A70, and W85N sulfide bodies. Other examples undoubtedly exist, but this list indicates that major sulfide concentrations are commonly associated with detritus zones.

It is also apparent from this study that some sulfide-bearing zones lack major amounts of associated detritus. These zones correspond to the tabular ore bodies in the upper barrier complex (Skall, 1972). Although there are small areas of massive sulfide concentration in these zones, most of the ore consists of stratabound sulfides confined to a relatively narrow stratigraphic interval (Plate 8). Tabular sulfide zones are common in the lower part of the coarse-crystalline

Facies K dolostone in some areas; many of the prismatic ore bodies have contiguous tabular sulfide concentrations.

M40 is located in the central portion of the Main Hinge Zone within the cluster of N38A, N42, and O42 prismatic ore bodies (Fig. 3). M40 is the only active underground mining operation in the district and offers a more complete view of the mineralized zone than is generally possible in the open pits. The sulfide concentration in M40 is stratabound in the lower part of the coarse-crystalline Facies K dolostone and averages about three meters in thickness, although it reaches a maximum of 15 meters (Fig. 5). Most of the ore occurs as open-space filling of vuggy porosity (Plate 8:1-4), and local collapse breccias also host sulfides (Plate 8:7, 8). Some massive sulfide concentrations are present (Plate 8:5); sulfide textures indicate growth from the walls and suggest that these zones were large voids prior to mineralization. Some of these zones are thin and tabular and contain gravity-controlled stalactitic sulfide forms (Plate 8:6). Dolostone detritus of the type common in prismatic ore bodies has not been recognized in M40.

Solution features associated with sulfide concentrations within the coarse-crystalline dolostone of the upper barrier differ somewhat from the sulfide-hosting features within the fine-crystalline dolostones of the lower barrier (Plate 9). The latter sulfide-bearing zones occur northeast of the present-day erosional limit of the Presqu'ile (Fig. 3) but presumably once were covered by the coarse-crystalline dolostone. Both the W17 and X15 ore bodies are largely within Facies D-1 and the J subfacies (Fig. 5), and W17 was chosen for study of a

mineralized zone in the fine-crystalline dolostones of the lower barrier. Sulfide concentrations may be either massive without lithic components or distributed in intercrystalline porosity in reefal and back-reef lithologies. In addition to intraformational reefal breccias, two other types are present in W17. One type consists of fragments of Facies J fine-crystalline dolostone in a matrix of light gray, sandy, fine-crystalline dolostone; appreciable amounts of sulfides occur within breccia matrix and fragments (Plate 9:2, 3). The second type consists of Facies J fragments in a dark gray, dense micritic, calcareous matrix (Plate 9:4). Fragments are largely dolostone, but calcareous dolostone and limestone fragments are also present; some blocks have bleached rims (Plate 9:4). Sulfides are uncommon in this type. In addition, some breccias consist of Facies J dolostone blocks cemented by sulfides without apparent rock matrix (Plate 9:5), and some irregular areas of sulfides occur in Facies J dolostone lacking evidence of pre-mineralization disruption by major fracturing or brecciation (Plate 9:6). These breccias are local features and are largely coextensive with the mineralized zone. A local zone of sticky green clay occurs in the upper part of W17 (Figs. 21 and 22). The green clay has a maximum preserved thickness of about ten meters and contains pyrite and sphalerite. The green clay is similar to the waxy green shales of the disconformity and the Watt Mountain Formation, but the exact relationship between these units is indeterminable.

N204 is the most northeasterly and the lowest stratigraphically of the presently known mineralized zones (Fig. 3). Sulfides occur in the upper part of a laterally extensive zone of vuggy and

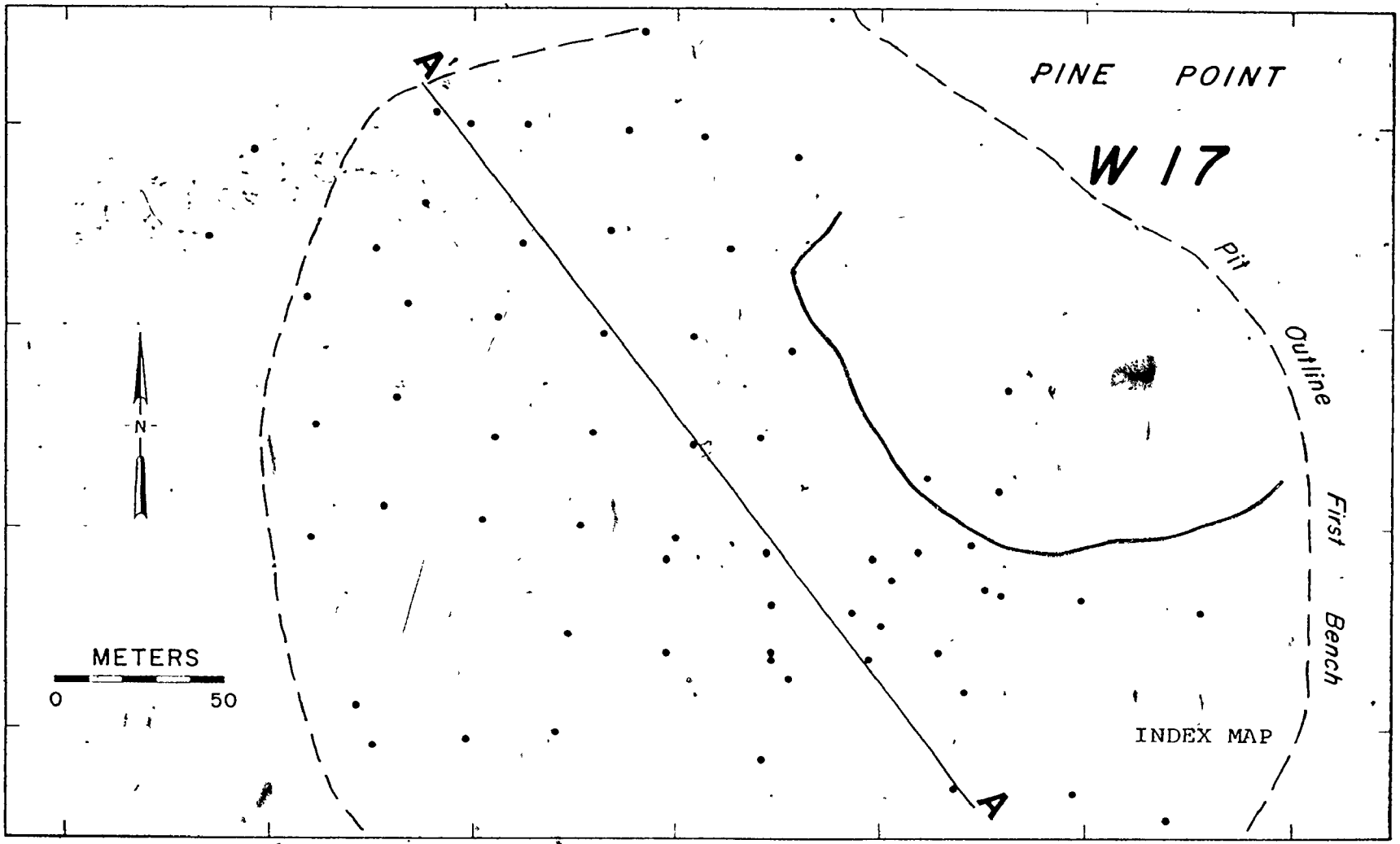

Fig. 20. Index Map of W17 Area.

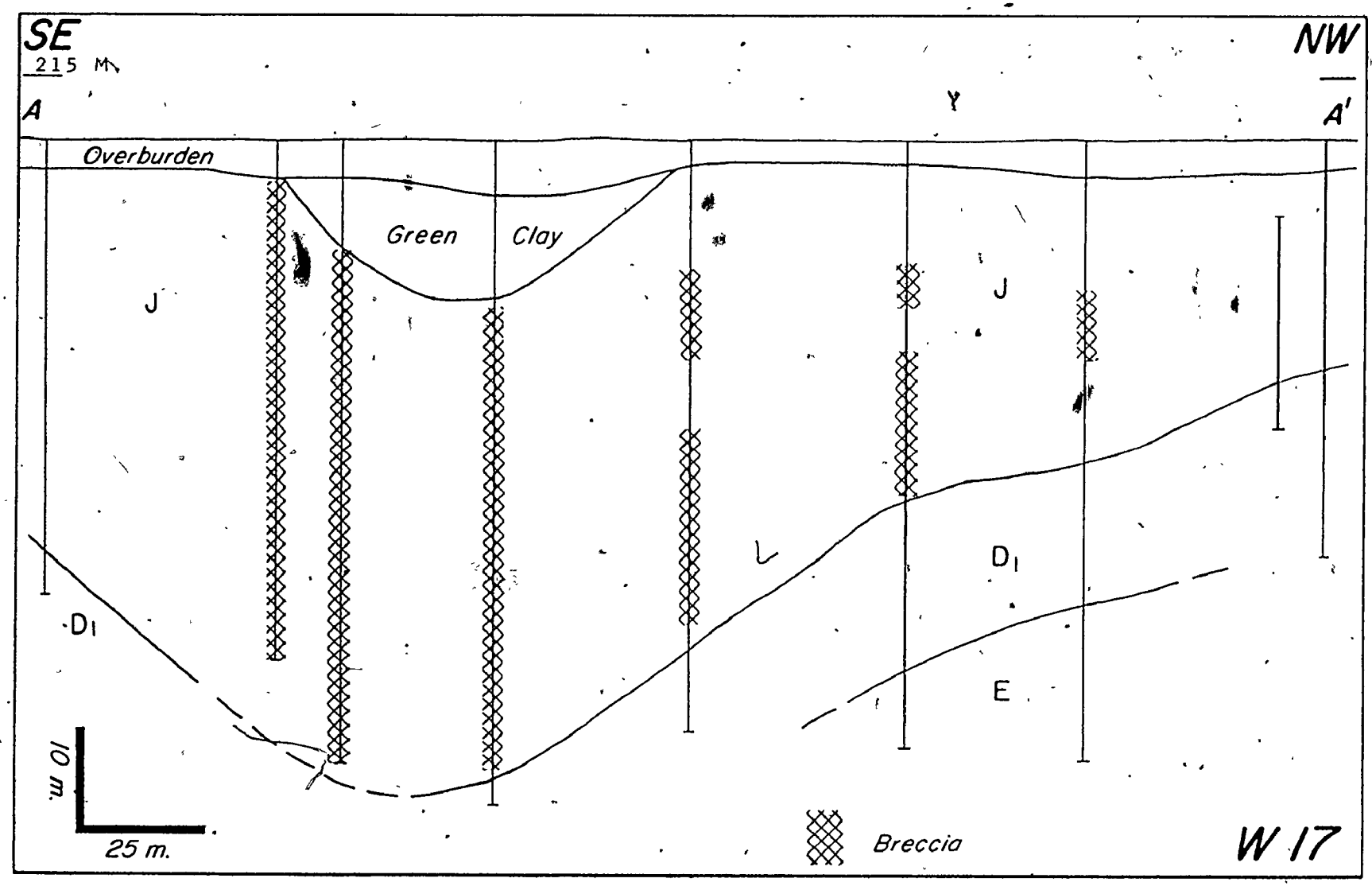

Fig. 21. Geologic Cross Section, W17 Area

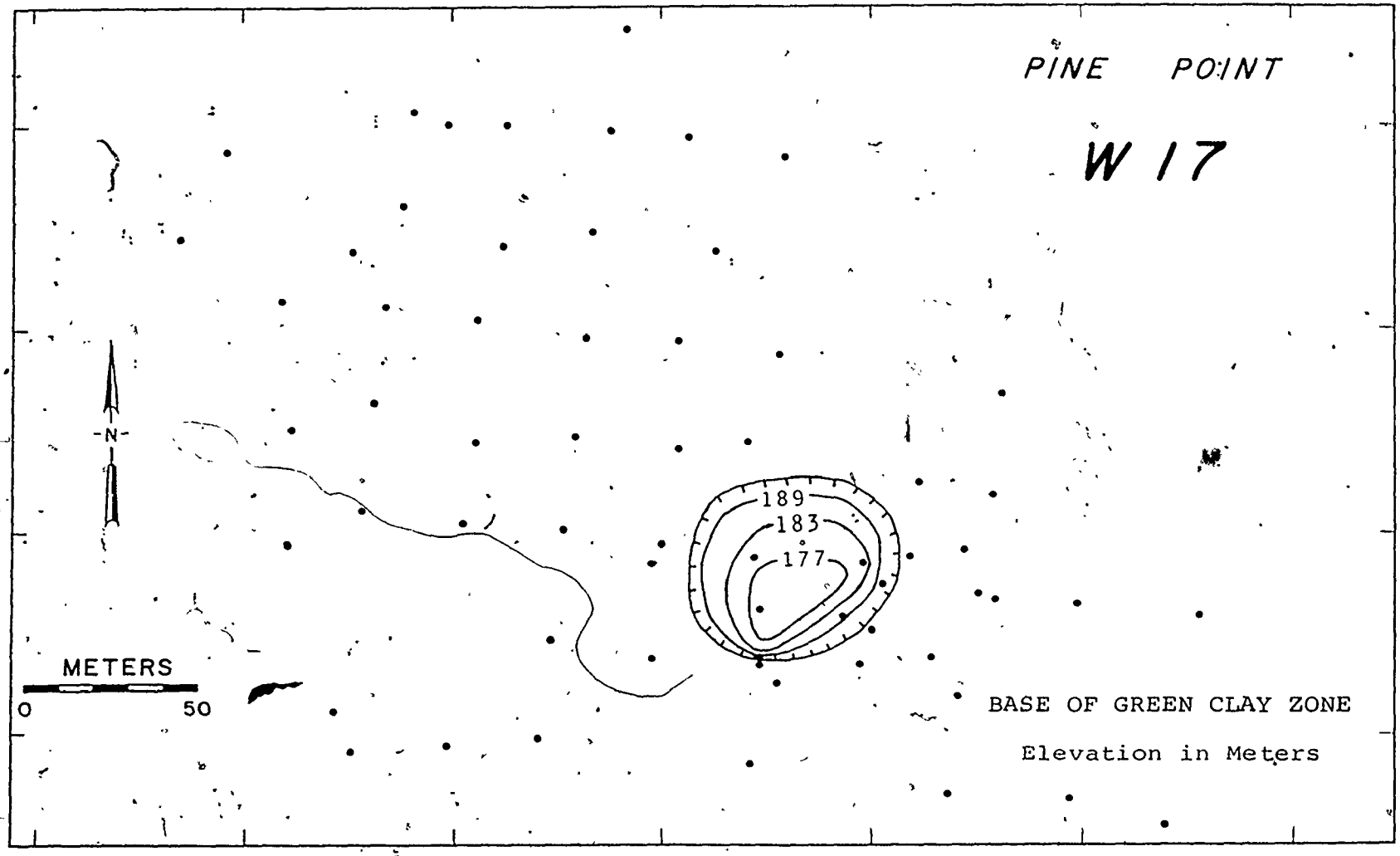

Fig. 22. Structural Contour Map on Base of Green Clay Zone, W17 Area

intercrystalline porosity and incipient fracturing (Plate 9:8-10), known as the Spongy Horizon, in the fine-crystalline dolostones of subfacies B-3 just above the Keg River Formation (Fig. 5).

Relationship of Sulfide Concentrations to Solution Features

Upper Barrier

Solution features in the Pine Point barrier complex were of considerable importance in the localization of sulfide concentrations. The detritus zones appear to have been the loci for the deposition of the prismatic ore bodies and contiguous sulfide concentrations in the upper barrier. This association can be demonstrated readily by comparing the distribution of detritus in the Z53N, A70, and K57 areas (Figs. 10, 13-15, and 17-19) with the corresponding "Total Sulfide Index" (Appendix I) as plotted in Figs. 23-27.

Because of the depth of recent erosion in the Z53N area, this prismatic sulfide body is only 18 meters in thickness and contains a maximum of 25 percent total sulfides by volume (Fig. 23). The dominant sulfide concentrations occur within the detritus zone adjacent to the deepest detritus penetrations (Fig. 10). Areas of low sulfide content occur within the detritus zone, as well as in the coarse-crystalline Facies K dolostone adjacent to the detritus zone.

A70 has a maximum of over 40 volume percent total sulfides over a 53-meter interval (Fig. 24). The prismatic portion of the sulfide concentration is coincident with the major detritus zone (Figs. 14 and 15), but a broad stratabound zone of lower sulfide concentration occurs within the coarse-crystalline Presqu'ile dolostone, particularly

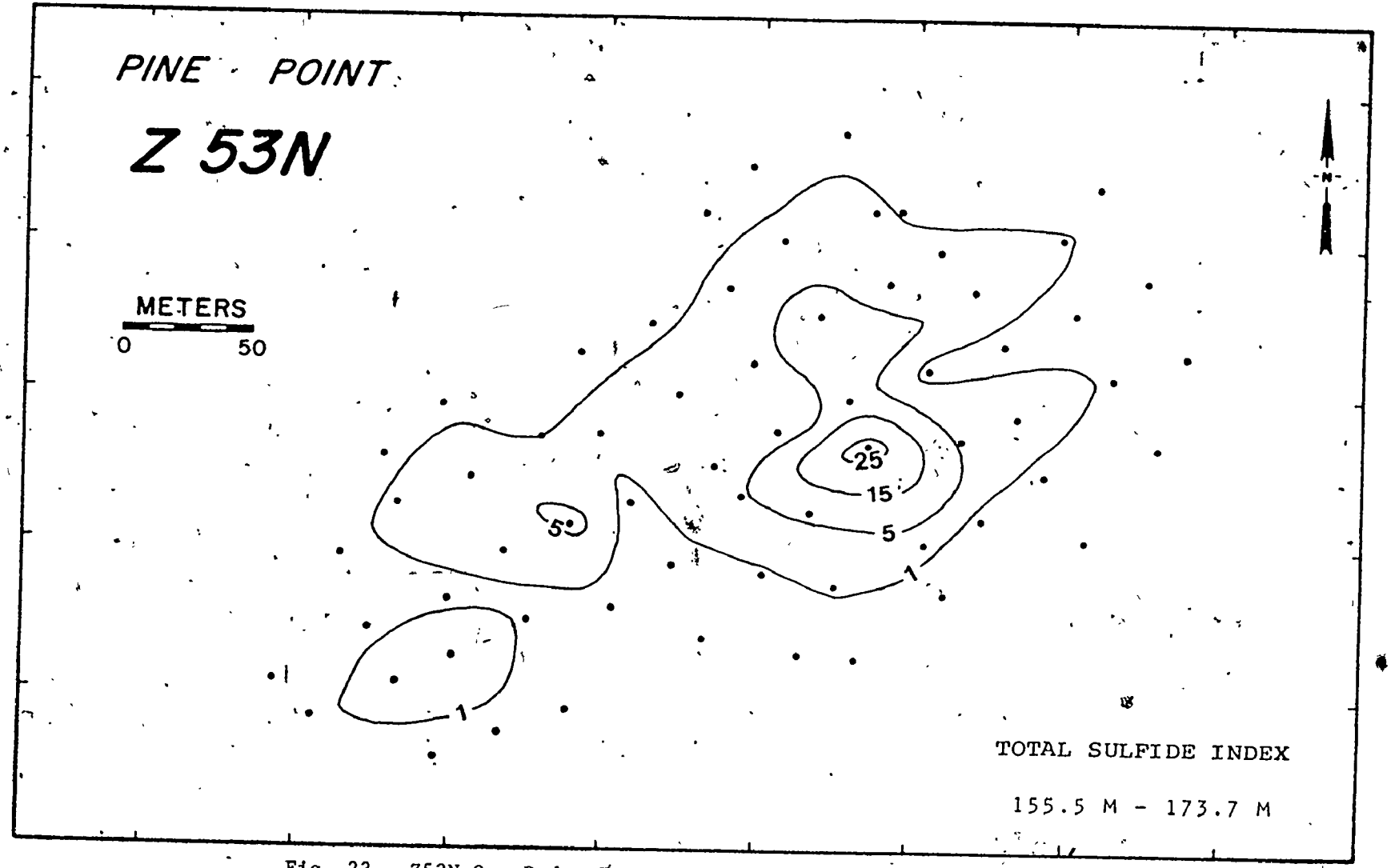

Fig. 23. Z53N Ore Body, Total Sulfide Index, 155.5 m - 173.7 m

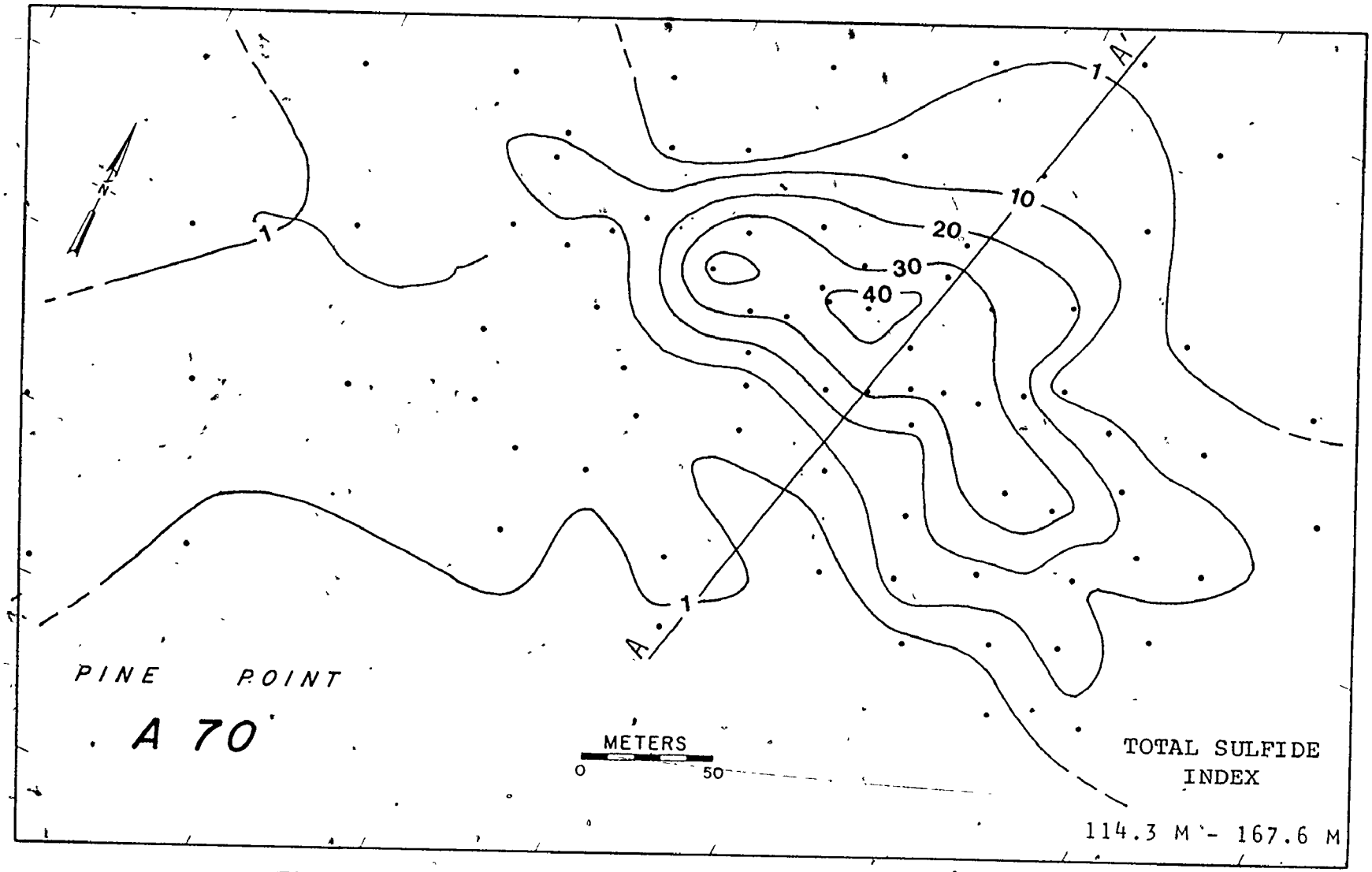

Fig. 24. A70 Ore Body, Total Sulfide Index, 114.3 m - 167.6 m

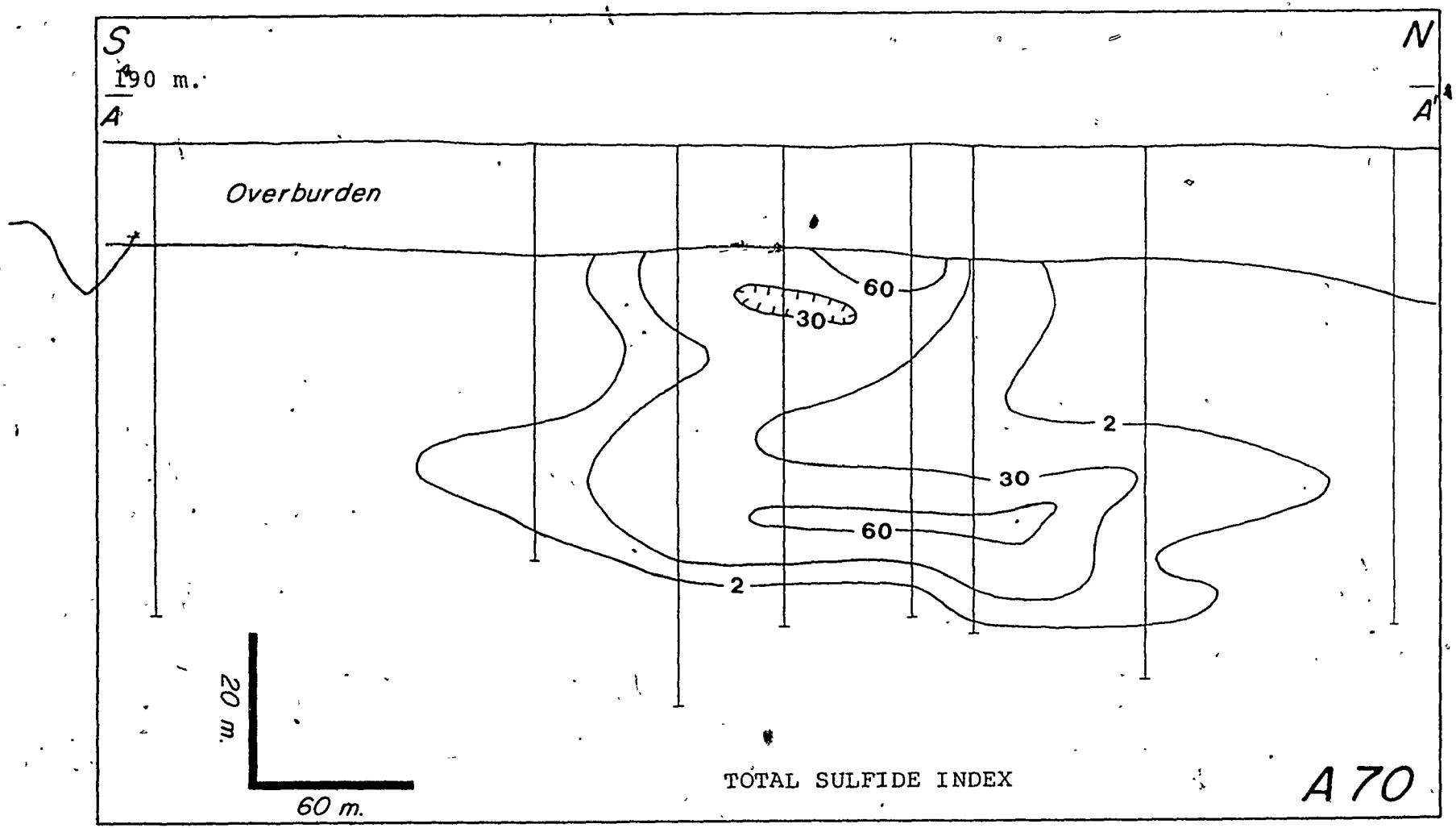

Fig. 25. A70 Ore Body, Total Sulfide Index, Section A-A'

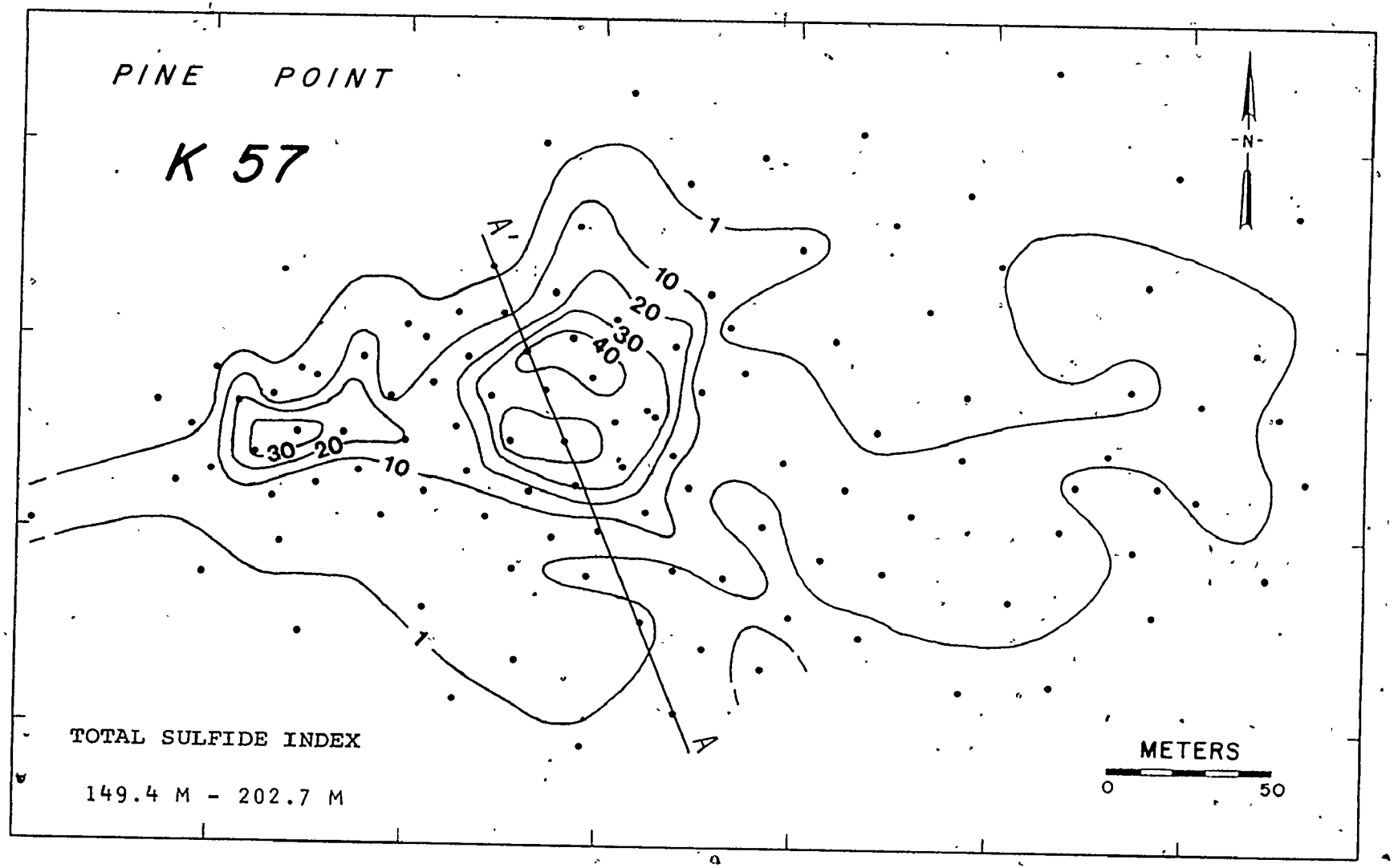

Fig. 26. K57 Ore Body, Total Sulfide Index, 149.4 m - 202.7 m

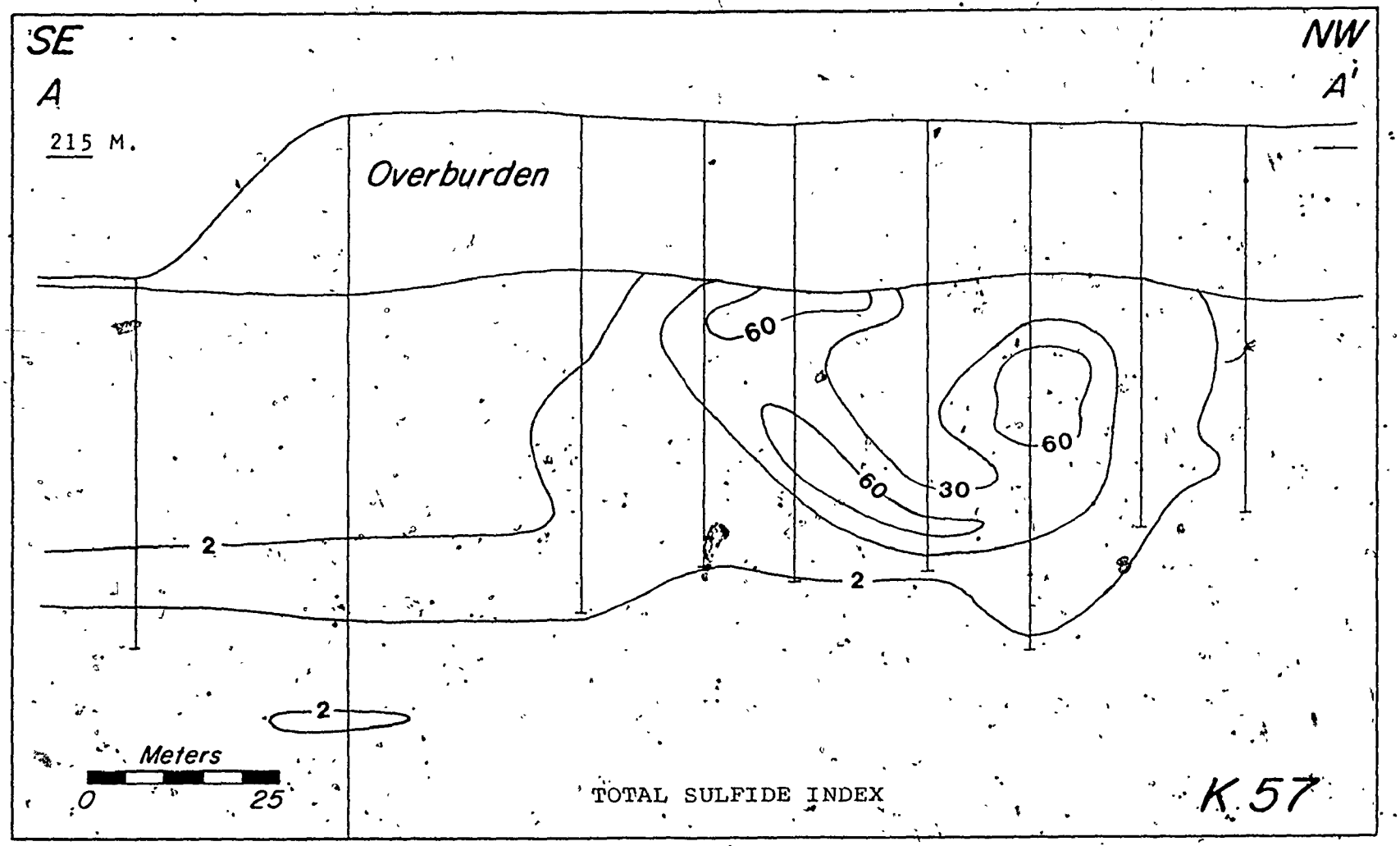

Fig. 27. K57 Ore Body, Total Sulfide Index, Section A-A'

2

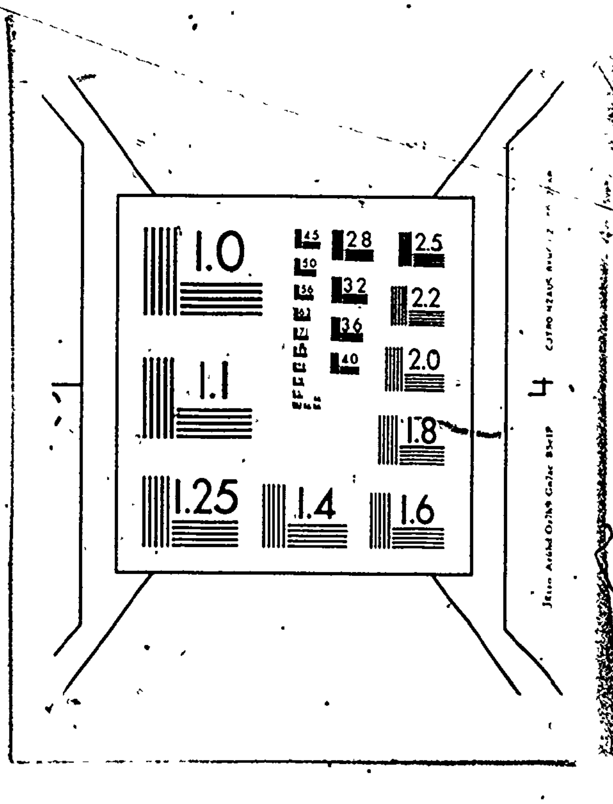

northeast and southwest of the detritus zone (Fig. 24). Downward displacement of late Givetian strata has taken place in an irregularly elliptical area overlying the detritus zone (Fig. 13). The late Givetian strata and the detritus zone are fractured and brecciated. Sulfides fill fractures and form concentrations at the expense of pre-existing materials, particularly the carbonate detritus (Fig. 25; Plate 7:6, 10, 11).

K57 has a maximum total sulfide concentration of about 50 volume percent over a 53 meter interval (Fig. 26). The greatest sulfide concentration is within the detritus zone (Figs. 18 and 19), but an irregular stratabound zone of lower sulfide content is present to the east of the massive zone (Figs. 26 and 27). Most of the sulfides in the stratabound zone occur as pore-filling of the uniform granular lithology (proximal fore-reef) in the lower unit of the coarse-crystalline Facies K dolostone (Fig. 17; Plate 8:2, 3). Sulfide minerals within the detritus zone fill fractures and breccia interstices, but large intervals are massive. Despite extensive vuggy porosity within the pervasive white dolomite of the upper Facies K (Plate 4), the boundary of the prismatic ore body is sharp, and the upper Presqu'ile does not contain megascopic sulfides. Minor sulfides occur in intercrystalline porosity in the Facies B dolostone which underlies the Presqu'ile (Figs. 17 and 27).

Lower Barrier

A definite relationship also exists between areas of collapse (Plate 9:1) and the sulfide concentrations in the fine-crystalline

dolostones of the lower barrier. W17 has a maximum of over 50 volume percent total sulfides over a 99-meter interval (Fig. 28), and some 25-meter intervals contain over 85 percent sulfides (Fig. 29). The area of greatest sulfide concentration is largely coincident with the green clay zone which represents the central area of collapse (Fig. 22). A correlation exists between sulfide concentrations and the various breccia types (Figs. 21 and 29). Sulfides fill fractures and replace breccia matrix and fragments (Plate 9:2-6). Most sulfides appear to be present in intervals of brecciated Facies J dolostone (Fig. 21), but in high sulfide intervals, there is little lithic material remaining (Plate 9:7).

Detritus or collapse breccias do not appear to have been of major importance in the localization of the N204 sulfide concentrations. However, local downward displacement affects strata as deep as the underlying E-Shales. Highest sulfide concentrations occur in the "Spongy Horizon" adjacent to these local slump areas, but sulfides also occur at higher stratigraphic levels overlying the downward displaced zones (Adams, 1973).

Development of Sulfide-bearing Solution Features

Solution features associated with sulfide concentrations in the coarse-crystalline Facies K dolostone of the upper barrier are either large detritus-filled depressions open to the disconformable surface or macropores and stratabound zones of increased porosity in the lower Presqu'ile without apparent direct connection with the disconformable surface. These features are thought to have formed during prolonged

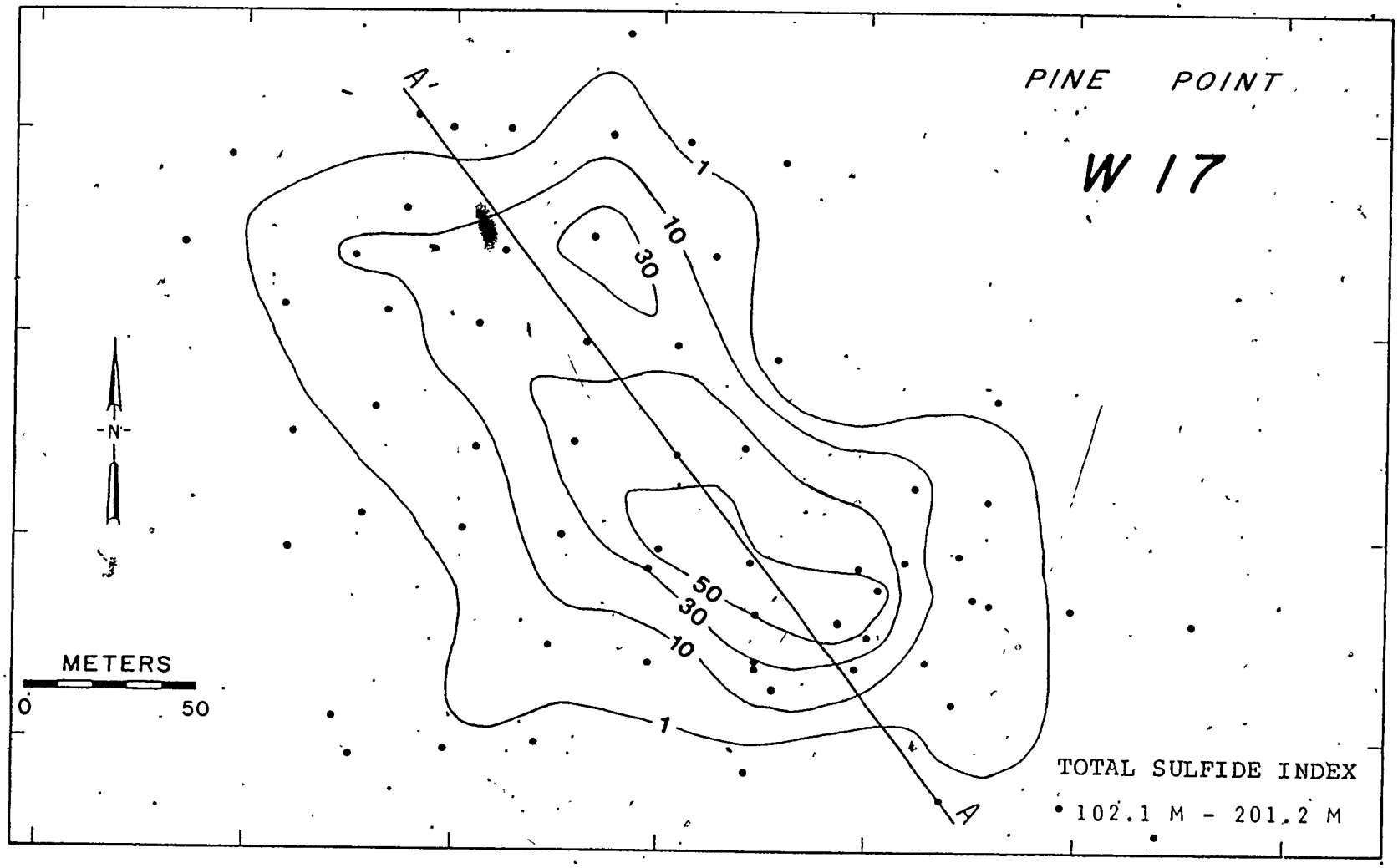

Fig. 28. W17 Ore Body, Total Sulfide Index, 102.1 m - 201.2 m

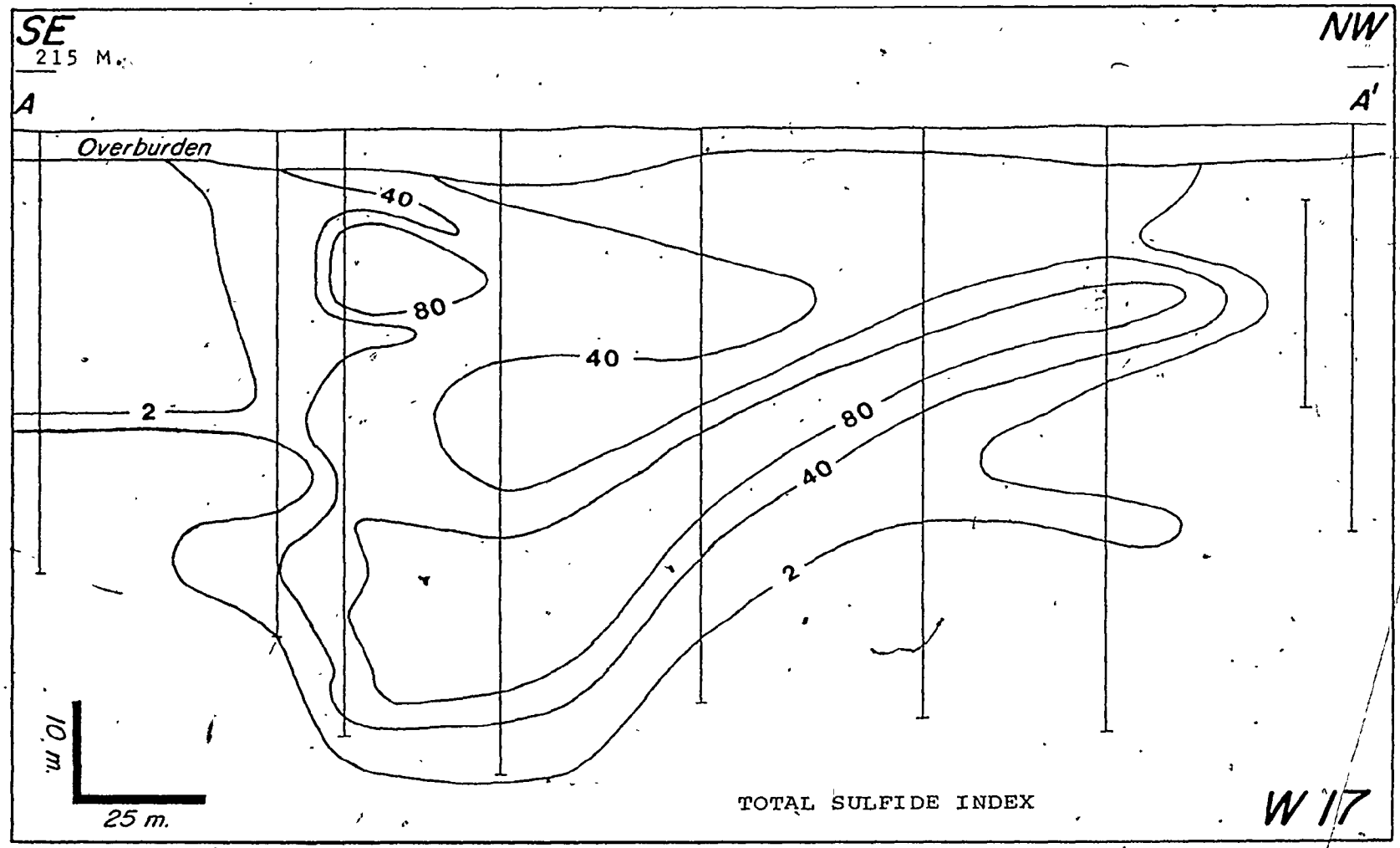

Fig. 29. W17 Ore Body, Total Sulfide Index, Section A-A'

subaerial exposure with attendant karstification and carbonate diagenesis during post-middle Givetian emergence.

Dolines

The detritus zones are interpreted as filled compound dolines (sinkholes) (Sweeting, 1973) which developed largely by solution activity in the limestone Facies C, D-2, H, and I of the upper barrier (Fig. 30, situation B). Original stratigraphic facies was not the major factor controlling development of the dolines because they occur in back-reef (e.g. N38A, 042), reefal (e.g. K57, K62), and intercalated facies (e.g. A70). The dolines are elongate in a northeasterly direction parallel to the Hinge Zones, suggesting that karstification was controlled by the same structural factors that governed carbonate sedimentation. The dolines are as much as 400 meters in length and have length to width ratios ranging from about 2 to 3.5. Doline walls were relatively steep and irregular as suggested by the abrupt transition from detritus to wall rock, and depths of at least as much as 35 meters are indicated. In addition to detritus-filled dolines, green clay and carbonate detritus occur in solution-enlarged joints, bedding planes, and vugs near the disconformity.

The developmental sequence envisaged for the formation of the sulfide-bearing, detritus-filled dolines is shown in Fig. 31A-D. During subaerial exposure, the upper barrier limestones were subject to chemical attack by rainwater, which is undersaturated with respect to calcite (Thrailkill, 1968). Dissolution was concentrated at joint intersections, generally along the dominant northeasterly trend.

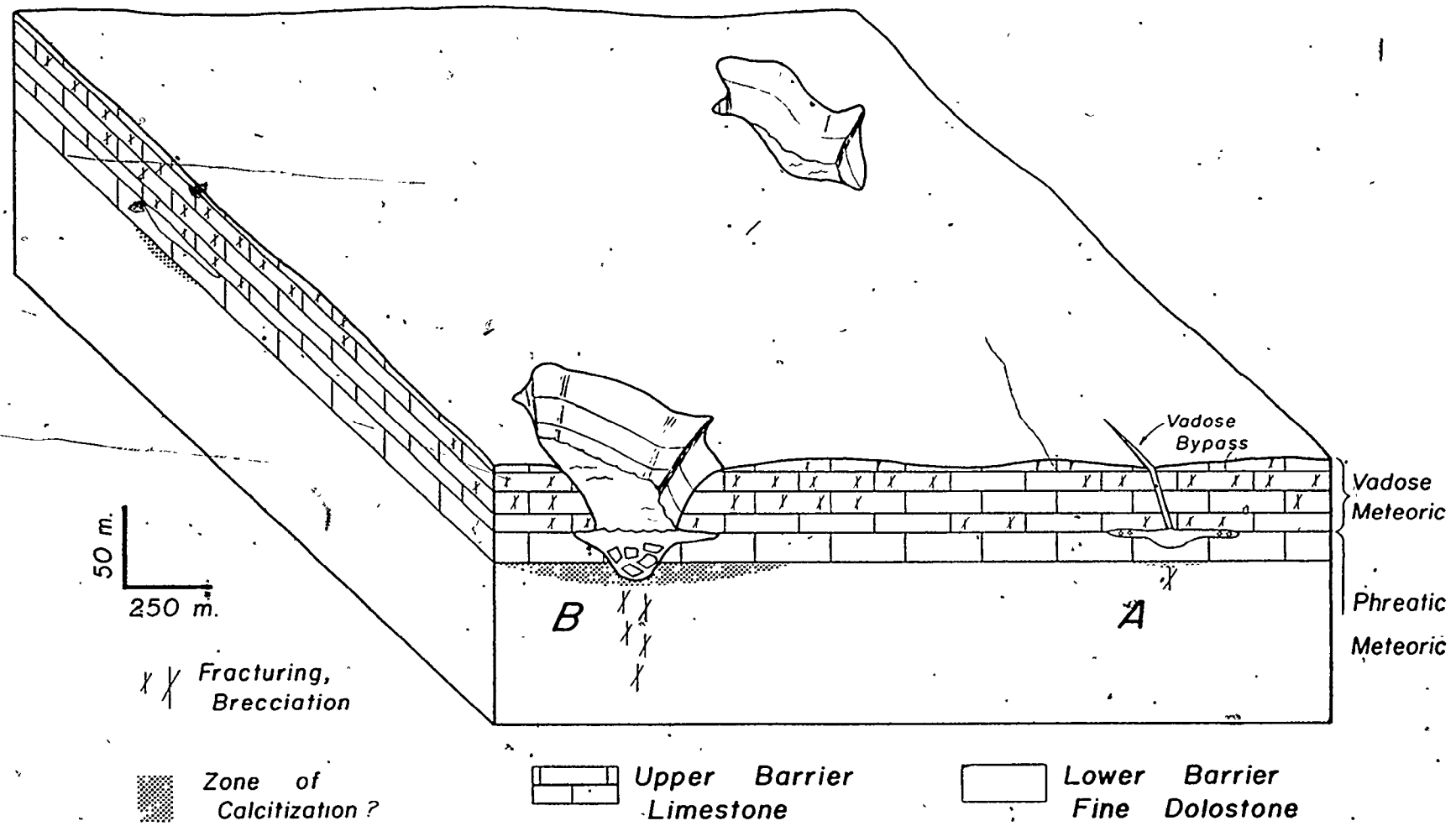

Fig. 30. Vadose and Phreatic Zones in the Upper Pine Point Barrier during the Post-Middle Givetian Erosional Period

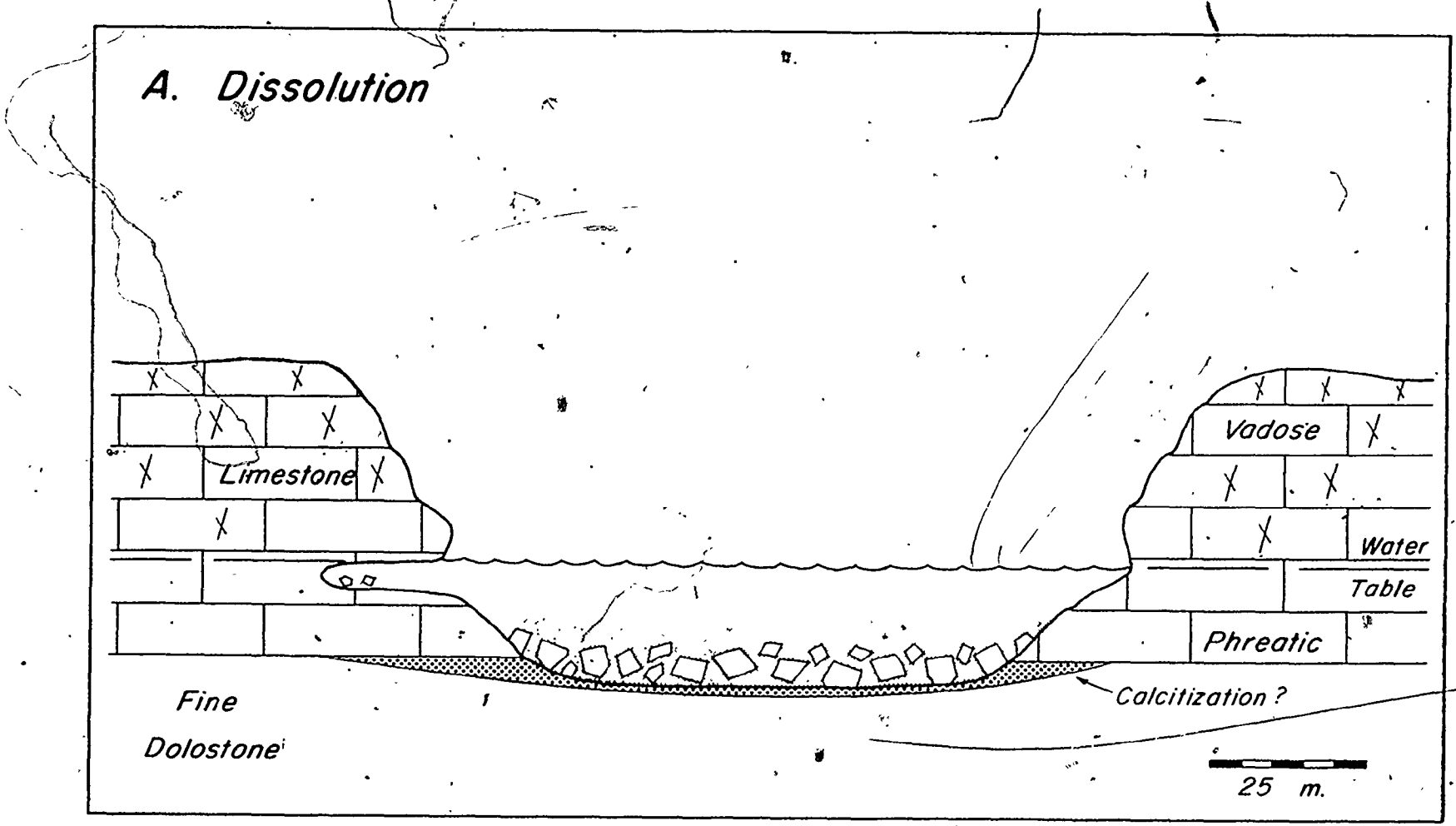

Fig. 31. Developmental Sequence of Sulfide-bearing, Detritus-filled Dolines

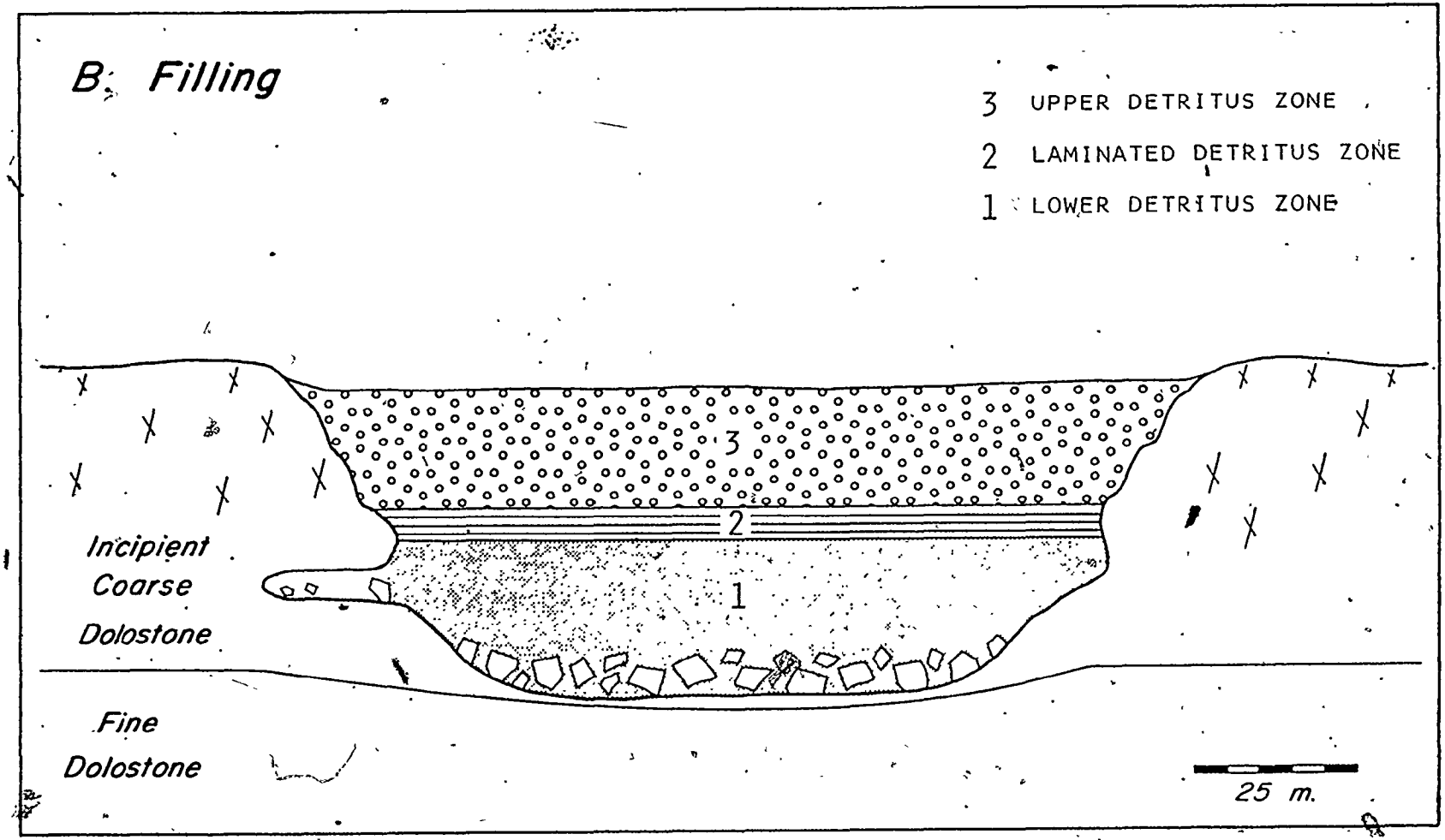

Fig. 31 (continued).

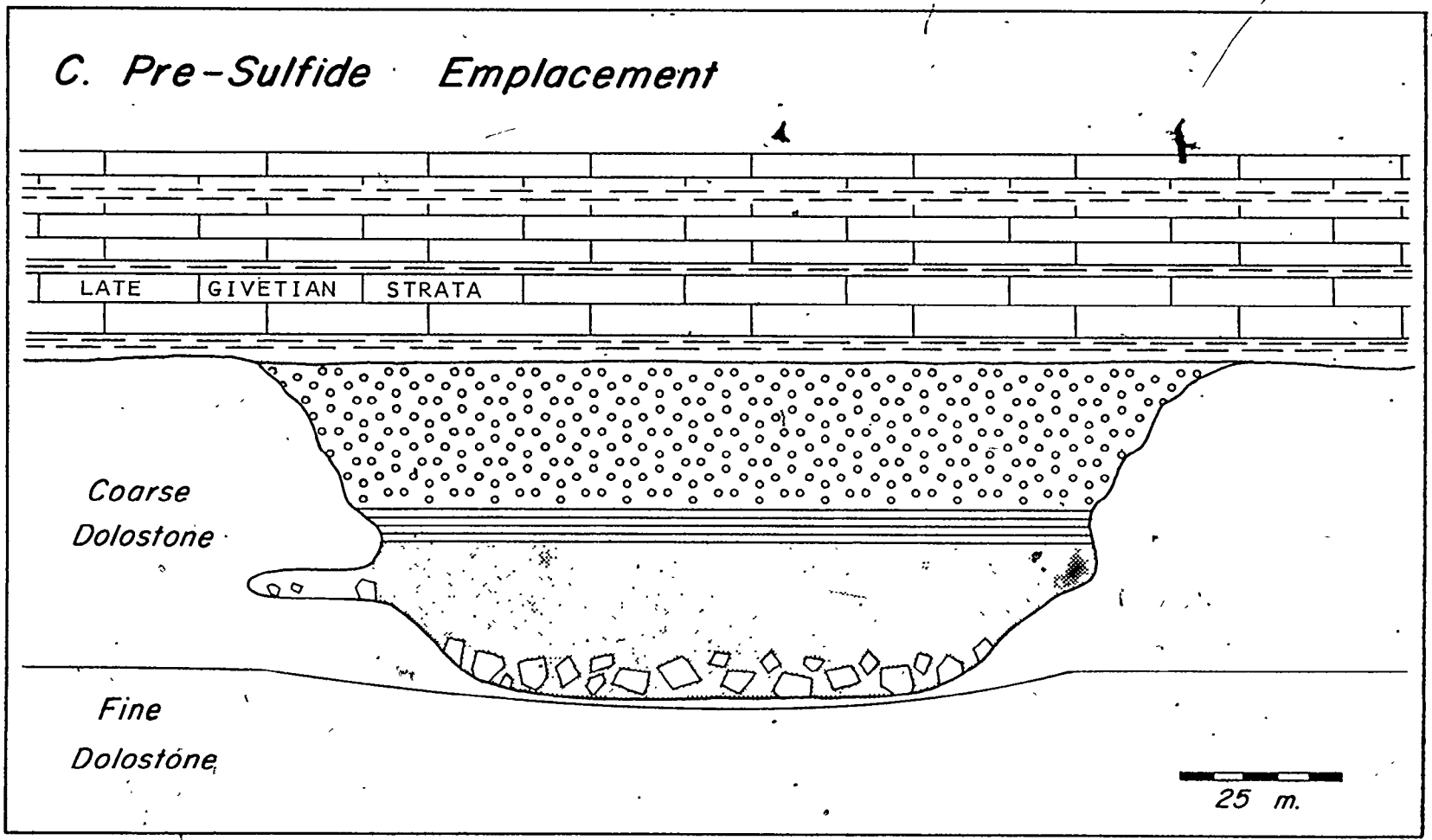

Fig. 31 (continued)

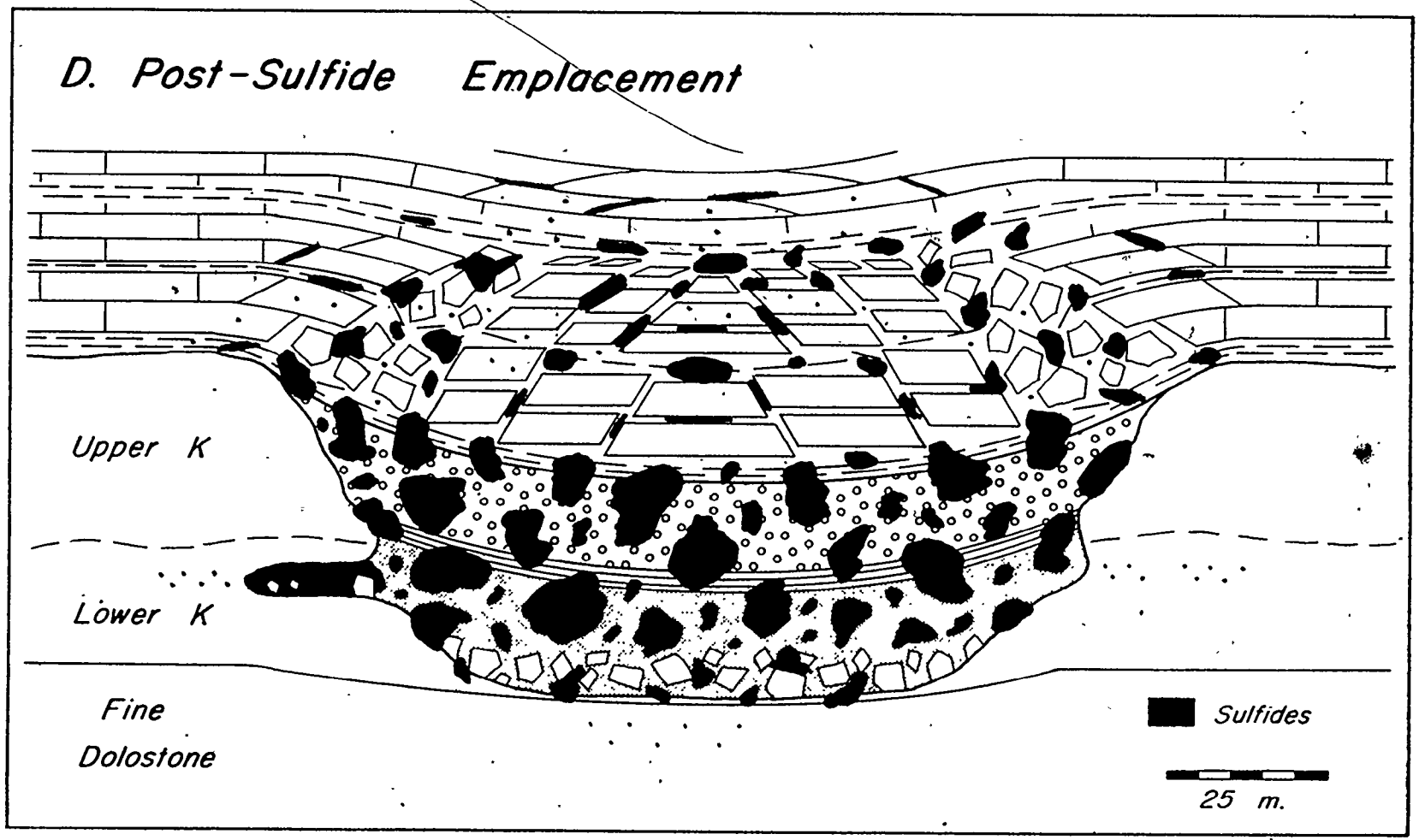

Fig. 31 (continued)

Dissolution proceeded until the entire limestone sequence was penetrated (Fig. 30). Additional dissolution was slowed at this stage, not only by the underlying chemically more resistant fine-crystalline dolostone, but also by hydrologic factors. The position of the meteoric water table may have been controlled indirectly by sea level on the fore-reef side of the exposed barrier (Fig. 9). Since most carbonate dissolution takes place in the upper part of the meteoric phreatic zone (Thrailkill, 1968) which apparently was confined within the upper barrier, extensive dissolution of the fine-crystalline dolostones by meteoric water was greatly inhibited. The water table eventually became relatively stable at a level within the lower part of the limestone units of the upper barrier (Fig. 31A). Lateral dissolution of limestone occurred near the water table adjacent to the dolines, and macropores were developed. Slumping of oversteepened doline walls resulted in a rubble pile of large limestone blocks and finer debris on the doline floor as in the lower detritus zone in K57. Slumping of the doline walls may have effectively sealed off part of the macropores so that they were not completely filled with detritus.

Following the post-middle Givetian erosional period and development of the karstified barrier, marine transgression first affected the low-lying "nearshore" areas, and local tidal flat conditions were established. Periodically, probably during major storms, fine carbonate detritus was swept into the standing body of water in the dolines and sedimented in thin layers (Fig. 31B) as in the laminated detritus in K57. Inundation of the erosional surface was sporadic with

several periods of transgression and minor regression (Wiley, 1970). During the final closing of the erosional period, the regolith developed on the karstified barrier was swept into depressions on the surface, the largest of which were the dolines (Fig. 31B). This erosional material consisted of fine carbonate detritus with some green clay and tidal flat dolostone fragments eroded from the ephemeral tidal flat and lacustrine deposits of initial transgression. This material forms the upper detritus zone in K57. Marine transgression appears to have been effective in filling the dolines. In the A70 area, the waxy green shale which usually overlies the rubble contact also extends across the detritus zone. It and the succeeding intervals are not consistently thicker over the detritus zone, indicating that the doline was completely filled with detritus during marine transgression and that little compaction of detritus occurred during late Givetian sedimentation (Fig. 31C). Collapse of late Givetian strata overlying the detritus zones occurred at least in part as the result of volume reduction during sulfide emplacement (Fig. 31D).

Caves

The sulfide-filled macropores in the lower part of Facies K (e.g. M40, Plate 8) that lack apparent direct connection with the disconformity are interpreted as former caves which developed in the upper part of the phreatic zone during the period of the stable water table (Fig. 30, situation A). Local collapse in the cave system created breccias which now also host sulfide minerals. Extensive dissolution of limestone is readily accomplished by meteoric water which has not

become saturated with respect to calcite due to CO_2 loss during seepage of rainwater through the vadose zone to the water table (Thrailkill, 1968). Therefore, macropores and caves developed in the limestones of the upper Pine Point barrier where a bypass permitted vadose flow instead of vadose seepage to the water table (Fig. 30). The vadose bypasses did not remain open enough to permit complete filling of the caves by detritus during the close of the erosional period.

Other Effects of Subaerial Exposure

Horizons of increased porosity and permeability apparently were created in the upper part of the phreatic zone adjacent to the zones of major dissolution. This process was responsible for creation of most of the hosting porosity for the tabular sulfide concentrations such as M40, which are common in the lower Presqu'ile (Plate 8), particularly along the Main Hinge. The development of horizons of increased permeability probably was controlled by the local supply of meteoric water with the chemical capacity to produce increased porosity. Once meteoric water became saturated with respect to calcite, effective porosity enlargement ceased. This restriction may account for the apparent limited lateral extent of these horizons in the lower Presqu'ile rather than development of a continuous zone of increased permeability along the position of the upper part of the paleo-phreatic zone.

Mineralogic stabilization of skeletal material, that is, conversion from high-Mg calcite and aragonite to low-Mg calcite probably took place in the phreatic zone; this effect has been

demonstrated in modern carbonates (Matthews, 1974; Friedman, 1975). This process resulted in partial preservation of the relic faunal textures in the lower part of the upper barrier limestone (now coarse-crystalline dolostone). Mineralogically unstable skeletal components in the vadose zone were leached by percolating meteoric water, thereby creating abundant void space; the effects of this process are evident in modern vadose environments (Matthews, 1974; Friedman, 1975). After the paleo-vadose zone was buried by post-middle Givetian strata, the vuggy horizons of the upper barrier were subject to loading with eventual void collapse and development of intricately brecciated upper barrier strata. This interval is now represented by the upper part of the Presqu'ile which contains pervasive white dolomite often with breccia-moldic textures (Plate 4).

Another possible effect of meteoric water flushing of the upper barrier is suggested by the nature of the contact between the coarse-crystalline dolostones of Facies K and the underlying fine-crystalline dolostones. Near the detritus zones in the K57 and A70 areas, the upper part of the usually fine-crystalline Facies B dolostone becomes considerably coarser and the faunal components become indistinct. There is no simple geochemical reason why the fluid which converted the upper barrier limestones to coarse-crystalline dolostone and was therefore in equilibrium with dolomite should have any effect on the pre-existing fine-crystalline dolostone. The apparently coarsened dolostones could have resulted from the "presquilization" of incompletely dolomitized limestones, but the association with the detritus zones suggests a more complex mechanism. If meteoric water

with a high Ca/Mg ratio flowed at high rates through the fine-crystalline dolostones (Fig. 20), a situation which would have existed near the dolines, the upper part of the fine-crystalline dolostones might have been calcitized (dedolomitized) locally (De Groot, 1967; Evamy, 1967). Later, this material was converted into coarse-crystalline dolostone with relic color and fauna of the pre-existing fine-crystalline dolostone as the zone of mixed sea water and meteoric water moved upward in the barrier and began to convert limestone to coarse-crystalline dolostone.

The relationship of post-middle Givetian episode of karsification to the sulfide-hosting structures in the fine-crystalline dolostones of the lower barrier complex is unclear. The collapse zone and local rock matrix breccias in W17 bear some resemblance to sulfide-hosting features in the upper barrier, but the upper part of the W17 zone has been eroded, and it is impossible to determine if it originally extended into the upper barrier. None of the Facies K mineralized zones extend for any appreciable distance into the fine-crystalline dolostones. The vuggy and intercrystalline porosity which hosts sulfide minerals in N204 is the result of leaching of mineralogically unstable skeletal components and burrows; such horizons result from vadose leaching in modern carbonates (e.g. Matthews, 1974), but intrastratal dissolution could produce similar effects.

It seems unlikely that the zone of most intensive carbonate dissolution, the upper phreatic, could have extended into the lower levels of the barrier complex during the post-middle Givetian erosional period. However, carbonate dissolution may have occurred in the zone

of mixing of fresh water and sea water which existed within the lower barrier during this period. Another possibility is that the sulfide-hosting structures in the fine-crystalline dolostones resulted from an earlier period of subaerial exposure and carbonate diagenesis, as Maiklem (1971) has proposed for the middle Givetian of the Pine Point barrier complex.

In summary, carbonate diagenesis related to post-middle Givetian subaerial exposure of the Pine Point barrier complex was important in the development of fluid-transporting permeability and of sulfide-hosting features. Dolines were formed by dissolution of the limestones of the upper barrier by meteoric water (Fig. 30). Caves and lateral horizons of increased permeability developed in the limestones in the upper part of the phreatic zone; partial collapse resulted in the formation of local breccias. Mineralogic stabilization and preservation of skeletal components occurred in the phreatic zone; leaching of mineralogically unstable material took place in the vadose zone, thus creating vuggy stratabound horizons in the upper barrier. Calcitization of fine-crystalline dolostone may have occurred in areas of rapid flushing by meteoric water. Conversion of upper barrier limestones to coarse-crystalline Facies K dolostone was accomplished in the zone of mixing of meteoric water and sea water (Fig. 9). Increase in sea level during marine transgression at the cessation of the erosional period resulted in sporadic raising of the level of the various diagenetic environments and filling of the dolines with detritus from the erosional surface. The upper barrier limestones and detritus zones were converted to coarse-crystalline dolostones as the zone of mixed

sea water and meteoric water moved upward through the barrier complex. Dolomitization ceased as the meteoric water supply was terminated by marine inundation of the erosional surface. Following late Givetian and later? sedimentation, "hydrothermal" fluids utilized the aquifer systems and porosity developed during the erosional period to transport and deposit sulfides within the detritus-filled dolines and in open spaces in the paleo-caves. Collapse of late Givetian strata overlying the detritus zones took place during sulfide emplacement in the detritus zones, thus creating additional porosity for sulfide deposition. Neomorphic growth of white dolomite occurred in the intricately brecciated upper part of the coarse-crystalline Presqu'ile dolostone.

CHAPTER FOUR

ORE BODIES

General Characteristics

The Pine Point district consists of about 50 known Pb-Zn-Fe sulfide bodies in an area of about 1,000 square kilometers (Fig. 3); these bodies vary considerably in size, geometry, metal percentages and ratios, sulfide textures, and host rock relationships. Sulfide bodies range in size from less than 100 thousand to as much as 15 million tons and are elongate in a northeasterly direction generally parallel to the Hinge Zones. Individual bodies are stratabound in relatively narrow intervals, but major sulfide bodies occur in several stratigraphic positions in a 200-meter section of the Pine Point barrier complex (Fig. 5). Some ore bodies may be classified as either tabular or prismatic (Skall, 1972), but this division is somewhat artificial because some sulfide zones have both prismatic and tabular concentrations (e.g. K57, A70) and because it separates ore bodies of otherwise similar characteristics (e.g. X15, W17). Most of the sulfide concentrations are incomplete because of erosional truncation, and the following discussion will reflect the current nature of the sulfide bodies at different levels of preservation.

The metal content of the ore bodies ranges from about 3 to 11.5 percent Zn and from about 0.8 to 9 percent Pb; the district average

is about 5.8 percent Zn and 2.2 percent Pb (Fig. 32). The combined Zn-Pb content of the bodies ranges from about 3 to 20.5 percent (Fig. 33). Significant tonnages of massive ore exist in some ore bodies and account for almost 1.5 million tons of direct shipping material averaging over 45 percent combined Pb-Zn (Table 1). The Fe content of the ore bodies varies from less than 0.5 to about 10.5 percent with a district average of about 3.5 percent (Fig. 33). Some relatively small "barren" sulfide bodies consist of Fe sulfides with only minor Pb and Zn.

The Zn/(Pb + Zn) ratios of the Pine Point sulfide bodies range from 0.4 to 0.9 with a district average of about 0.7 (Fig. 34). The strongest peak at about 0.75 is greatly influenced by the large X15 ore body with this ratio. The Fe/(Pb + Zn + Fe) ratios of the Pb-Zn ore bodies range from about 0.05 to 0.6 (Fig. 35). The district average is about 0.3, but several distinct peaks are evident. Again, the strongest peak at about 0.5 is dominated by the X15 ore body. The small "barren" Fe sulfide bodies have Fe/(Pb + Zn + Fe) ratios greater than 0.9.

A plot of the Pb-Zn-Fe ratios of individual sulfide bodies indicates considerable variation within the district (Fig. 36). Although these ratios are for incompletely preserved sulfide bodies, the apparent absence of vertical metal zoning within individual bodies and the presence of district-wide metal zoning (to be discussed in following sections) suggest that these ratios reflect real variations. Ore bodies in which the greatest sulfide content is in a prismatic zone, particularly those within the upper barrier, are usually Pb-rich

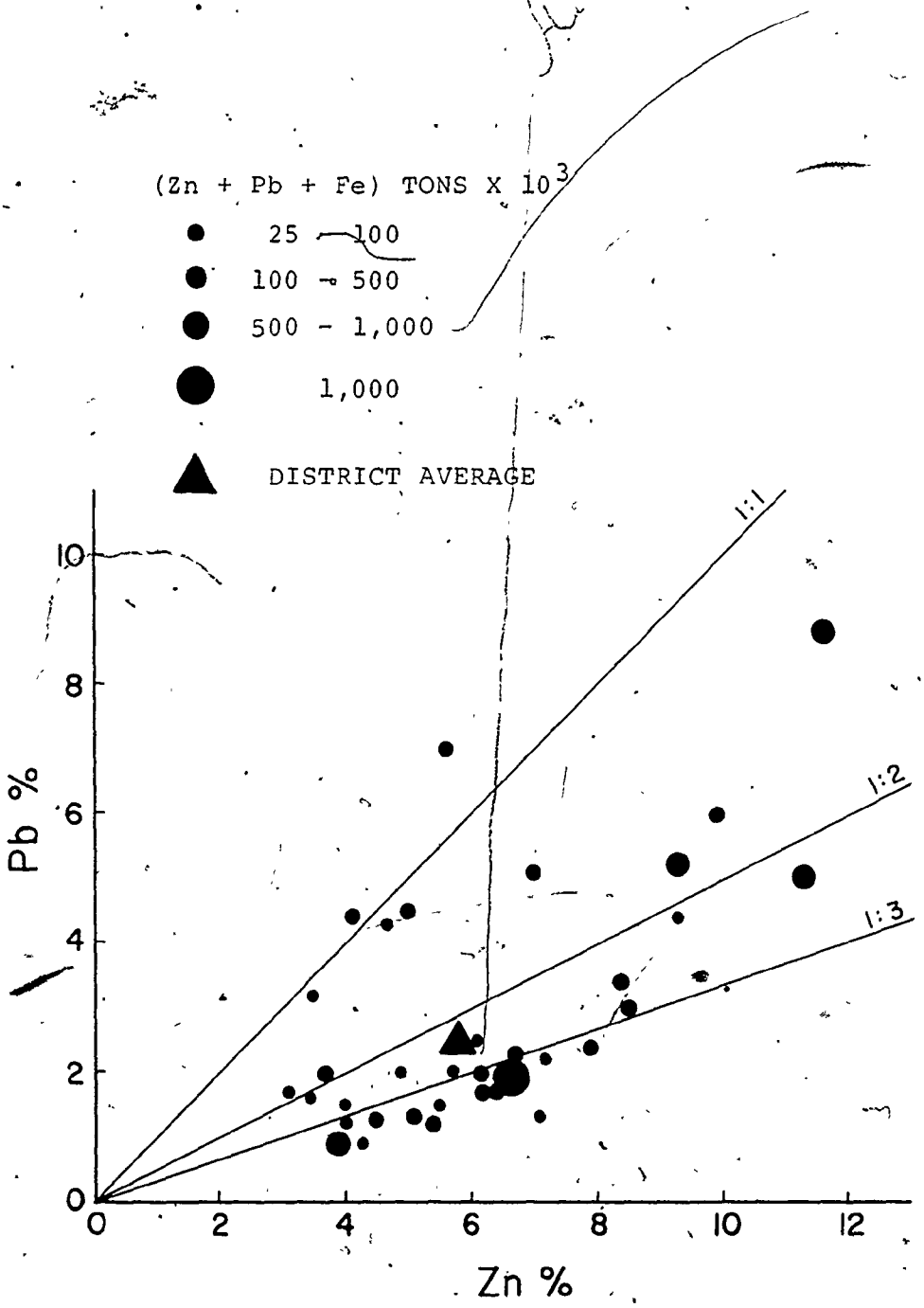

Fig. 32. Weight Percent of Pb and Zn in Major Ore Bodies

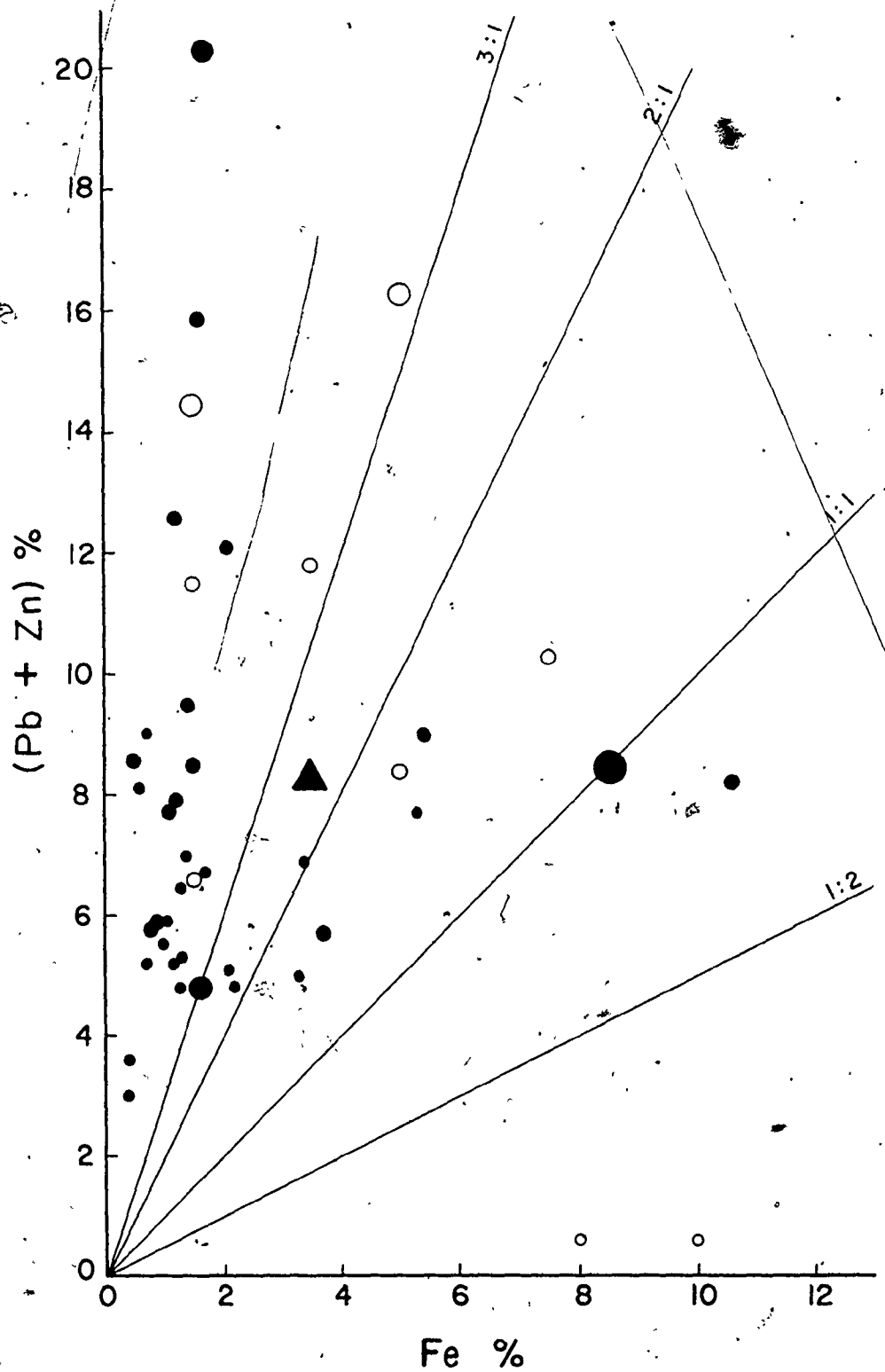

Fig. 33. Weight Percent of Combined Pb-Zn and Fe in Major Sulfide Bodies

Data points as defined in Fig. 32; open circles indicate deposits for which one or more metal percentages are poorly defined by present data.

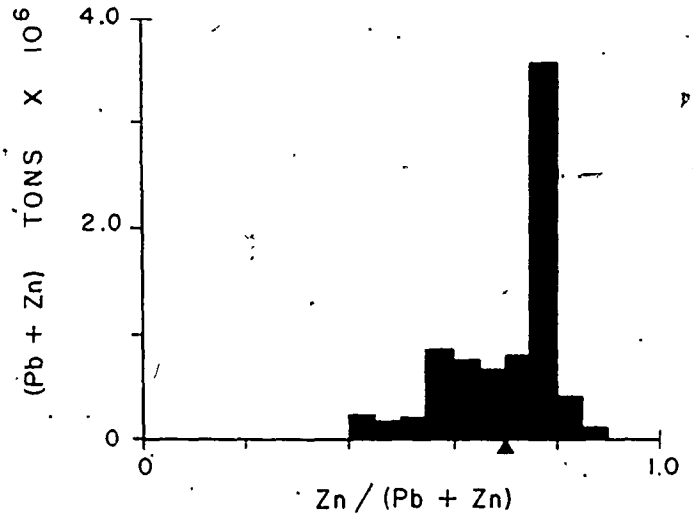

Fig. 34. Zn/(Pb + Zn) Ratios for Cumulative Ore Tonnages

Defined by ore reserve data for individual ore bodies; triangle is district weighted average.

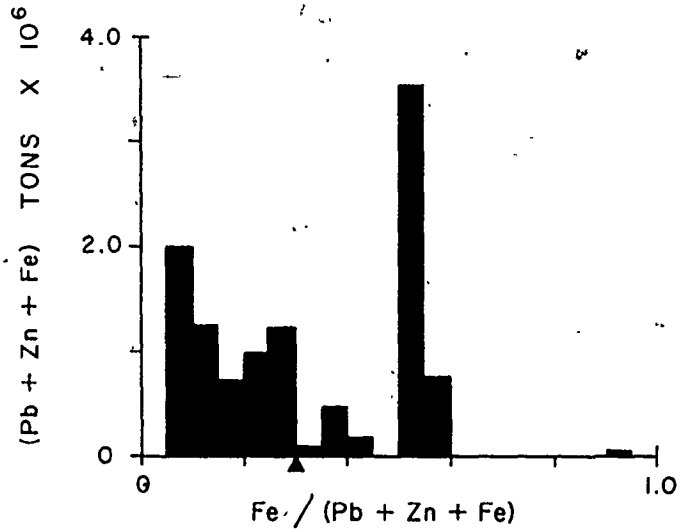

Fig. 35. Fe/(Pb + Zn + Fe) Ratios for Cumulative Ore Tonnages

Defined by ore reserve data for individual ore bodies; triangle is district weighted average.

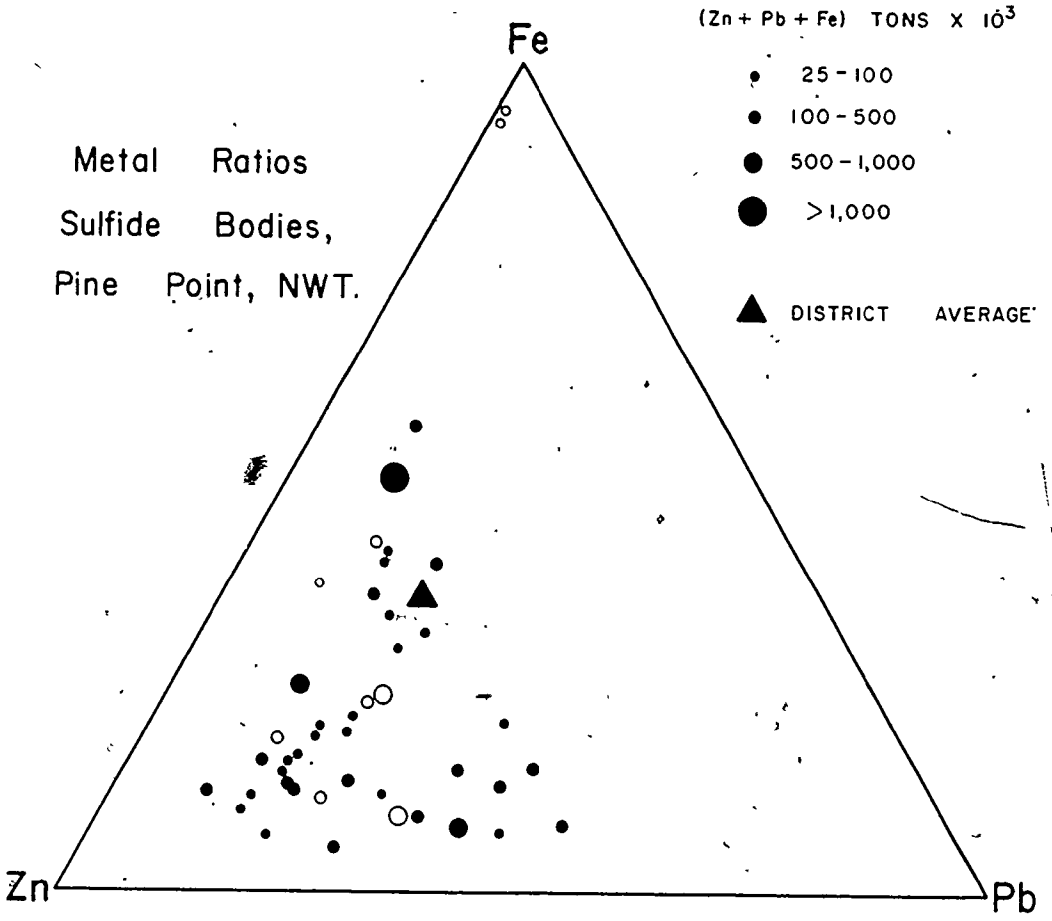

Fig. 36.. Pb-Zn-Fe Ratios of Major Sulfide Bodies

Open circles indicate those deposits for which one or more metal percentages, usually Fe, are poorly defined by present data; district average is weighted.

with Pb/(Pb + Zn) averaging about 0.4. Conversely, tabular ore bodies are relatively Zn-rich with Pb/(Pb + Zn) averaging less than 0.3. There does not appear to be a consistent relationship between geometry and Fe content of the sulfide bodies.

Zoning of Major Metals

District

A district-wide pattern of major metal zoning can be demonstrated using metal ratios determined from ore reserve data. The Pb/(Pb + Zn) ratios of ore bodies increase from about 0.2 in the southeast to about 0.5 in the northwest in zones parallel to the Main Trend (Fig. 37). A similar pattern, less well defined by present data, exists along the North Trend of ore bodies. The Fe/(Pb + Zn + Fe) ratios decrease strikingly from about 0.5 in the southeast to about 0.1 in the northwest in zones parallel to the Main Trend (Fig. 38). Again, a similar pattern exists along the North Trend. Three barren Fe sulfide bodies fit well in this pattern as determined by the metal ratios of all ore bodies (Fig. 38).

The weighted averages of Pb, Zn, and Fe from sulfide bodies in various stratigraphic positions within the Pine Point barrier suggest weak vertical metal zoning within the district (Table 5). Although the stratigraphic distribution of major sulfide bodies does not permit statistical verification of metal trends, sulfide bodies in the upper barrier (Facies K, L, M) have relatively higher Pb and lower Fe than those in the lower barrier (Facies A, D, J). However, there is

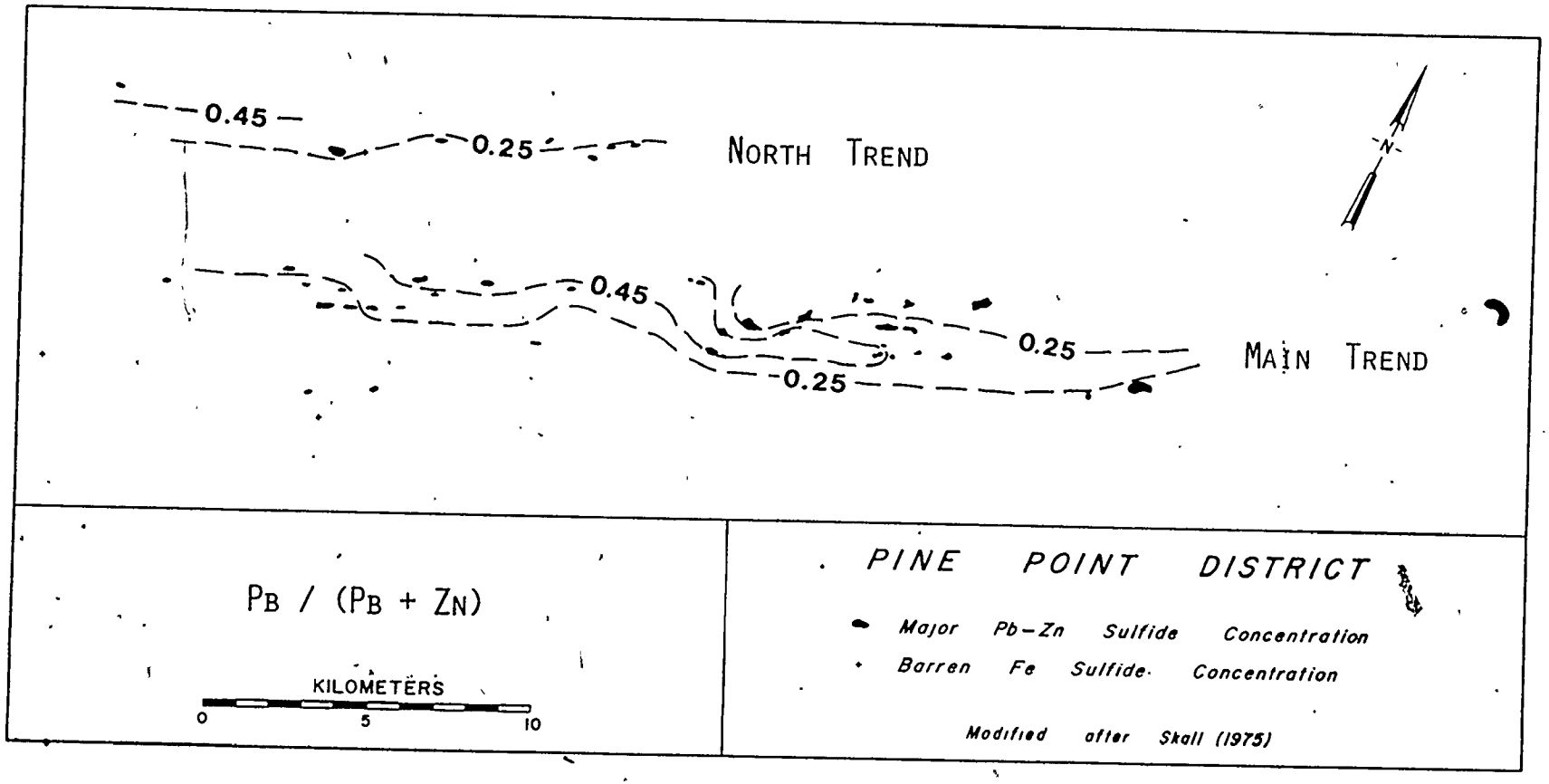

Fig. 37. District Contour Plot of Pb/(Pb + Zn) Ratios of Ore Bodies

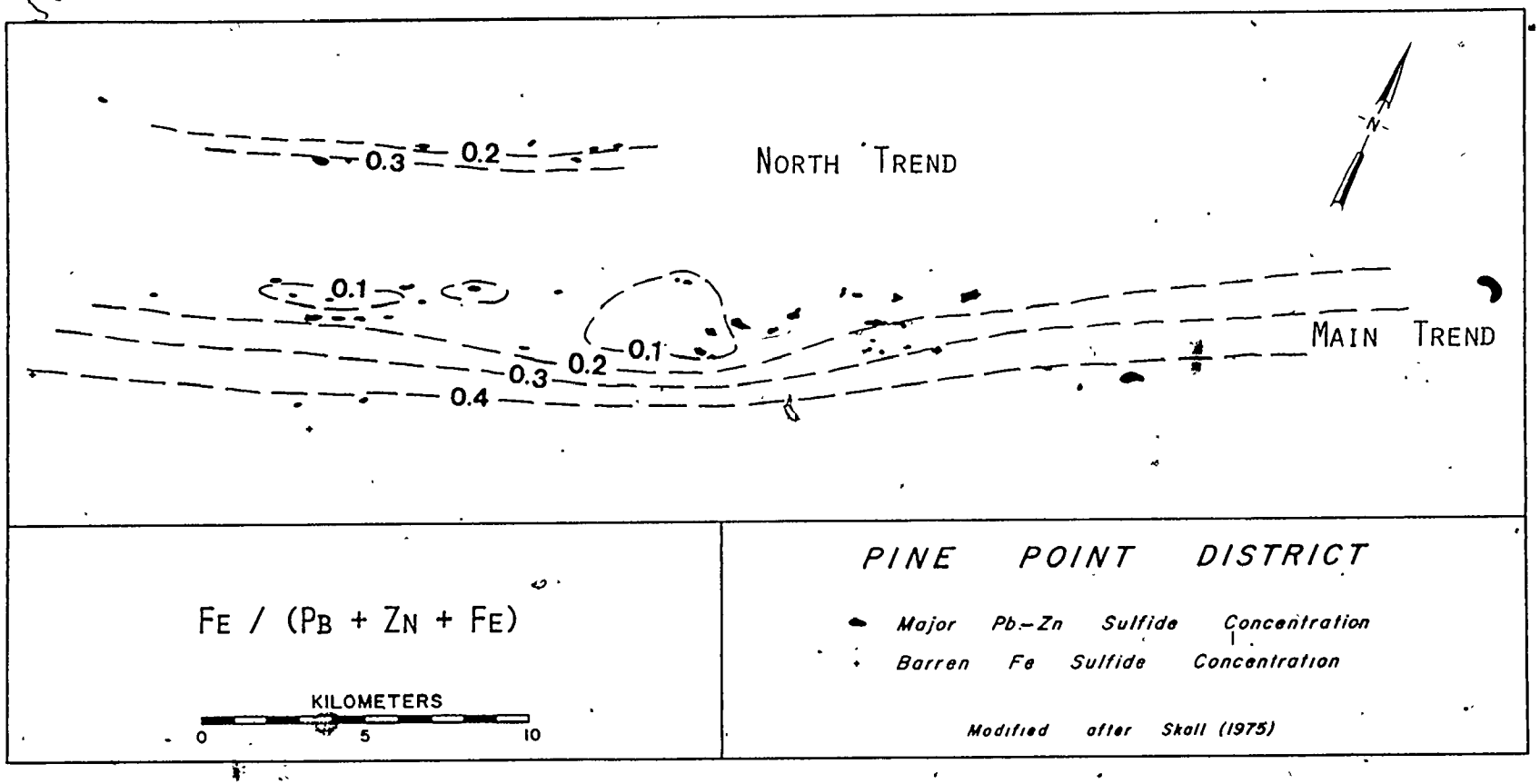

Fig. 38. District Contour Plot of Fe/(Pb + Zn + Fe) Ratios of Ore Bodies

TABLE 5

Metal Ratios of Sulfide Bodies Relative to Hosting Facies

Dominant Host Rock Facies	Total Number Sulfide Bodies	Number Sulfide Bodies 100,000 Tons (Pb + Zn)	Cumulative Tons (Pb + Zn) X 10^6	Pb/(Pb + Zn)	Fe/(Pb + Zn + Fe)
K, L, M	50	17	5.6	0.33	0.17
J, D	2	2	2.1	0.23	0.49
A	1	1	0.8	0.20	0.27

considerable variation in the metal ratios of the upper barrier ore bodies, and some (e.g. A70, R61) have metal ratios similar to the sulfide bodies of the lower barrier.

Individual Sulfide Bodies

K57

K57 is a prismatic sulfide body with an adjacent discontinuous tabular sulfide zone (Figs. 39, 40); some intervals of essentially massive sphalerite and galena are present with over 75 weight percent combined Pb-Zn (Fig. 40). Preproduction ore reserves were 1.8 million tons averaging 7.0 percent Pb, 5.6 percent Zn, and 1.2 percent Fe. The high grade portion is about 150 meters long and a maximum of about 75 meters wide; it contains a maximum of 38.7 weight percent combined Pb-Zn over a 53-meter interval (Fig. 39). Major amounts of Pb are restricted to the prismatic zone and reach a maximum of 32.9 percent in the northeastern part (Fig. 41). Maxima of 14.3 percent Zn (Fig. 42) and 3.7 percent Fe (Fig. 43) are reached in the prismatic zone. The Pb/(Pb + Zn) ratio increases from 0.3 on the periphery of the sulfide body to 0.7 in the center (Fig. 44), thus reflecting the Zn-rich zone surrounding the Pb-rich core. The relative abundance of Fe in the perimeter of the sulfide body is shown by outward increase of Fe/(Pb + Zn + Fe) from less than 0.1 to 0.3 (Fig. 45). There does not appear to be a simple vertical metal zonation (Figs. 46, 47); instead, zoning appears to consist of a three-dimensional Fe envelope around the Pb-rich center.

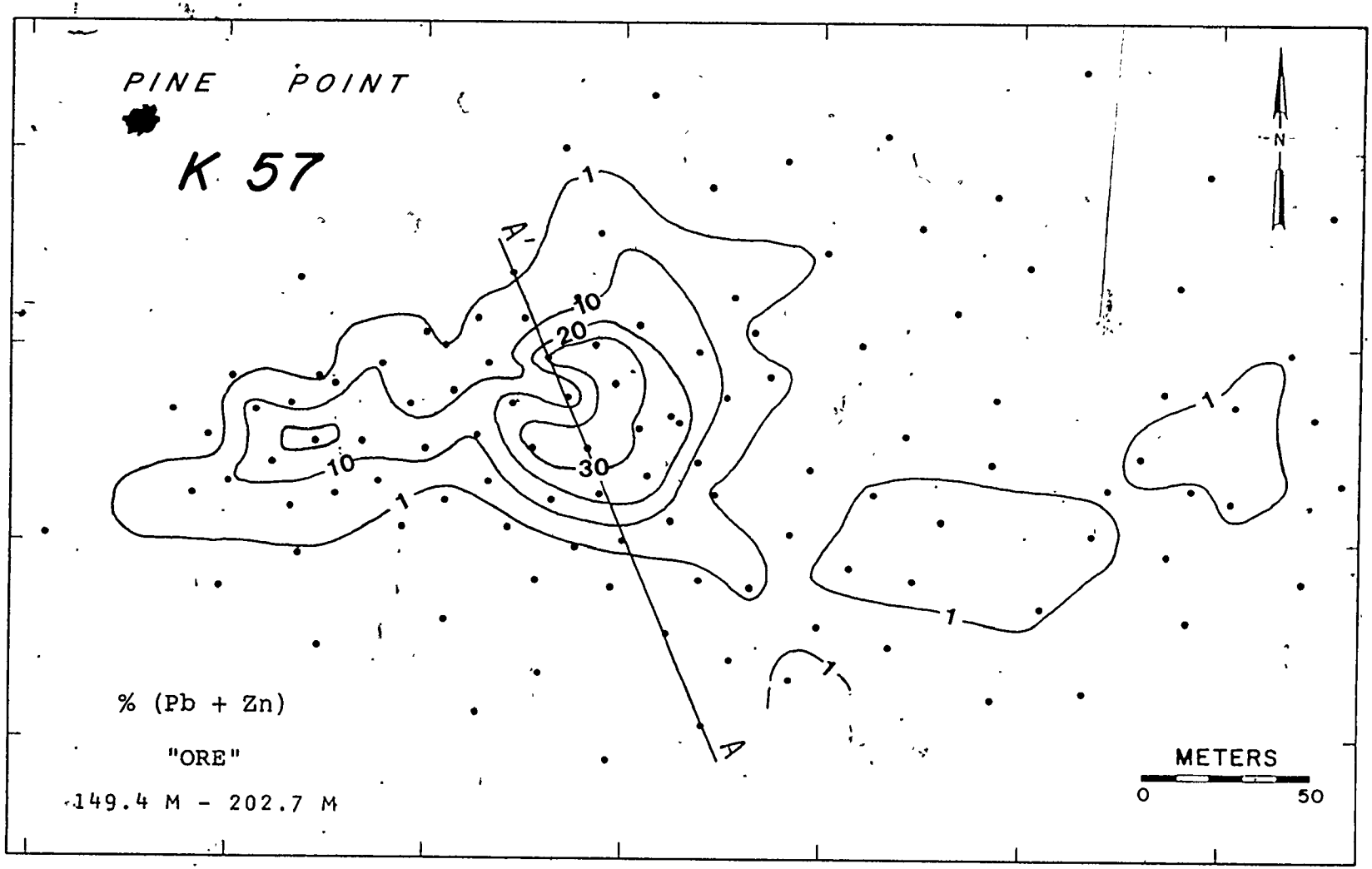

Fig. 39. K57 Ore Body, % (Pb + Zn), 149.4 m - 202.7 m

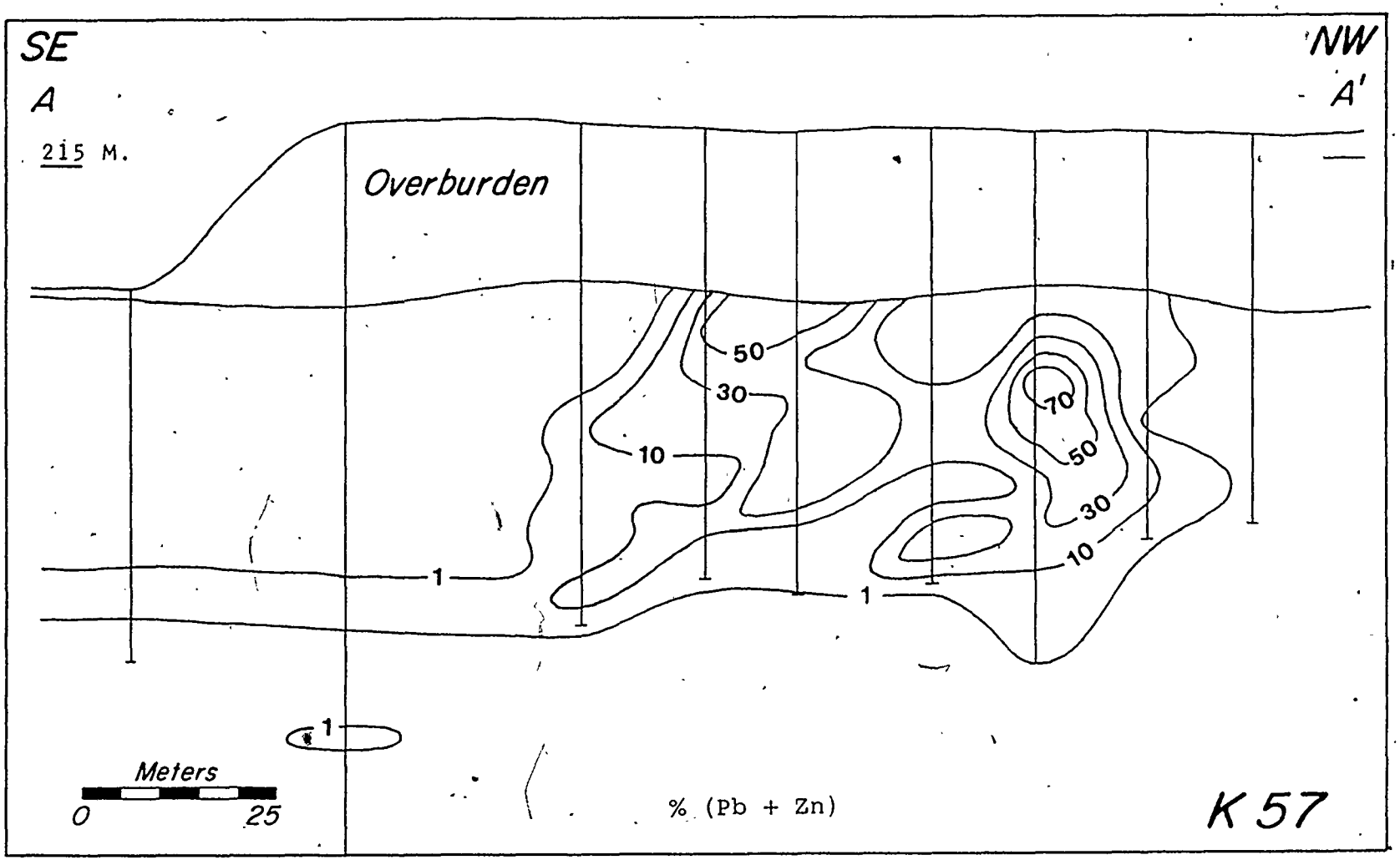

Fig. 40. K57 Ore Body, % (Pb + Zn), Section A-A'

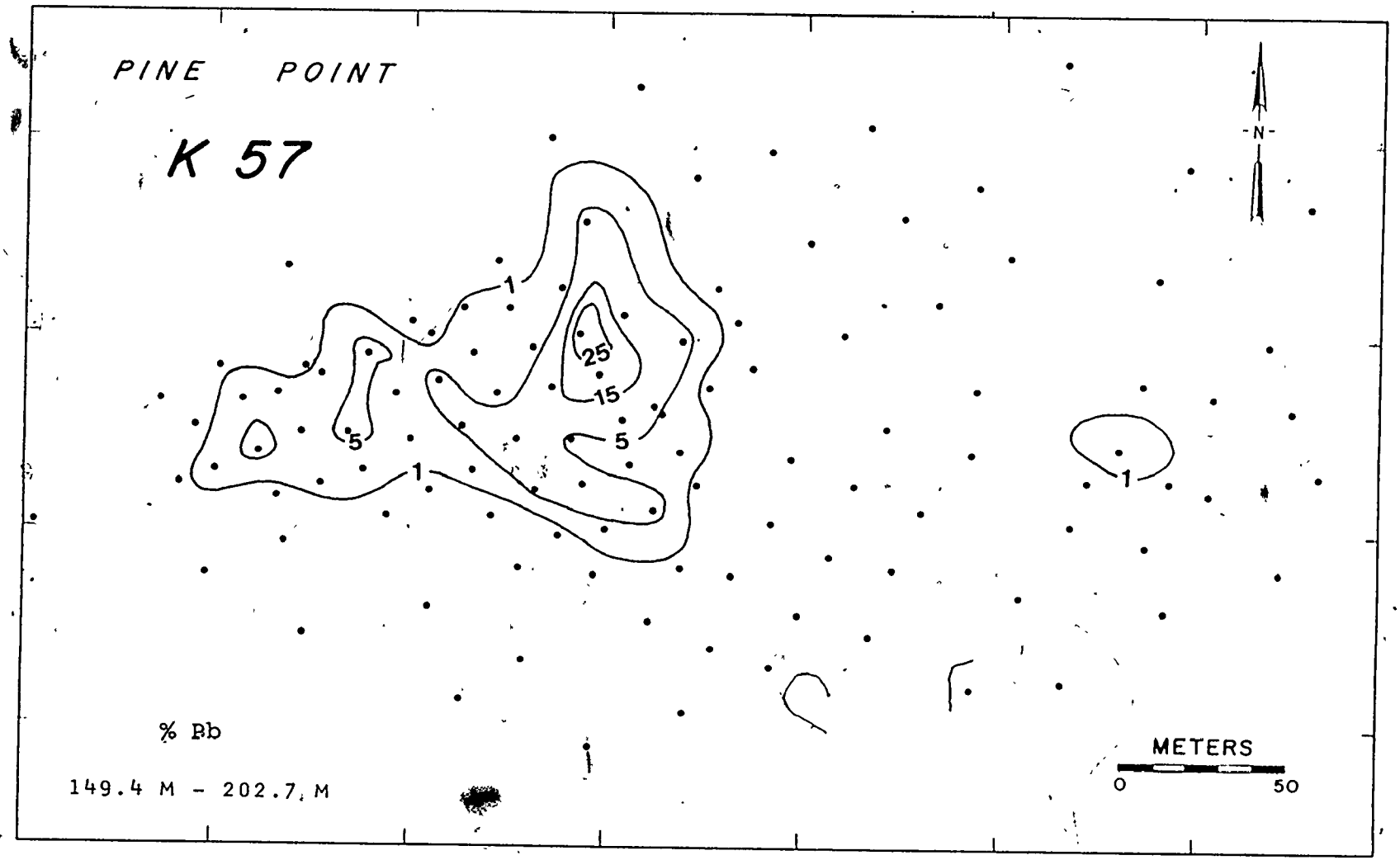

Fig. 41. K57 Ore Body, % Pb, 149.4 m - 202.7 m

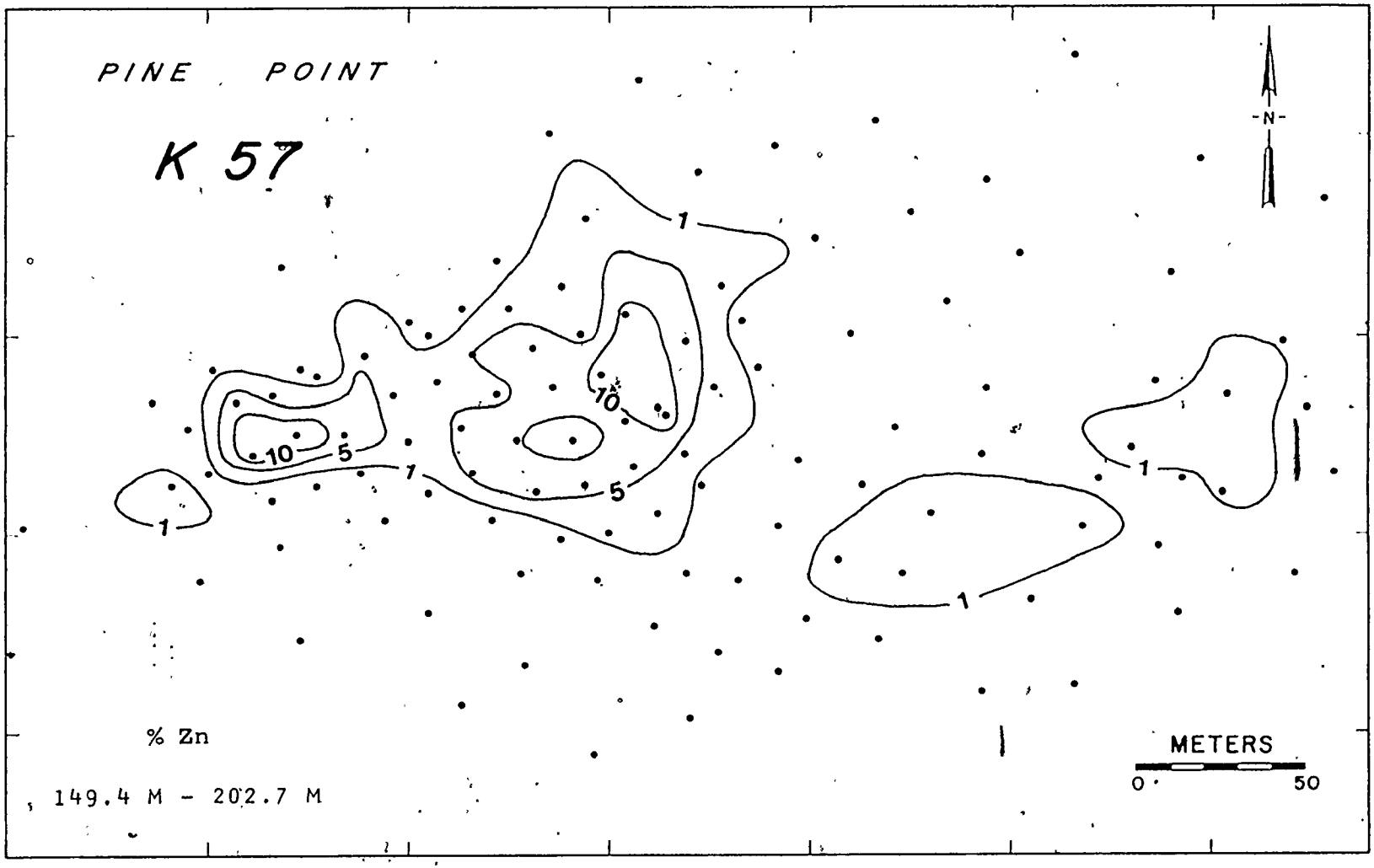

Fig. 42. K57 Ore Body, % Zn, 149.4 m - 202.7 m

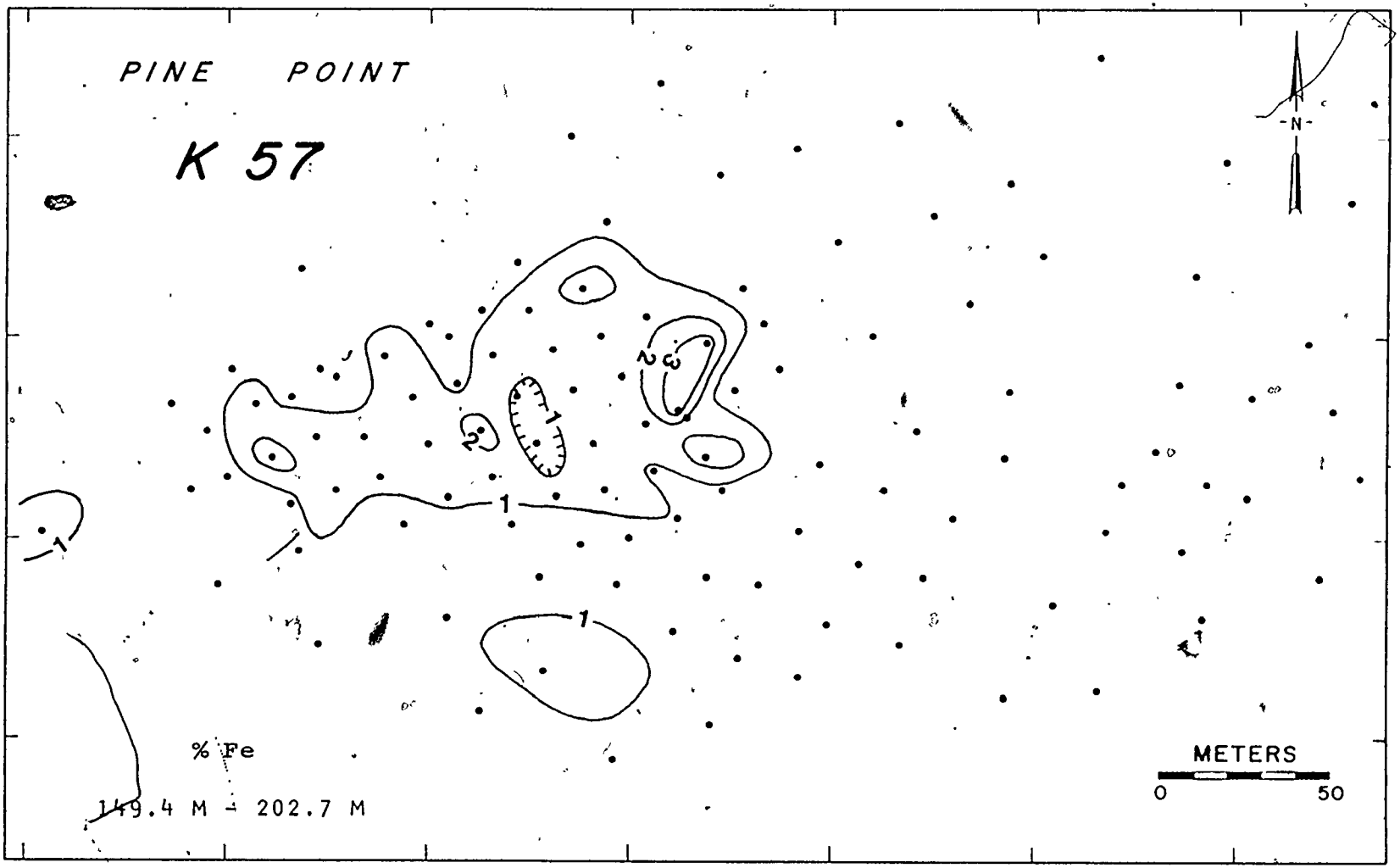

Fig. 43. K57 Ore Body, % Fe, 149.4 m - 202.7 m

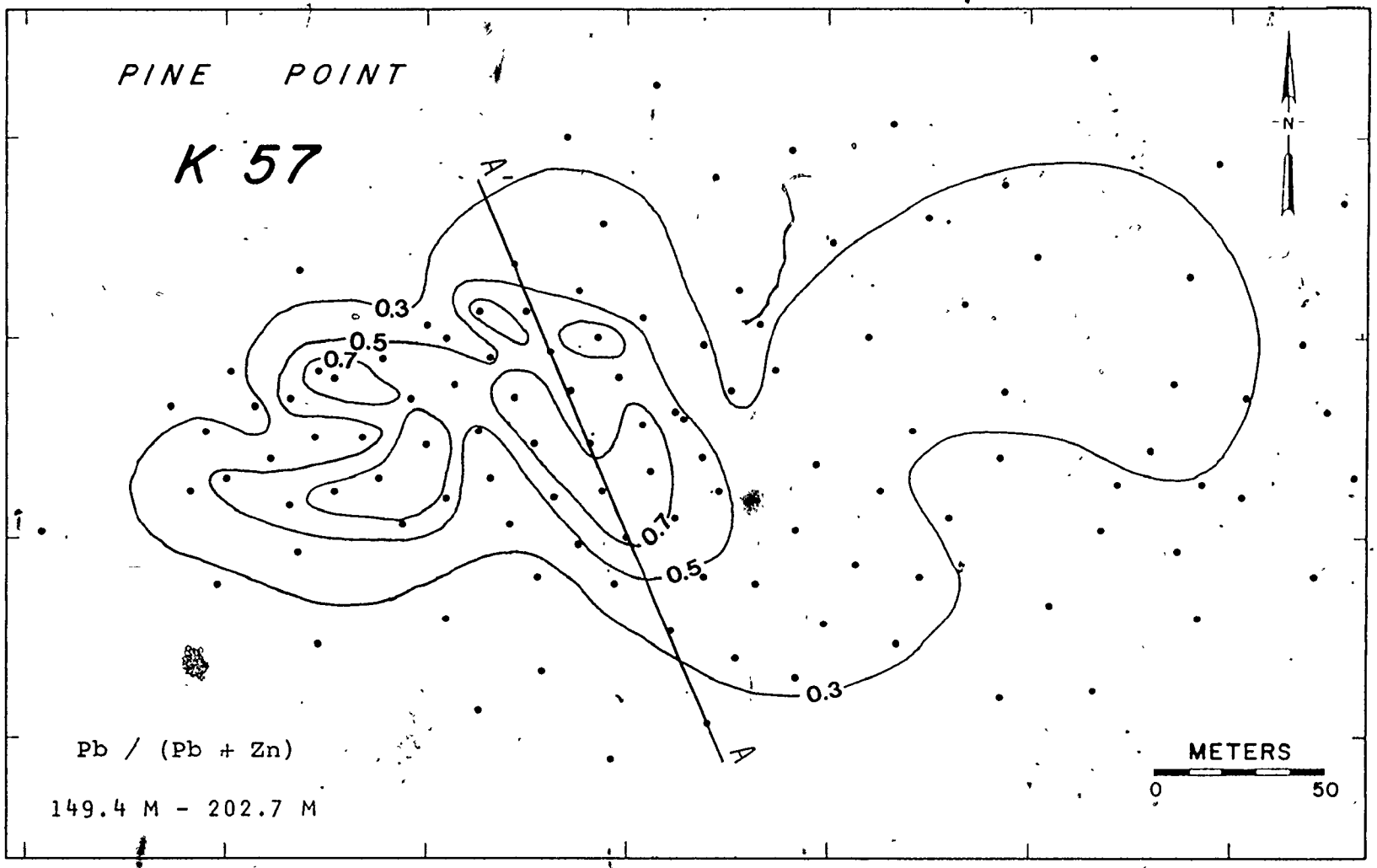

Fig. 44. K57 Ore Body, Pb/(Pb + Zn), 149.4 m - 202.7 m

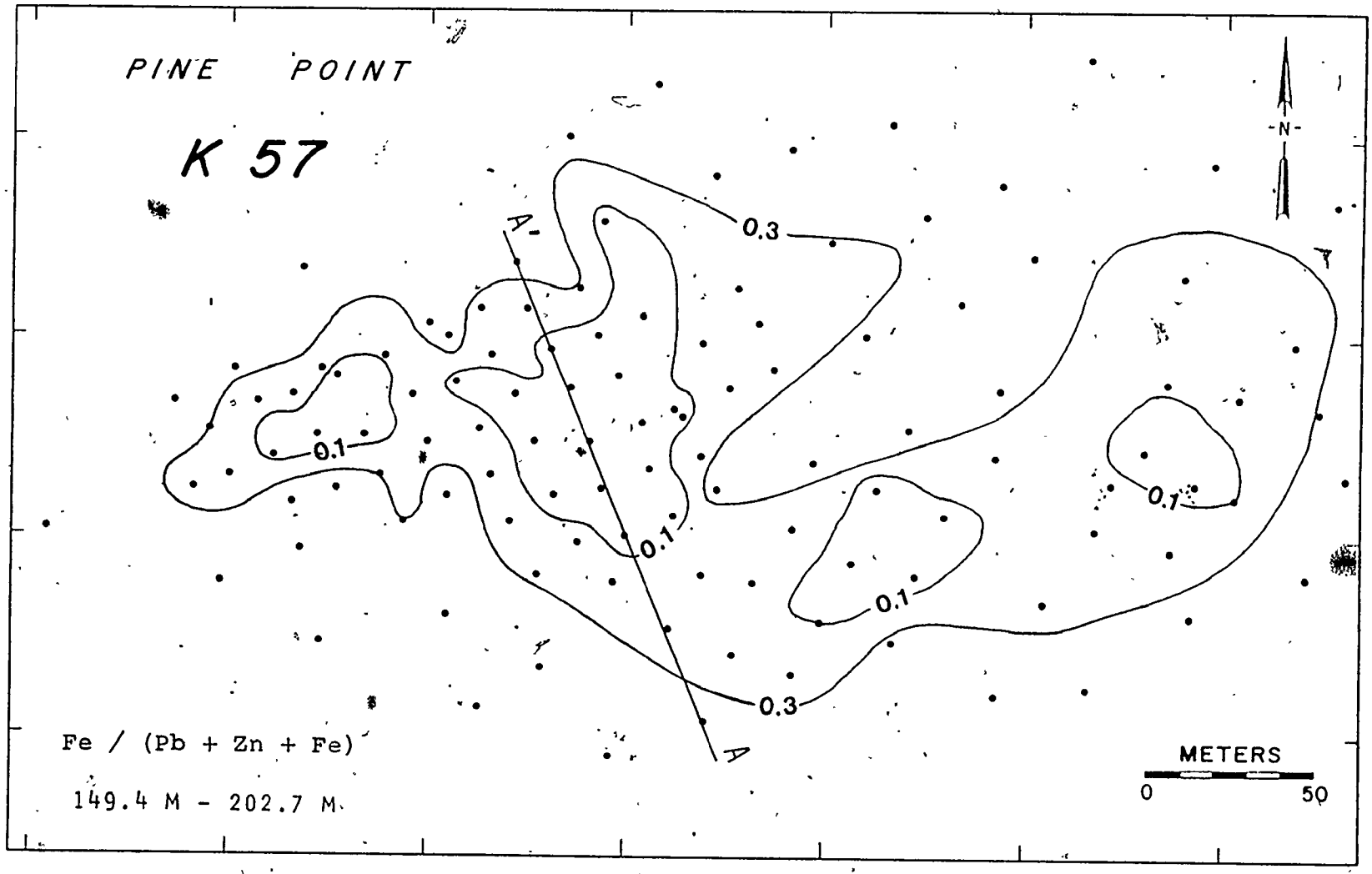

Fig. 45. K57 Ore Body, Fe/(Pb + Zn + Fe), 149.4 m - 202.7 m

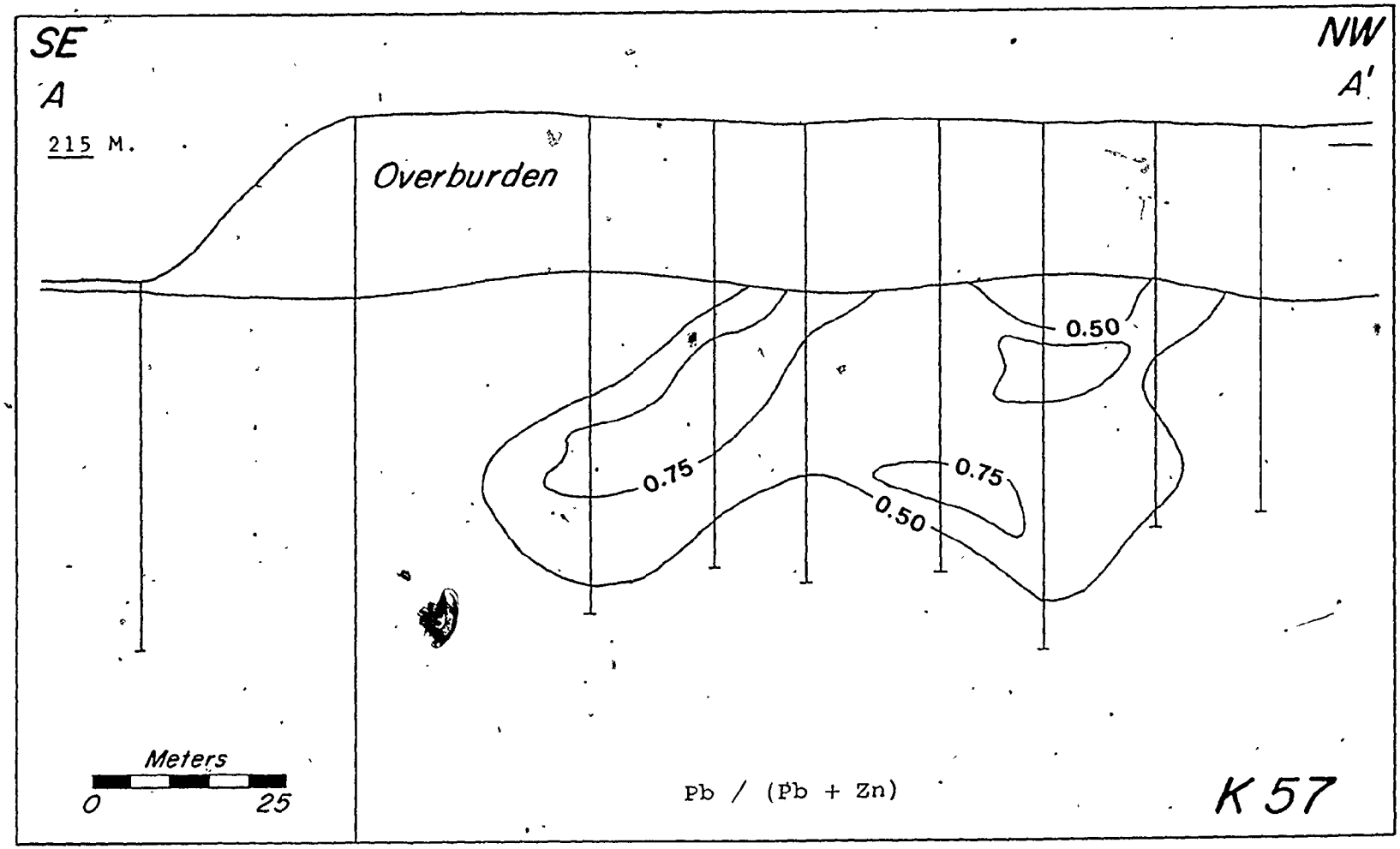

Fig. 46. K57 Ore Body, Pb/(Pb + Zn), Section A-A'

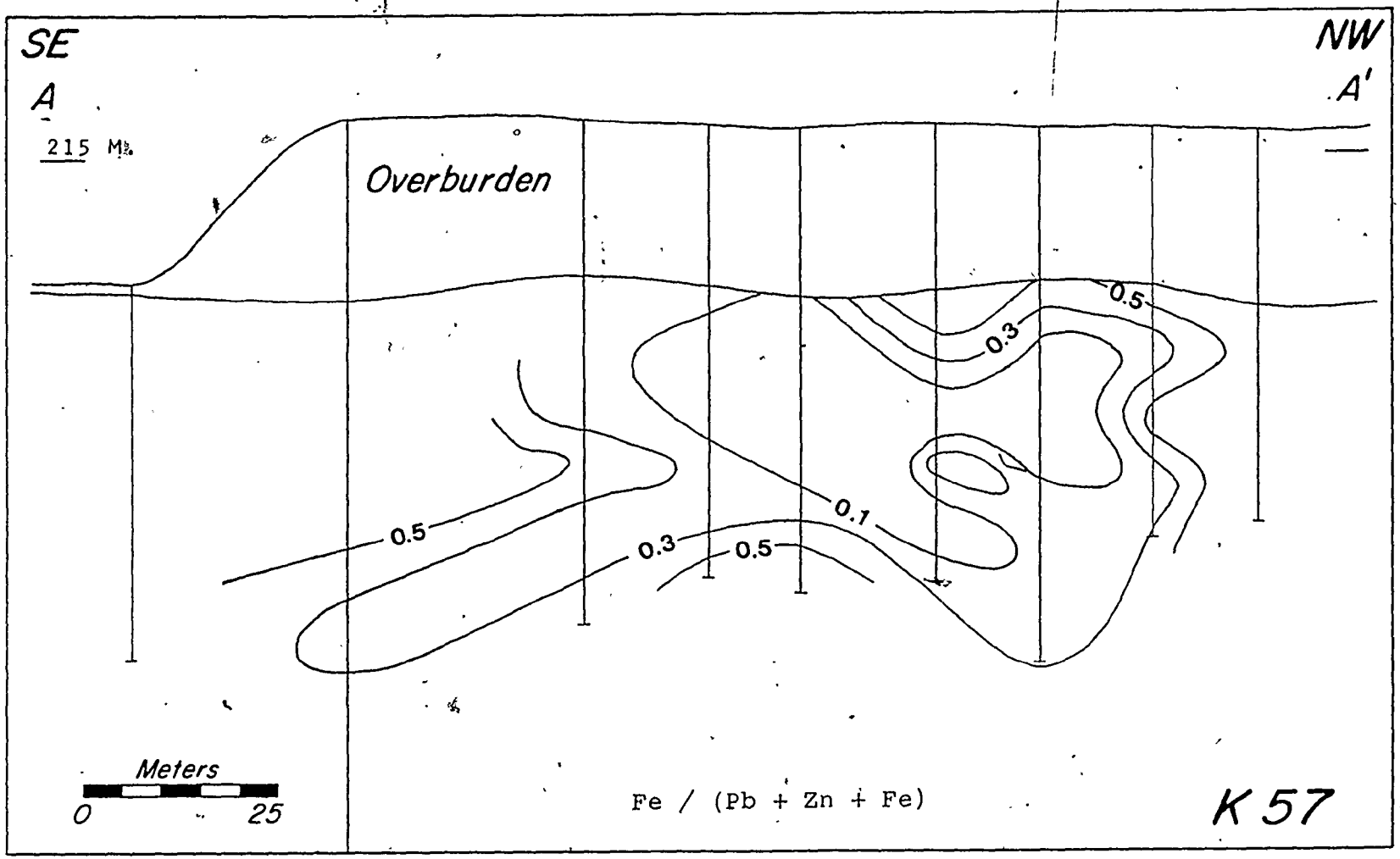

Fig. 47. K57 Ore Body, Fe/(Pb + Zn + Fe), Section A-A'

A70

A70 is a prismatic sulfide body (Figs. 48, 49) containing 2.8 million tons of ore averaging 5.0 percent Pb, 11.3 percent Zn, and about 5 percent Fe. An extensive contiguous tabular sulfide zone containing primarily Fe sulfides with only minor Pb and Zn is present northeast and southwest of the ore body (Fig. 24). The high grade core is about 200 meters long and 80 meters wide and contains a maximum of 27.8 percent combined Pb-Zn over a 53-meter interval (Fig. 48). Major amounts of Pb and Zn are restricted to the prismatic body and reach maxima of 8.8 and 19.6 percent, respectively (Figs. 50, 51). Iron content of the ore body is quite variable and attains a maximum of about 7 percent around the perimeter of the prismatic body (Fig. 52). The relative abundance of Pb in the high grade core is shown by the increase of Pb/(Pb + Zn) from 0.25 around the periphery to 0.35 in the center (Fig. 53). There appears to be a decrease in relative Pb content from south to north as reflected by the decrease of Pb/(Pb + Zn) from more than 0.3 to less than 0.2 (Fig. 54). The abundance of Fe on the perimeter of the prismatic body is shown by the marked increase of Fe/(Pb + Zn + Fe) from more than 0.7 to less than 0.1 (Fig. 55). Again, metal distribution consists of a three-dimensional Fe envelope around the Zn-rich zone which surrounds the Pb-rich center (Figs. 53-56).

W17

W17 is a prismatic sulfide body (Figs. 57, 58) containing preproduction ore reserves of 3.9 million tons averaging 2.0 percent Pb, 6.2 percent Zn, and 10.6 percent Fe. The high grade portion is about

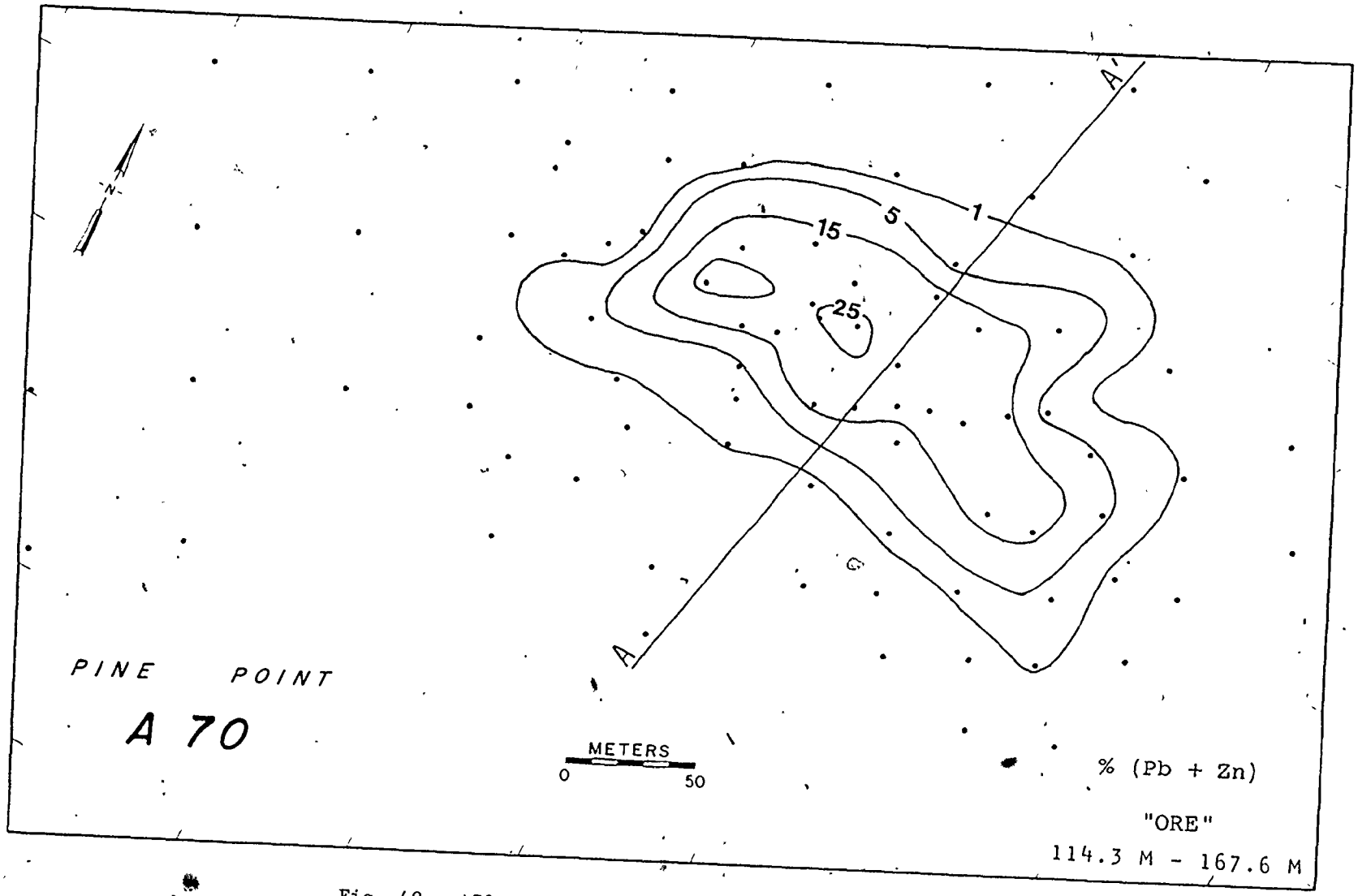

Fig. 48. A70 Ore Body, % (Pb + Zn), 114.3 m - 167.6'm

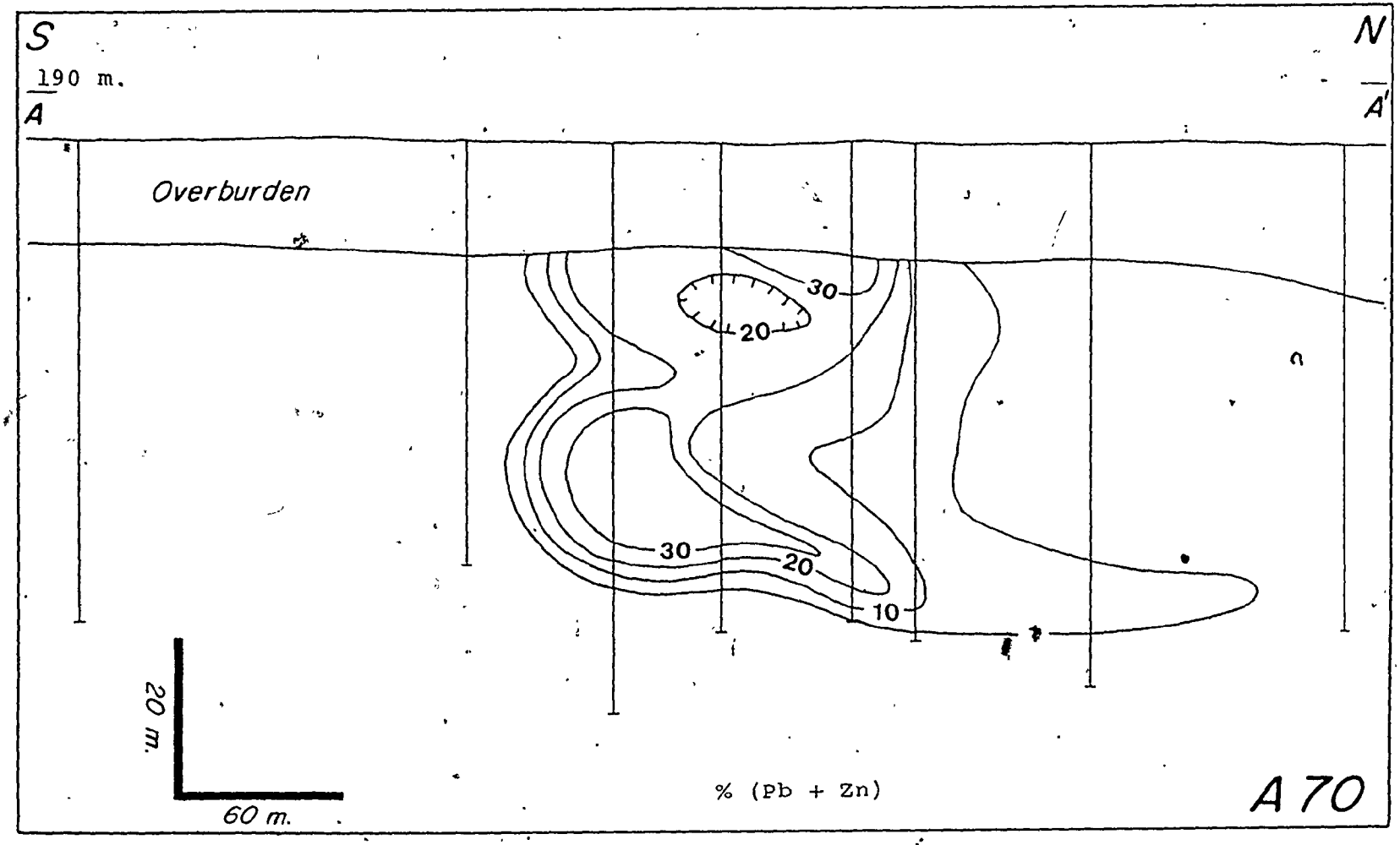

Fig. 49. A70 Ore Body, % (Pb + Zn), Section A-A'

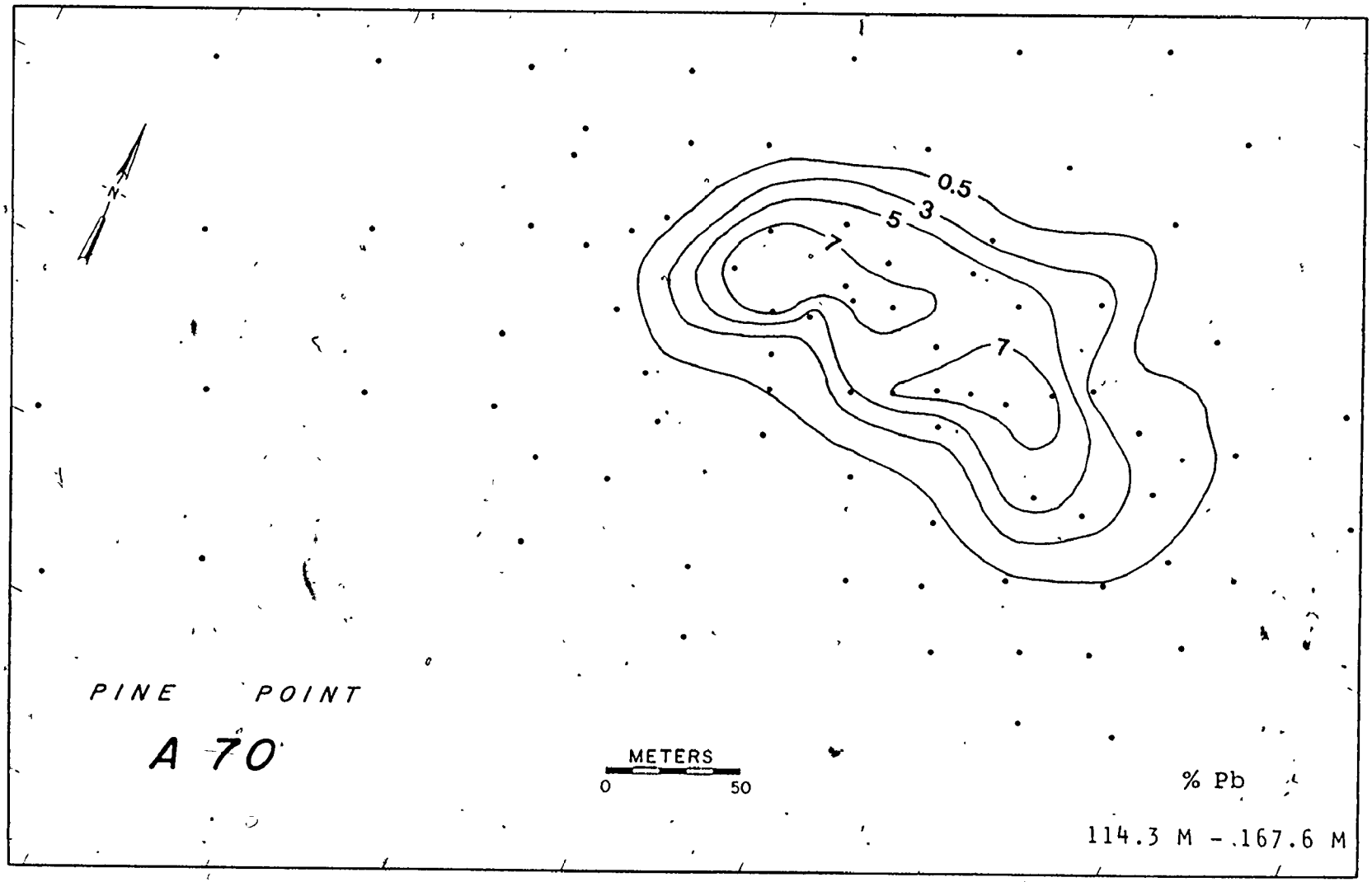

Fig. 50. A70 Ore Body, % Pb, 114.3 m - 167.6 m

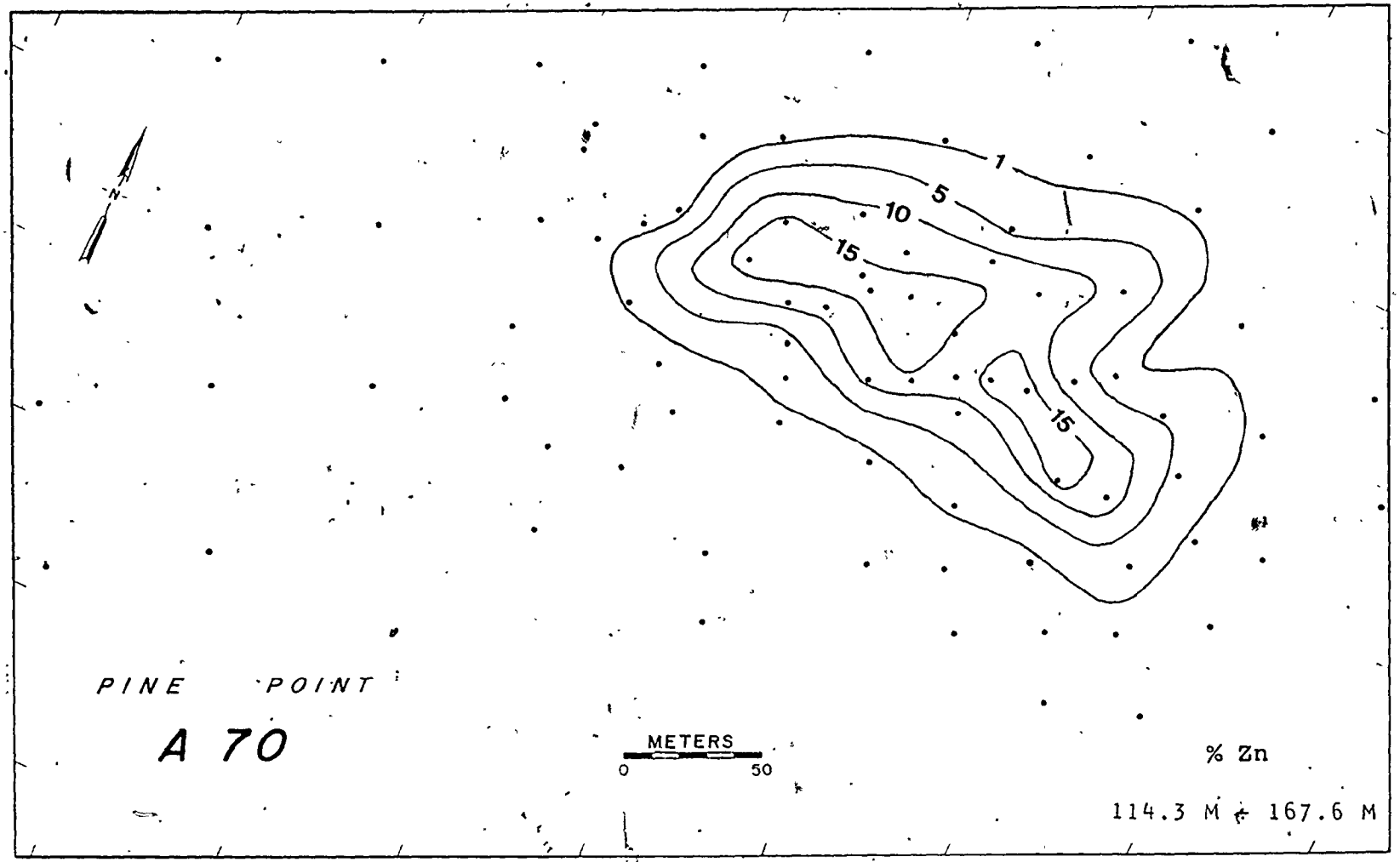

Fig. 51. A70 Ore Body, % Zn, 114.3 m - 167.6 m

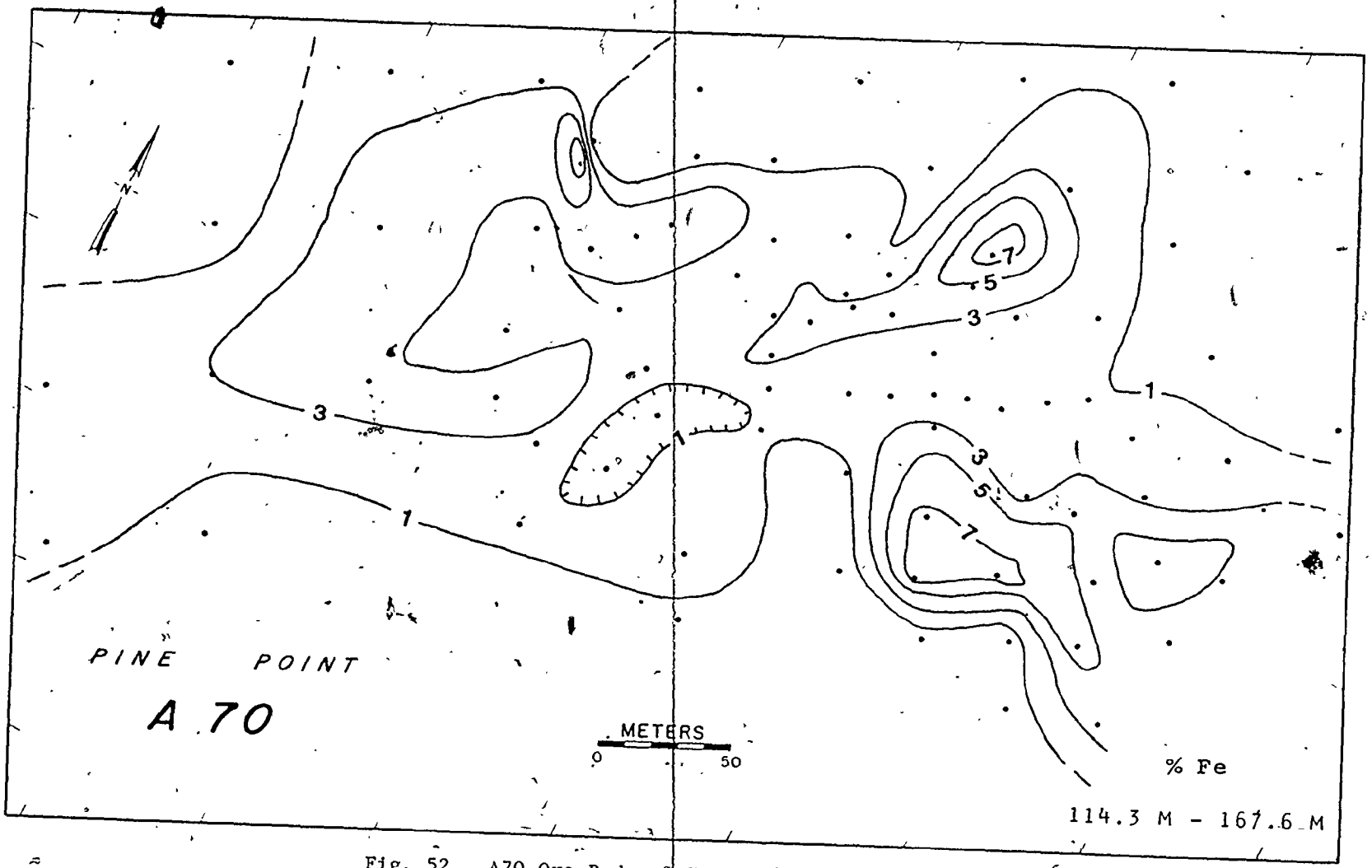

Fig. 52. A70 Ore Body, % Fe, 114.3 m - 167.6 m

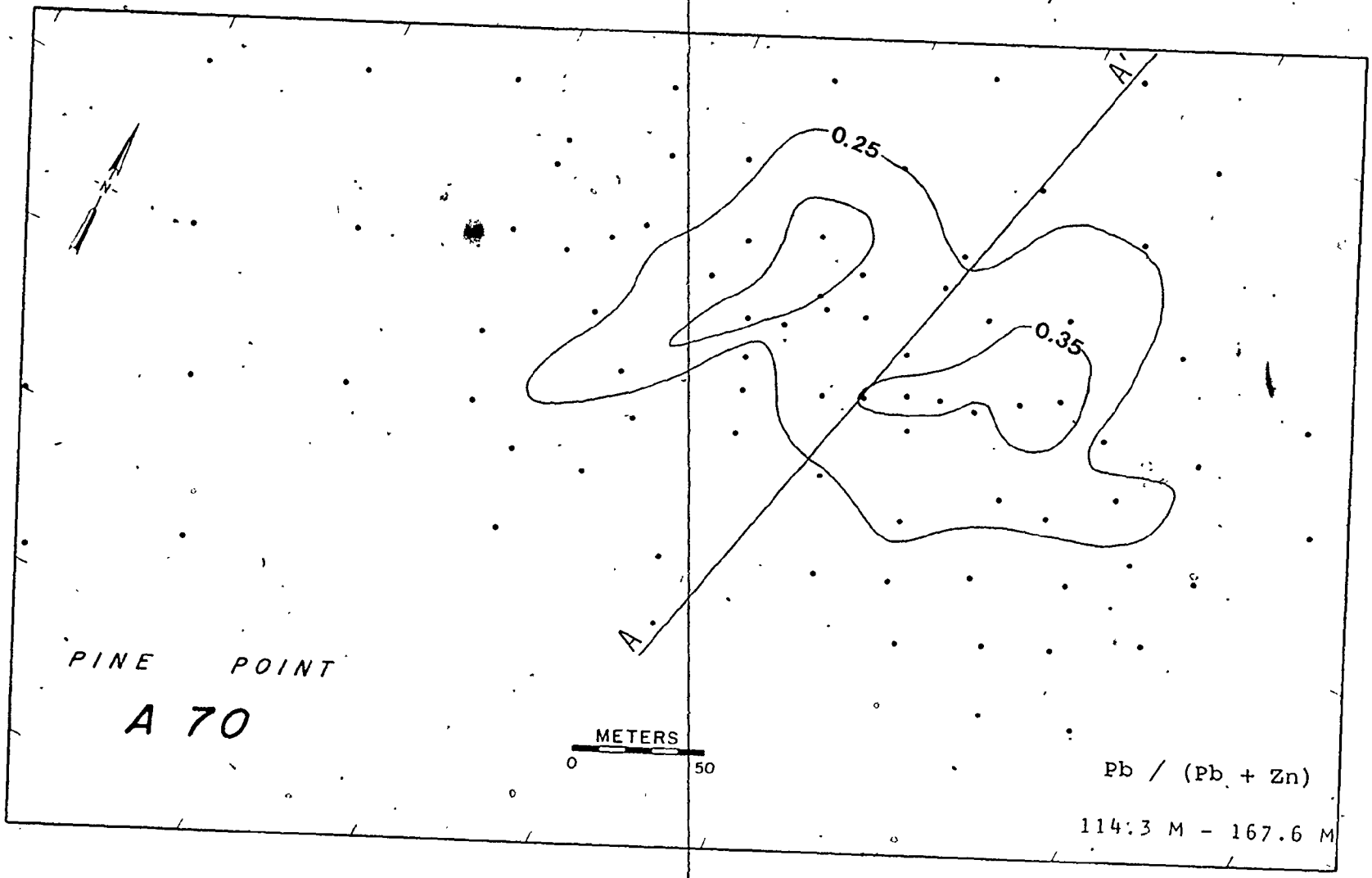

Fig. 53. A70 Ore Body, Pb/(Pb + Zn), 114.3 m - 167.6 m

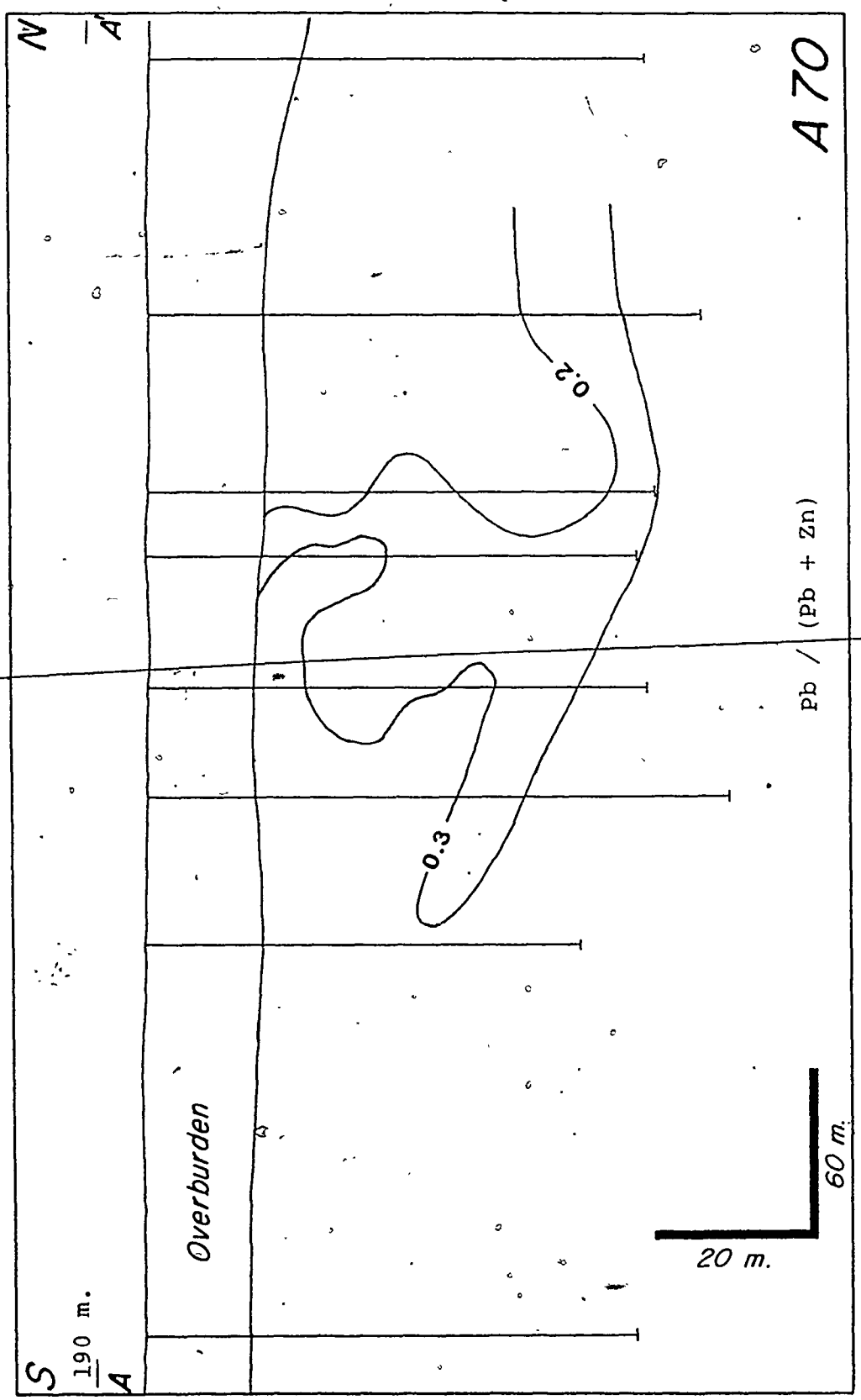

Fig. 54. A70 Ore Body, Pb/(Pb + Zn), Section A-A'

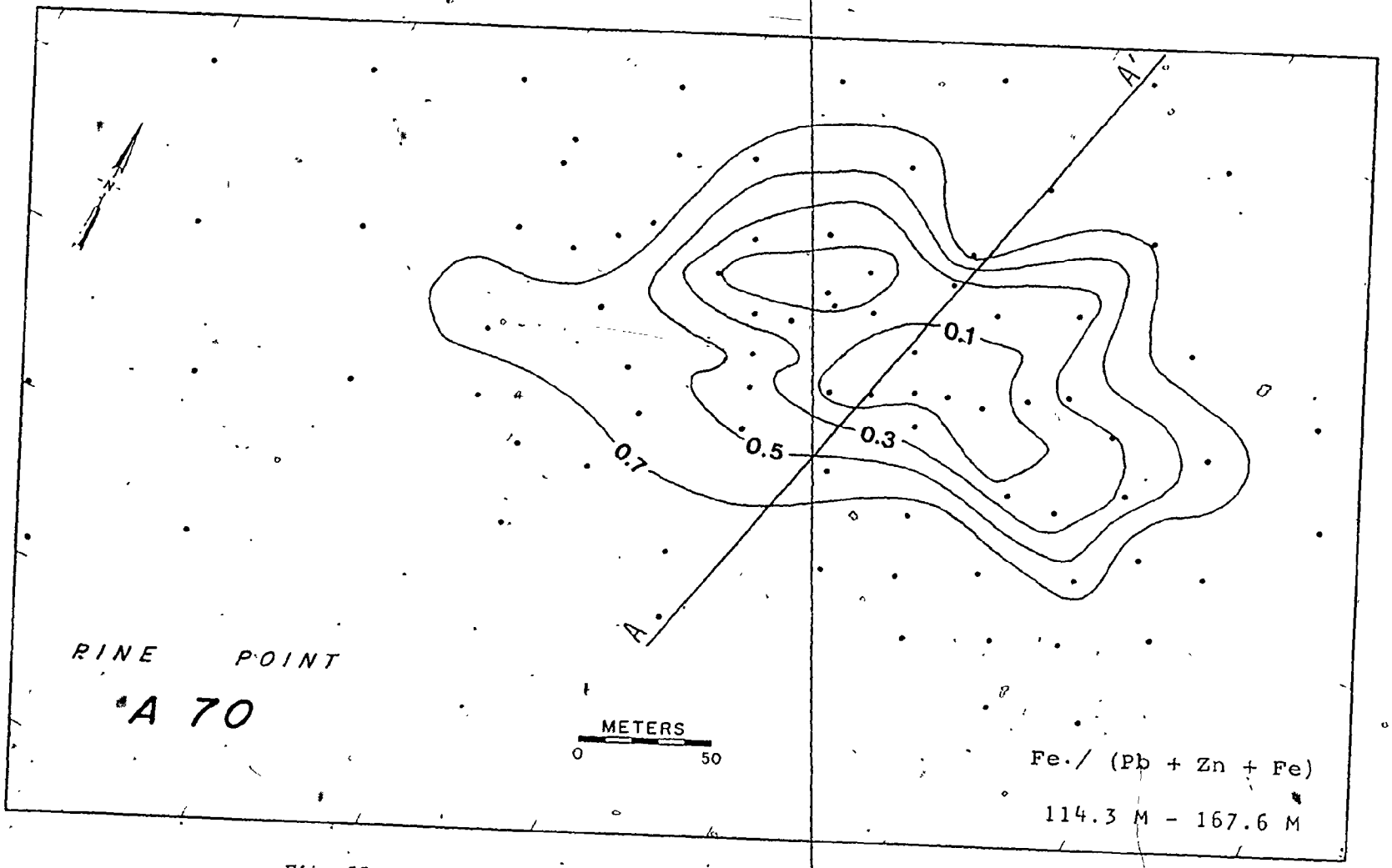

Fig. 55. A70 Ore Body, Fe/(Pb + Zn + Fe), 114.3 m - 167.6 m

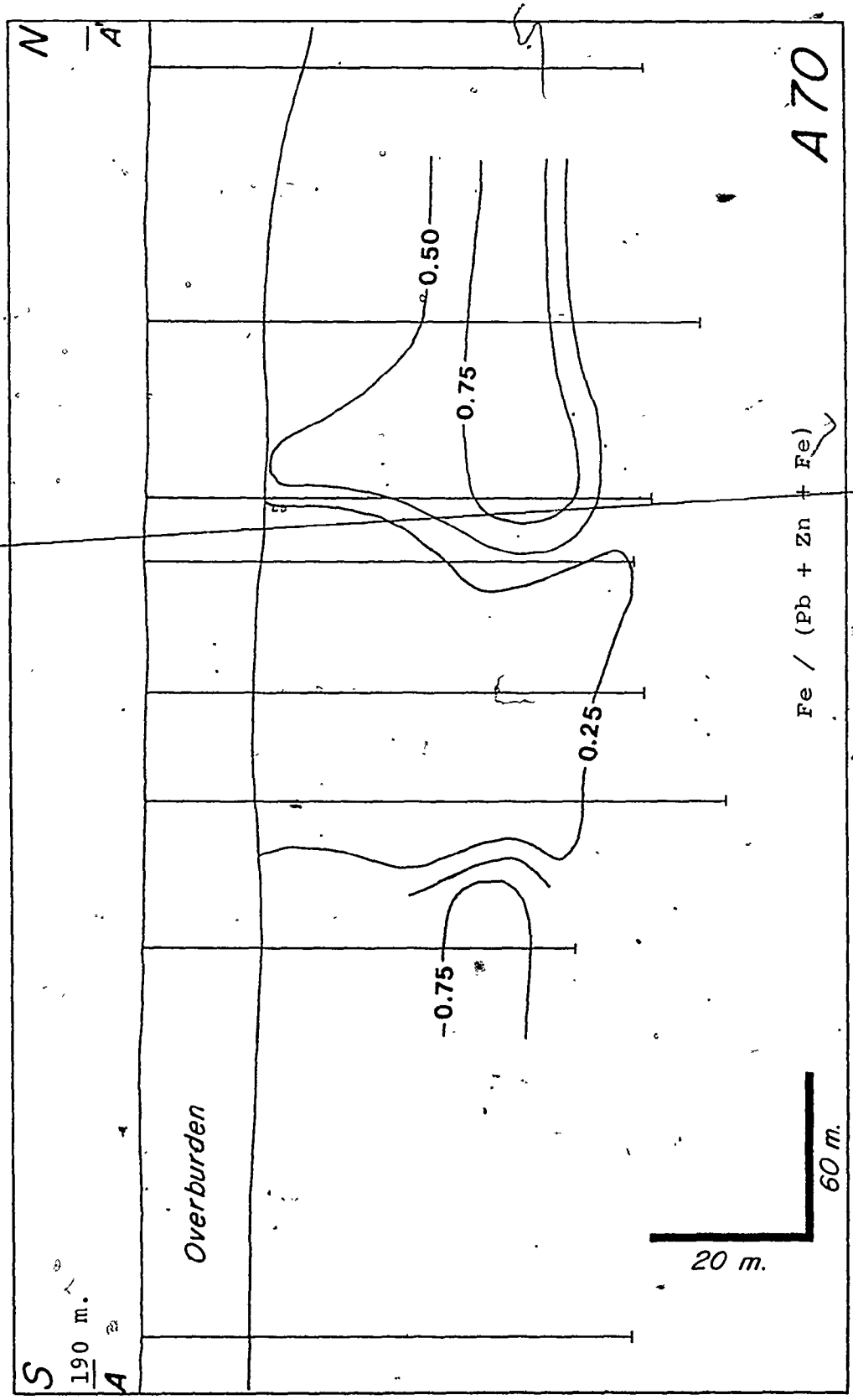

Fig. 56. A70 Ore Body, Fe/(Pb + Zn + Fe), Section A-A'

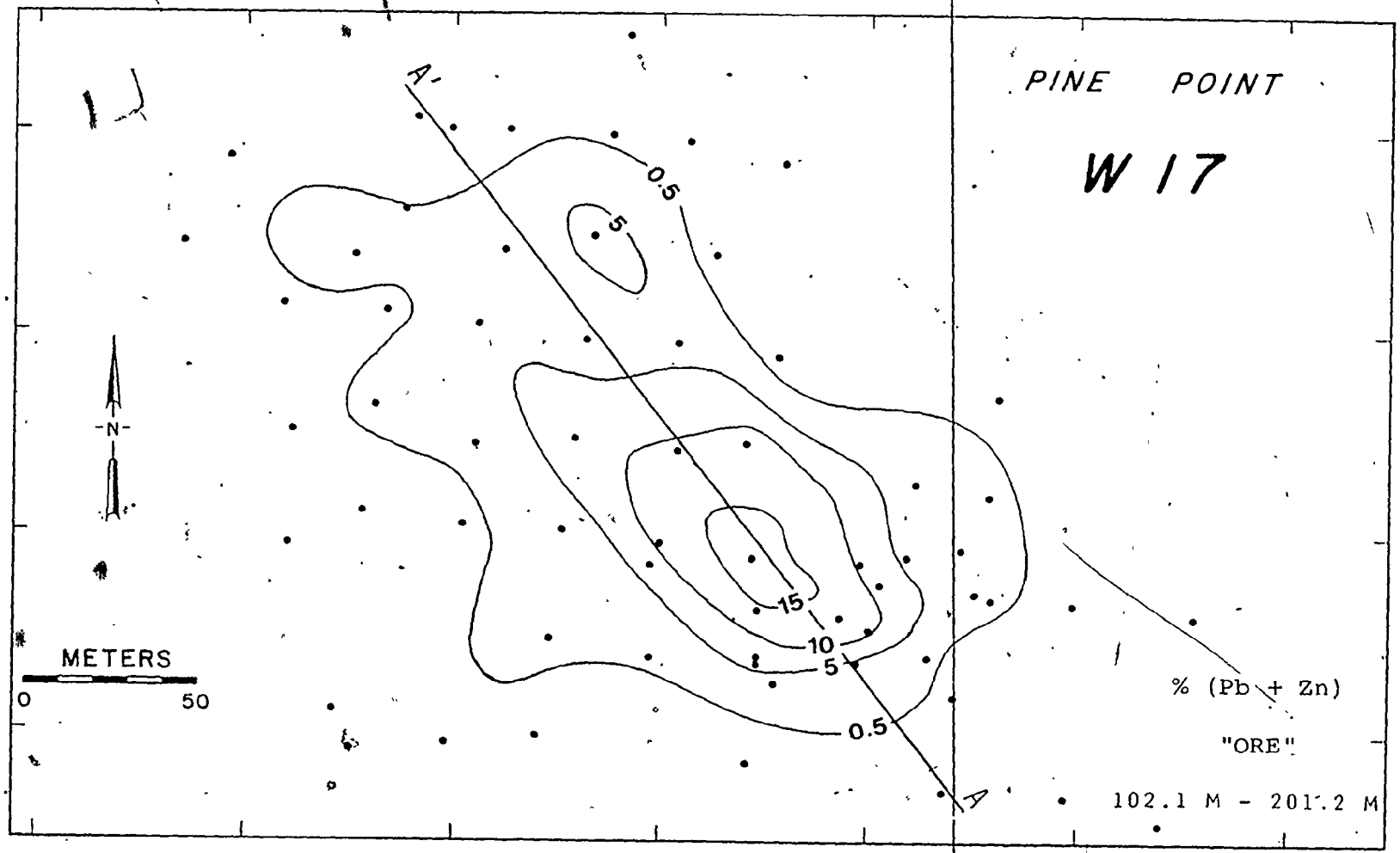

Fig. 57. W17 Ore Body, % (Pb + Zn), 102.1 m - 201.2 m

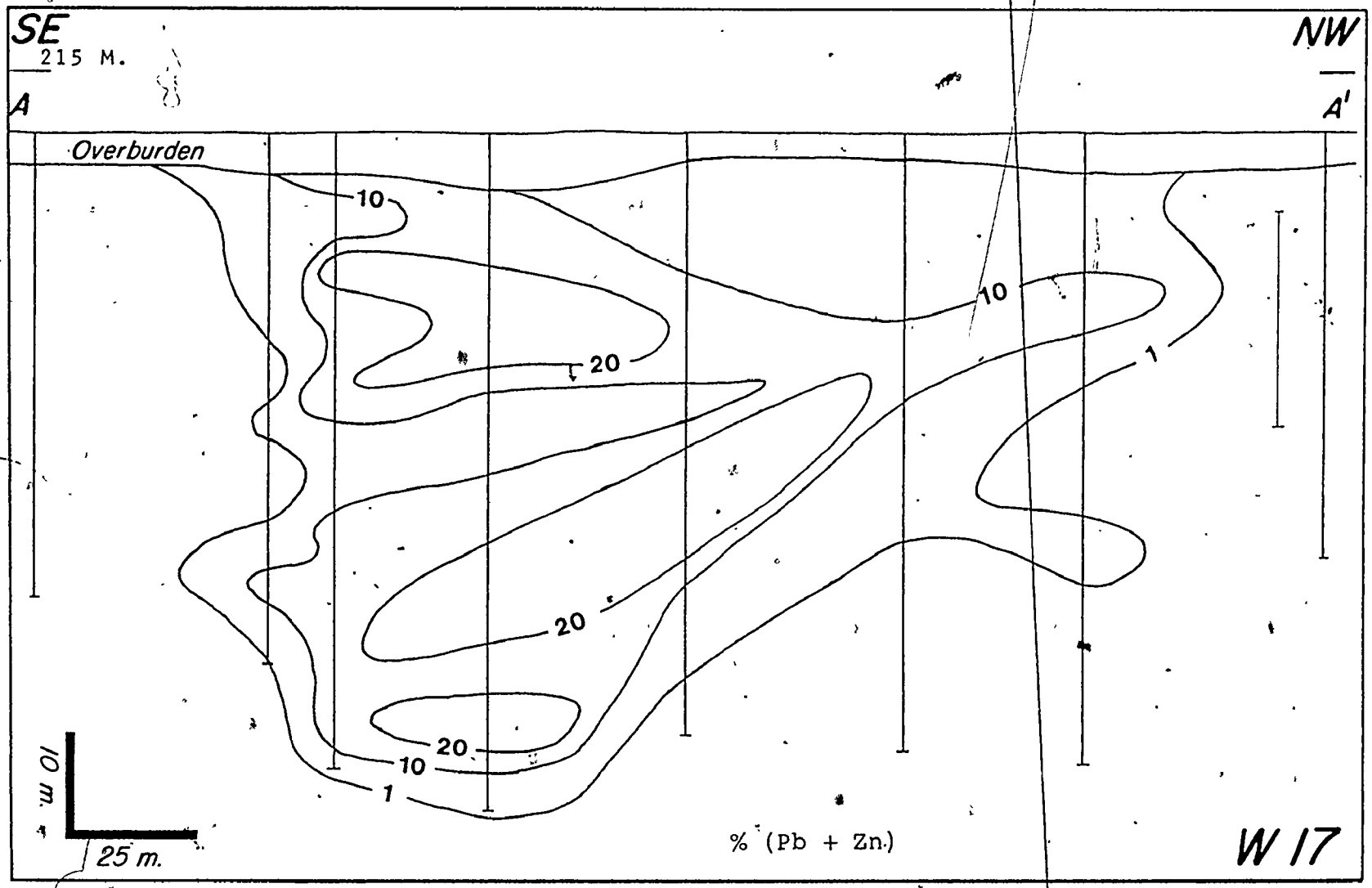

Fig. 58. W17 Ore Body, % (Pb + Zn), Section A-A'

140 meters long and 85 meters wide and contains a maximum of about 18 percent combined Pb-Zn over a 99-meter interval (Fig. 57). Although major concentrations of Pb, Zn, and Fe are largely coincident and reach maxima of 4.9, 12.9, and 23.1 percent, respectively (Figs. 59, 60, 61), the high Fe zone is more extensive. Lead appears to decrease slightly from southwest to northeast as indicated by the decrease of Pb/(Pb + Zn) from 0.3 to 0.2 (Fig. 62). In section, Pb/(Pb + Zn) varies irregularly between 0.4 and 0.2 (Fig. 63). The three-dimensional increase in relative Fe content is shown by the increase of Fe/(Pb + Zn + Fe) from less than 0.5 in the center to more than 0.7 on the periphery (Figs. 64, 65).

N204

N204 is an extensive low grade tabular sulfide body with a Pb/(Pb + Zn) ratio varying irregularly between 0.25 and 0.15 in the principal mineralized zone. The absolute Fe content is greatest on the east side and is part of a discontinuous relatively high Fe envelope with Fe/(Pb + Zn +Fe) greater than 0.4 (Fig. 66).

General Trends

Although individual sulfide bodies differ greatly in metal percentages and ratios, some consistent trends in relative metal distribution are apparent. The generalized pattern of metal distribution in the Pine Point ore bodies is a Pb-rich, high grade center with high Pb/(Pb + Zn) and low Fe/(Pb + Zn + Fe) passing outward into a Zn-rich, high grade zone with lower Pb/(Pb + Zn) and low Fe/(Pb + Zn + Fe) which

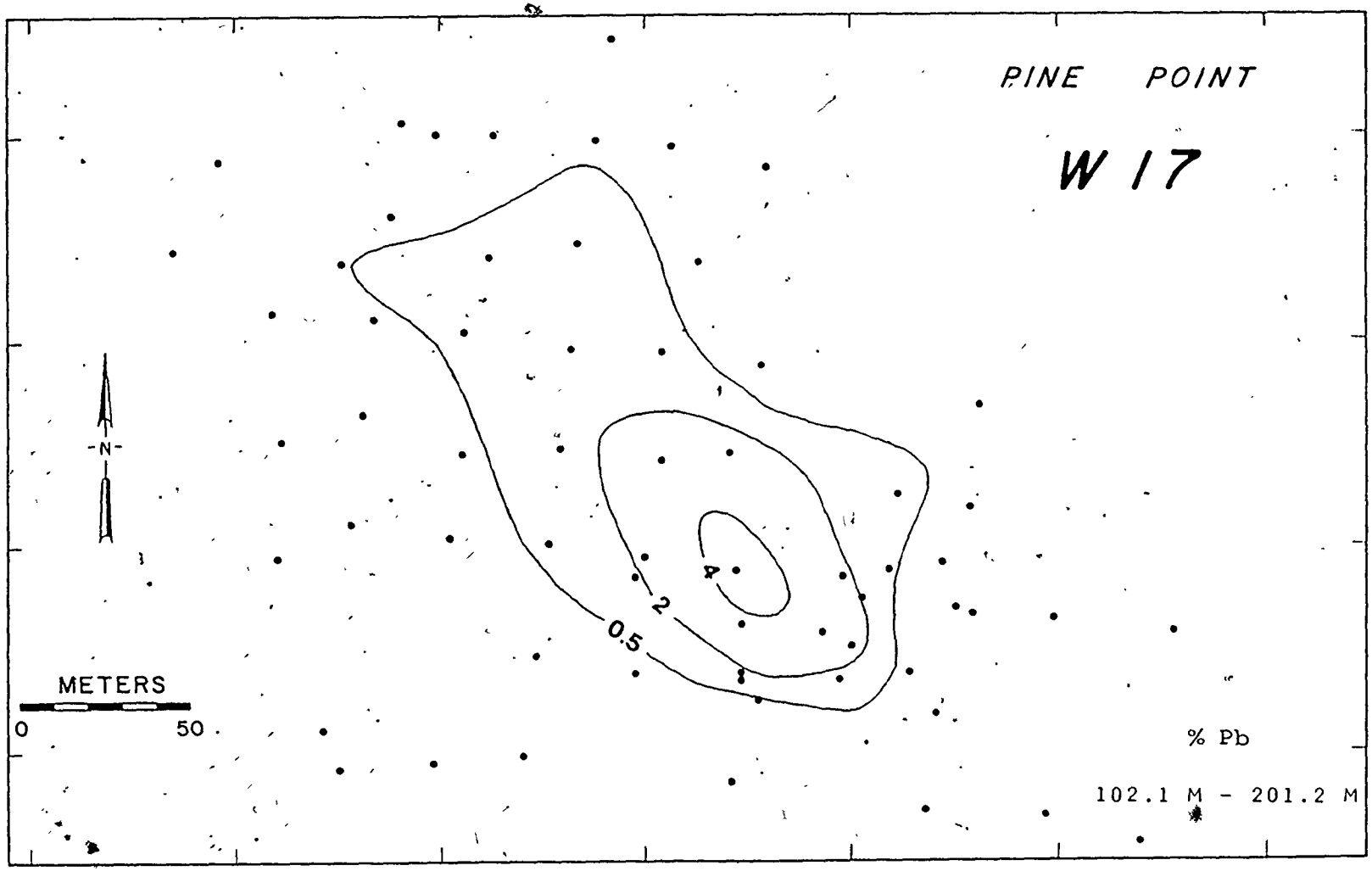

Fig. 59. W17 Ore Body, % Pb, 102.1 m - 201.2 m

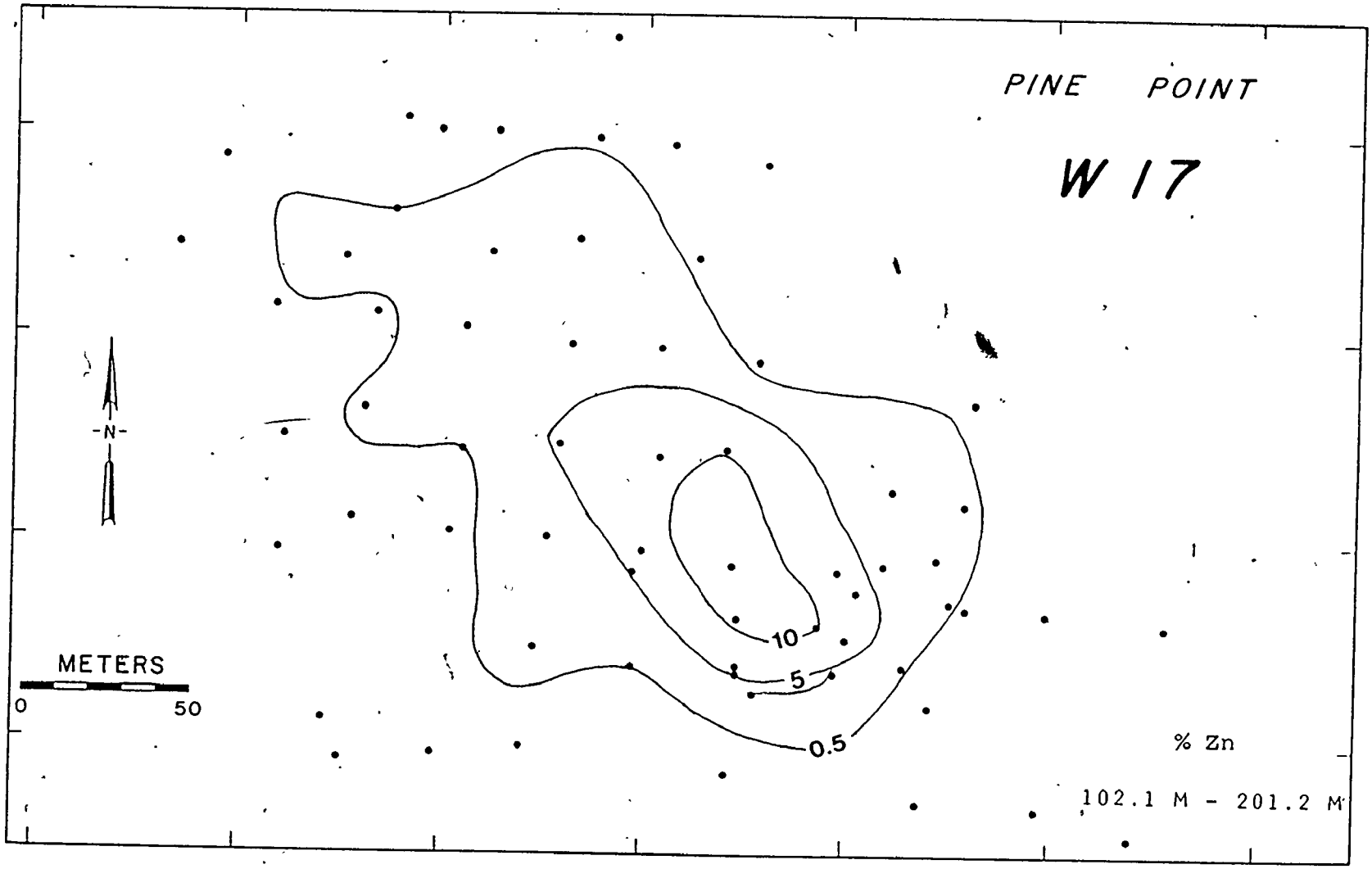

Fig. 60. W17 Ore Body, % Zn, 102.1 m - 201.2 m

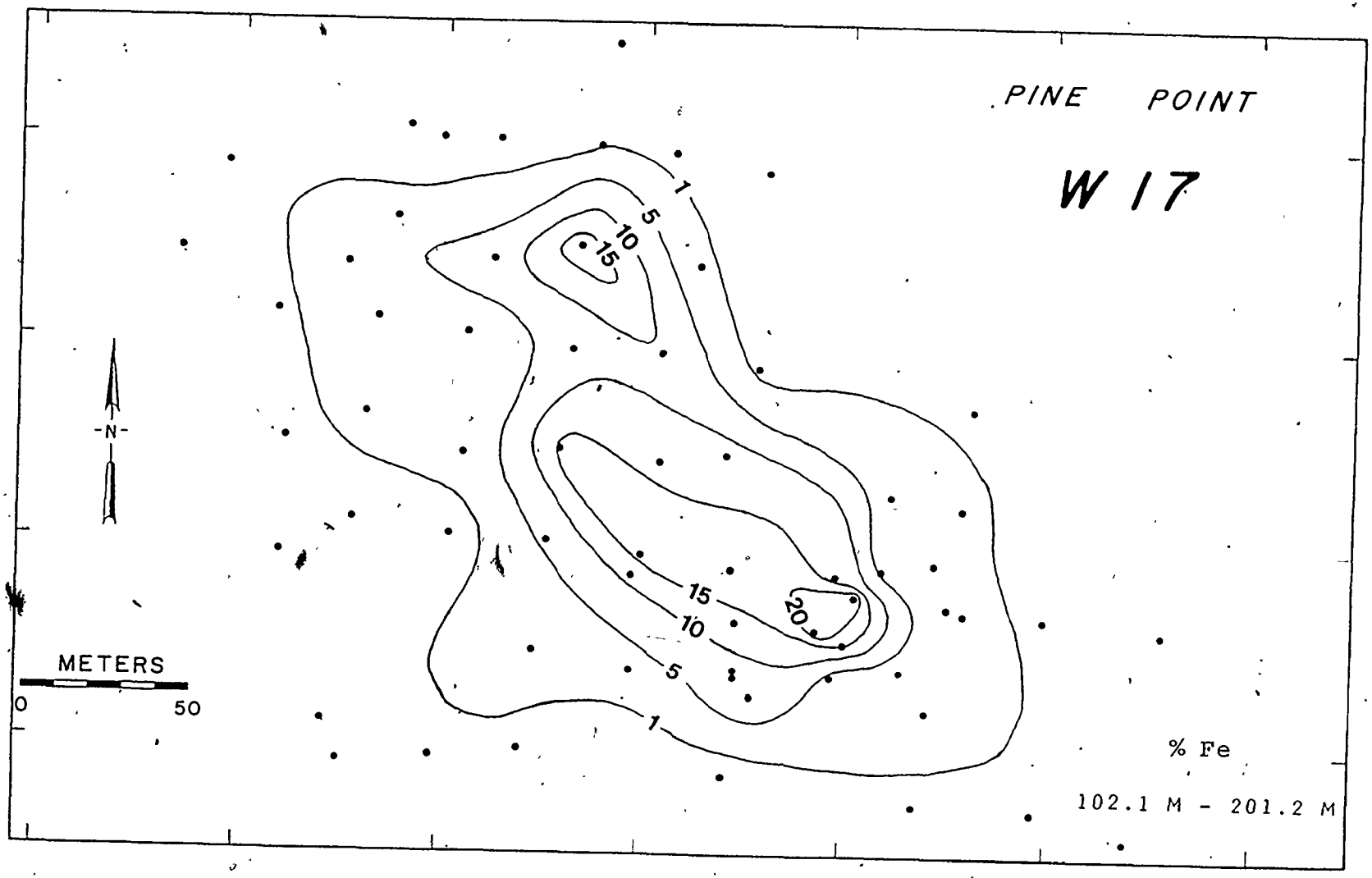

Fig. 61. W17 Ore Body, % Fe, 102.1 m - 201.2 m

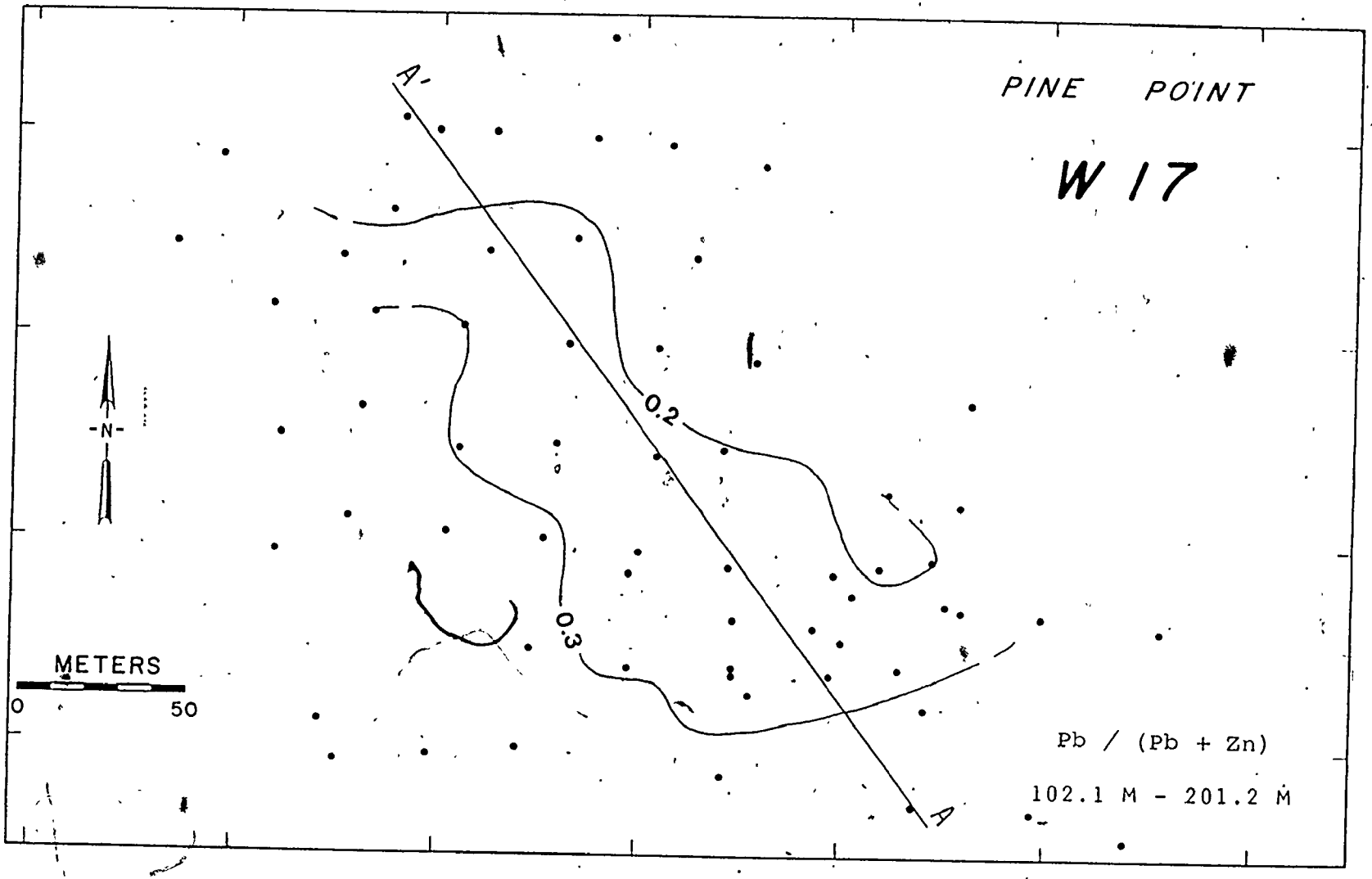

Fig. 62. W17 Ore Body, Pb/(Pb + Zn), 102.1 m - 201.2 m

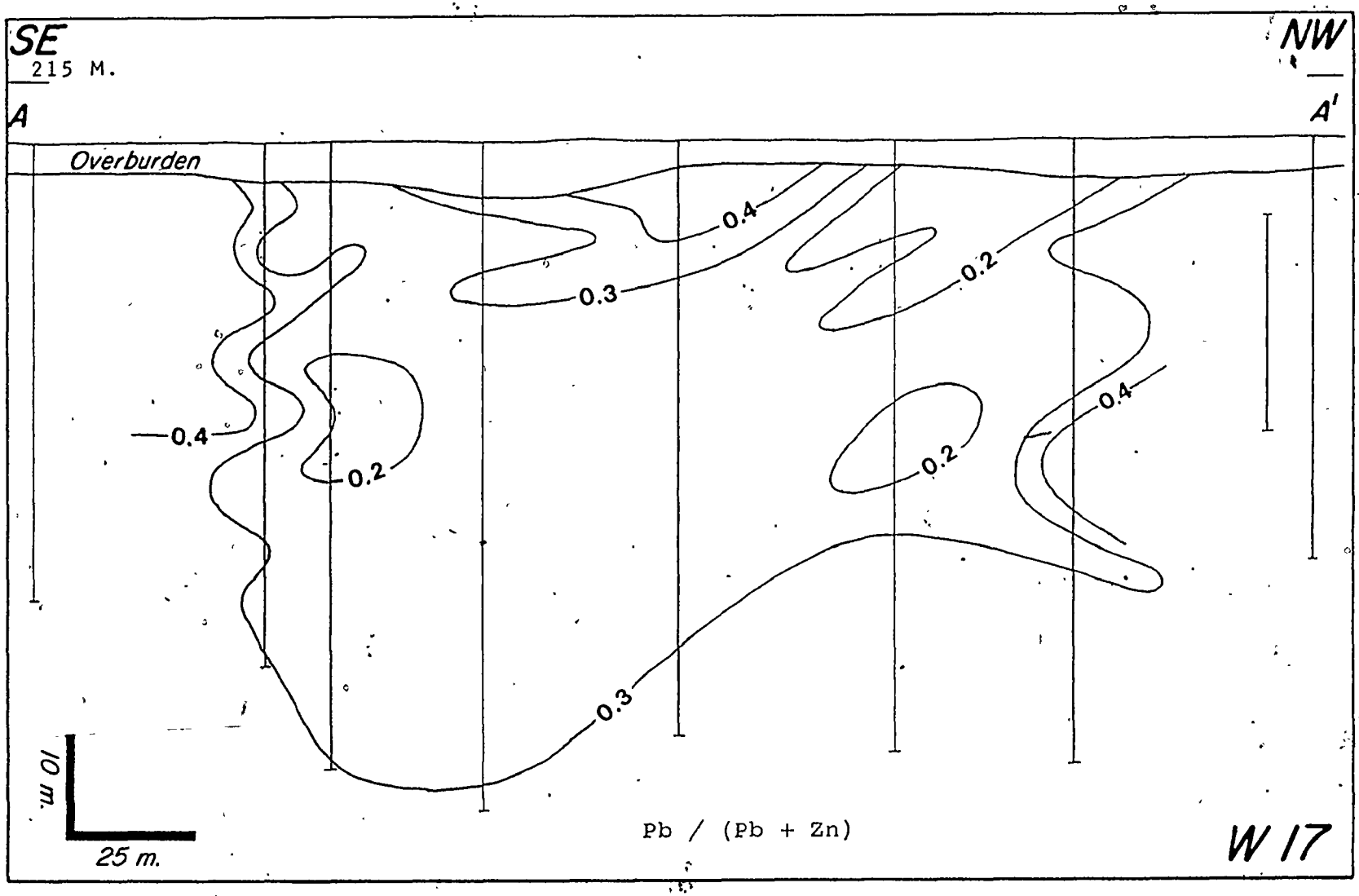

Fig. 63. W17 Ore Body, Pb/(Pb + Zn), Section A-A'

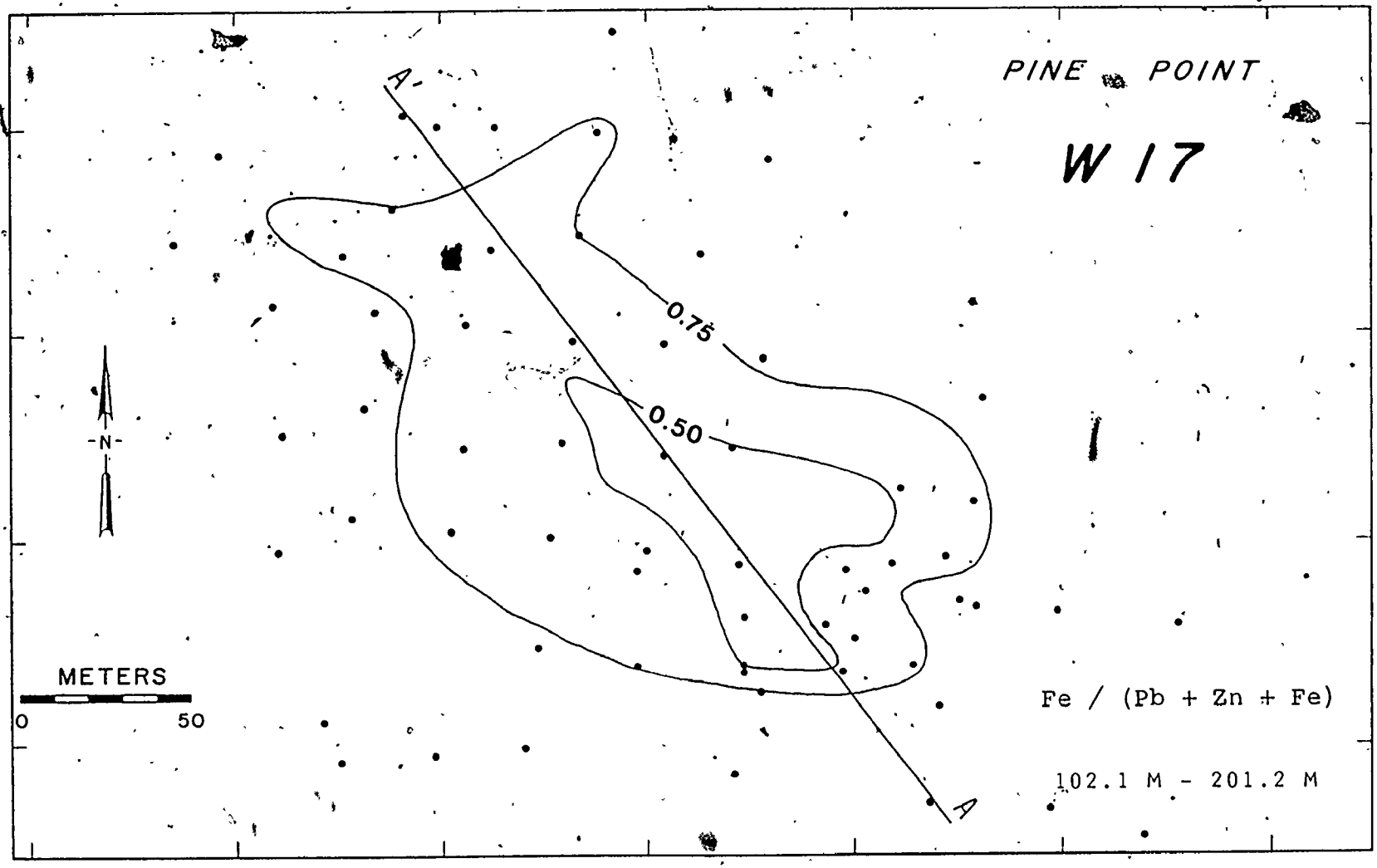

Fig. 64. W17 Ore Body, Fe/(Pb + Zn + Fe), 102.1 m - 201.2 m

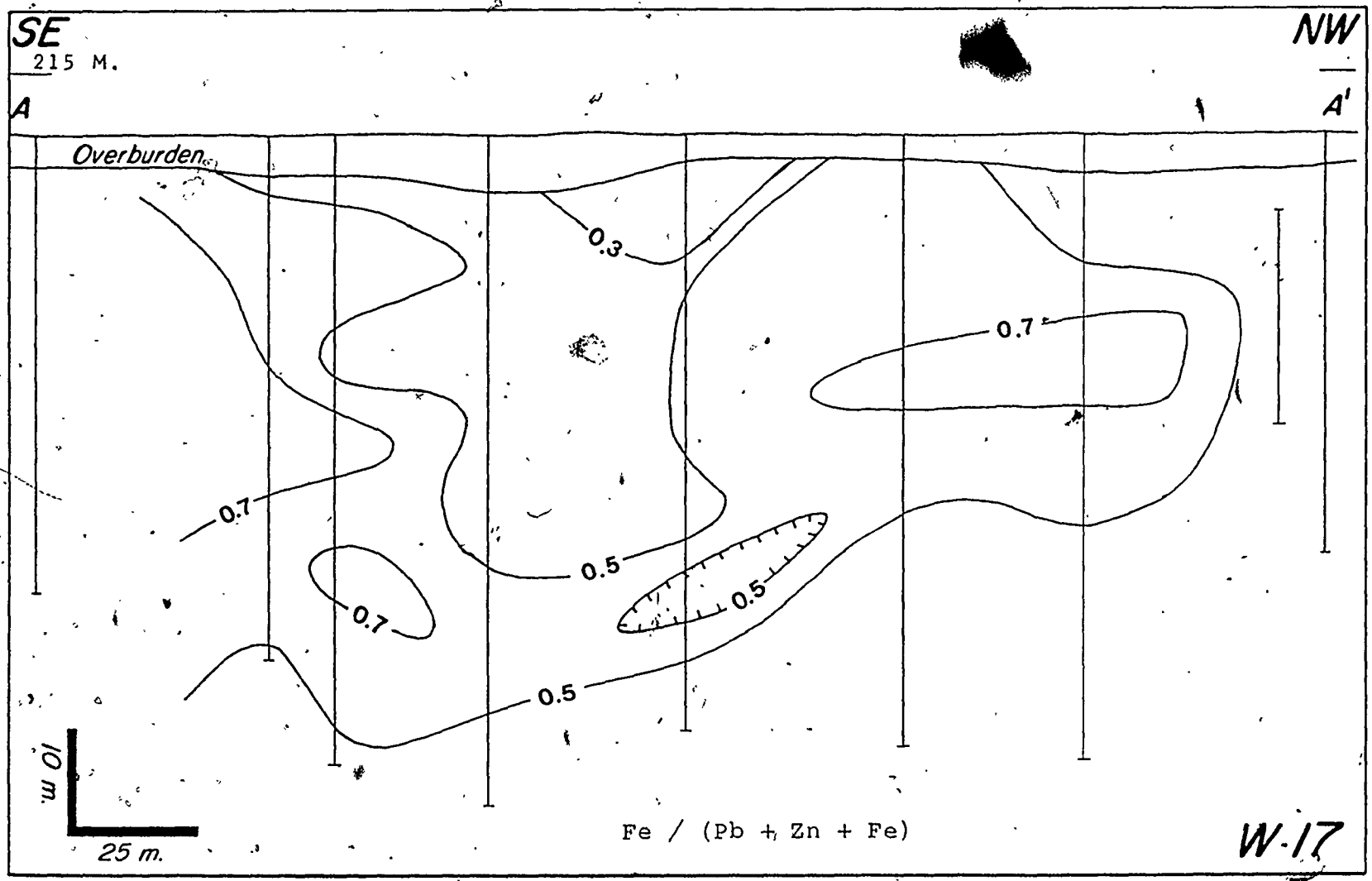

Fig. 65. W17 Ore Body, Fe/(Pb + Zn + Fe), Section A-A'

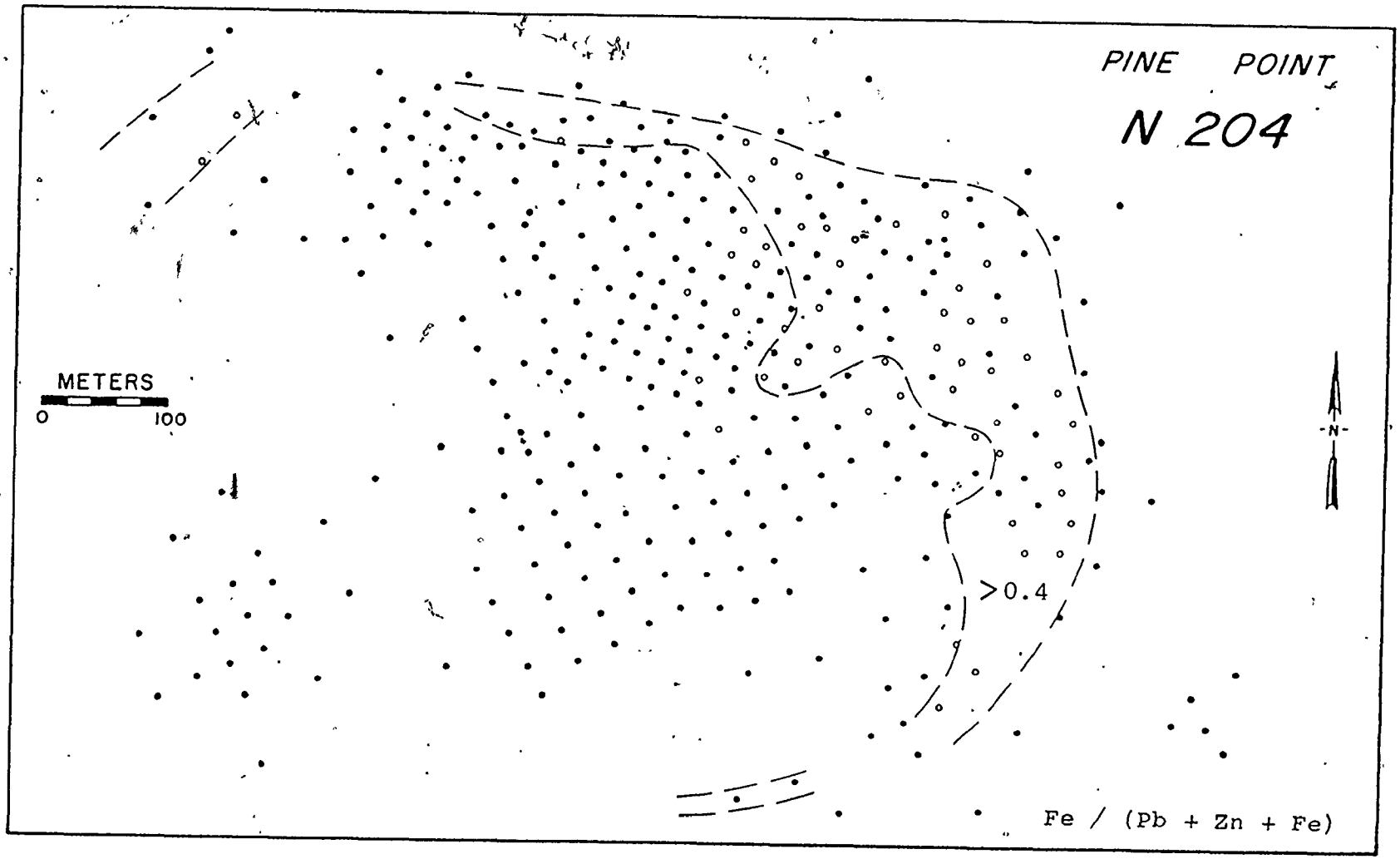

Fig. 66. N204 Ore Body, Fe/(Pb + Zn + Fe), Principal Zone
Open circles indicate drill holes with greater than 4% Fe.

grades into an Fe-rich, low grade envelope with low Pb/(Pb + Zn) and high Fe/(Pb + Zn + Fe) (Fig. 67). This zonation appears to be applicable to both prismatic and tabular sulfide bodies throughout the barrier complex. Low grade sections exist locally in the high grade center, and tabular sulfide concentrations may be present adjacent to the prismatic zone. Transition between high total sulfide material and barren host rock is commonly abrupt.

Mineralogy

The Pine Point sulfide bodies are composed almost exclusively of sphalerite, galena, pyrite, and marcasite with a non-metallic gangue of dolomite and calcite. Minor amounts of pyrrhotite, celestite, barite, gypsum, anhydrite, fluorite, sulfur, and bitumen are present within the host rocks.

Sulfides

Sphalerite

Sphalerite, ZnS, is the most common sulfide mineral in most of the ore bodies and occurs as individual tetrahedral crystals, as "colloform" and banded crusts, as ramose and dendritic forms, and as intimate intergrowths with other sulfides (Plates 10-13). Individual crystals range from less than 1 mm to as much as 4 cms; many project into open spaces, but some occur without associated porosity in fine-crystalline sulfide aggregates and within dense host dolostone (Plate 10:7-9). Sphalerite occurs in yellow, tan, orange, light

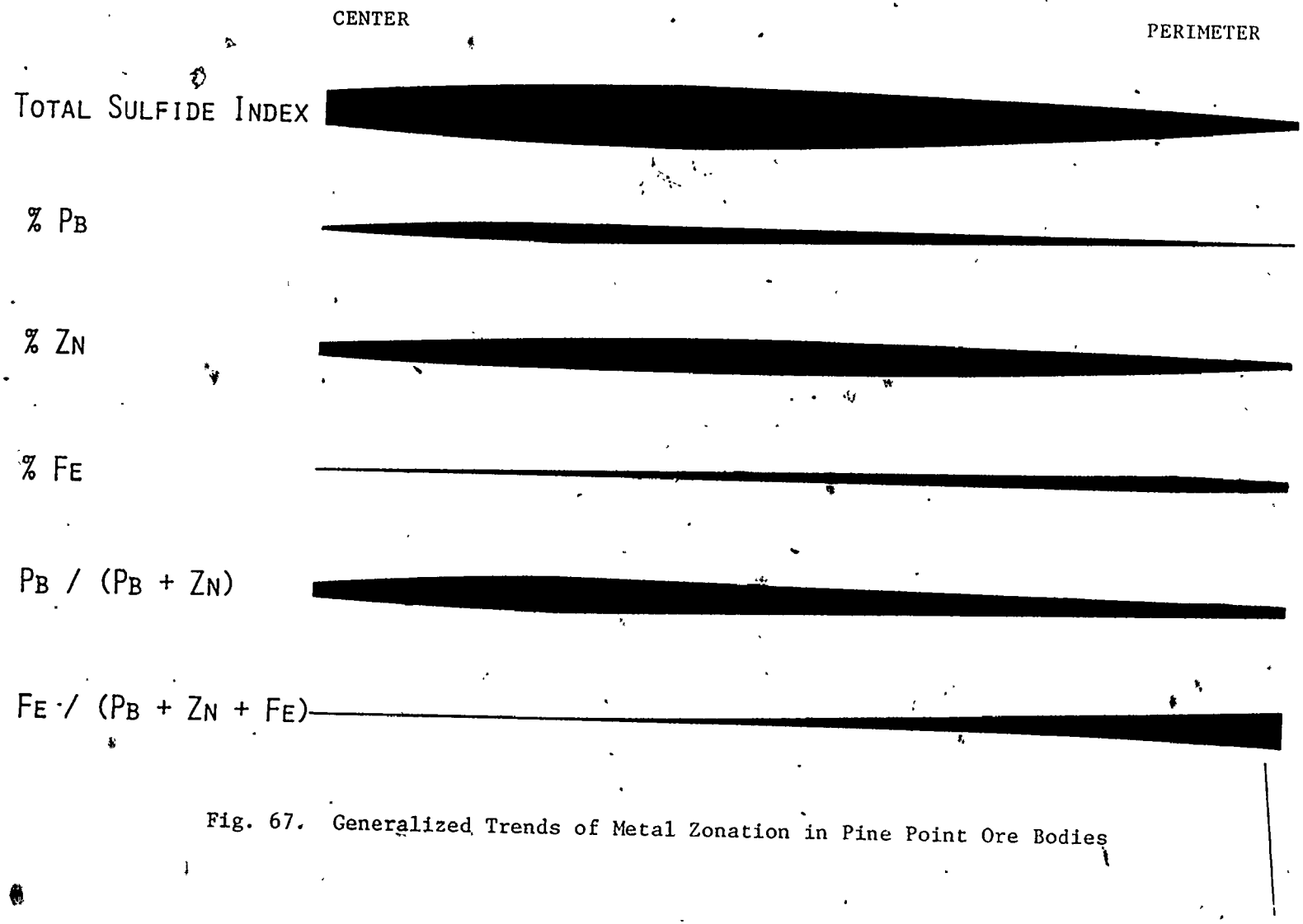

Fig. 67. Generalized Trends of Metal Zonation in Pine Point Ore Bodies

reddish-brown, dark reddish-brown, and dark brown varieties; some irregular laminae are purple in transmitted light. Commonly sphalerite occurs in "colloform" crusts of varying thicknesses composed of differently colored layers (Roedder, 1968b) (Plate 11); crystals are optically continuous across many color bands and often extend across the entire crust (Plate 11:5). Some colloform sphalerite appears to be stalactitic in form (Plate 11:1, 2), but this material is generally broken and is not in growth position. All ZnS appears to be in the form of sphalerite, although some local birefringent areas suggest up to 30 percent wurtzite polytype layers (M. E. Fleet, pers. commun., 1976).

A preliminary study of "stratigraphy" in colloform sphalerites from a number of ore bodies has shown that sphalerite bands ("strata") can be traced consistently among samples from individual ore bodies, using megascopic criteria of color, habit, relative thickness, associated minerals, and stratigraphic sequence (Plate 11:4, 5). Certain sphalerite strata and sequences of strata are absent from individual samples; their absence is apparently due to non-deposition rather than chemical erosion. Gross sequences of strata ("groups") can be correlated between some ore bodies, but the textural details of the stratigraphic sequence are commonly quite different, even among adjacent ore bodies (Plate 11:4, 5). These features suggest that local conditions greatly influenced sulfide precipitation. A detailed study of sphalerite stratigraphy and related topics such as trace elements, isotopes, and fluid inclusions is an area of research which could provide important information on the mechanism of sulfide deposition.

Microprobe analyses of sphalerites from several Pine Point ore

bodies reveal that Fe is the most common trace element and ranges from 0.15 to 10.3 weight percent (Table 6; Appendix II). Although Roedder and Dwornik (1968) did not find a direct correlation between color and Fe content of colloform sphalerite layers, microprobe analyses of sphalerite of several colors indicate a general pattern of greater Fe content with darker color (Fig. 68). Since Fe is the only common trace element, there also appears to be a complementary correlation between lower Zn content and darker color. In general these analyses are in agreement with the findings of Scott and Barnes (1972) which suggested that dark color in sphalerite is indicative of decreased metal and increased sulfur content (Fig. 68). There does not appear to be a positive relationship between Fe sulfide content of individual ore bodies and Fe content of sphalerite from those bodies. For instance, sphalerite from the Fe-rich X15 ore body is generally lower in Fe than the average of all sphalerite samples (Appendix II). Pb, Cu, Cd, and Mn are highly erratic in distribution and reach maxima of 1.05, 0.16, 0.32, and 0.02 percent, respectively (Table 6). Pb, Cu, and Mn do not appear to vary with sphalerite color; Cd, on the other hand, appears to be most abundant in the tan, pulverulent microcrystalline variety (Fig. 68, Plate 11:1, 2, 5). Ni, Co, and Ag were not detected in any sample. These analyses do not reveal a consistent trend in the composition of sphalerite relative to paragenetic stage, associated minerals, host rock type, or location within the district; admittedly, many more analyses are needed to substantiate this general statement.

TABLE 6

Composition of Pine Point Sulfide Minerals

Mineral		Zn	S	Pb	Fe	Mn	Cu	Cd	Total
Sphalerite	Maximum	66.64	33.61	1.05	10.30	0.02	0.16	0.32	100.04
	Minimum	55.47	31.48	0.00	0.15	0.00	0.00	0.00	98.07
	Mean(69)	64.16	33.38	0.21	2.23	0.01	0.02	0.05	99.67
Galena	Maximum	1.30	13.66	86.60	0.15	n.a.	0.24	n.a.	99.98
	Minimum	0.00	13.09	84.47	0.00	n.a.	0.00	n.a.	98.44
	Mean(24)	0.23	13.34	85.76	0.01	n.a.	0.08	n.a.	99.44
Pyrite/ Marcasite	Maximum	n.a.	53.95	n.a.	46.82	n.d.	1.27	n.a.	100.04
	Minimum	n.a.	51.95	n.a.	45.00	n.d.	0.00	n.a.	98.63
	Mean(31)	n.a.	53.26	n.a.	46.10	n.d.	0.16	n.a.	99.54

n.a. — not analysed; n.d. not detected

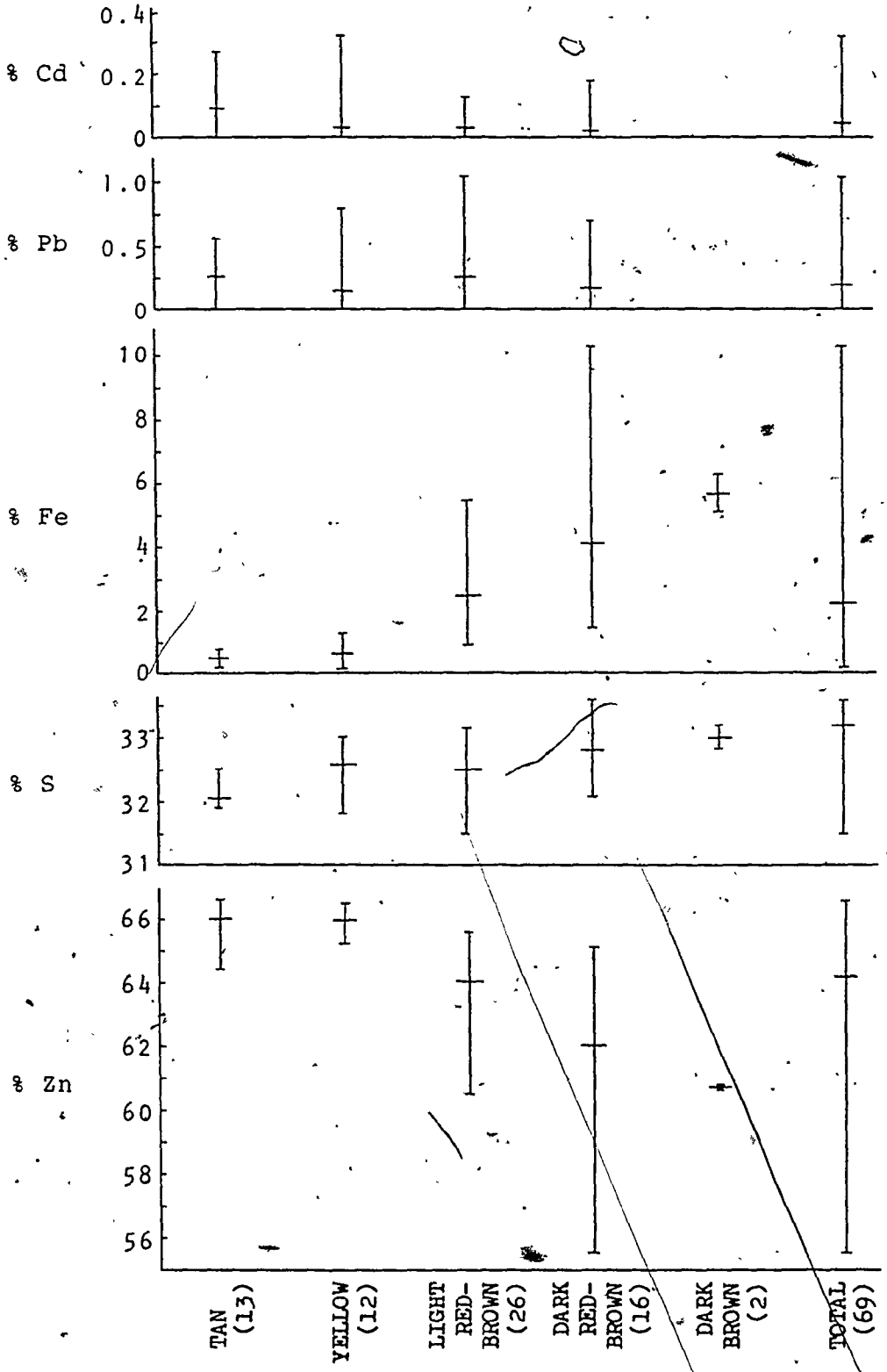

Fig. 68. Composition of Pine Point Sphalerite Relative to Color
Vertical bar is the range; horizontal bar is the mean.

Galena

Galena, PbS, is present in varying amounts in all ore bodies and occurs as individual cubic and cubo-octahedral crystals, as skeletal, hopper, bladed, and ramose forms, and as intimate intergrowths with other sulfides (Plates 10-13). Individual crystals range from less than 1 mm to as much as 5 cms (Plate 12), and galena has essentially the same modes of occurrence as sphalerite. Galena is present within colloform and stalactitic sphalerite, generally oriented subperpendicular to sphalerite growth bands (Plate 11:7). These and other forms are crystallographic entities which often extend for several centimeters in the direction of growth and commonly transect sphalerite stratigraphy. Galena co-precipitation with sphalerite is indicated by intimate intergrowths (Plate 11:3, 4, 6, 7) and by the apparent response of sphalerite growth bands to galena crystal interference (Plate 11:9).

Microprobe analyses of galena reveal little variation in composition relative to ore body, associated minerals, paragenetic position, or crystal habit (Appendix III). Zn, Cu, and Fe are the only trace elements present and reach maxima of 1.30, 0.24, and 0.15 percent (Table 6), respectively; Ag was not detected in any sample.

Pyrite, Marcasite, and Pyrrhotite

The polytypes of FeS_2, pyrite and marcasite, are present in varying amounts in all Pine Point sulfide bodies (Plates 12 and 13); pyrrhotite, $Fe_{1-x}S$, is rare, and its distribution is not well known (Plate 13:10). Approximately 75 polished surfaces containing Fe sulfides

were examined in this study; the pyrite/marcasite ratio varied greatly among specimens, even between polished surfaces from the same hand specimen. However, marcasite appears to be the dominant Fe sulfide, particularly in those sulfide bodies which contain abundant Fe. The decomposition of Fe-rich ore upon exposure further suggests the abundance of easily oxidized marcasite. Marcasite and pyrite are often intimately intergrown with other sulfides (Plate 12:10), and the Fe sulfides may be brecciated and enclosed in a matrix of sulfides (Plate 13:9). Iron sulfides are commonly massive, but locally have vuggy, boxwork, radiating, and ramose forms (Plate 13). Marcasite generally occurs as the characteristic bladed orthorhombic crystals, sometimes twinned on (101), ranging from less than 0.1 mm to as much as 1 cm (Plate 13:4, 5). Pyrite is usually in poorly formed cubes (Plate 12:10), occasionally with octahedral faces, and individual crystals up to 3 cms are present in the Green Clay Zone of W17 (Plate 13:3).

Microprobe analyses of Fe sulfides from several ore bodies indicate little compositional variation between marcasite and pyrite or between the same mineral from different ore bodies, mineral assemblages, or crystal habits (Appendix IV). Cu is erratic in distribution and reaches a maximum of 1.27 percent (Table 6); Co, Ni, Mn, and Ag were not detected in any sample.

Sulfates

Celestite

Colorless, orthorhombic celestite, $SrSO_4$, is present within the coarse-crystalline Facies K dolostone and is usually associated with

dolomite, calcite, and native sulfur (Plate 14:8). Coarse-crystalline celestite associated with calcite usually is not recognized in routine core examination and is more abundant than previously acknowledged. It has not been observed in association with sulfide minerals.

Barite

Barite, $BaSO_4$, is commonly listed among the minerals which occur at Pine Point (Beales and Jackson, 1968). The writer has not seen this mineral, and W. E. Wiley (pers. commun., 1974) suggests that some of the reported barite may have been misidentified dolomite or celestite. Barite is not a common mineral at Pine Point and is not associated with the sulfide bodies.

Anhydrite and Gypsum

Anhydrite, $CaSO_4$, and its hydrated analogue, gypsum, $CaSO_4 \cdot 2H_2O$, occur as extensive back-reef evaporite strata of the Muskeg Formation. They also fill porosity in and locally replace barrier lithologies, particularly in the fine-crystalline reefal rocks of the lower Pine Point Group. Gypsum and anhydrite occasionally have been observed in spatial proximity to sulfide bodies (Jackson, 1971), but the relationship between sulfides and sulfates has not been clearly established.

Carbonates

Dolomite

Dolomite, $CaMg(CO_3)_2$, is extremely abundant in the coarse-crystalline Facies K dolostone, particularly in the upper part

(Plate 14), and minor amounts occur locally throughout the Givetian strata in the Pine Point area. Dolomite occurs as single crystals, thick banded crusts, fracture and breccia cement, breccia-moldic forms, and pervasive replacement of coarse dolostone (Plates 4 and 5). Individual rhombohedral crystals commonly reach 1 cm in size and are generally curved. Most of the dolomite is white, some is light to medium gray, and a minor amount is pink (Plate 14). The white color is, at least in part, due to the presence of a vast number of fluid inclusions; fine-crystalline iron sulfides impart the gray color. The pinkish dolomite is probably caused by a trace element, perhaps Mn. The relationship between the white and gray dolomites is complex. They may be interlayered, one may pass abruptly into the other in the same layer, or one may fill fractures in the other (Plate 14:1-4). Dolomite in direct contact with iron sulfides is commonly pale gray, but most gray dolomite is not directly associated with megascopic iron sulfides. White and gray dolomite are much more extensive than sulfide mineralization; commonly, there is less dolomite in the sulfide bodies than in the adjacent unmineralized Facies K. Dolomite is both earlier and later than sulfide minerals (Plate 11:3, 5, 10; 14:1, 2). Brecciated sulfides cemented by dolomite (Plate 14:2-4) and the absence of sulfides with the white dolomite in the very porous upper Facies K dolostone suggest that a great deal of white dolomite may have formed later than the main period of sulfide deposition. Vague boundaries between white dolomite and coarse-crystalline dolostone (Plate 4:7, 5:8, 14:5) further suggest that white dolomite largely formed by isochemical replacement of pre-existing dolostone.

Calcite

Calcite, $CaCO_3$, is rather erratic in its distribution and abundance in the district. It occurs as single crystals, as thick crusts, and as vug, fracture, and breccia cement and is commonly colorless, white, or amber (Plate 14). Simple and complex scalenohedral crystals are the most common forms; individual crystals reach as much as 25 cms in the longest dimension. Calcite occurs also as medium gray, radiating, acicular crystals within the fine-crystalline reefal lithologies in the lower Pine Point Group. Except for calcite interlayered with white dolomite, calcite was one of the last minerals to form and its distribution reflects the distribution of pre-existing porosity.

Other Introduced Components

Fluorite

Fluorite, CaF_2, is commonly listed as occurring in the Pine Point district (Beales and Jackson, 1968). To the best of the writer's knowledge, it has been observed only in one short section of drill core in the coarse-crystalline Facies K dolostone (W. E. Wiley, pers. commun., 1975) and must be regarded as very rare.

Sulfur

Coarse-crystalline, yellow native sulfur, S, is relatively common in the district and is associated with dolomite, calcite, celestite, and bitumen (Plate 14:8). It has been observed throughout

the Givetian carbonate facies but is abundant only in Facies K. This relationship may be due in part to the greater availability of late porosity in the coarse-crystalline dolostone. Sulfur occurs also as the result of present-day decomposition of marcasite. Native sulfur occurs occasionally in spatial proximity to sulfide minerals, but the genetic association is inconclusive.

Bitumen

Bitumen, a complex mixture of devolitized hydrocarbons, is present in vuggy and intergranular porosity in the carbonate rocks (Plate 14:9, 10). It forms spheres as much as 2 cms in diameter when present in open vugs and is most abundant in Facies K. White dolomite appears to have formed around bitumen in some instances (Plate 14:10). Bitumen occurs within the sulfide bodies, but in all of the observed examples, bitumen is later than the sulfide minerals (Plate 14:9).

Sulfide Textures and Sulfide-Carbonate Relationships

Upper Barrier Ore Bodies

Colloform and banded sulfide textures are common in the ore bodies in Facies K and younger strata (Plate 11). These textures and some well-formed coarse sulfide crystals undoubtedly were formed in open space, but in view of other textures, some of this porosity may not have existed prior to sulfide emplacement. That is, fluids of the sulfide-depositing system may have significantly enlarged pre-existing porosity by dissolution of carbonates, particularly within the detritus

and breccia zones, and collapse of overlying strata may have created additional porosity (Fig. 31D). Dissolution enlargement is suggested by fragments of paragenetically early sulfides within later sulfides (Plate 11:1), remnants of carbonate detritus within coarse-crystalline sulfides (Plate 7), corroded edges of dolomite rhombs in dolostone (Plate 13:7, 8), and sulfides within dense dolostone (Plate 10:7). Beales (1975) has proposed that sulfides formed in equilibrium with the white dolomite of the Pine Point ore bodies because of apparent distinct contacts between the two. However, at higher magnification the contact of the white dolomite and sulfides is irregular locally, and detailed study is needed to better define this relationship. Evidence for carbonate dissolution is associated more commonly with the prismatic ore bodies (Plate 7). The tabular sulfide bodies generally appear to be simple open-space filling of pre-existing porosity (Plate 8).

Lower Barrier Ore Bodies

Colloform sphalerite textures are present (Plate 12:9) in the ore bodies in the fine-crystalline dolostones of the lower barrier but are not as common as in the upper barrier ore bodies. Instead, the dominant early generation sphalerite consists of dark reddish-brown coalesced spherules, often with yellow rims and generally less than 1 mm in diameter (Plate 10:4). Massive ore consists of a complex aggregate of fine and coarse sphalerite, marcasite, pyrite, and galena (Plate 9:7, 10:4, 12:10); fragments of sulfides in a matrix of later sulfides of coarse-crystalline calcite are common (Plate 10:2, 4; 12:8; 13:9). Sulfide breccia textures and highly irregular contacts between massive

sulfides and dolostone or dolostone breccia suggest local conditions of disequilibrium between the fluids of the sulfide-depositing system and dolomite (Plate 9:2, 3, 6).

Paragenesis

A detailed paragenetic sequence applicable throughout the district is difficult to establish because of the highly variable sulfide textures and modes of occurrence and the rather individual nature of the ore bodies. The generalized sequence is shown schematically in Fig. 69. White and gray dolomite deposition generally precedes sulfide precipitation in the ore bodies within Facies K. Marcasite is the earliest sulfide mineral in most ore bodies, followed by, and often intergrown with, pyrite. Sphalerite deposition overlaps the iron sulfide stage, and the early textures may be fine-crystalline, colloform, dendritic, or ramose. Galena may be intergrown with this sphalerite and is commonly skeletal. Coarse bands and crystals of late sphalerite associated with cubic and cubo-octahedral galena are generally the last sulfides deposited. A stage of white and gray dolomite and massive white calcite deposition follows sulfide precipitation. This generation of dolomite is believed to be more extensive than the pre-sulfide generation. Celestite, fluorite, and native sulfur belong to a later period of deposition. Coarse crystals of calcite fill remaining porosity. Most bitumen is a late feature, but some may be of an earlier generation.

It is possible to define more detailed sequences of mineral deposition for some individual ore bodies. The orderly paragenesis of the tabular M40 ore body in the coarse-crystalline dolostone of the

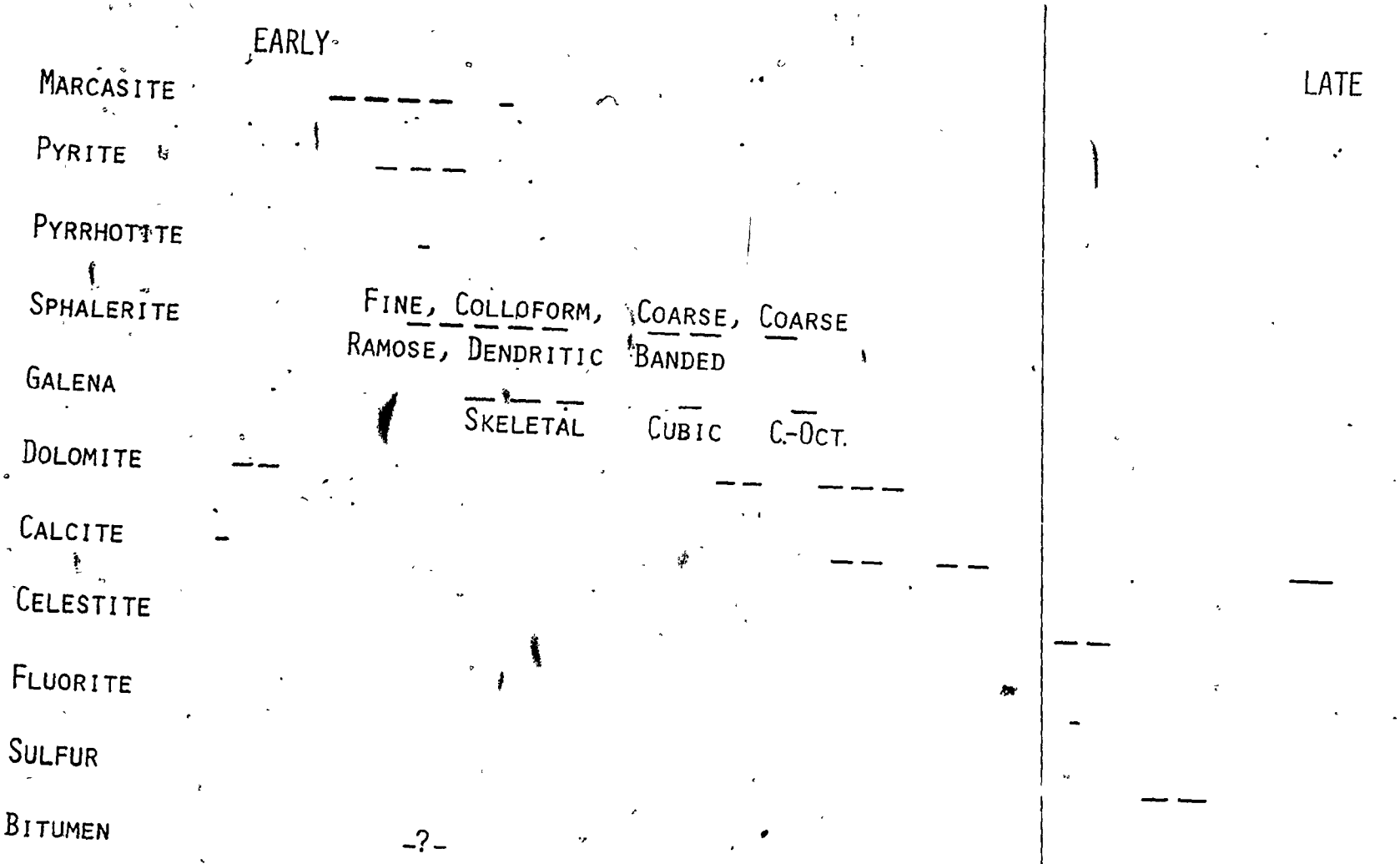

Fig. 69. Generalized Paragenetic Sequence for the Pine Point District

lower Facies K is shown schematically in Fig. 70 (Plate 11:3). The earliest sulfides consist of dark reddish-brown dendritic sphalerite with some skeletal galena and minor iron sulfides on a white dolomite substrate. The dendritic zone passes into a thick ramose network of orange sphalerite and abundant intergrown skeletal galena; thin bands of orange and yellow sphalerite with minor skeletal galena cap this zone. Yellow sphalerite is overlain by reddish-brown sphalerite with common cubic galena. White dolomite encloses the latest sulfide stage of coarse-crystalline dark brown sphalerite and cubo-octahedral galena. Coarse-crystalline calcite has filled much of the remaining open space. The sequence is best developed in the thick zone of massive sulfides in the central area of tabular mineralization (Plate 8:5).

The paragenetic sequence in the W17 ore body in the fine-crystalline dolostone of the lower Pine Point Group is shown schematically in Fig. 71; the sequence of sulfide deposition is not as readily apparent as it is in M40. Abundant marcasite and pyrite are the first sulfides to form on the dolostone substrate; rare pyrrhotite occurs along fractures and grain boundaries of massive pyrite. Dark reddish-brown fine-crystalline sphalerite spherules are intergrown with the iron sulfides. Tan, pulverulent colloform sphalerite is another paragenetically early form and may contain some skeletal galena. Coarse yellow and greenish-brown and cubic galena are a later sulfide stage. Calcite may cement fragments of these sulfides and fill porosity. Dolomite rarely occurs in the sulfide body.

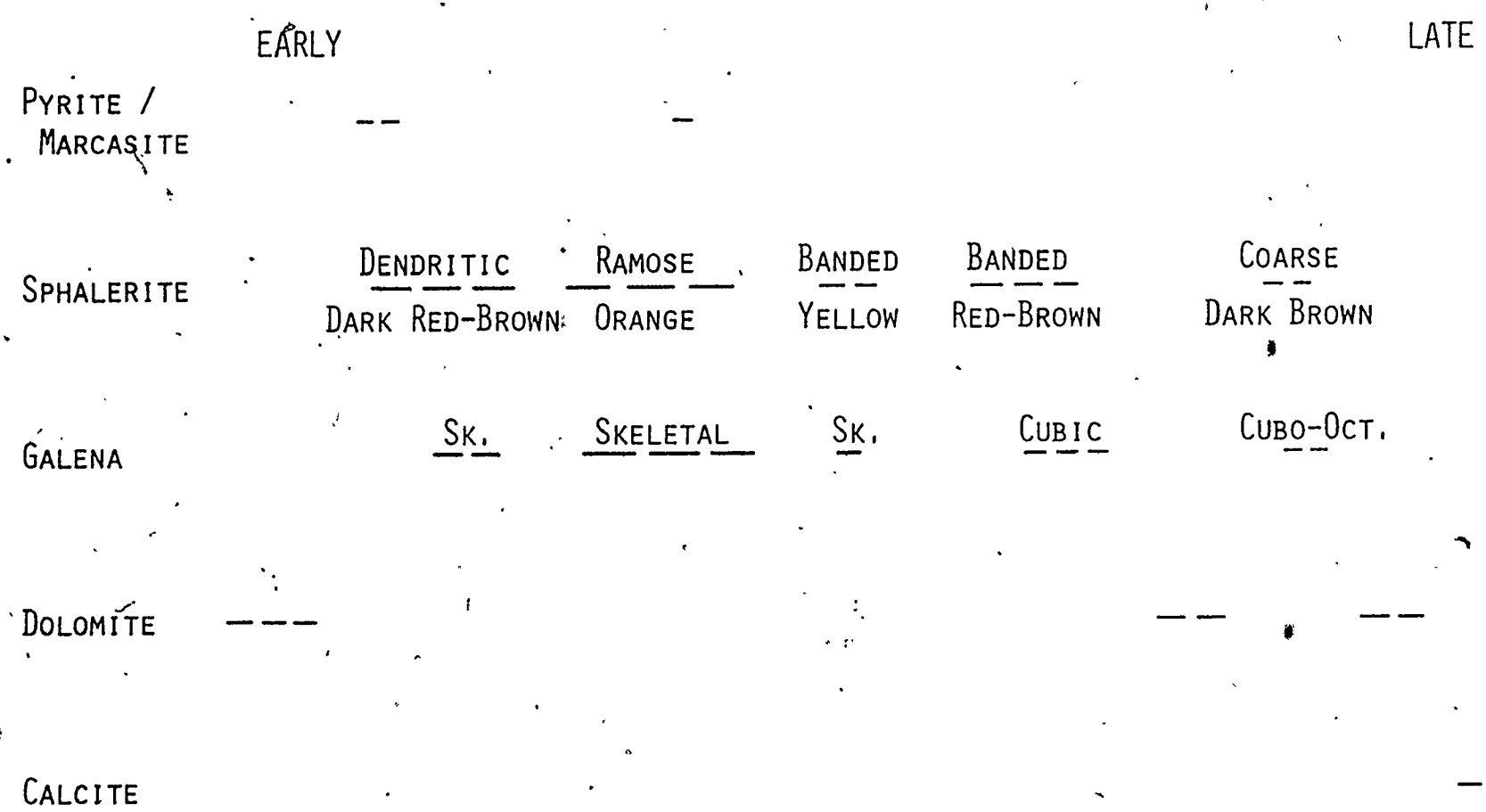

Fig. 70. Paragenetic Sequence for the M40 Ore Body

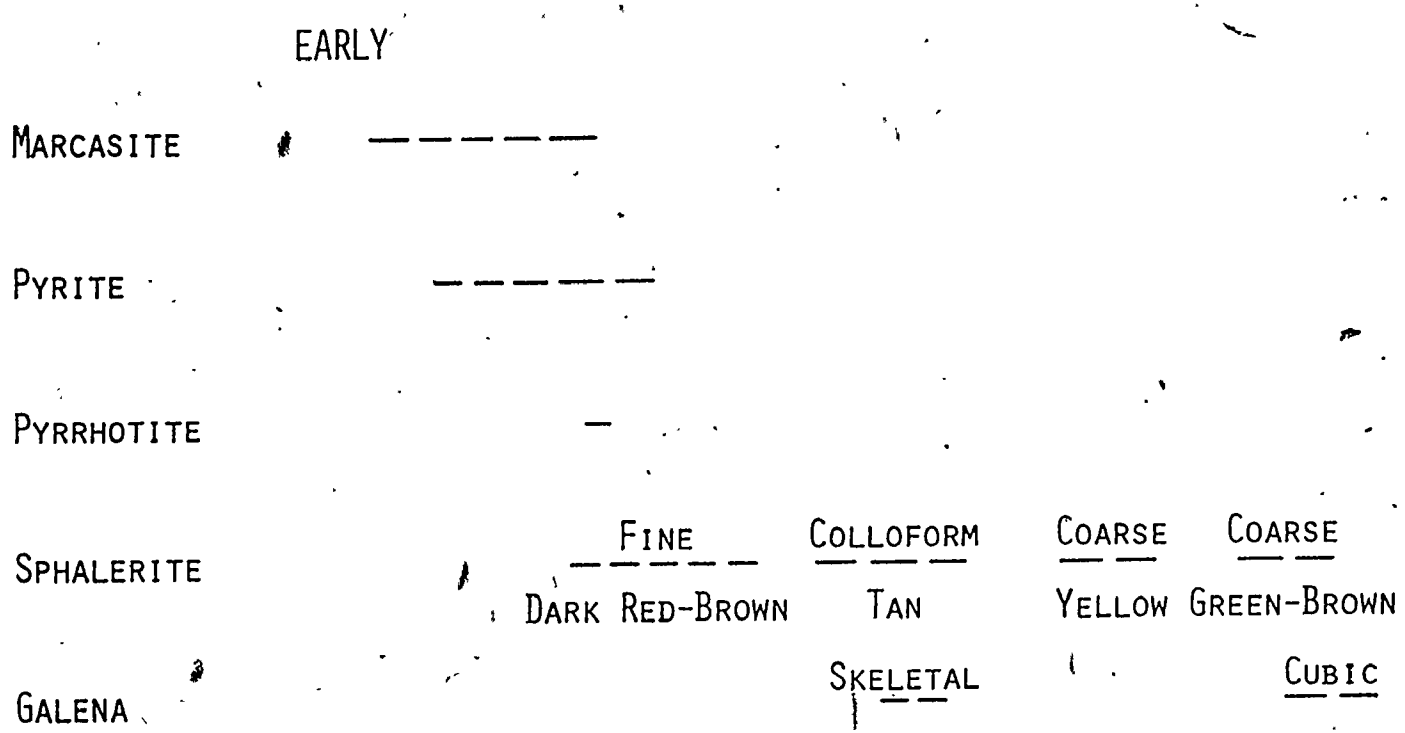

Fig. 71. Paragenetic Sequence for the W17 Ore Body

CHAPTER FIVE

MINERALIZATION: DISCUSSION

Introduction

The origin of carbonate-hosted Pb-Zn-Fe deposits of the so-called Mississippi Valley-type has been the subject of considerable debate for over 50 years. The following discussion will review briefly modern concepts of ore genesis, particularly as it pertains to Pine Point. The basinal evolution model developed at Pine Point (Beales and Jackson, 1966) has been applied widely to explain the origin of other carbonate-hosted deposits. Only now that development and diagenetic modification of the Pine Point barrier complex and the characteristics of the sulfide bodies have been determined is it possible to consider fully the complex problem of ore genesis. Genetic aspects to be considered for any mineral deposit are the nature of the transporting fluid, source of the components in the deposit, primarily metals and sulfur in this case, direction of fluid movement, reasons for mineral precipitation and concentration, and timing of mineralization.

Composition and Temperature of the Transporting Fluid

Major and Trace Element Components

Based on available production and reserve information, the Pine Point district contains about 75 million tons of ore averaging about 2.5% Pb, 6.0% Zn, and 3.5% Fe. A reasonable addition to this figure based on subeconomic sulfide occurrences and undiscovered ore bodies

would indicate a total metal concentration of about 2 million tons of Pb, 5 million tons of Zn, and 3 million tons of Fe. These sulfide concentrations also contain 15 million tons of S, not including the native S throughout the barrier. Assuming that the present mineral assemblages and the trace element content of the sulfides represents the content of the mineralizing fluid, Pb, Zn, and Fe were the only common metals and were present in a ratio of 2:5:3. Cu, Mn, and Cd are present locally in minor quantities, but separate minerals have not been recognized. Ca-, Mg-, and Sr-bearing minerals are present, but their relationship to the sulfide minerals is unclear because of paragenetic and fluid inclusion differences; Ca, Mg, and Sr are common components of carbonate rocks.

Fluid Inclusions

Minute quantities of the transporting fluid trapped during mineral growth, termed primary fluid inclusions, generally provide the best samples of the "ore-forming fluid" (Roedder, 1976). Although extraction and direct measurement of the composition and properties of the trapped fluid are possible only in exceptional cases, *in situ* measurement of homogenization and freezing temperatures of inclusions in non-opaque minerals indicates formation temperature and total salt content of the fluid, respectively.

Inclusions in sphalerite from the Pine Point ore bodies generally are difficult to study because of their small size and the dark color of much of the sphalerite. The earlier fluid inclusion study (Roedder, 1968a) and related study of "colloform" sphalerite (Roedder, 1968b)

provide much valuable information. Roedder's study material consisted of unlocated samples (probably N42 and O42 ore bodies) and did not represent many of the geologic variables apparent with subsequent developments and studies in the district. Therefore, additional fluid inclusion data were needed to supplement the findings of Roedder (1968a). The nature of the sulfide-depositing fluids for the ore bodies in the fine-crystalline dolostones of the lower barrier, particularly the fine-crystalline early sphalerite not present in the upper barrier ore bodies, and for the stalactitic sphalerite of the Facies K ore bodies was of particular interest. However, suitable inclusions were not found in the polished doublets prepared from this material, and this information remains unavailable. New fluid inclusion data are shown in Fig. 72; determinations for X15, W17, and N204 samples are for late generation, coarse-crystalline sphalerite.

Homogenization temperature determinations for primary fluid inclusions in sphalerite by Roedder (1968a) and the author indicate that the depositing fluids ranged in temperature from 51° to 99° C. Freezing temperatures commonly ranged from -10° to -35° C; many inclusions remained as unfrozen, supercooled liquid at -78° C after several hours (Roedder, 1968a). These freezing temperatures indicate that the sphalerite-depositing solutions were highly saline, ranging from about 15 to over 23 percent total salts, calculated on the basis of pure NaCl. No daughter minerals are present, but Roedder (1968a) recognized $NaCl \cdot 2H_2O$ (?) hydrate crystals in many inclusions as the last solid phase to melt on warming. Inclusions in white dolomite crystals associated with sulfide minerals had similar homogenization temperatures

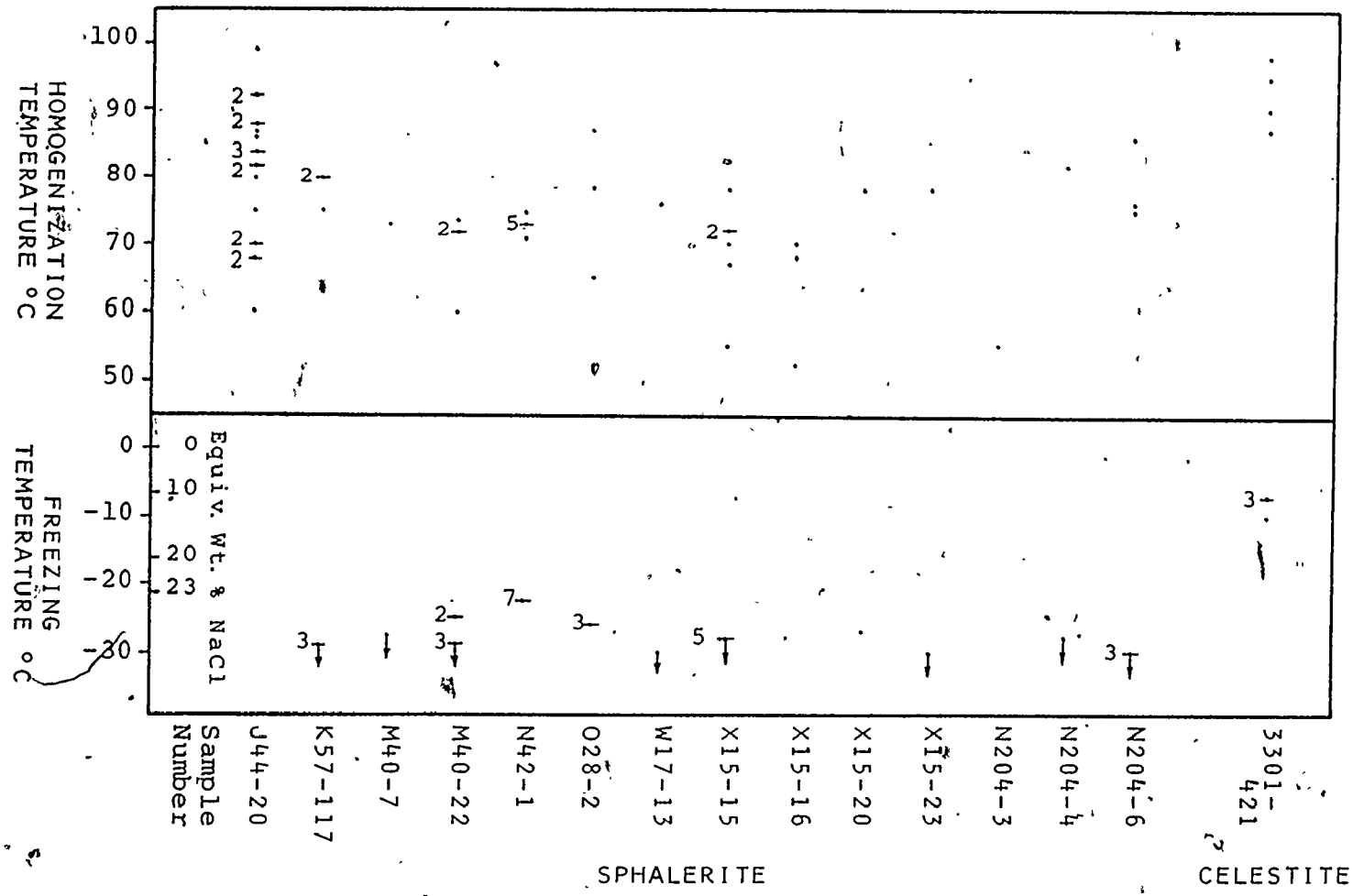

Fig. 72. Plot of Freezing and Homogenization Temperatures of Primary Fluid Inclusions, Pine Point District

Individual inclusions are indicated by a dot; an accompanying number and a line through the dot signifies that the indicated number of inclusions gave identical results. Arrows with the freezing temperatures indicate that these inclusions remain unfrozen after several hours at these temperatures.

ranging from 90° to 100° C, but salinities from 15 to 20 percent NaCl are indicated (Roedder, 1968a). Similar results were obtained for celestite from the Facies K dolostone with homogenization temperatures of 86° to 98° C and salinities of 10 to 15 percent NaCl (Fig. 72). Coarse calcite crystals from the ore bodies have salinities less than 10 percent (Roedder, 1968a). Particular care had to be taken to avoid leakage in the inclusions in dolomite, calcite, and celestite.

The relatively low temperatures and high salinities of the Pine Point fluid inclusions are characteristic of the carbonate-hosted Pb-Zn deposits (Roedder, 1967). The distinct temperature and composition differences between inclusion fluids from magmatic mineral deposits and from carbonate-hosted deposits (Roedder, 1976) and the general absence of evidence for magmatic or volcanogenic processes in the carbonate-hosted mineral districts (Ohle, 1959) suggest that the carbonate-hosted deposits originated by non-magmatic processes. This discussion will develop further the concept of a "sedimentogenic" origin (Sangster, 1976a). Chemical analyses of fluid inclusions from carbonate-hosted deposits show that the contained solutions are dense brines with Cl, Na, Ca, K, and Mg, in order of decreasing weight percent (Roedder, 1976). These brines are remarkably similar to the subsurface brines present in many oil fields (White, 1968).

Modern metal-rich subsurface brines have been discovered in the Salton Sea, the Red Sea (White, 1968), the Cheleken Peninsula (Lebedev, 1972), the Western Canada basin (Billings et al., 1969), and the Gulf Coast (Carpenter et al., 1974). The last two occurrences are far removed from areas of igneous activity and high geothermal gradients

and have geologic settings compatible with carbonate-hosted Pb-Zn deposits. These subsurface brines have characteristics similar to those determined from fluid inclusions. The metal source for these brines and for carbonate-hosted deposits is unclear but can be considered relative to the processes which have affected sedimentary basins.

Source of Metals

General

Similarities between oil field brines and inclusion fluids and the spatial association of some hydrocarbon and sulfide accumulations have prompted some authors to suggest genetic affiliations between hydrocarbons and carbonate-hosted Pb-Zn deposits (Beales and Jackson, 1966, 1968; Jackson and Beales, 1967; Skinner, 1967; Dozy, 1970; Dunsmore, 1973, 1975; Macqueen, 1976; and others). Although there are different opinions among these authors concerning metal sources and causes of sulfide precipitation, all suggest that carbonate-hosted Pb-Zn sulfide deposits, like petroleum and natural gas, are the result of normal processes active during the evolution of sedimentary basins.

Inherent in the basinal evolution model for development of carbonate-hosted Pb-Zn deposits is the concept of an original source "bed" from which metals were extracted prior to concentration as metal sulfides in a suitable "trap." Because source beds for hydrocarbons can be demonstrated to have been organic-rich, fine-grained clastic sediments (e.g. Erdman and Morris, 1974), such sediments have been considered by some authors to have been the most likely source of metals as well. Other

authors have proposed that the immediate metal source for the deposits was either the host carbonate strata, associated evaporites, or sandstone aquifers through which the brines passed.

Fine-grained Clastic Sediments

The basinal evolution model for Pine Point (Beales and Jackson, 1966) invokes metal supply from compacting shales in the Mackenzie Basin and sulfur supply from the evaporites in the Elk Point Basin (Fig. 7). Favorable sites for sulfide precipitation were provided by the porous rocks of the Pine Point barrier complex. Jackson and Beales (1967) emphasize that shales generally contain more Pb and Zn than do carbonate rocks and that the large amount of water originally present in argillaceous sediments would have to be expelled during compaction and could transport released metals. However, argillaceous sediment dewatering is a complex process involving not only compactional release of interpore water, but also the dehydrational release of interlattice water (Burst, 1976). Salinity of pore water increases with depth due to ionic filtration by clays, thus indicating that relatively "fresh" water is expelled during compaction (Magara, 1974b; Burst, 1976). Petroleum is highly soluble in and could be readily transported by "fresh" water, whereas increases in salinity cause hydrocarbon exsolution (Price, 1976). On the other hand, base metal solubility in the 100° C region under consideration increases radically with increasing salinity because of metal-chloride complexing (Nriagu and Anderson, 1971). Therefore, the relationship between hydrocarbon accumulations and carbonate-hosted Pb-Zn deposits cannot be simple because the fluids which can

effectively transport petroleum and base metals are of greatly different salinities. Transport of metals as organic-metal complexes is a possibility (Saxby, 1973) but introduces other problems. If metal-bearing brines are derived from basinal shales, metal extraction must have taken place during a later phase of clay mineral dehydration as suggested by Macqueen (1976). These reactions could take place at depths of a few kilometers (Magara, 1974b) which, assuming normal geothermal gradients, would be in the 75° to 175° C range generally applying to carbonate-hosted mineral deposits (Macqueen, 1976).

Shales, particularly organic-rich ones, do contain more Pb and Zn than most other sedimentary rocks; this fact does not necessarily mean that metals were released at an earlier stage in their diagenetic history. Also, shales are enriched in many metals, including uranium (Macqueen et al., 1975), and thus they seem too complex a source for the simple element suite present in the carbonate-hosted deposits. In addition, shale sequences which could serve as potential source rocks are absent in the vicinity of many of the important carbonate-hosted deposits of the Mississippi Valley.

Coarse-grained Clastic Sediments

A Pb-isotope study (Doe and Delevaux, 1972) suggests that the Pb-rich ores of Southeast Missouri were derived from the carbonate cement of the Lamotte Sandstone, the aquifer which overlies the Precambrian basement and underlies the host Bonneterre Dolostone. Sangster (1976b) points out that the few analyses presented do not eliminate the potash feldspar component of the basal arkosic Lamotte as

the immediate Pb source with the granitic basement constituting the original source. The geologic setting of the Pine Point district is similar to Southeast Missouri because the host dolostones are not more than 300 meters above the Precambrian basement and an arkosic sandstone, the Old Fort Island Formation, overlies the basement (Table 2). Pine Point ores also are Pb-rich relative to most of the other major carbonate-hosted districts (Sangster, 1976a). On the other hand, Pine Point lead isotopes lack the distinct anomalous character of the Southeast Missouri deposits (Appendix V; Sangster, 1976b). Also, circulation of the metal-bearing brine from the basal sandstone to the host dolostone would be greatly inhibited by the intervening impermeable Chinchaga evaporite sequence.

Carbonate Sediments

Because of their ubiquitous carbonate host rocks, it is reasonable to consider the possibility that trace amounts of Pb and Zn from these rocks were concentrated into economic sulfide deposits. Collins and Smith (1972) and Bernard (1973) suggest that metal concentration is accomplished during the weathering cycle that creates the "karstic" porosity which hosts much of the ore. Metals are released by mechanical weathering and chemical leaching in the vadose zone; deposition of sulfides takes place in areas of inhibited circulation below the layer of active circulation at the top of the phreatic zone (Bernard, 1973). Paterson (1975) emphasizes the textural similarities between Pine Point ores and carbonate speleothems from modern caves. However, meteoric water at near-surface temperature is markedly different from the highly

saline, 50° to 100° C (to 175° C in other districts) mineralizing solutions indicated for Pine Point by fluid inclusion evidence. The explanation of Bernard (1973) that these hot, saline fluids are the result of recrystallization of "karstic" sulfides in the deep subsurface is reviewed and judged invalid by Roedder (1976). The differences in timing of karstification and sulfide deposition as shown for Pine Point are also difficult to reconcile by the model of Bernard (1973). Johnson (1972) advocates that subsurface brines are enriched in metals during dolomitization of reefal complexes. This process may not be feasible considering that many diagenetic processes which affect carbonates, including dolomitization, appear to be near-surface phenomena, and metals released to this dynamic system probably would be lost through reflux to the open ocean.

Although the mechanism is not clear, a strong case can be developed for metal supply from carbonate rocks. Probably the most supportive evidence is the common association of galena, sphalerite, fluorite, and barite with carbonate rocks, particularly dolostones, not only in major and minor mining districts (Heyl, 1968), but also in porosity in most shelf carbonate sequences of Phanerozoic age. These minor occurrences have fluid inclusion characteristics which are indistinguishable from the major districts (E. Roedder, pers. commun., 1975). Economic concentrations thus appear to be the result of a favorable combination of hosting structures, hydrology, and timing.

Evaporites

Dunsmore (1975) emphasizes the evaporitic nature of many of the host carbonate rocks, an association previously noted by Davidson (1966).

He shows that the residual brines from modern sea water evaporitic pans when adjusted for diagenetic changes have chemical compositions essentially identical to typical fluid inclusion brines from carbonate-hosted deposits. Thiede (1975) provides the first systematic study of the base metal content of an evaporitic sequence. Although there is considerable variation among evaporite lithologies, lead and zinc are concentrated in the Elk Point evaporites of Saskatchewan by factors of 10^2 to 10^6 over that of sea water. Considerable tonnages of metals were available for release during gypsum dehydration at depths of 600 to 900 meters (Burst, 1976) or during evaporite solution in the deep subsurface (Thiede, 1975). One serious objection previously noted for shale metal sources is that evaporite sequences generally are not as spatially related to Pb-Zn deposits as at Pine Point, and certainly there are many major evaporite basins without known Pb-Zn deposits. However, supply of metals and sulfur in a single solution eliminates the problem of having two solutions arrive at the same site in order for sulfide precipitation to occur (Dunsmore, 1975).

Source of Sulfur

Approximately 15 million tons of S are present in sulfide form in the Pine Point ore bodies, not considering the native S and sulfates within the host rocks which have an uncertain relationship to the sulfides. Since the role of S is that of chemically "trapping" metals to form an economic sulfide accumulation, its ultimate source and subsequent history is a vital aspect of ore genesis. Sulfur isotope compositions provide some limitations as to source.

Sulfur has four stable isotopes--^{32}S, ^{33}S, ^{34}S, and ^{36}S. Isotopes ^{32}S and ^{34}S are the most abundant, and isotopic data are expressed generally in terms of the per mil difference between the ratio of these isotopes in a sample to that of an accepted standard, according to the formula:

$$^{34}S\ ^{o}/_{oo} = \frac{(^{34}S/\ ^{32}S)\ \text{sample} - (^{34}S/\ ^{32}S)\ \text{standard}}{(^{34}S/\ ^{32}S)\ \text{standard}} \times 1{,}000$$

Positive and negative per mil values represent ^{34}S enrichment and depletion, respectively, relative to the accepted standard. Formation of metal sulfides from S of a fixed isotopic composition generally results in sulfides of a different composition than the source because of isotopic fractionation. Temperature of reaction and biological action are the two most important factors governing fractionation. (Sangster, 1976b).

Sasaki and Krouse (1969) provide extensive S isotope data for sulfides from P29, N32, N42, 042, and X15 ore bodies at Pine Point. The average of 118 sulfide samples is +20.1 per mil with a standard deviation of 2.6. The means for galena, marcasite, pyrite, and sphalerite are +18.4, +19.3, +19.7, and +21.6 per mil, respectively. These values are very similar to the ratios (+19 to +20 per mil) determined for Middle Devonian evaporites, although there is some question whether the evaporite samples of Sasaki and Krouse (1969) truly represent the laterally equivalent Muskeg Formation. The most reasonable source for the sulfide sulfur is Middle Devonian sea water sulfate, perhaps supplied in connate brines from the Elk Point

evaporites (Sasaki and Krouse, 1969). The small range of sulfide S isotopes could be the result of isotopic homogenization of H_2S before fixation as sulfides (Sangster, 1976b).

Fluid Movement

Consideration of the evidence for fluid movement is pertinent to evaluation of the concept of sulfide precipitation by fluid mixing. Skall (1975) demonstrates conclusively the importance of Middle Devonian tectonic adjustments along the N 65° E trend of the Hinge Zones to the establishment of depositional environments; subsequent adjustments along the Hinge Zones were responsible for the creation of the diagenetic environments during the post-middle Givetian erosional period. The combined effect of depositional and superimposed diagenetic facies formed permeability zones subparallel to the N 65° E trend. The uniform crystalline dolostones of Facies E and to a lesser extent Facies D and B appear to be the most permeable units in the lower barrier. The lower part of Facies K is highly permeable, whereas the upper, highly vuggy Facies K section is probably not an effective aquifer. The thick, impermeable Chinchaga evaporite section is a barrier to vertical fluid movement, as is the intercalated shale and dense carbonate sequence of the late Givetian Facies L, M, and N. These relationships suggest that fluid movement was channeled along the Hinge Zones and within the rocks of the Pine Point Group.

Kesler et al. (1972) show that horizontal asymmetry of 43 single sulfide crystals and groups in ten Pine Point ore bodies suggest that the principal flow directions of the mineralizing fluid were both

northeast and southwest along the barrier trend. A strong flow vector is directed towards the southeast, and other divergences of flow from the barrier trend are apparent. This pattern can be interpreted to represent sulfide deposition spreading from point sources along joint patterns.

Speculation concerning the direction of mineralizing fluid movement is permitted also by metal zoning in the district and in individual ore bodies. Based on the decreasing relative solubilities of Fe, Zn, and Pb sulfides (Barnes and Czamanske, 1967), the metal distribution pattern for the Main and North Trends (Figs. 37, 38) indicates overall fluid movement from southeast to northwest; similarly, the ratios of the cumulative metal tonnages relative to stratigraphic position (Table 5) suggest a vertical component to fluid movement. In addition, the concentric metal zonation of individual ore bodies is most readily explained by local vertical movement of the mineralizing fluid.

Causes of Sulfide Precipitation and Concentration

Certain mineral assemblages and textures in carbonate-hosted Pb-Zn ores may aid in defining geochemical characteristics of the depositing fluids. The relationship between sulfides and carbonates is important particularly in indicating the cause of precipitation; if carbonates are stable during sulfide deposition, increase in reduced sulfur is the most likely reason for precipitation (Anderson, 1973, 1975). Beales (1975) points out instances of apparent carbonate-sulfide equilibrium, and this study reveals numerous examples suggesting carbonate instability (dissolution) <u>during</u> the sulfide-depositing episode

at Pine Point (e.g. Plates 7:2,6,11; 9:2,3,6). This evidence does not necessarily indicate that carbonates were undergoing active dissolution during sulfide precipitation; rather, it may indicate alternating episodes of carbonate dissolution and sulfide precipitation. Similarly, reduced sulfur may have been supplied periodically; as Anderson (1975) emphasizes, regular replenishment of reduced sulfur is a requirement for large sulfide concentrations because of the small amount of H_2S which can occupy available porosity.

Solubility data for galena at 100° C indicate that the transporting brine must be extremely acid if both lead and reduced sulfur are carried in the same solution (Anderson, 1975); yet, it is certain that any solution within a thick carbonate sequence would have been quickly buffered by calcite and dolomite. Therefore, the most reasonable mechanism for producing local conditions of carbonate disequilibrium is through mixing of solutions of differing character (Runnells, 1969; Plummer, 1975), probably one containing metals and another reduced sulfur. The mixing of these solutions is likely to cause rapid crystallization resulting from the relatively large degree of supersaturation (Anderson, 1975). Such a phenomenon is suggested by the early stage of colloform sphalerite and skeletal galena at Pine Point. Skeletal and other incomplete forms of galena have been produced experimentally by mixing aqueous lead chloride with a solution containing H_2S (Leleu and Goni, 1974).

The Cheleken Peninsula is an excellent example of a modern stratigraphic section with separate aquifers which contain fluids of greatly differing salinities, metal percentages, sulfur oxidation states,

and temperatures (Lebedev, 1972). Artificial mixing of these fluids produces spectacular growth of sulfides and sulfates. It is proposed that natural mixing of fluids from separate aquifers in paleo-dolines and breccia zones in the Pine Point barrier complex resulted in slower but just as spectacular growth of sulfides. This mechanism is supported by the association of the prismatic ore bodies with dolines and breccia zones within an otherwise undisturbed stratigraphic section, by the sharp boundaries and individual nature of these ore bodies, by the concentric metal zoning pattern in individual ore bodies, and by the divergences in fluid flow directions which appear to indicate point sources for the ore bodies.

Timing of Mineralization

Probably the single most enigmatic aspect of carbonate-hosted Pb-Zn deposits is the general problem of determining the age of mineralization. Yet, timing is of paramount importance in any genetic model for these deposits. It is clear from geologic evidence that many of these sulfide accumulations post-date the deposition of their host rocks, that is, they are "epigenetic" rather than "syngenetic." In the case of Pine Point, sulfides occur in strata as young as the late Givetian Facies N, but there is no geologic evidence to indicate a precise age of mineralization during the 375 million years from the Givetian to the present.

It is possible to determine the age of mineralization for some deposits through the use of lead isotopes. Lead exists in four isotopes--

^{204}Pb, ^{206}Pb, ^{207}Pb, and ^{208}Pb, of which ^{204}Pb is the least abundant. Isotopes ^{206}Pb, ^{207}Pb, and ^{208}Pb are radiogenic isotopes derived from the radioactive decay of ^{238}U, ^{235}U, and ^{232}Th parents, respectively, whereas ^{204}Pb is nonradiogenic (Doe and Stacey, 1974). Single-stage lead isotopes are those in which the present parent:daughter ratio is the result of sequential radioactive decay of the parents. Single-stage lead isotopes thus approximate the time of formation of the mineral deposit. Anomalous lead isotopes are those which result from the decay of sources with two or more parent:daughter ratios. Ages of formation determined from anomalous leads tend to be greatly in error (Sangster, 1976b).

Most of the classic carbonate-hosted Pb-Zn deposits of the Mississippi Valley are characterized by markedly radiogenic lead isotopes of the so-called J-type with $^{206}Pb/^{204}Pb$ ratios of 20 or greater (Heyl et al., 1974). Isotopic zonation in some districts has been interpreted to represent solution flow vectors; some individual galena crystals are zoned with more radiogenic isotopes on the perimeter (Heyl et al., 1974). The six previous Pb isotope determinations for galena from Pine Point (Cumming and Robertson, 1969) were considered to be poor representatives of the entire district because three were from the same sample and the other three were collected in 1916 from the original weathered surface occurrences. Thirteen carefully selected additional samples were analysed in this study in an attempt to represent variables of geographic location, hosting facies, galena habit, associated minerals, and paragenetic position (Appendix V). Although a slightly greater range is shown by the new data, the non-radiogenic

nature of the Pb indicated by the earlier analyses is verified (Fig. 73). The analyses are spread out along the "204-error" line, suggesting that analytical error of the least abundant isotope is the probable cause of most variation. Thus, the analyses can be considered as a single population, and a single-stage model for their evolution can be applied (D. F. Sangster, pers. commun., 1976). Using the methods of Cumming and Richards (1975), a model age of about 310 million years can be calculated from the mean isotopic composition. The mid-Carboniferous age thus determined can be considered as the valid age of mineralization in the absence of other evidence. The non-radiogenic character of the Pb may be interpreted to indicate either a juvenile source, or a source thoroughly mixed during sedimentation or transport so as to approximate single-stage conditions (Sangster, 1976b). District zonation or variation in lead isotopic percentages or ratios due to stratigraphic position, associated minerals, galena habit, or paragenetic stage is not indicated by present data.

The study by Beales et al. (1974) demonstrates great potential for the use of natural remnant magnetism to determine age of mineralization. Paleomagnetic pole positions computed for ores and their host rocks from two carbonate-hosted Pb-Zn districts are identical within statistical uncertainty. These results suggest that the ores, although clearly epigenetic, are of approximately the same age as the host rock (within 25 million years at their limit of accuracy), which is in agreement with geologic evidence. This method of age determination should become increasingly beneficial as apparent polar wandering curves are better defined by future work and as more

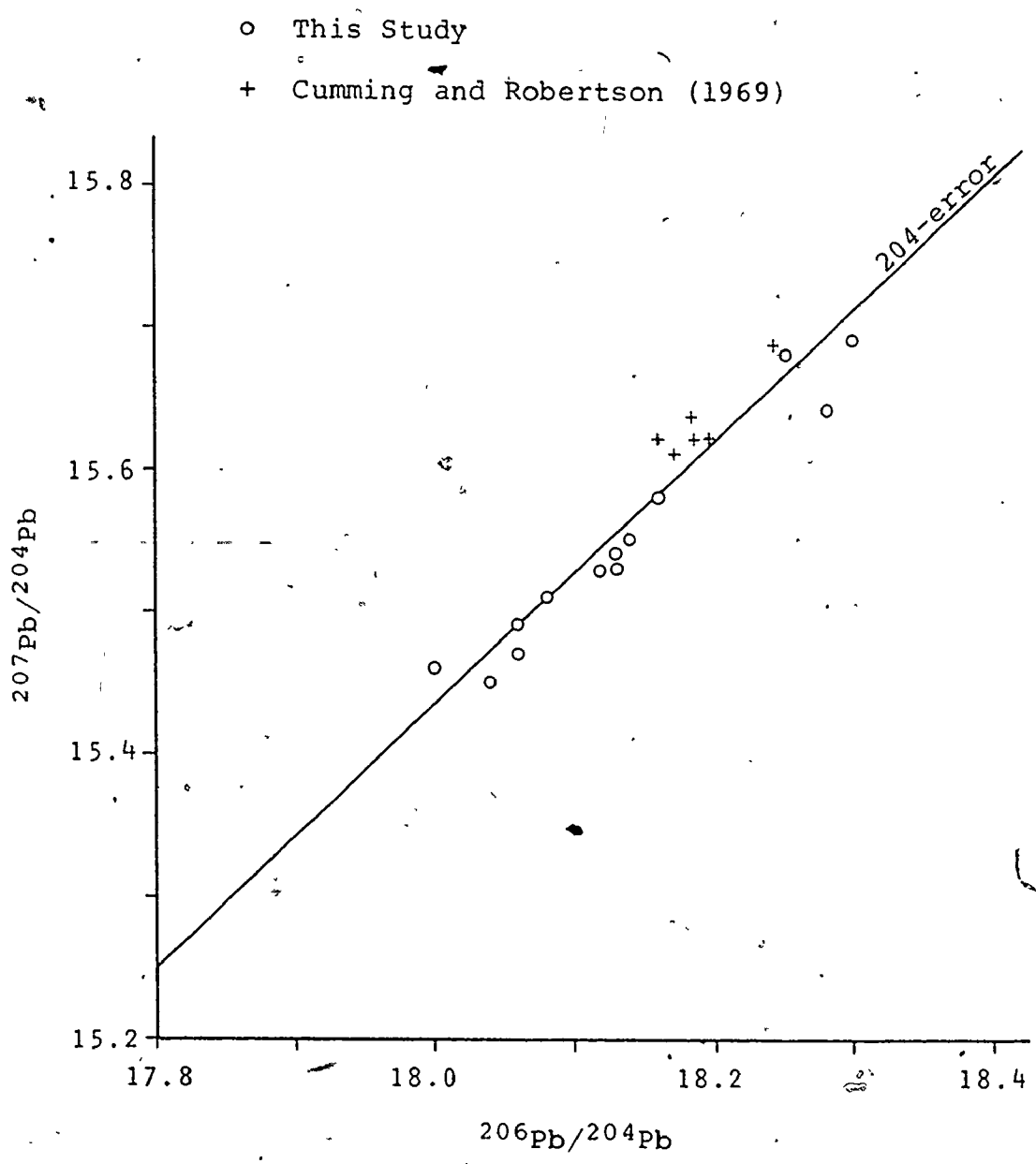

Fig. 73. Lead Isotope Ratios in Galena, Pine Point District

Data are presented in Appendix V.

sensitive techniques are developed to measure low levels of remnant magnetism. Beales et al. (1974) were unable to detect the remnant magnetism for a sample of Pine Point ore.

In addition to the geologic age of mineralization, the length of time involved in sulfide deposition is also of interest. For example, as Roedder (1976) shows, 100 million tons of 10 percent ore could be deposited within a time span of 1,000 to 10 million years with a precipitation change of 1,000 to 10 ppm, respectively, using geologically reasonable values for fluid flow rates, quantity of flow, fluid density, and bulk porosity. Roedder (1968a) recognized regular ("periodic") color bands in Pine Point colloform sphalerites and interpreted them to be annual varves, perhaps resulting from seasonal mixing of fluids of different compositions. If the total ore deposition consists of about 7 cm thick colloform crusts on many substrates, as Roedder assumes, and each varve has a thickness of 7 μm, then 100 million tons of 10 percent ore could be deposited in about 350,000 years with a precipitation change of 1,000 ppm and flow rates of 10 gallons per minute. Extremely rapid sulfide growth has been demonstrated for the Cheleken Peninsula where the artificial mixing of natural metal- and sulfur-bearing brines results in colloform sphalerite precipitation at the rate of 1 cm per year (Lebedev, 1972). Periods of rapid precipitation are suggested also by Pine Point sulfide textures such as colloform sphalerite, skeletal galena, and intimate intergrowths (Plate 11:3-8; 12:5); also periods of slower growth are indicated by large crystals (Plate 12:2, 4; 13:3). Interruptions in sulfide deposition are indicated by intergrown dolomite (Plate 11:3).

CHAPTER SIX

CONCLUSIONS

Post-middle Givetian subaerial exposure of the Pine Point barrier complex resulted in the formation of major solution structures and the Facies K dolostone. Dolines developed through the dissolution of upper barrier limestones by meteoric water; caves and tabular zones of increased permeability formed in the upper part of the meteoric phreatic zone. The upper barrier limestones were converted into coarse-crystalline Facies K dolostone in a zone of mixed fresh water and sea water during subaerial exposure, as indicated by stratigraphic relations, paleogeography, hydrologic principles, dolostone Na-contents, and comparison with recent carbonates. Increase in sea level during marine transgression at the cessation of the erosional period resulted in sporadic raising of the level of the various diagenetic environments and filling of the dolines with erosional detritus. Dolomitization of upper barrier limestones and detritus-filled dolines ceased as the meteoric water supply was terminated by marine inundation of the erosional surface. These solution features were aquifers for mineralizing fluids and loci for sulfide deposition in the coarse-crystalline Facies K dolostone. Dolines host prismatic ore bodies, whereas caves and tabular permeable zones contain tabular ore bodies. Origin of the sulfide-hosting breccias in the fine-crystalline dolostones of the lower barrier is less apparent, but these also are believed to be

3 3

OF/DE

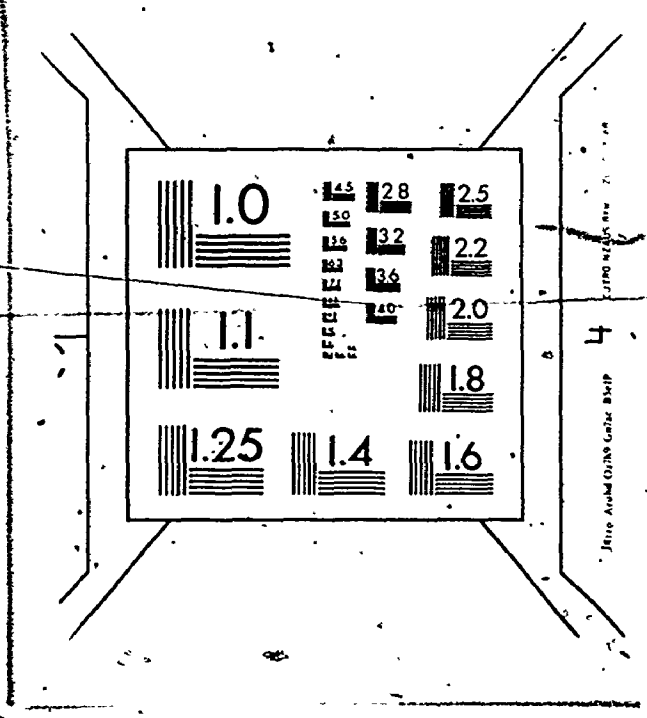

ARC - 374

solution features.

The Pine Point sulfide bodies range in size from less than 100,000 tons to more than 15 million tons and contain up to 20 percent combined Pb-Zn as sphalerite and galena. Marcasite and pyrite are common accessories, and Fe content of ore bodies ranges from less than 1 to more than 10 percent. Individual ore bodies are zoned with a Pb-rich, high grade core passing outward into a Zn-rich, high grade zone which grades into an Fe-rich, low grade envelope. A district metal zonation is indicated by ore bodies along both the Main and North Trends which are progressively more Pb-rich and less Fe-rich from southeast to northwest in zones parallel to the Hinge Zones.

Fluid inclusion evidence indicates that the Pine Point sulfides were deposited by highly saline brines at temperatures of 50° to 100° C, probably upon encountering a supply of reduced sulfur. These brines appear to have originated within the sedimentary sequence, but the immediate metal source cannot be defined by present data. Major and trace element composition of the ores indicates only abundant Pb, Zn, and Fe components in a 2:5:3 ratio. The most likely sulfur source is the Middle Devonian evaporites, probably supplied in the form of H_2S. Lead isotope analyses of a variety of district galena types confirm their non-radiogenic nature and indicate a mean $^{206}Pb/^{204}Pb$ ratio of about 18.1. These data suggest a mid-Carboniferous (310 million years) age of mineralization, considerably younger than the middle Givetian (375 million years) dolostone host. Colloform sphalerite and skeletal galena indicate an early phase of rapid sulfide deposition, while coarse crystals suggest a later period of slower

sulfide growth. Evidence for both sulfide-carbonate equilibrium and disequilibrium conditions are apparent, perhaps relating to periodic fluctuations in supply of reduced sulfur.

High-grade sulfide concentrations are localized in paleodolines and breccia zones because these transgressive features were the bypasses between different aquifers and acted as natural mixing sites for fluids of different character, one of which contained metals and the other reduced sulfur. This model is supported by the occurrence of prismatic ore bodies in dolines and breccia zones within an otherwise undisturbed stratigraphic section, the sharp boundaries and individual nature of the ore zones, the concentric metal zoning pattern in ore bodies, and apparent divergences in fluid flow directions.

Many questions remain unanswered for the Pine Point district, including the source of metals and the timing of mineralization. The concept of multiple phases of metal enrichment should be considered. Exhalative supply of metals to the sea floor along the N 65° E Hinge Zones perhaps resulted in metal concentration in shales, carbonates, or evaporites. Subsequent metal enrichment of sedimentary brines occurred, and metals were fixed as sulfides upon encountering reduced sulfur. Mechanical (and chemical?) reworking of sulfides as a result of carbonate dissolution accompanying sulfide deposition appears to have resulted in further sulfide concentration in some ore bodies.

PLATE 1

Lower Paleozoic and Lower Pine Point Barrier Rock Types

(Samples are polished cores, 35 mm in horizontal dimension)

1:1 Old Fort Island Formation -- reddish, fine-grained, friable quartz sandstone.

1:2 Mirage Point Formation -- orange, fine-crystalline dolostone with blebs and veins of anhydrite.

1:3 Mirage Point Formation -- reddish- and greenish-gray dolomitic mudstone with abundant scattered sand grains.

1:4 Chinchaga Formation -- light to medium brown anhydrite with thin dolostone laminae and anhydrite-filled fractures.

1:5 Keg River Formation -- Facies A -- medium brown, argillaceous limestone with abundant crinoid ossicles and scattered brachiopod fragments.

1:6 Keg River Formation -- E-Shale -- bluish-gray, dolomitic shale with scattered crinoid ossicles.

1:7 Pine Point Group -- Facies B-1 -- light gray brown, dense dolostone with scattered stromatoporoid fragments.

1:8 Facies B-1 -- medium brown, sandy dolostone with Thamnopora impregnated with bitumen.

1:9 Facies B-2 -- dark gray brown, dense dolostone with abundant crinoid ossicles and thin-shelled brachiopods (partly silicified).

1:10 Facies B-3 -- light brown, dense dolostone with fine fractures and areas of good intergranular ("spongy") porosity after leached fossils and burrows.

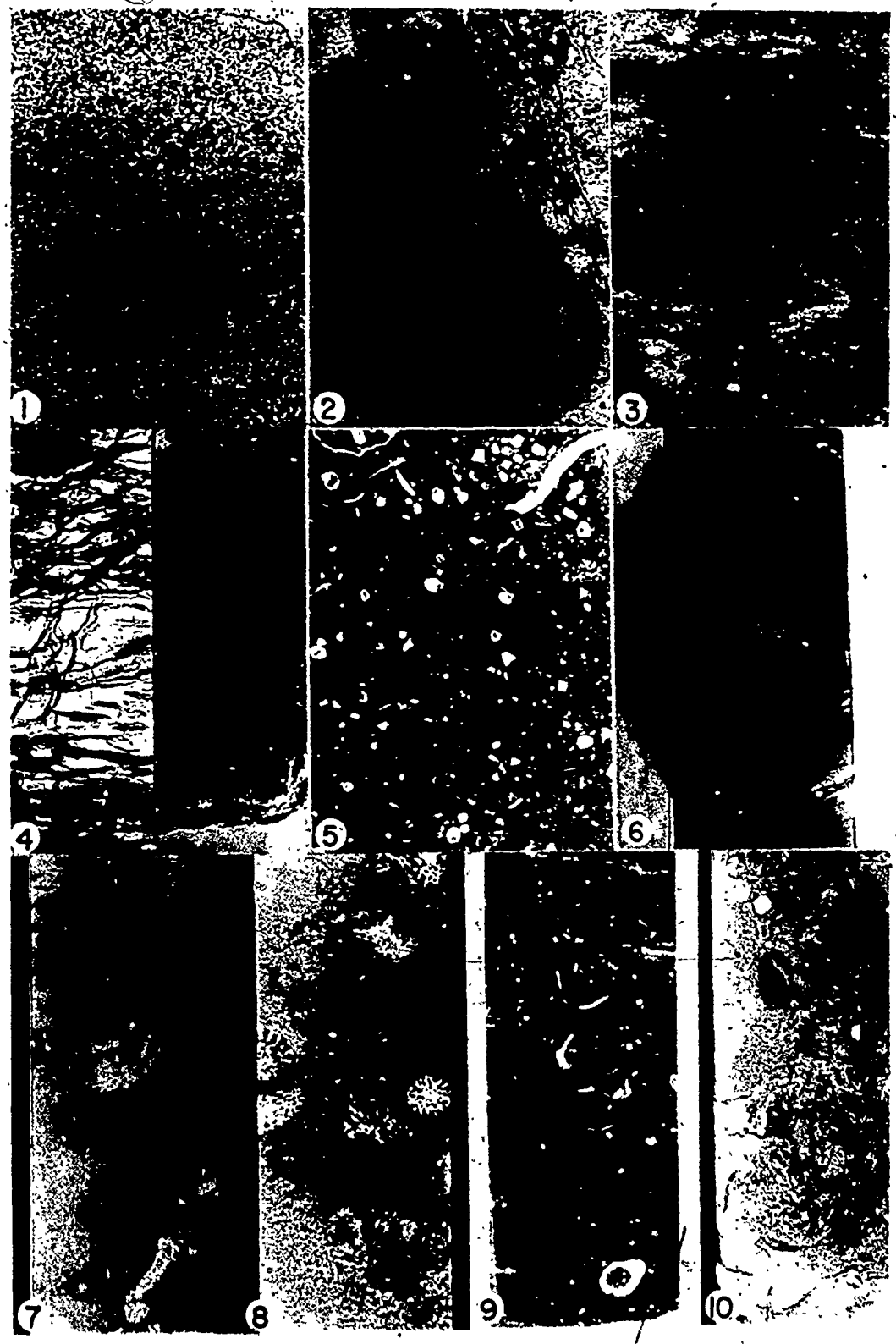
1
2
3
4
5
6
7
8
9
10

PLATE 2

Pine Point Group Rock Types

(Samples are polished cores, 35 mm in horizontal dimension, unless another scale is shown)

2:1 Facies C -- very light gray limestone composed of uniform skeletal sand.

2:2 Facies D-1

a. Medium brown dolostone with tabular stromatoporoid fragments.

b. Buff, sandy dolostone with vague "micritized" tabular stromatoporoids.

2:3 Facies D-3

a. Light brown to gray fragmental dolostone.

b. Blue gray, dense, vuggy dolostone with vague fossil forms.

2:4 Facies D-1 -- medium brown dolostone with abundant leached stromatoporoids. X15 ore body, north side, 4th bench.

2:5 Facies D-2

a. Very light gray limestone composed of massive stromatoporoids. K62 ore body, south side, 1st bench.

b. Very light gray limestone composed of large fragments of massive stromatoporoids.

2:6 Facies E -- light brown, sandy, friable dolostone with good intergranular porosity.

2:7 Facies F -- black, very bituminous, micritic limestone with Tentaculites and Styliolina.

2:8 Facies F -- photomicrograph of Tentaculites in dense, bituminous limestone. Scale is 0.4 mm.

2:9 Facies G -- Buffalo River Shale -- bluish-gray, fissile shale with disseminated iron sulfides.

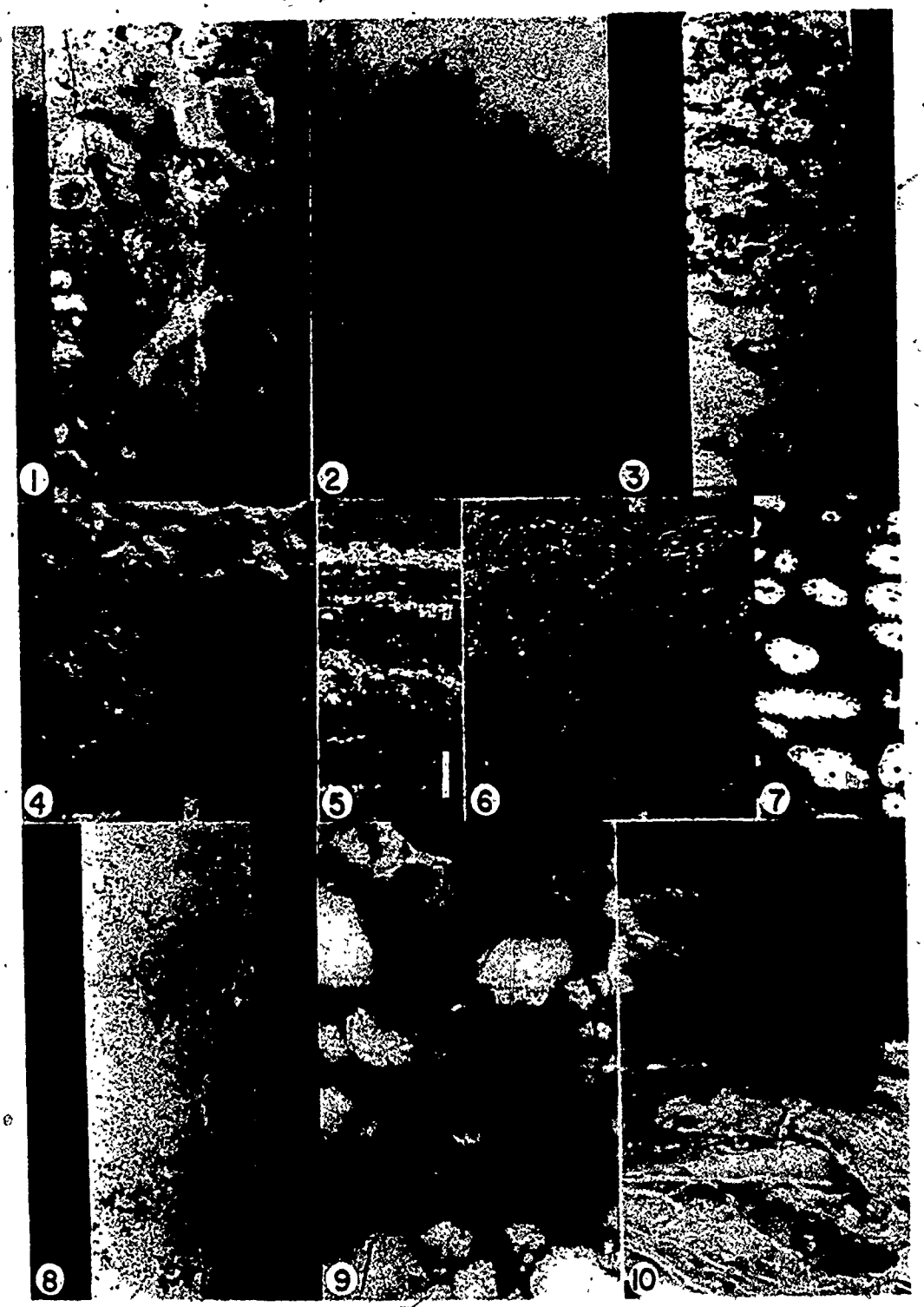
1
2
3
4
5
6
7
8
9
10

PLATE 3

Pine Point Group Rock Types

(Samples are polished cores, 35 mm in horizontal dimension, unless another scale is shown)

3:1 Facies H -- very light gray limestone with gastropods and algally-coated skeletal grains.

3:2 Facies I -- very light gray, micritic limestone with common Amphipora.

3:3 Facies J-1 -- light blue gray, dense dolostone with blotchy mottling.

3:4 Facies J-2 -- medium brown, faintly laminated, dense dolostone; lens cap is 54 mm in diameter. W17 ore body, west side, 3rd bench.

3:5 Facies J-2 -- polished core showing crenulated laminae, probably of algal origin; scale is 5 mm.

3:6 Facies J-4 -- medium brown, dense dolostone with abundant Amphipora; lens cap is 54 mm in diameter. X15 ore body, west side, 3rd bench.

3:7 Facies J-4 -- polished core with abundant Amphipora; scale is 5 mm.

3:8 Facies J-3 -- light brown, sandy dolostone with good intergranular porosity.

3:9 Muskeg Formation -- white, nodular gypsum.

3:10 Muskeg Formation -- light to medium brown, dense anhydrite.

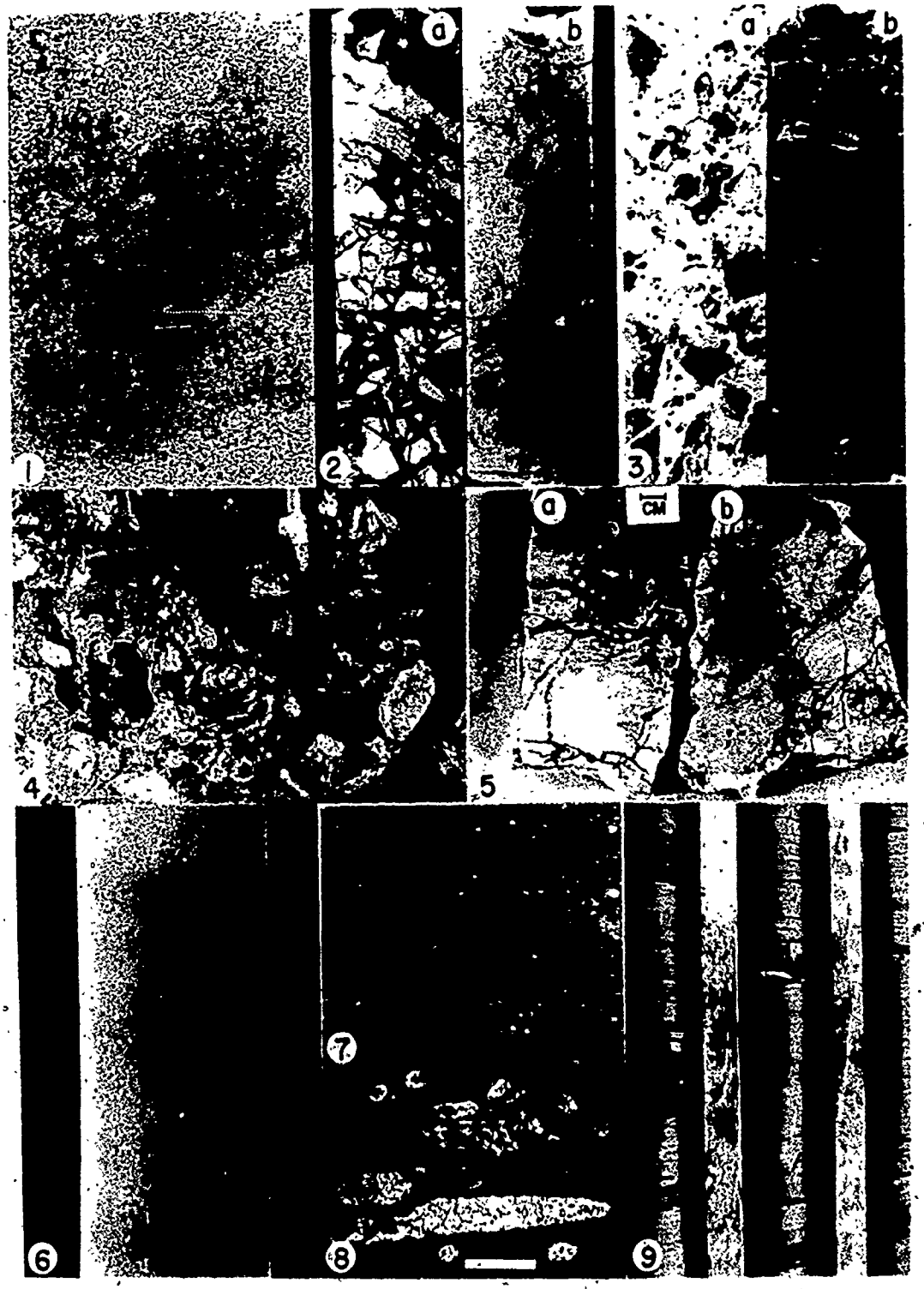
a
b
a
b
1
2
3
a
cm
b
4
5
6
7
8
9

PLATE 4

Presqu'ile Facies K

4:1 Bedded Facies K in west wall of N38A open pit, first bench. Note abundant zones of white dolomite above thin bed of Facies J-2 dolostone (C-Horizon). Bench height is about 8 meters.

4:2 Well-bedded back-reef Facies K in south wall of N42 open pit. Height of exposed section is about 25 meters.

4:3 White dolomite-healed "breccia" in upper K in south wall of K57 open pit, fourth bench.

4:4 Pervasive white dolomite in upper K in southeast wall of K57 open pit, fourth bench.

4:5 Boxwork white dolomite in west wall of K57 open pit, fourth bench.

4:6 Boxwork white dolomite with porosity-occluding coarse calcite. K57 open pit, west side, fourth bench.

4:7 Pervasive white dolomite in upper K, core specimens from K57 ore outline drilling.

4:8 Buff, coarse-crystalline dolostone in lower K, K57 ore outline drilling.

a,b. Massive, vuggy dolostone with relic massive stromatoporoids.

c,d. Uniform granular dolostone, probably relic skeletal debris; pervasive iron sulfides account for darker color of d.

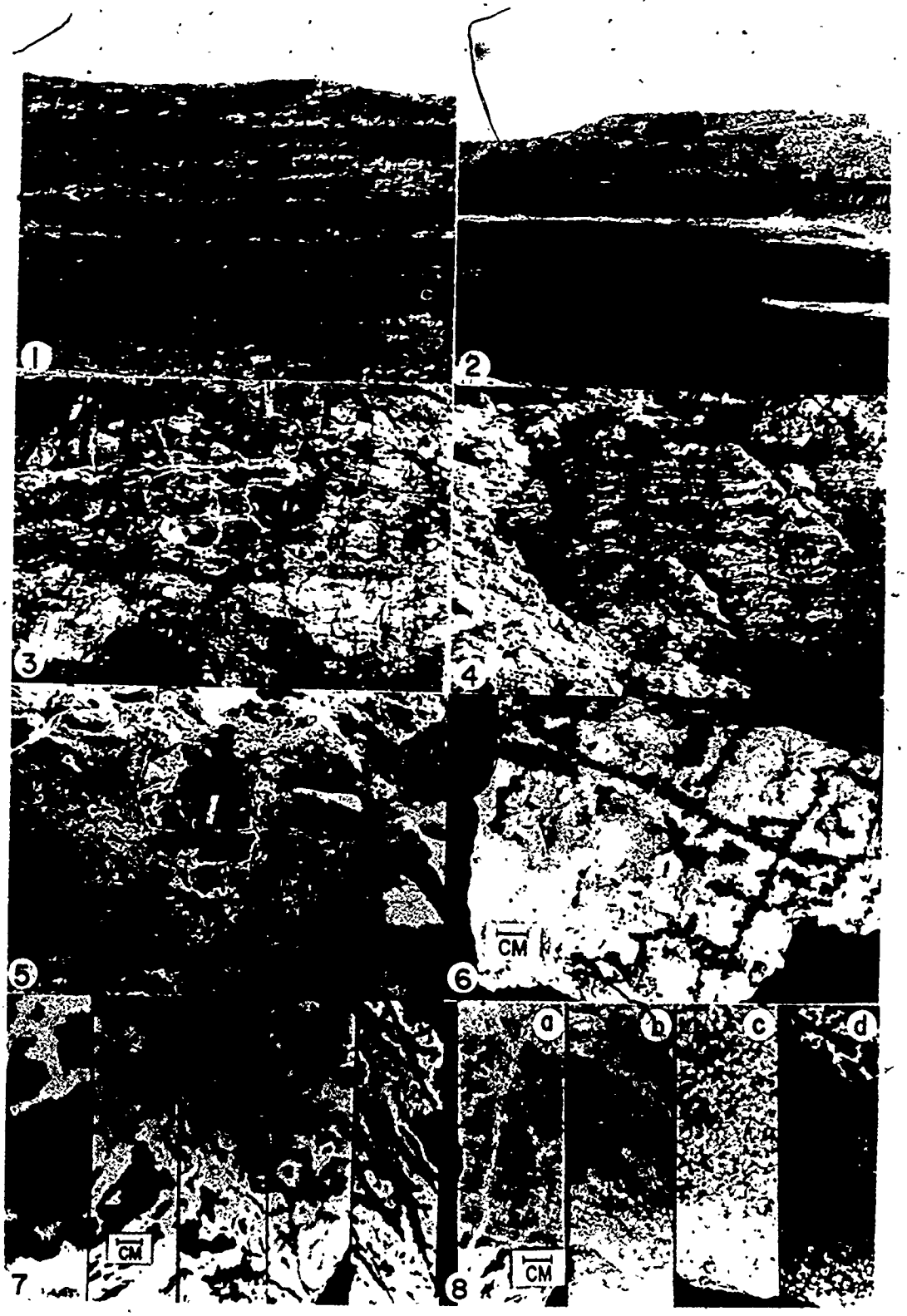
1
2
3
4
5
6
CM
7
CM
8
a
b
c
d
CM

PLATE 5

Presqu'ile Facies K

5:1 Irregular contact of coarse-crystalline Facies K dolostone with unaffected near-reef Facies D-2 limestone in J44 ramp; steeply-dipping fracture is filled with gray-green clay.

5:2 Interbedded coarse-crystalline dolostone of Facies K and micritic limestone of Facies I on right passing to left into section of entirely coarse-crystalline dolostone, N42 ramp.

5:3 Close-up of part 5:2.

5:4 Specimens of interbedded lithologic types, N42 ramp.

a. Very light gray Facies I limestone with skeletal sand and gravel.

b. Buff coarse-crystalline Facies K dolostone with granular texture.

5:5 Transformation of carbonate sediment into Facies K; interbedded and gradational lithologies from drill core.

a. Skeletal gravel, largely dendroid stromatoporoid fragments.

b. Lithified skeletal gravel (Facies D-2).

c. Coarse-crystalline Facies K dolostone derived from D-2 limestone.

5:6 Light gray, coarse-crystalline Facies K dolostone consisting of massive stromatoporoids with some corals.

5:7 Light brown, coarse-crystalline dolostone with parallel layers of white dolomite ("zebra rock").

5:8 Coarse-crystalline, granular Facies K dolostone types with varying amounts of white dolomite.

5:9 Coarse-crystalline Facies K dolostones, possibly derived from pre-existing fine-crystalline dolostones.

a. Light gray, laminated coarse-crystalline dolostone associated with C-Horizon; possibly former Facies J dolostone.

b. Light brown, coarse-crystalline dolostone occurring in lower part of Facies K; possibly former Facies E dolostone.

c. Medium brown, argillaceous, coarse-crystalline dolostone with relic thin-shelled brachiopods and crinoid ossicles from lower part of Facies K; probably former Facies B dolostone.

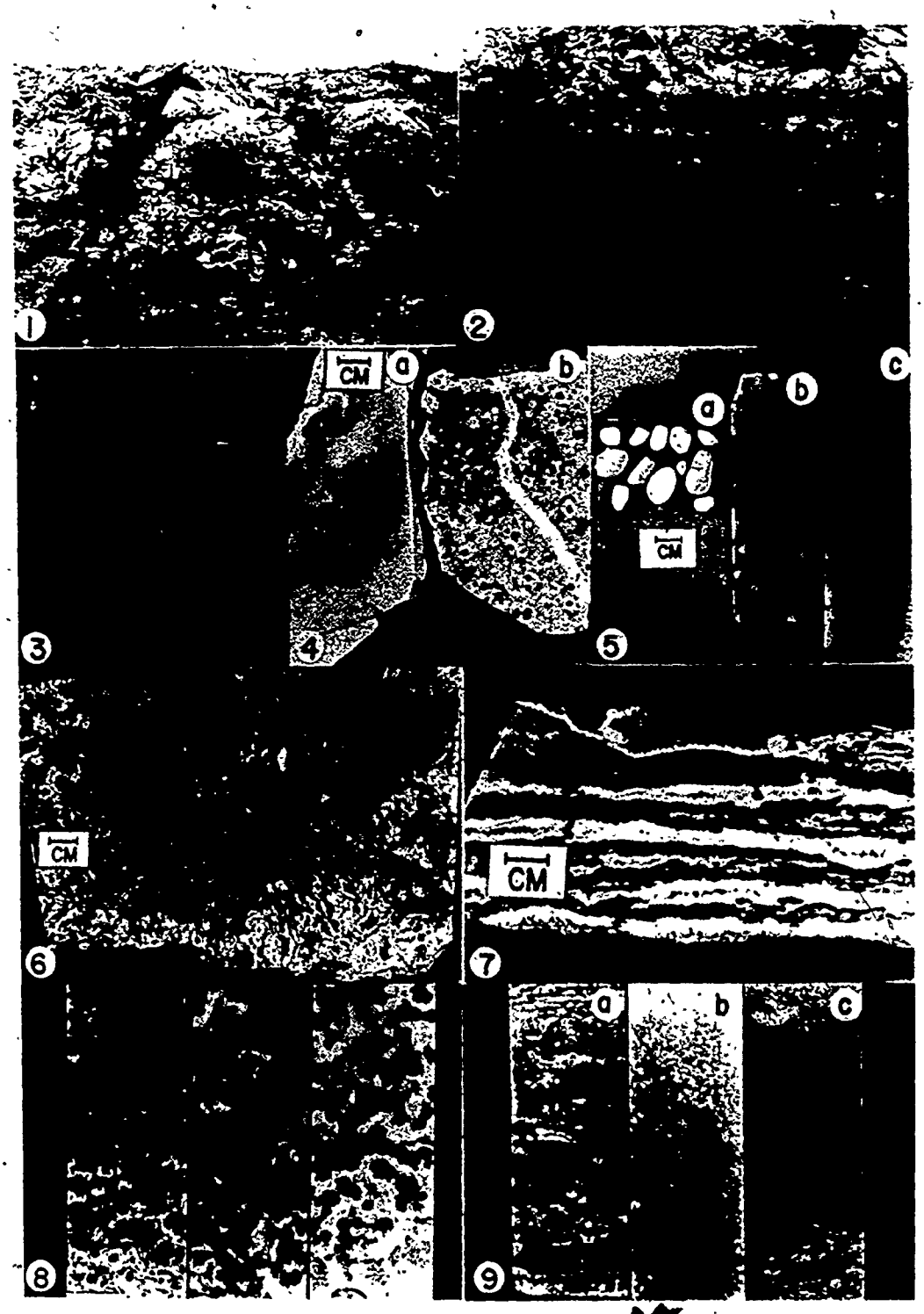
1
2
CM
a
b
c
3
4
5
6
7
8
9

PLATE 6

Watt Mountain and Slave Point Formations

(Samples are polished cores, 35 mm in horizontal dimension)

6:1 Watt Mountain Formation -- Facies L -- light gray, dense limestone with algal and skeletal sand laminae.

6:2 Facies L -- light green gray, argillaceous dolostone with scattered blotchy mottling and shale chip conglomerate.

6:3 Facies L -- very light gray, micritic limestone impregnated with bitumen.

6:4 Slave Point Formation -- Facies M-2 -- light brown limestone with bulbous stromatoporoids impregnated with bitumen.

6:5 Slave Point Formation -- Facies N -- light gray brown, laminated limestone.

6:6 Slave Point Formation -- Facies O -- dark brown, micritic limestone with abundant irregular argillaceous laminae.

6:7 Slave Point Formation -- Facies P -- medium brown limestone with common thin-shelled brachiopods and small intraclasts.

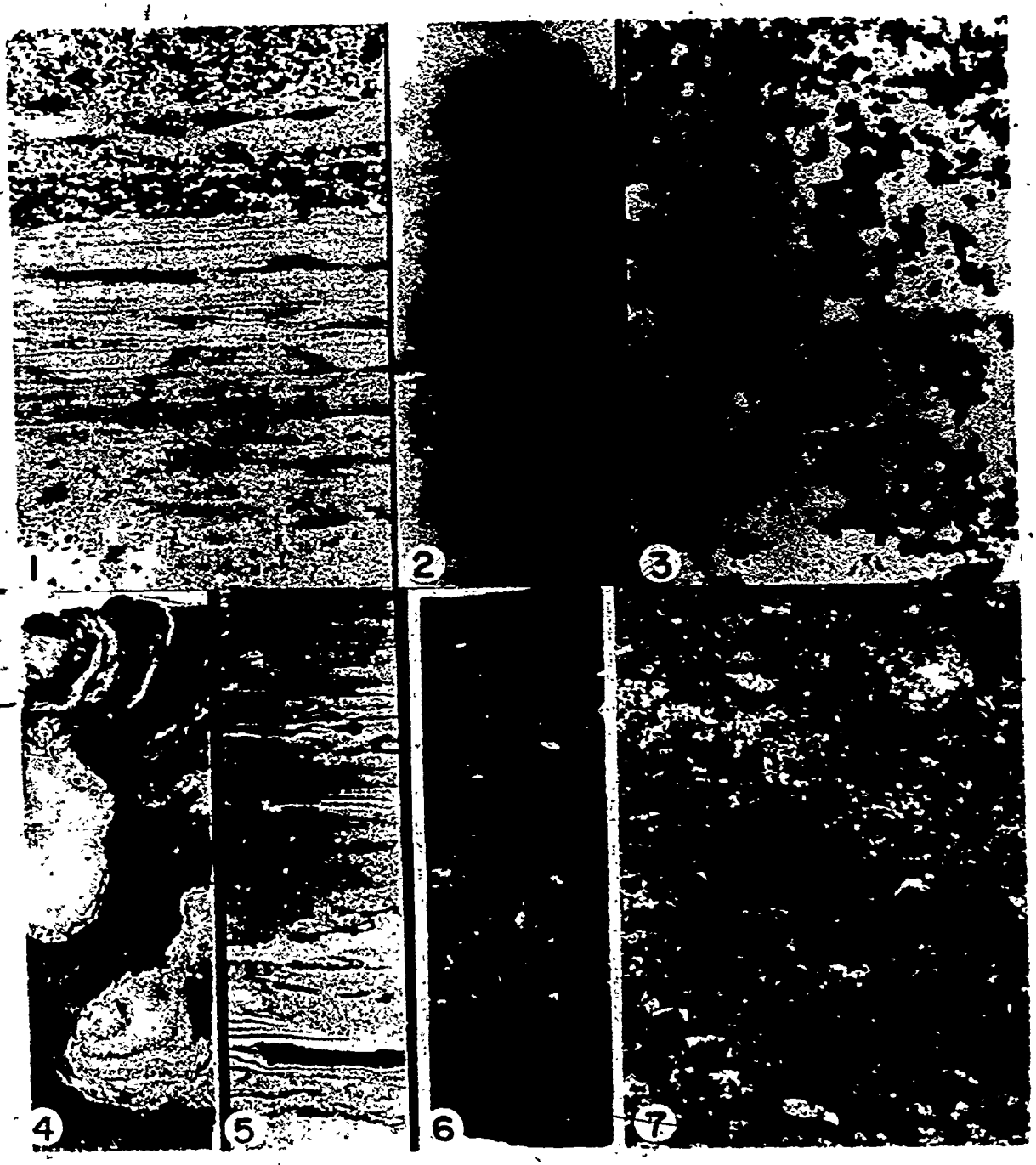
1
2
3
4
5
6
7

PLATE 7

Sulfide-hosting Features Associated with
Prismatic Ore Bodies in Facies K

7:1 Abrupt transition (dashed line) from the iron-rich perimeter (S) of N38A ore body to sulfide-deficient coarse-crystalline dolostone of upper Facies K. N38A open pit, southeast side, first bench; width of scene is about 8 meters.

7:2 Isolated remnant block of laminated detritus (D) within massive sphalerite and galena (S); K62 open pit, first bench.

7:3 Medium-gray, laminated detritus with scattered green clay blebs and white dolomite. Sample K57-29-80; scale is 1 cm.

7:4 Light gray, laminated detritus (D) with introduced sphalerite (S1) and galena (Ga). Sample K62-25; scale is 1 cm.

7:5 Detritus (D) with scattered tidal flat dolostone fragments; irregular fractures cemented by sphalerite and galena (S). K62 open pit, first bench; lens cap is 54 mm in diameter.

7:6 Dolostone detritus with pervasive introduction of about 75% sphalerite and galena; note preserved blebs of green clay (C). Sample A70-4-193; scale is 1 cm.

7:7 Large tidal flat dolostone fragments in detritus; K62 open pit, center, first bench.

7:8 Detritus "fragments" (D) cemented by colloform sphalerite (S1) and galena (Ga); note isolated colloform crusts without substrates and galena veinlet transecting detritus fragment and its colloform sphalerite rim (A). Sample N38A-7.

7:9 Fragments of tidal flat dolostone and green clay (C) in detritus; galena crystals (Ga) in matrix. K62 open pit, east side, first bench; coin is 23 mm in diameter.

7:10 Photomicrograph of dolostone detritus (D) with intercrystalline galena (Ga) and clay (C). Sample Z53N-1-52, polished surface 6320. Reflected light; scale is 0.4 mm.

7:11 Photomicrograph of galena in dolostone detritus; irregular crystal edges and remnants of detritus within the single crystal suggest that the crystal formed by successive stages of detritus dissolution and galena precipitation. Sample K62-5; polished surface K-5. Reflected light; scale is 0.4 mm.


1
2
3
4
5
6
7
8
9
10
11

PLATE 8

Sulfide-hosting Features Associated with
Tabular Ore Bodies in Facies K

8:1 Coarse-crystalline sphalerite in stratabound porosity zones in lower Facies K dolostone. M40 ore body, stope 3336-7; scale is 30 cm.

8:2 Uniform granular Facies K dolostone with fine- to very coarse-crystalline dark reddish-brown sphalerite. Cores from tabular sulfide zone east of K57 open pit; samples, left to right, K57-142-101, K57-128-78, K57-128-92.

8:3 Uniform granular Facies K dolostone with coarse-crystalline galena. Sample K57-20.

8:4 Uniform granular Facies K dolostone with fine-crystalline dark reddish-brown sphalerite. Sample N38A-25.

8:5 Facies K dolostone surrounded by massive sphalerite and galena (S) in a macropore. M40 ore body; scale is 30 cm.

8:6 Stalactitic sphalerite in tabular macropore. M40 ore body, 3134 drift east; scale is 10 cm.

8:7 Collapse breccia in lower Facies K dolostone cemented by sphalerite and galena (S). M40 ore body, stope 3337-16; scale is 30 cm.

8:8 Breccia of uniform granular Facies K dolostone fragments cemented by massive coarse-crystalline galena (Ga). Sample K62-9.

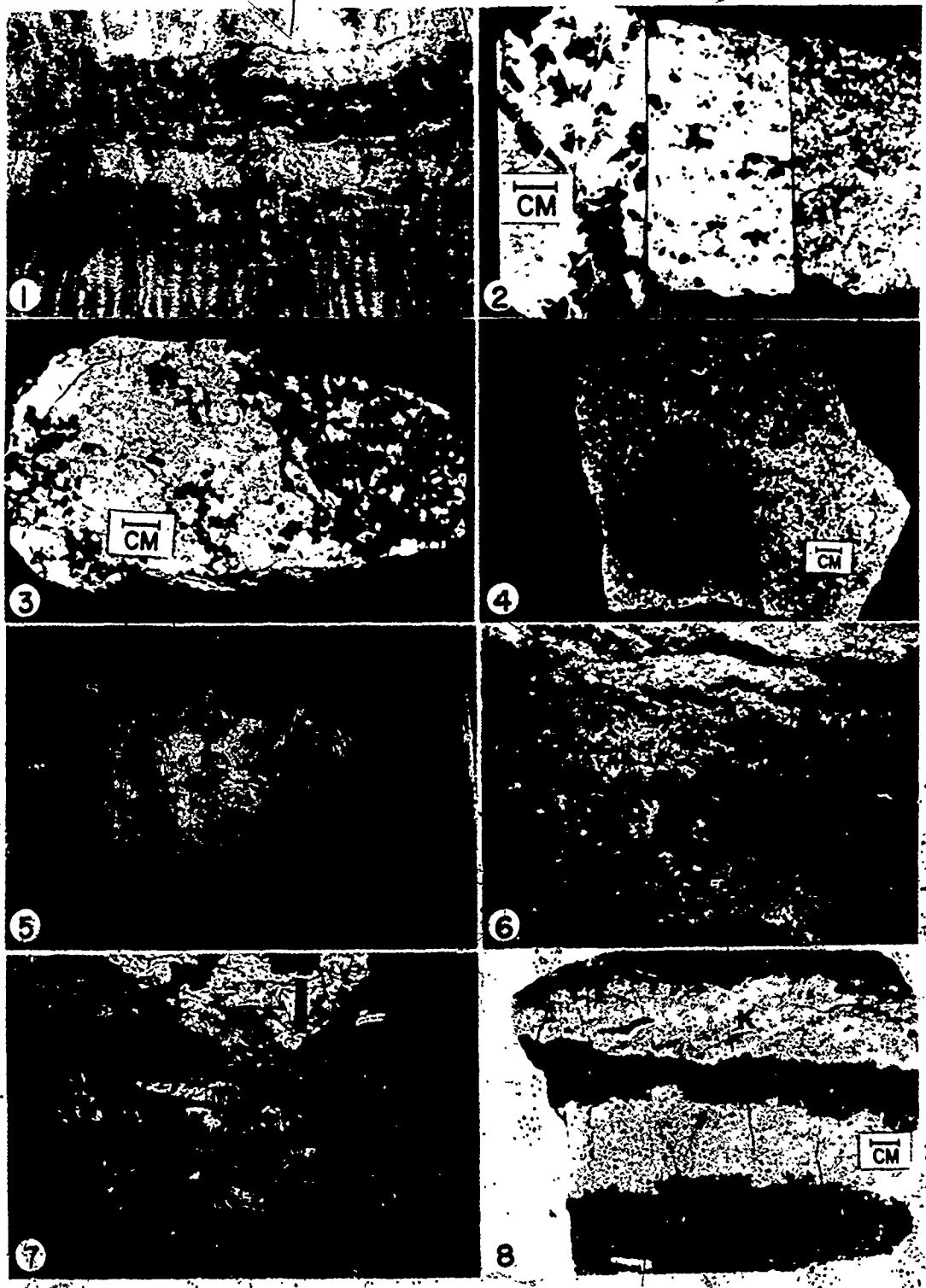
1
2
CM
3
CM
4
CM
5
6
7
8
K
CM

PLATE 9

Sulfide-hosting Features in the Fine-crystalline Dolostones of the lower Pine Point Group

9:1 Depression in Facies J dolostone exposed in west wall of W17 open pit; note boundary "fault". Height of exposed section is about 45 meters.

9:2 Rock matrix breccia with pervasive massive sulfides (S); note extremely irregular edges on fragment of J-4 dolostone. W17 open pit, sixth bench; scale is 15 cm.

9:3 Rock matrix breccia (BR) consisting of J-2 and J-3? dolostone fragments in fine-crystalline, light gray dolostone matrix; note irregular contact with massive sulfides (S). The absence of sulfide encrusting growth forms on the irregular contact suggests that the sulfides formed by successive stages of carbonate dissolution and sulfide precipitation. Sample W17-17.

9:4 Fragments of dolostone and limestone in micritic, calcareous matrix; note bleached rims on some fragments. W17 open pit, sixth bench; lower scale in cms.

9:5 Breccia of J-2 dolostone fragments cemented by encrusting sulfides. W17 open pit, third bench; lens cap is 54 mm in diameter.

9:6 J-2 dolostone with irregular areas of massive sulfides (S); note that tidal flat laminations are not displaced adjacent to the sulfides. W17 open pit, sixth bench; scale is 20 cm.

9:7 Massive ore composed of intimate mixture of marcasite, pyrite, sphalerite, and galena. W17 open pit, third bench.

9:8 Facies B dolostone with sulfides in intercrystalline porosity and galena in thin fractures. Core, N204 ore body; scale is 1 cm.

9:9 Facies B dolostone with dark brown coarse-crystalline sphalerite in vugs and in intercrystalline porosity in burrows. Core, N204 ore body; scale is 1 cm.

9:10 Pervasive sulfides in intercrystalline porosity in Facies B dolostone. Core, N204 ore body; scale is 1 cm.

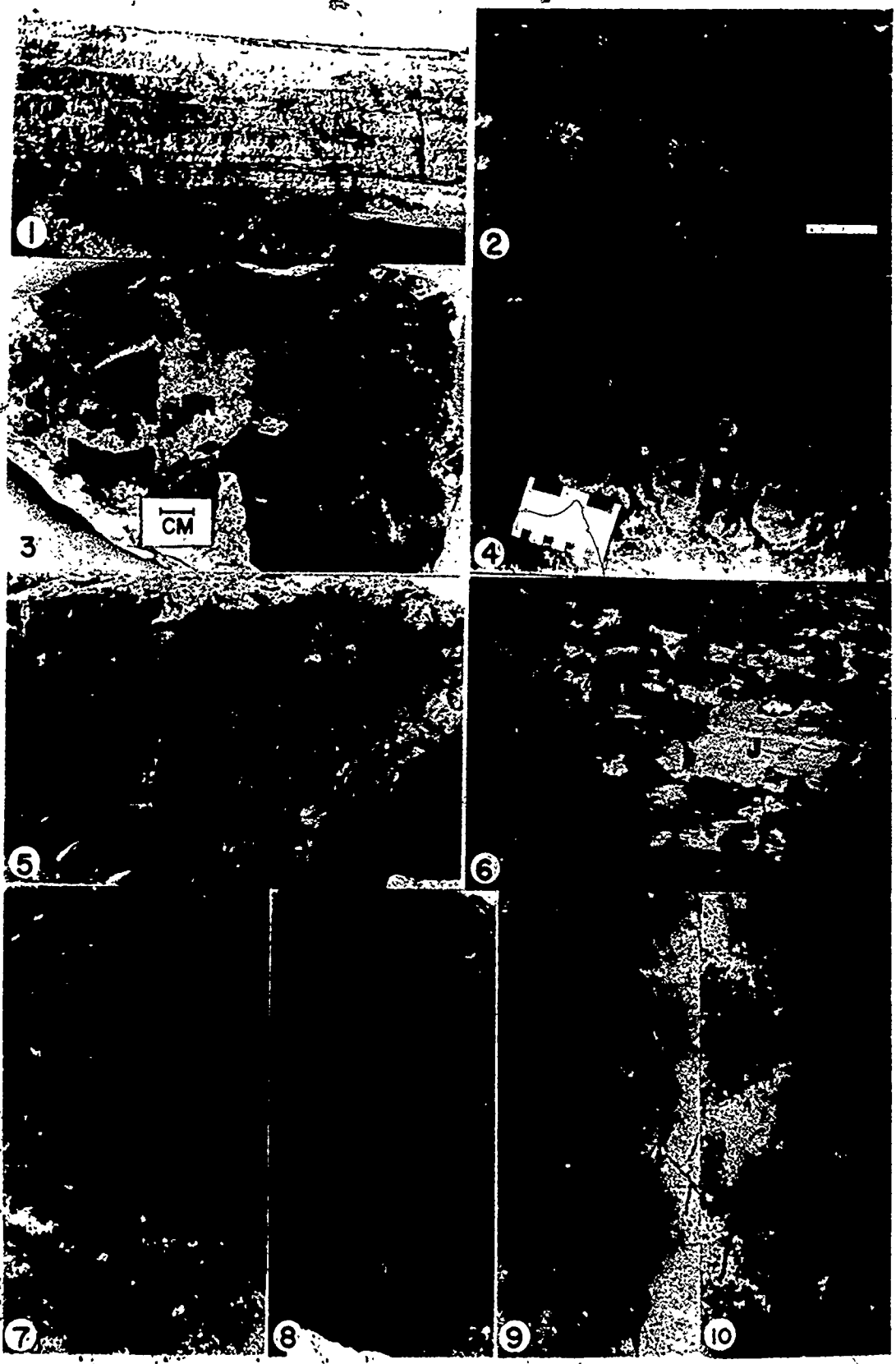
1
2
3
CM
4
5
6
7
8
9
10

PLATE 10

Sulfide Textures

10:1 Zoned tetrahedral crystals of reddish-brown sphalerite (S1) with encrusting white dolomite (Do). Sample J44-20; scale is 1 cm.

10:2 Yellow sphalerite crystals, fragments, and broken crusts in a matrix of calcite; calcite has been stained with Alizarin red-S and appears dark. Sample X15-15.

10:3 Photomicrograph of X15-15; sphalerite (S1) appears dark in the coarse-crystalline calcite (Ca). Transmitted light; scale is 0.4 mm.

10:4 Three textural types of sphalerite in X15 and W17 ore bodies. Type 1 consists of coalescing fine-crystalline spherules of dark reddish-brown sphalerite, often with yellow rims. Type 2 is the yellow variety of 10:2, and type 3 is greenish-brown coarse-crystalline sphalerite with associated cubic galena. Interstitial calcite has been stained with Alazarin red-S and appears dark. Sample X15-20; scale is 1 cm.

10:5 Irregularly banded coarse-crystalline Facies K dolostone with introduced banded fine-crystalline greenish-brown sphalerite. N38A open pit, first bench, northeast side; coin is 23 mm in diameter.

10:6 Fine-crystalline sphalerite bands with interlayer galena and marcasite from location in 10:5. Sample N38A-8.

10:7 Zoned reddish-brown sphalerite crystals in dense very fine-crystalline dolostone of Facies L. Sample A70-1-80; scale is 1 cm.

10:8 Concentration "front" of sulfides, largely sphalerite, in fine-crystalline Facies J-3 dolostone. Polished surface 6789, sample X15-38. Transmitted light; scale is 1 cm.

10:9 Anastomosing network of concentration "fronts" in Facies J-3 dolostone; note apparent bleached areas adjacent to sulfide concentrations. X15 open pit, fourth bench, north side.

10:10 Dendritic and ramose sphalerite forms with galena growing on substrates of dolostone breccia fragments and encrusted by coarse calcite. J44 stockpile, exact location unknown; lens cap is 54 mm in diameter.

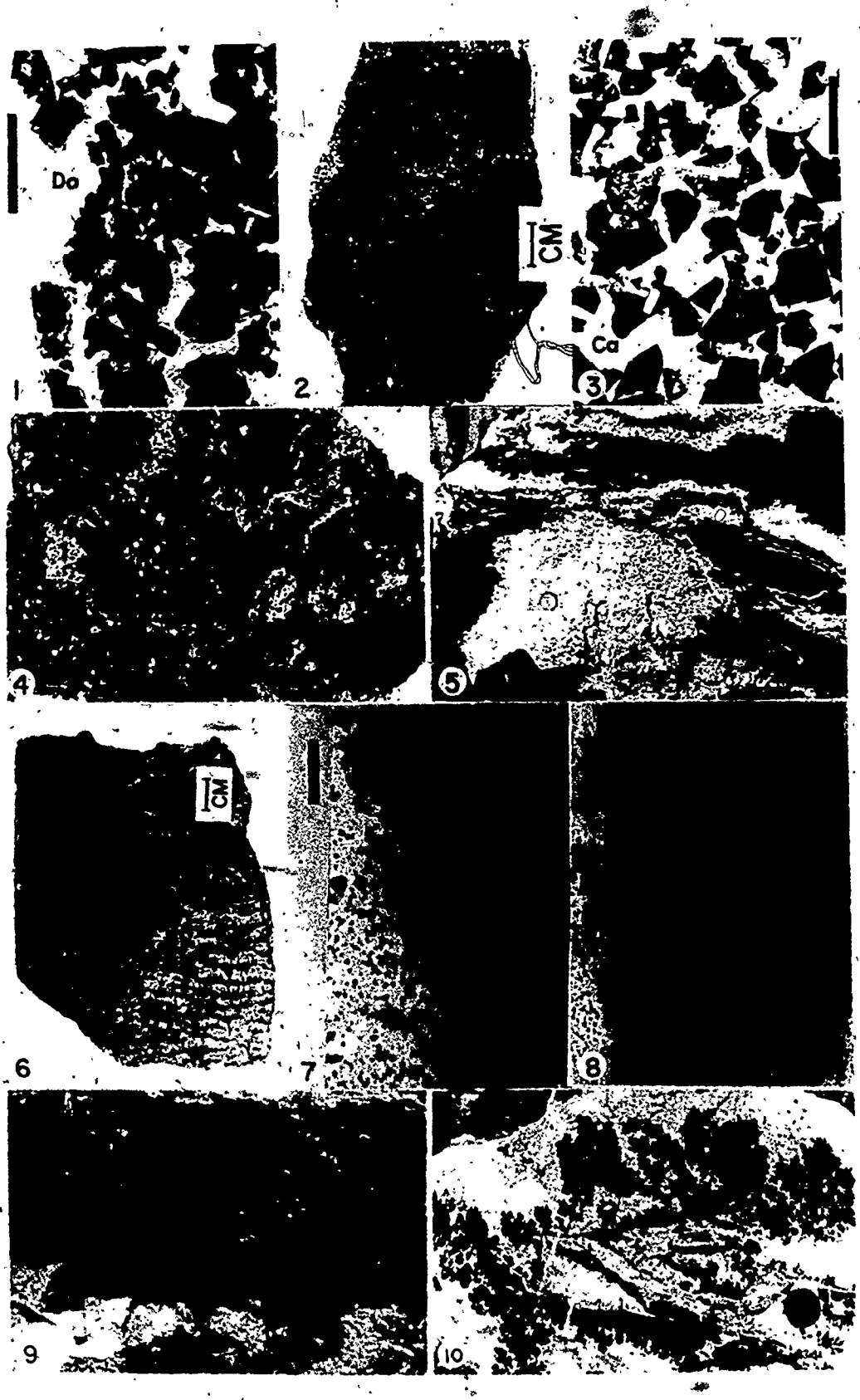
Da
CM
Ca
1
2
3
4
5
CM
6
7
8
9
10

PLATE 11

Sulfide Textures

11:1 Broken colloform sphalerite (Sl) in a matrix of skeletal galena (Ga). Sample 042-1.

11:2 Dark and light reddish-brown and tan colloform sphalerite in a matrix of sphalerite and galena. Sample 11,676; 024 open pit.

11:3 Thick sulfide crust consisting of the following units, in order of deposition: (1) dolomite; (2) dendritic dark reddish-brown sphalerite with minor galena; (3) ramose orange sphalerite with about 30% skeletal galena and rare pyrite; (4) orange sphalerite with minor skeletal galena; (5) yellow sphalerite; (6) reddish-brown sphalerite with cubic galena; (7) dolomite; and (8) dark brown sphalerite crystals with octahedral galena. Sample M40-7.

11:4 Layers 3-7, sample M40-7 (11:3). Transmitted light; scale is 1 cm.

11:5 Thick sulfide crust consisting of the following units: (1) dolomite; (2) alternating light and dark reddish-brown sphalerite with minor skeletal galena; (3) reddish-brown sphalerite with about 10% skeletal galena; (4) alternating yellow and tan microcrystalline sphalerite layers; initial yellow sphalerite layer fills skeletal galena molds transecting several layers of 3 strata (A); (5) alternating yellow and orange sphalerite bands; unit crystals extend across the stratigraphic sequence, and (6) yellow and orange sphalerite bands with octahedral galena crystals. Sample N42-1; scale is 1 cm.

11:6 Photomicrograph of skeletal galena in sphalerite, sample M40-7 (11:3). Polished surface K32; reflected light; scale is 0.4 mm.

11:7 Photomicrograph of "molar tooth" of galena with crown extending beyond growth limit of sphalerite stalactite. Polished surface 6334; sample M40-27. Reflected light; scale is 0.4 mm.

11:8 Photomicrograph of skeletal galena with sphalerite and dolomite. Polished surface M40-8. Reflected light; scale is 0.4 mm.

11:9 Photomicrograph of galena in colloform sphalerite showing the response of sphalerite precipitation to the presence of the galena crystal. Polished surface 350-[redacted]; sample 042-1. Reflected light, partly crossed nicols; scale is 0.4 mm.

11:10 Thick crust of colloform sphalerite with galena; note white dolomite underlying and overlying sulfides. Sample 028-2.

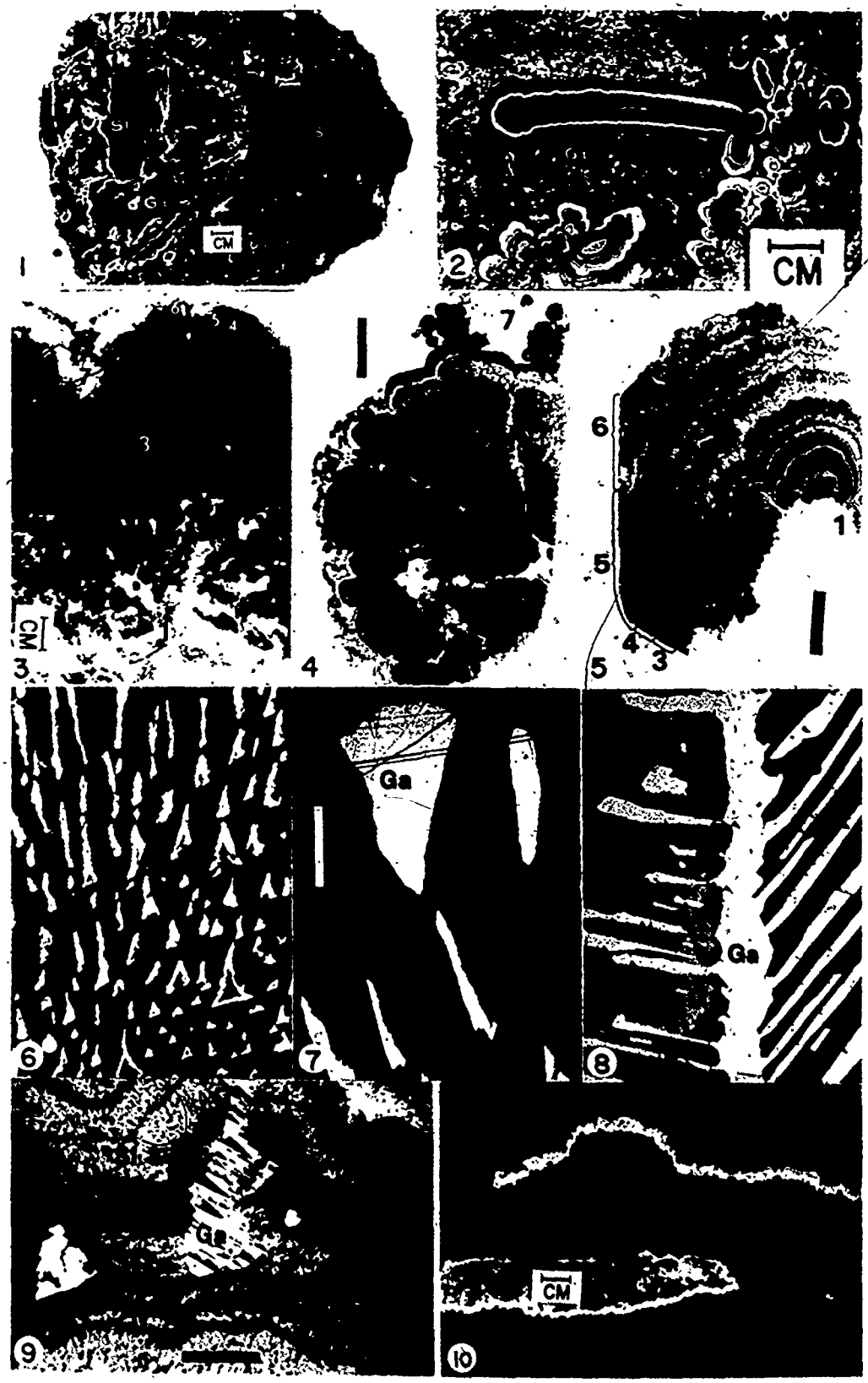
CM
CM
CM
Ga
Ga
Ga
CM

PLATE 12

Sulfide Textures

12:1 Skeletal galena aggregate containing 3 cm. cubic galena crystals. Sample K62-34.

12:2 Large cubic galena crystals from clay-filled vug in X15 ore body.

12:3 Photomicrograph of galena crystals with colloform sphalerite; massive galena associated with colloform sphalerite (e.g. 11:1, 12:1) commonly is composed of skeletal crystal aggregates. Polished surface 4653; sample 8341, 042 open pit. Reflected light; scale is 0.4 mm.

12:4 Coarse reddish-brown sphalerite (Sl) overgrown by late cubo-octahedral galena (Ga) and white dolomite. Sample N42-15; scale is 1 cm.

12:5 Hopper galena crystals overgrown by white dolomite; arrow shows relative direction of mineralizing fluid movement as indicated by crystal asymmetry (Kesler et al., 1972). Sample M40-36; scale is 1 cm.

12:6 Bladed galena crystals in center of banded reddish-brown sphalerite. Sample K57-22.

12:7 Coarse cubic galena crystals in a matrix of fine-crystalline, pulverulent, tan sphalerite and skeletal galena. Sample K62-10.

12:8 High-grade ore consisting of sulfide and Facies D-1 dolostone fragments cemented by calcite; note large iron sulfide fragments (A) and marcasite rind on one lithic fragment (B). sample X15-26.

12:9 Pulverulent, tan colloform sphalerite formed around irregular masses of iron sulfides (FS); colloform sphalerite is uncommon in the ore bodies in the fine-crystalline dolostones of the lower Pine Point Group. Sample X15-6.

12:10 Photomicrograph of fine-crystalline ramose sphalerite enclosing marcasite and pyrite within massive iron sulfides (FS); euhedral large crystals on periphery are pyrite (Py). Polished surface K19; sample X15-9. Reflected light, scale is 0.4 mm.

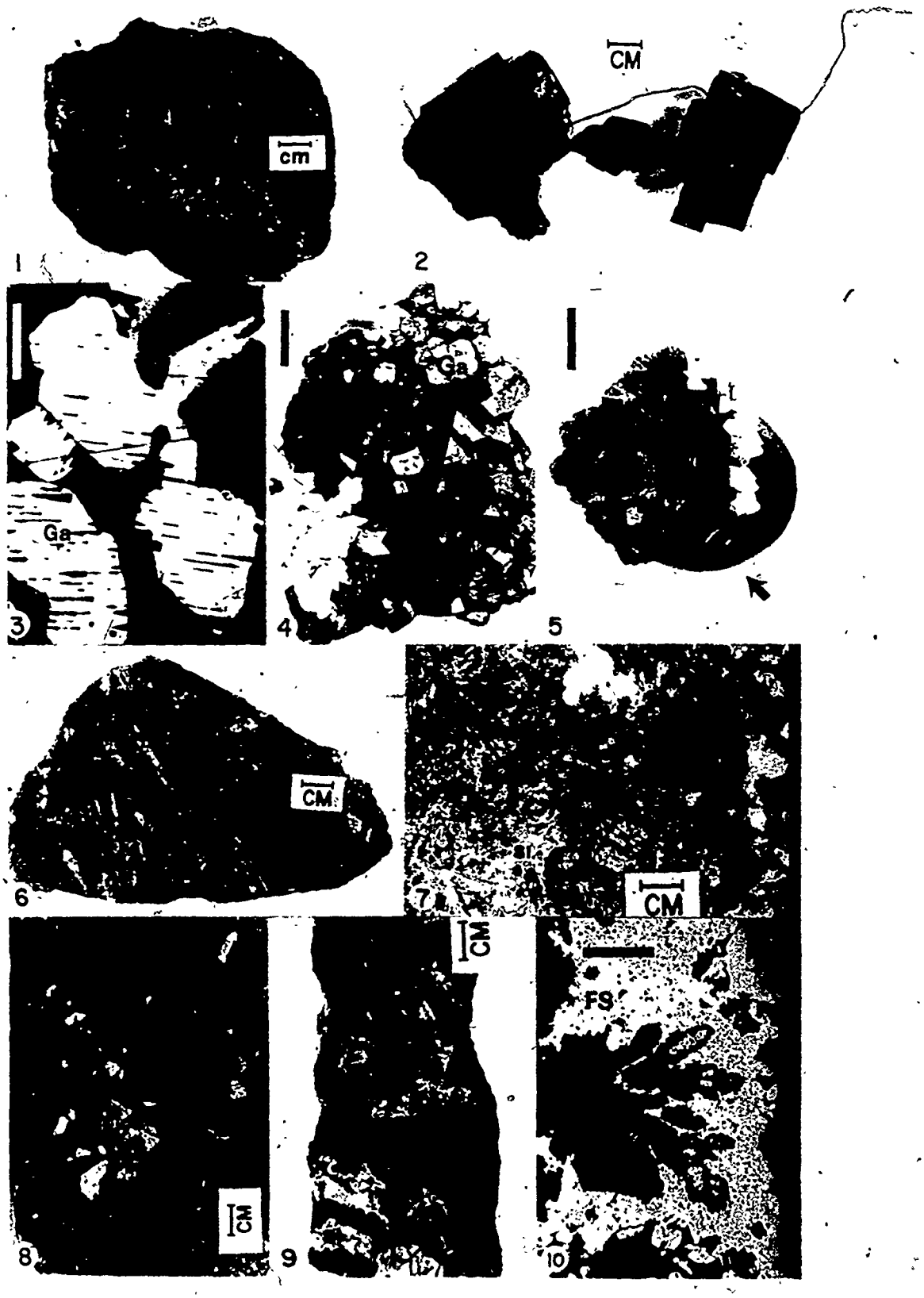
cm
CM
1
2
Ga
3
Ga
4
t
5
CM
6
CM
7
CM
CM
8
9
FS
10

PLATE 13

Sulfide Textures

13:1 Rare example of acicular crust of marcasite on massive iron sulfides. Sample P31-1.

13:2 Vuggy boxwork of pyrite with marcasite and minor colloform sphalerite. Sample X15-12.

13:3 Pyrite crystal groups and nodules with minor encrusting coarse-crystalline, dark reddish-brown sphalerite from Green Clay Zone of W17.

13:4 Photomicrograph of twinned orthorhombic marcasite crystals. K17 polished surface; sample X15-6. Reflected light, partly crossed nicols; scale is 0.2 mm.

13:5 Acicular crystals of marcasite with intercrystal filling of galena. K-31 polished surface; sample X15-26. Reflected light, scale is 0.2 mm.

13:6 Pervasive introduction of iron sulfides along fracture in Facies L tidal flat dolostone. Sample R61-1.

13:7 Photomicrograph of iron sulfide rim in R61-1 (13:6); introduction of acicular marcasite crystals along dolostone crystal contacts has resulted in irregular rhombic outlines, particularly toward fracture (extreme top). Polished surface 6296. Reflected light; scale is 0.2 mm.

13:8 Photomicrograph illustrating pervasive introduction of iron sulfides (FS) along irregular rhombic crystal boundaries in dolostone. Polished surface 6330; sample R61-38-64. Reflected light; scale is 0.2 mm.

13:9 Fragments of massive iron sulfides in a matrix of fine-crystalline marcasite, pyrite, sphalerite, and galena. Sample W17-2.

13:10 Photomicrograph showing rare occurrence of interstitial pyrrhotite (Po) along grain boundaries in massive pyrite (Py). Polished surface K23; sample X15-12. Reflected light; scale is 0.2 mm.


1
CM
2
CM
4
3
CM
5
6
CM
7
8
FS
9
CM
10
Py

PLATE 14

Gangue Mineral Textures

14:1 White dolomite overlain by gray dolomite, dark reddish-brown coarse-crystalline sphalerite, and white dolomite; the gray dolomite passes abruptly to white dolomite with a faint pink tint on the right. Sample M40-31; scale is 1 cm.

14:2 Central area (1) of white dolomite containing coarse-crystalline dolostone with relic fossil outlines overlain by gray dolomite (2) with dark reddish-brown sphalerite, grayish white dolomite (3), gray dolomite (4), and a thick rim of white dolomite (5). Units 3 and 4 fill fracture in gray dolomite and sphalerite of unit 2 at A. Sample J44-26.

14:3 Fragments of massive iron sulfides (FS) with coarse-crystalline reddish-brown sphalerite cemented by white dolomite. Sample N38A-30.

14:4 Fragments and bands of fine-crystalline, light reddish-brown sphalerite cemented by light gray and white dolomite; compare with 12:6. Sample N38A-21.

14:5 Coarse-crystalline orange sphalerite with white dolomite in uniform granular dolostone of lower facies K. Vague boundaries between dolostone and white dolomite suggest that some white dolomite grew by cannibalization of the coarse dolostone. Sample K57-25-158; scale is 1 cm.

14:6 Thick carbonate crust with massive white calcite and white dolomite on gray dolomite. Right half of core has been stained with Alazarin red-S so that calcite appears dark and dolomite remains unchanged. Sample K57-95-131.

14:7 Large calcite crystals from vug in J44 ore body; coin is 23 mm in diameter.

14:8 Tabular crystals of colorless celestite (Ce) overgrown by coarse-crystalline yellow native sulfur (S) from vug in Facies K. Sample 3301-421; scale is 1 cm.

14:9 Banded light reddish-brown sphalerite (Sl) with bitumen (Bi) and calcite (Ca). Sample K62-36.

14:10 White dolomite crust on gray dolomite with bitumen. Bitumen sphere has white dolomite around it and may have been present during white dolomite growth. Sample K57-32.

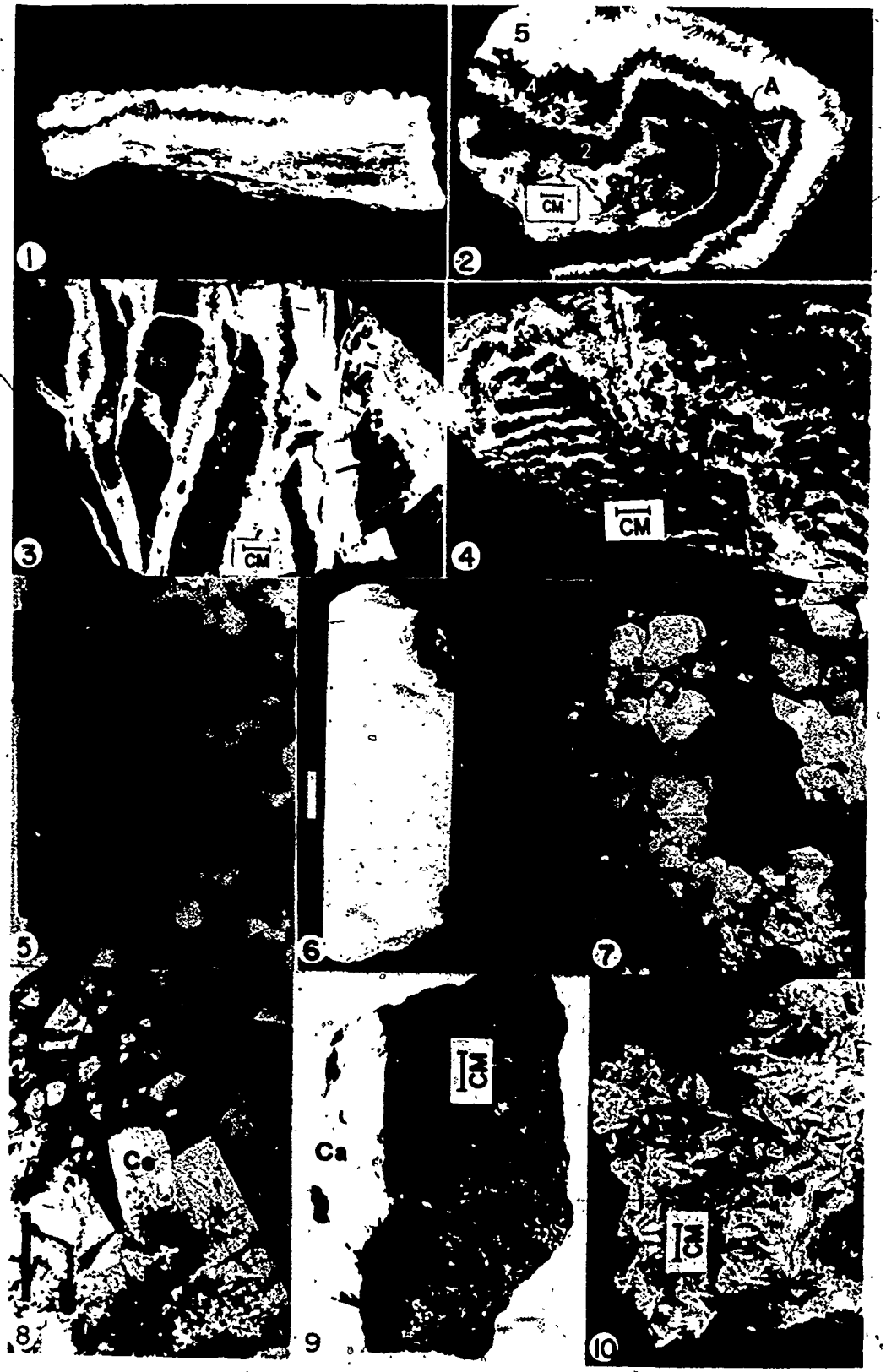
1
2
5
4
3
2
A
CM
3
FS
CM
4
CM
5
6
7
Ca
CM
8
9
CM
10

APPENDIX I

Calculation of Metal Percentages and Ratios

The plan maps and sectional plots of metal percentages and ratios presented in this study are generalized after data and computer plots generated by the MEPS system of the Data Processing Section of Cominco Ltd. in Trail, B. C. This system utilized Pb, Zn, and Fe assay data provided by Pine Point Mines Ltd. from the cores of closely spaced, vertical diamond drill holes in the K57, A70, and W17 areas. The intervals selected for study were those previously determined by Pine Point Mines to have economically recoverable amounts of Pb-Zn. Computer plots of metal values and ratios were made for 25-foot (7.5-meter) mining bench intervals and for the total ore interval on a scale of 1 inch equals 40 feet (1 cm = 4.8 m). The weighted averages of Pb, Zn, and Fe for the appropriate interval of each drill hole were utilized in constructing the plan maps of slices between certain elevations. The assay intervals are highly variable, ranging from less than 1 to more than 10 feet (0.3 to 3 m) with a mean of about 5 feet (1.5 m). Metal values of assayed intervals range from not detectable in barren rock to essentially stoichiometric percentages for Pb, Zn, and Fe in galena, sphalerite, and pyrite, respectively, in massive sulfide intervals. Core intervals which do not contain megascopic sulfides, and therefore were not assayed, were assigned zero metal

percentages. Drill holes with incomplete information for certain intervals because of lack of core recovery, overburden extending below the upper elevation of the interval, or insufficient penetration were not used for the plan maps of those intervals. Sectional plots were made by compositing assay values into 5-foot (1.5-meter) intervals of elevation. In order to emphasize metal trends, final contouring of sectional data is based on the moving average of data including the 5-foot intervals above and below the central interval. Metal ratios were originally plotted as Zn/Pb, Zn/Fe, and (Pb + Zn)/Fe, but at the suggestion of D. F. Sangster, these data were recalculated and contoured as Pb/(Pb + Zn) and Fe/(Pb + Zn + Fe) for better definition of metal trends.

Galena, (PbS), sphalerite (ZnS), pyrite (FeS_2), and marcasite (FeS_2) are the only common sulfide minerals in the Pine Point ore bodies. Composition of these sulfides does not vary greatly from stoichiometric as trace elements are usually minor. Therefore, the weight percentages of Pb, Zn, and Fe determined from assay data can be used to calculate an index of the total volumetric percentage of sulfides present.

$$\text{Total Sulfide Index} = \frac{\%\ \text{Pb}}{0.866} + \frac{\%\ \text{Zn}}{0.671} + \frac{\%\ \text{Fe}}{0.465}$$

Total Sulfide Index avoids misconceptions caused by the use of "ore" or the sum of Pb, Zn, and Fe weight percentages to express overall metal distribution and facilitates evaluation of sulfide distribution

relative to geologic features.

Only the contour maps of metal percentages and ratios for the entire ore intervals of K57, A70, and W17 are presented in this study. Although metal percentages vary greatly among the 25-foot (7.5 m) mining intervals, even in individual ore bodies, metal ratios and trends are consistently those demonstrated by the composited total ore interval. Similarly, only selected sections showing general metal trends are included.

APPENDIX II

Composition of Sphalerite from Pine Point Ore Bodies*

Section & Sample No. Description	Sphalerite Habit	Zn	S	Pb	Fe	Mn	Cu	Cd	Total
K-32A; M40-7 Ramose sphalerite and skeletal galena passing outward into banded sphalerite with coarse galena; layers 3-7 of Plate II:3,4	Ramose lt. red-brown	62.09	32.59	0.00	5.25	0.00	0.00	0.00	99.94
	Ramose lt. red-brown	62.59	33.28	0.00	3.78	0.02	0.06	0.00	99.95
	Ramose lt. red-brown	62.85	33.06	0.00	3.88	0.00	0.06	0.00	99.85
	Lt. red-brown band	64.23	32.61	0.09	2.29	0.00	0.07	0.00	99.29
	Lt. red-brown band	64.13	32.70	0.23	2.59	0.00	0.09	0.00	99.74
	Dk. red-brown band	63.97	32.59	0.23	2.66	0.01	0.10	0.00	99.56
	Dk. red-brown band	63.85	32.38	0.71	2.30	0.00	0.00	0.00	99.23
	Dk. red-brown band	63.73	32.23	0.30	2.13	0.00	0.00	0.00	98.39
	Yellow band	66.50	32.57	0.00	0.65	0.00	0.10	0.00	99.82
	Yellow band	66.27	32.58	0.00	0.39	0.00	0.11	0.00	99.35
	Dk. brown crystal	60.64	33.19	0.00	5.09	0.00	0.08	0.00	99.13
	Dk. brown crystal	60.79	32.84	0.00	6.27	0.00	0.00	0.00	99.91

*Microprobe Analyses

APPENDIX II (Continued)

Section & Sample No. Description	Sphalerite Habit	Zn	S	Pb	Fe	Mn	Cu	Cd	Total
K-6A; M40-6 Ramose sphalerite with abundant intergrown skeletal galena	Ramose lt. red-brown	60.50	33.17	0.00	5.29	0.00	0.00	0.00	98.96
	Ramose lt. red-brown	62.71	33.04	0.00	3.47	0.02	0.00	0.00	99.24
	Ramose lt. red-brown	60.89	33.16	0.00	4.78	0.01	0.00	0.00	98.84
	Ramose lt. red-brown	60.88	32.97	0.00	5.48	0.00	0.00	0.03	99.36
	Ramose dk. red-brown	55.47	33.61	0.00	10.30	0.00	0.00	0.00	99.38
	Ramose dk. red-brown	56.25	33.23	0.07	8.89	0.00	0.00	0.00	98.44
	Ramose dk. red-brown	59.71	33.13	0.05	6.12	0.00	0.01	0.00	99.02
4846; M40-22 Coarse crystals of sphalerite and galena with white dolomite	Light red-brown	65.61	32.34	0.27	1.73	0.00	0.00	0.00	99.95
	Light red-brown	65.58	32.22	0.00	1.77	0.00	0.00	0.00	99.57
4848; K57-22 Banded sphalerite with bladed galena; Plate 12:6	Light red-brown	65.47	32.90	0.06	1.17	0.02	0.00	0.06	99.68
	Light red-brown	65.51	32.66	0.34	0.97	0.00	0.00	0.00	99.48
	Light red-brown	65.04	32.18	0.53	0.87	0.00	0.00	0.00	98.62

APPENDIX II (Continued)

Section & Sample No. Description	Sphalerite Habit	Zn	S	Pb	Fe	Mn	Cu	Cd	Total
350-003; 042-1 Concentrically banded colloform sphalerite with skeletal galena (Plate 11:1)	Tan colloform rim	66.64	32.29	0.29	0.20	0.00	0.00	0.20	99.62
	Tan colloform band	66.46	31.82	0.29	0.30	0.00	0.00	0.27	99.14
	Tan colloform band	65.55	31.86	0.55	0.66	0.00	0.00	0.17	98.79
	Tan colloform rim	66.19	32.07	0.08	0.42	0.00	0.00	0.12	98.88
	Tan colloform band	66.25	32.01	0.40	0.36	0.00	0.00	0.10	99.12
	Tan colloform band	64.44	30.79	0.52	0.52	0.00	0.00	0.26	98.64
	Yellow colloform band	65.32	31.83	0.79	0.79	0.00	0.00	0.10	98.83
	Yellow colloform band	66.47	32.16	0.57	0.61	0.00	0.00	0.23	100.04
	Yellow colloform band	66.20	31.80	0.32	0.59	0.00	0.01	0.16	99.08
	Lt. red-brown band	64.98	31.54	0.79	0.98	0.00	0.00	0.09	98.38
	Lt. red-brown center	65.28	31.43	0.76	1.17	0.00	0.00	0.10	98.74
	Lt. red-brown band	64.54	32.28	0.67	1.45	0.00	0.00	0.09	99.06
	Lt. red-brown band	64.48	31.48	1.05	1.03	0.00	0.00	0.13	98.17
	Lt. red-brown band	64.75	31.88	0.57	1.23	0.00	0.00	0.09	98.52
	Lt. red-brown center	65.43	32.05	0.52	1.18	0.00	0.00	0.09	99.27
	Dk. red-brown band	64.49	32.08	0.40	2.03	0.00	0.16	0.16	99.16

APPENDIX II (Continued)

Section & Sample No. Description	Sphalerite Habit	Zn	S	Pb	Fe	Mn	Cu	Cd	Total
350-003 (continued)	Dk. red-brown band	65.14	32.29	0.41	1.98	0.00	0.00	0.11	99.93
	Dk. red-brown center	64.35	32.06	0.61	1.45	0.00	0.00	0.18	98.64
K-29; X15-22 Coarse sphalerite with galena, pyrite, marcasite, and calcite	Coarse lt. red-brown	64.55	32.63	0.00	2.19	0.01	0.00	0.00	99.38
	Coarse lt. red-brown	64.64	32.50	0.00	1.82	0.00	0.00	0.00	98.96
	Coarse lt. red-brown	63.83	32.66	0.00	2.41	0.00	0.00	0.00	98.90
	Coarse lt. red-brown	64.87	32.65	0.00	2.36	0.00	0.00	0.00	99.88
	Coarse yellow	66.16	32.79	0.00	0.50	0.02	0.00	0.00	99.47
	Coarse yellow	66.18	32.73	0.00	0.15	0.00	0.00	0.00	99.06
	Coarse yellow	66.22	32.56	0.00	0.68	0.01	0.00	0.32	99.79
7518; X15-20 Spherules of dark red-brown sphalerite rimmed by yellow sphalerite; associated with galena, marcasite, pyrite, and calcite	Dark red-brown core	64.06	32.51	0.00	2.97	0.00	0.00	0.00	99.55
	Dark red-brown band	62.53	32.85	0.00	3.84	0.00	0.00	0.00	99.19
	Dark red-brown core	62.18	32.95	0.00	4.49	0.00	0.00	0.00	99.61
	Dark red-brown band	62.96	32.93	0.00	3.58	0.00	0.00	0.00	99.48
	Dark red-brown core	59.80	33.23	0.00	5.99	0.00	0.00	0.00	99.02
	Dark red-brown band	60.40	33.36	0.00	5.78	0.00	0.00	0.00	99.54
	Dark red-brown band	63.83	33.04	0.00	2.98	0.00	0.00	0.00	99.85

APPENDIX II (Continued)

Section & Sample No. Description	Sphalerite Habit	Zn	S	Pb	Fe	Mn	Cu	Cd	Total
7518 (continued)	Yellow crystal rim	65.38	32.97	0.00	1.16	0.00	0.00	0.00	99.50
	Yellow crystal rim	65.73	33.02	0.00	1.21	0.00	0.00	0.00	99.98
	Yellow crystal rim	65.45	33.03	0.00	0.91	0.00	0.00	0.00	99.38
	Yellow crystal rim	65.25	32.76	0.00	1.30	0.00	0.00	0.00	99.31
5967; N204-48 Colloform sphalerite with galena from vug in friable dolostone	Tan colloform band	66.48	32.41	0.16	0.78	0.00	0.05	0.05	99.93
	Tan colloform band	66.24	32.41	0.12	0.72	0.00	0.03	0.00	99.52
	Tan colloform band	66.38	32.29	0.00	0.43	0.00	0.05	0.00	99.15
	Tan colloform band	66.53	32.53	0.03	0.63	0.00	0.04	0.00	99.76
	Tan colloform band	66.03	32.13	0.21	0.72	0.00	0.02	0.00	99.11
	Tan colloform band	65.57	31.78	0.36	0.32	0.00	0.04	0.00	98.07
	Tan colloform band	65.71	31.95	0.43	0.21	0.01	0.04	0.00	98.35
	Lt. red-brown band	64.54	32.35	0.21	1.81	0.00	0.05	0.00	98.96
	Lt. red-brown band	63.38	32.26	0.37	2.79	0.00	0.02	0.00	98.82
Summary of 69 Analyses	Maximum	66.64	33.61	1.05	10.30	0.02	0.16	0.32	100.04
	Minimum	55.47	31.48	0.00	0.15	0.00	0.00	0.00	98.07
	Mean	64.16	33.38	0.21	2.23	0.01	0.02	0.05	99.67

APPENDIX III

Composition of Galena from Pine Point Ore Bodies*

Section & Sample No Description	Galena Habit	Pb	S	Zn	Cu	Fe	Total
K-32A; M40-7 Skeletal galena in ramose sphalerite passing outward into banded sphalerite with coarse galena layers 3-7 of Plate 11:3,4.	Skel.	85.82	13.32	0.00	0.21	0.00	99.35
	Skel.	85.29	13.33	0.05	0.18	0.00	98.85
	Skel.	84.77	13.47	0.00	0.22	0.00	98.45
	Skel.	86.02	13.37	0.00	0.18	0.00	99.57
	Skel.	84.91	13.47	0.36	0.17	0.01	98.92
	Skel.	85.02	13.40	1.30	0.24	0.00	99.96
	Coarse	86.15	13.23	0.21	0.21	0.00	99.80
	Coarse	86.27	13.30	0.17	0.24	0.00	99.98
K-6A; M40-6 Skeletal galena in ramose sphalerite	Skel.	86.19	13.43	0.05	0.00	0.00	99.67
	Skel.	85.90	13.40	0.00	0.00	0.01	99.31
	Skel.	86.22	13.20	0.00	0.00	0.00	99.42
	Skel.	85.60	13.39	0.93	0.04	0.00	99.96
	Skel.	85.67	13.51	0.27	0.01	0.00	99.46
4846; M40-22 Coarse galena, sphalerite with dolomite	Coarse	86.60	13.30	0.01	0.01	0.00	99.92
	Coarse	85.93	13.41	0.04	0.00	0.00	99.38
4848; K57-22 Bladed galena with banded sphalerite	Bladed	85.78	13.65	0.34	0.00	0.00	99.77
	Bladed	86.07	13.66	0.00	0.02	0.00	99.75
K-29; X15-22 Coarse galena with sphalerite, pyrite marcasite, and calcite	Coarse	85.79	13.24	0.12	0.04	0.00	99.19
	Coarse	86.14	13.17	0.28	0.02	0.02	99.62
	Coarse	85.59	13.15	0.71	0.00	0.05	99.90
	Coarse	85.41	13.09	0.47	0.06	0.04	99.06
	Coarse	84.95	13.10	0.18	0.06	0.15	98.44

*Microprobe Analyses

APPENDIX III (Continued)

Section & Sample No. Description	Galena Habit	Pb	S	Zn	Cu	Fe	Total
5967; N204-48	Coarse	86.12	13.32	0.00	0.01	0.00	99.45
Coarse galena with colloform sphalerite	Coarse	86.04	13.26	0.00	0.00	0.00	99.30
Summary of 24 Analyses	Maximum	86.60	13.66	1.30	0.24	0.15	99.98
	Minimum	84.47	13.09	0.00	0.00	0.00	98.44
	Mean	85.76	13.34	0.23	0.08	0.01	99.44

APPENDIX IV

Composition of Pyrite and Marcasite from Pine Point Ore Bodies*

Section & Sample No. Description	Mineral & Habit	Fe	S	Cu	Total
K-6a; M40-6	Marcasite	45.11	53.09	0.63	98.83
Minor marcasite in ramose sphalerite and skeletal galena	Interstitial				
	Marcasite	45.76	53.55	0.34	99.65
	Interstitial				
	Marcasite	45.99	53.57	0.48	100.04
	Interstitial				
	Marcasite	45.30	53.05	0.13	98.90
	Interstitial				
	Marcasite	45.20	52.80	1.15	99.15
	Interstitial				
	Marcasite	45.00	53.20	1.27	99.47
	Interstitial				
	Marcasite	45.30	53.50	1.01	99.91
	Interstitial				
K57-8	Marcasite	46.15	53.71	0.01	99.87
Marcasite with white dolomite	Blade				
	Marcasite	46.52	53.34	0.00	99.86
	Blade				
	Marcasite	46.54	53.32	0.00	99.86
	Blade				
	Marcasite	46.30	53.06	0.00	99.36
	Blade				
	Marcasite	46.76	51.95	0.01	98.72
	Blade				
5987; A70-96-166	Marcasite	46.58	53.08	0.00	99.66
Marcasite with coarse red-brown sphalerite	Interstitial				
	Marcasite	46.82	53.18	0.00	100.00
	Interstitial				
	Marcasite	46.04	53.15	0.00	99.19
	Interstitial				
	Marcasite	46.45	52.90	0.00	99.35
	Interstitial				
	Marcasite	46.46	53.11	0.00	99.57
	Interstitial				
6344; N204-179-126	Marcasite	46.05	53.20	0.03	99.28
Marcasite with pyrite, galena, and sphalerite	Blade				
	Marcasite	46.53	52.36	0.00	98.89
	Blade				

*Microprobe Analyses

APPENDIX IV (Continued)

Section & Sample No. Description	Mineral & Habit	Fe	S	Cu	Total
K-11; W17-3 Co-existing pyrite and marcasite from dolostone breccia	Marcasite Blade	45.80	53.78	0.00	99.58
	Marcasite Blade	46.59	53.40	0.00	99.99
	Marcasite Blade	46.75	53.28	0.00	100.03
	Marcasite Blade	45.90	53.95	0.00	99.85
	Marcasite Blade	46.08	53.73	0.00	99.81
	Pyrite Cubic	46.05	53.73	0.00	99.78
	Pyrite Cubic	46.07	53.59	0.00	99.66
K-30; X15-23 Pyrite and marcasite with sphalerite, galena, and calcite	Marcasite Blade	46.75	53.14	0.00	99.89
	Marcasite Blade	45.71	52.92	0.00	98.63
	Marcasite Blade	45.78	53.93	0.00	99.71
	Pyrite Cubic	46.15	53.31	0.00	99.66
	Pyrite Cubic	46.73	52.93	0.00	99.66
Summary of 31 Analyses	Maximum	46.82	53.95	1.27	100.04
	Minimum	45.00	51.95	0.00	98.63
	Mean	46.10	53.26	0.16	99.54

APPENDIX V

Lead Isotope Percentages and Ratios in Galena, Pine Point District

Sample and Description	^{204}Pb	^{206}Pb	^{207}Pb	^{208}Pb	206/204	207/204	208/204
A70-17-106; bladed Ga associated with colloform S1	1.367	24.948	21.370	52.315	18.28	15.64	38.29
A70-30-172; coarse Ga crystals	1.383	24.888	21.376	52.353	18.00	15.46	37.45
W85N-34-206; coarse Ga crystals associated with banded S1	1.373	24.928	21.386	52.313	18.16	15.58	38.10
K62-22; coarse Ga crystals in detritus	1.381	24.978	21.429	52.212	18.06	15.52	37.75
N42-3; cubo-octahedral Ga on white Do	1.366	24.936	21.415	52.283	18.25	15.68	38.26
N38A-11; massive skeletal Ga associated with colloform S1	1.379	24.932	21.384	52.305	18.08	15.51	37.93
M40-2; massive skeletal Ga	1.363	24.947	21.382	52.308	18.30	15.69	38.38
R61-20-67; coarse Ga associated with tan friable S1	1.381	24.935	21.366	52.318	18.06	15.47	37.88
X15-1; coarse Ga crystals in massive Ca	1.381	24.915	21.332	52.372	18.04	15.45	37.92
X15-27; fine Ga associated with fine S1	1.375	24.940	21.381	52.304	18.14	15.55	38.04
W17-45-207; coarse Ga	1.376	24.935	21.375	52.304	18.13	15.53	38.01
N204-204-202; Ga in sandy dolostone	1.376	24.933	21.370	52.321	18.12	15.53	38.02
N204-48-175; Ga in fractures in dolostone	1.376	24.941	21.382	52.301	18.13	15.54	38.01

REFERENCES

Adams, D.H., 1973, N204 study, in Pine Point Mines 1974 Exploration Proposal.

Adams, D.H., 1975, Stratigraphic correlations over the Pine Point area: unpubl. Pine Point Mines report.

Adams, J.E., and Rhodes, M.L., 1960, Dolomitization by seepage refluxion: Am. Assoc. Petroleum Geol. Bull., v. 44, pp. 1912-1920.

Anderson, G.M., 1973, The hydrothermal transport and deposition of galena and sphalerite near 100° C: Econ. Geol., v. 68, pp. 480-492.

_____, 1975, Precipitation of Mississippi Valley-type ores: Econ. Geol., v. 70, pp. 937-942.

Back, W., and Hanshaw, B.B., 1970, Comparison of chemical hydrogeology of the carbonate peninsulas of Florida and Yucatan: Jour. Hydrology, v. 10, pp. 330-368.

Badiozamani, K., 1973, The Dorag dolomitization model--application to the Middle Ordovician of Wisconsin: Jour. Sed. Petrology, v. 43, pp. 965-984.

Barnes, H.L., and Czamanske, G.K., 1967, Solubilities and transport of ore minerals, in Barnes, H.L. (ed.), Geochemistry of hydrothermal ore deposits: Holt, Rinehart, and Winston, pp. 334-381.

Beales, F.W., 1975, Precipitation mechanisms for Mississippi Valley-type ore deposits: Econ. Geol., v. 70, pp. 943-948.

Beales, F.W., Carracedo, J.C., and Strangway, D.W., 1974, Paleomagnetism and the origin of Mississippi Valley-Type ore deposits: Can. Jour. Earth Sci., v. 11, pp. 211-223.

Beales, F.W., and Jackson, S.A., 1966, Precipitation of lead-zinc ores in carbonate reservoirs as illustrated by Pine Point ore field, Canada: Trans. Inst. Min. Metall., v. 75, pp. B278-B285.

Beales, F.W., and Jackson, S.A., 1968, Pine Point--a stratigraphical approach: Can. Inst. Min. Metall. Bull., v. 61, pp. 867-878.

Bebout, D.G., and Maiklem, W.R., 1973, Ancient anhydrite facies and environments, Middle Devonian Elk Point Basin, Alberta: Bull. Can. Petroleum Geol., v. 21, pp. 278-343.

Bell, J.M., 1929, The lead-zinc deposits near Pine Point, Great Slave Lake: Trans. Can. Inst. Min. Metall., v. 32, pp. 122-139.

Bell, R., 1899, Annual Report, v. XII, part A: Geol. Surv. Can., pp. 104-109.

Bernard, A.J., 1973, Metallogenic processes in intra-karstic sedimentation, in Amstutz, G.C., and Bernard, A.J. (eds.), Ores in sediments: Springer-Verlag, pp. 43-57.

Billings, G.K., Kesler, S.E., and Jackson, S.A., 1969, Relation of zinc-rich formation waters, northern Alberta to the Pine Point ore deposit: Econ. Geol., v. 64, pp. 385-391.

Burst, J.F., 1976, Argillaceous sediment dewatering, in Donath, F.A. et al. (eds.), Annual review of earth and planetary sciences, v. 4, pp. 293-318.

Campbell, N., 1950, The Middle Devonian in the Pine Point area, N.W.T.: Proc. Geol. Assoc. Can., v. 3, pp. 87-96.

_____, 1966, The lead-zinc deposits of Pine Point: Can. Inst. Min. Metall. Bull., v. 59, pp. 953-960.

_____, 1967, Tectonics, reefs, and stratiform lead-zinc deposits of the Pine Point area, Canada, in Brown, J.S. (ed.), Genesis of stratiform lead-zinc-barite-fluorite deposits in carbonate rocks: Econ. Geol. Mon. 3, pp. 59-70.

Carpenter, A.B., Trout, M.L., and Pickett, E.E., 1974, Preliminary report on the origin and chemical evolution of lead- and zinc-rich oil field brines in central Mississippi: Econ. Geol., v. 69, pp. 1191-1206.

Collins, J.A., and Smith, L., 1972, Sphalerite as related to the tectonic movements, deposition, diagenesis and karstification of a carbonate platform: 24th Intern. Geol. Congress, Proceedings Section 6, pp. 208-215.

Cumming, G.L., and Richards, J.R., 1975, Ore lead isotope ratios in a continuously changing earth: Earth Planet. Sci. Letters, v. 28, pp. 155-171.

Cumming, G.L., and Robertson, D.K., 1969, Isotopic composition of lead from the Pine Point deposit: Econ. Geol., v. 64, pp. 731-732.

Davidson, C.F., 1966, Some genetic relationships between ore deposits and evaporites: Trans. Inst. Min. Metall., v. 75, pp. B216-B225.

De Groot, K., 1967, Experimental dedolomitization: Jour. Sed. Petrology, v. 37, pp. 1216-1220.

De Wit, R., Gronberg, E.C., Richards, W.B., and Richmond, W.O., 1973, Tathlina area, District of Mackenzie, in The future petroleum provinces of Canada: Can. Soc. Petroleum Geol. Mem. 1, pp. 187-212.

Doe, B.R., and Delevaux, M.H., 1972, Source of lead in Southeast Missouri galena ores: Econ. Geol., v. 67, pp. 409-435.

Doe, B.R., and Stacey, J.S., 1974, The application of lead isotopes to the problems of ore genesis and ore prospect evaluation: a review: Econ. Geol., v. 69, no. 6, pp. 757-776.

Douglas, R.J.W., 1959, Great Slave and Trout River map area, N.W.T.: Geol. Surv. Can. Rept. 58-11.

Dozy, J.J., 1970, A geological model for the genesis of the lead-zinc ores of the Mississippi Valley, U.S.A.: Trans. Inst. Min. Metall., v. 79, pp. B163-B170.

Dunsmore, H.E., 1973, Diagenetic processes of lead-zinc emplacement in carbonates: Inst. Min. Metall. Trans., v. 82, pp. B168-B173.

_____, 1975, Origin of lead-zinc ores in carbonate rocks: a sedimentary-diagenetic model: unpubl. Ph.D. thesis, Royal School of Mines, Imperial College, London.

Erdman, J.G., and Morris, D.A., 1974, Geochemical correlation of petroleum: Am. Assoc. Petroleum Geol. Bull., v. 58, pp. 2326-2337.

Evamy, B.D., 1967, Dedolomitization and the development of rhombohedral pores in limestones: Jour. Sed. Petrology, v. 37, pp. 1204-1215.

Folk, R.L., and Land, L.S., 1975, Mg/Ca ratio and salinity: two controls over crystallization of dolomite: Am. Assoc. Petroleum Geol. Bull., v. 59, pp. 60-68.

Friedman, G.M., 1975, The making and unmaking of limestones or the downs and ups of porosity: Jour. Sed. Petrology, v. 45, pp. 379-398.

Fritz, P., and Jackson, S.A., 1972, Geochemical and isotopic characteristics of Middle Devonian dolomites from Pine Point, Northern Canada: 24th Intern. Geol. Congress, Proceedings, Section 6, pp. 230-243.

Füchtbauer, H., 1974, Sediments and sedimentary rocks: Wiley, New York, 464 pp.

Hanshaw, B.B., Back, W., and Deike, R.G., 1971, A geochemical hypothesis for dolomitization and ground water: Econ. Geol., v. 66, pp. 710-724.

Heyl, A.V., 1968, Minor epigenetic, diagenetic, and syngenetic sulfide, fluorite, and barite occurrences in the central United States: Econ. Geol., v. 63, pp. 585-594.

Heyl, A.V., Landis, G.P., and Zartman, R.E., 1974, Isotopic evidence for the origin of Mississippi Valley-type mineral deposits: a review: Econ. Geol., v. 69, pp. 992-1006.

Hoffman, P.F., 1969, Proterozoic paleocurrents and depositional history of the east arm fold belt, Great Slave Lake: Can. Jour. Earth Sci., v. 6, pp. 441-462.

Hoffman, P., Dewey, J.F., and Burke, K., 1974, Aulacogens and their genetic relations to geosynclines, in Dott, R.H., Jr. and Shaver, R.H. (eds.), Modern and ancient geosynclinal sedimentation: Soc. Econ. Paleon. Mineral. Spec. Publ. 19, pp. 38-55.

Hsu, K.J., and Siegenthaler, C., 1969, Preliminary experiments on hydrodynamic movement induced by evaporation and their bearing on the dolomite problem: Sedimentology, v. 12, pp. 11-26.

Jackson, S.A., 1971, The carbonate complex and lead-zinc ore bodies, Pine Point, Northwest Territories, Canada: unpubl. Ph.D. thesis, Univ. of Alberta, Edmonton.

Jackson, S.A., and Beales, F.W., 1967, An aspect of sedimentary basin evolution: the concentration of Mississippi Valley-type ores during late stages of diagenesis: Bull. Can. Petroleum Geol., v. 15, pp. 383-433.

Jackson, S.A., and Folinsbee, R.E., 1969, The Pine Point lead-zinc deposits, N.W.T., Canada--Introduction and paleoecology of the Presqu'ile reef: Econ. Geol., v. 64, pp. 711-717.

Johnson, A.M., 1972, Metal-bearing brines from reef complexes (abs.): Geol. Soc. Amer., Abstracts with programs, v. 4, no. 7, p. 553.

Kahout, F.A., 1960, Cyclic flow of salt water in the Biscayne aquifer of southeastern Florida: Jour. Geophysical Research, v. 65, pp. 2133-2141.

Kesler, S.E., Stoiber, R.E., and Billings, G.K., 1972, Direction of flow of mineralizing solutions at Pine Point, N.W.T.: Econ. Geol., v. 67, pp. 19-24.

Land, L.S., 1973a, Contemporaneous dolomitization of middle Pleistocene reefs by meteoric water, North Jamaica: Bull. Marine Sci., v. 23, pp. 64-92.

_____, 1973b, Holocene meteoric dolomitization of Pleistocene limestones, North Jamaica: Sedimentology, v. 20, pp. 411-424.

Land, L.S., Salem, M.R.I., and Morrow, D.W., 1975, Paleohydrology of ancient dolomites: geochemical evidence: Am. Assoc. Petroleum Geol. Bull., v. 59, pp. 1602-1625.

Lebedev, L.M., 1972, Minerals of contemporary hydrotherms of Cheleken: Geochem. Intern., v. 9, pp. 485-504.

Leleu, M., and Goni, J., 1974, Sur la formation biogeochimique de stalactites de galene: Mineral. Deposita, v. 9, pp. 27-32.

Macqueen, R.W., 1976, Sediments, zinc and lead, Rocky Mountain Belt, Canadian Cordillera: Geoscience Can., v. 3, pp. 71-81.

Macqueen, R.W., Williams, G.K., Barefoot, R.R., and Foscolos, A.E., 1975, Devonian metalliferous shales, Pine Point region, District of Mackenzie, in Geol. Surv. Can., Paper 75-1, Part A, pp. 553-556.

Magara, K., 1974a, Aquathermal fluid migration: Am. Assoc. Petroleum Geol. Bull., v. 58, pp. 2513-2516.

_____, 1974b, Compaction, ion filtration, and osmosis in shale and their significance in primary migration: Am. Assoc. Petroleum Geol. Bull., v. 58, pp. 283-290.

Maiklem, W.R., 1971, Evaporative drawdown--a mechanism for water-level-lowering and diagenesis in the Elk Point Basin: Bull. Can. Petroleum Geol., v. 17, pp. 194-233.

Matthews, R.K., 1974, A process approach to diagenesis of reefs and reef associated limestones, in Laporte, L.F. (ed.)., Reefs in time and space: Soc. Econ. Paleon. Min., Spec. Publ. 18, pp. 234-256.

Milliman, J.D., 1974, Recent sedimentary carbonates, Part 1, Marine carbonates: Springer-Verlag, New York, 375 pp.

Murray, R.C., and Pray, L.C., 1965, Dolomitization and limestone diagenesis--an introduction, in Dolomitization and limestone diagenesis: a symposium: Soc. Econ. Paleon. Min., Spec. Publ. 13, pp. 1-2.

Norris, A.W., 1965, Stratigraphy of Middle Devonian and older Paleozoic rocks of the Great Slave Region, Northwest Territories: Geol. Surv. Can., Mem. 322.

Nriagu, J.O., and Anderson, G.M., 1971, Stability of the lead (II) chloride complexes at elevated temperatures: Chem. Geol., v. 7, pp. 171-183.

Ohle, E.L., 1959, Some considerations in determining the origin of ore deposits of the Mississippi Valley type: Econ. Geol., v. 54, pp. 796-789.

Paterson, D.M., 1975, A mineralographic investigation of Pine Point ores: unpubl. B.Sc. thesis, Univ. British Columbia, Vancouver.

Plummer, L.N., 1975, Mixing of sea water with calcium carbonate ground water, in Whitten, E.H.T. (ed.), Quantitative studies in the geological sciences: Geol. Soc. Amer., Mem. 142, pp. 219-236.

Price, L.C., 1976, Aqueous solubility of petroleum as applied to its origin and primary migration: Am. Assoc. Petroleum Geol. Bull., v. 60, pp. 312-244.

Richmond, W.O., 1965, Paleozoic stratigraphy and sedimentation of the Slave Point formation, southern Northwest Territories and northern Alberta: Unpubl. Ph.D. dissertation, Stanford Univ.

Roedder, E., 1967, Environment of deposition of stratiform (Mississippi Valley-type) ore deposits, from studies of fluid inclusions, in Brown, J.S. (ed.), Genesis of stratiform lead-zinc-barite-fluorite deposits: Econ. Geol. Mon. 3, pp. 349-361.

_____, 1968a, Temperature, salinity, and origin of the ore-forming fluids at Pine Point, Northwest Territories, Canada, from fluid inclusion studies: Econ. Geol., v. 63, pp. 439-450.

_____, 1968b, The noncolloidal origin of "colloform" textures in sphalerite ores: Econ. Geol., v. 63, pp. 451-471.

_____, 1976, Fluid-inclusion evidence on the genesis of ores in sedimentary and volcanic rocks, in Wolf, K.H. (ed.), Handbook of strata-bound and stratiform ore deposits, v. 2: Elsevier, Amsterdam, pp. 67-110.

Roedder, E., and Dwornik, E.J., 1968, Sphalerite color banding: lack of correlation with iron content, Pine Point, Northwest Territories, Canada: Am. Mineralogist, v. 53, pp. 1523-1529.

Runnels, D.D., 1969, Diagenesis, chemical sediments, and mixing of natural waters: Jour. Sed. Petrology, v. 39, pp. 1188-1201.

Sangster, D.F., 1976a, Carbonate-hosted lead-zinc deposits, in Wolf, K.H. (ed.), Handbook of strata-bound and stratiform ore deposits, v. 6: Elsevier, pp. 447-456.

_____, 1976b, Sulphur and lead isotopes in stratabound deposits, in Wolf, K.H. (ed.), Handbook of strata-bound and stratiform ore deposits, v. 2: Elsevier, pp. 219-266.

Sasaki, A., and Krouse, H.R., 1969, Sulfur isotopes and the Pine Point lead-zinc mineralization: Econ. Geol., v. 64, pp. 718-730.

Saxby, J.D., 1973, Diagenesis of metal-organic complexes in sediments: formation of metal sulphides from cystine complexes: Chem. Geol., v. 12, pp. 241-248.

Scott, S.D., and Barnes, H.L., 1972, Sphalerite-wurtzite equilibria and stoichiometry: Geochim. et Cosmochim. Acta, v. 36, pp. 1275-1295.

Sikabonyi, L.A., and Rodgers, W.J., 1959, Paleozoic tectonics and sedimentation in the northern half of the West Canadian Basin: Jour. Alberta Soc. Petroleum Geol., v. 7, pp. 193-216.

Skall, H., 1969, Special study 1969-8: unpubl. Cominco Ltd. report.

_____, 1970, Geology of the Pine Point Barrier Complex: unpubl. Cominco Ltd. report.

_____, 1972, Geological setting and mineralization of the Pine Point lead-zinc deposits, in Major lead-zinc deposits of western Canada, 24th Intern. Geol. Congress Guidebook A24-C24, pp. 3-18.

_____, 1975, The paleoenvironment of the Pine Point lead-zinc district: Econ. Geol., v. 70, pp. 22-45.

Sweeting, M.M., 1973, Karst landforms: Columbia Univ. Press, New York, 362 pp.

Thiede, D.S., 1975, Geological implications of variation in heavy metal content in the Elk Point evaporite sequence, Saskatchewan, Canada: unpubl. M.S. thesis, Univ. Wisconsin, Madison.

Thrailkill, J.V., 1968, Chemical and hydrologic factors in the excavation of limestone caves: Geol. Soc. Amer. Bull., v. 79, pp. 19-46.

White, D.E., 1968, Environments of generation of some base-metal ore deposits: Econ. Geol., v. 63, pp. 301-335.

Wiley, W.E., 1970, Middle Devonian Watt Mountain Formation, Pine Point, N.W.T.: unpubl. M.Sc. thesis. Univ. Saskatchewan.